



DESIGN AND SYNTHESIS OF NOVEL *P. falciparum* GDH INHIBITORS FOR USE AS POTENTIAL ANTIMALARIAL AGENTS

Edward Kumbirai Kasonde

School of Human Sciences

Ph. D

**A thesis submitted to London Metropolitan University for a degree
of DOCTOR OF PHILOSOPHY**

February 2021

“...Be strong and courageous and do the work. Do not be afraid or discouraged, for the Lord God, my God, is with you. He will not fail you or forsake you. He will see to it that all the work is finished correctly...”

“I wear the chains I forged in life, I made it link by link, and yard by yard; I girded it on my own free will and of my own free will I wore it. Is its pattern strange to you? ...”

Acknowledgements

I would like to thank Dr. Devine for having me as his research student, for his advice and guidance throughout the project. His attention to detail in all the work that I did, taking the time to go through every report, every presentation, all the analysis of NMR and chromatographic work which made this research project much easier for me. I have enjoyed the conversations we have shared and all the ideas we have discussed.

Special thanks to Dr. Don Green, Dr. Daniel Sykes, Dr. Bhaven Patel and Dr. Nick Wardle for all the advice you gave me during the course of this project, your input was very helpful and helped me improve as a researcher. I am very grateful for the time you took out of your busy schedules to help me improve my project. I am truly, truly thankful to Doreen Henry, for the measure of grace, hope and compassion you afforded me, for the helping hand at the beginning, for serendipity.

A very special thank you to Professor Terry Smith and the St Andrews group for testing my compounds against other parasitic organisms and to Professor Marcus Lee and the Sanger group of Cambridge University for testing my compounds against the Malaria parasite.

I would like to extend my sincere gratitude to Saron Eyob, Eric Coleman, Arun Rajan, Dr. Brigitte Awamaria, Louis Stott, Brunhilda Hasanaj, Elina Zalite, Lubica Tothova, Rohima Begum, Ruth Eyob, Shahrzad Nateghian, Bilkis Kazi, Alvin Sum, Ana Apostu, Beth Wallis, Karlene Marsh and all those who have left during the past four years, for their support in the laboratory, their assistance with the day to day equipment and chemical needs that made the project run as smoothly as possible, for the general safety updates checks and maintenance that were tedious at times but ensured that I got to the end of the project without any major incidents.

The assistance that the laboratory technicians and staff provided made it easier to work and helped with the health and safety aspects of the project, I am truly grateful for their advice and assistance.

Special thanks to John Morgan for the advice, papers and books that offered different perspectives on things, for bouncing off ideas for chemical reactions and alternate reagents that I could utilise for the project. John Crowder for running and processing all my NMR and mass spectra samples, Steven Boyer for running all my elemental analysis.

To all my fellow Ph.D. students past and present, the past four years has been a very unique experience that we have shared together. The pain, misery, the stress, the dinners and ice-cream the long hours in the laboratory. I am very grateful to Sarah Azam for the help she gave me with the biological evaluation section of my thesis. It may have not been the best four years of our lives, but there will be the ones that we will all remember. The bonds that were forged in adversity have unified and strengthened us. *The struggle continues!!*

I would like to thank my family for their support and encouragement throughout All my studies and this research programme as a whole. I want to thank my aunt Mrs Bessie Hardy for being flexible with her schedule to accommodate my rather rigid timetable. Special thanks to Mr Taurai Cosmas Marimo and Ms Normsa Zireba who supported and believed in me through a rather difficult period in my life. To Claudine Loicameka Brown, it is difficult to adequately and eloquently express in words what you have meant to me these past years, you chose to share my burden, one I would have struggled to carry on my own. You were a ray of sunshine that always broke through and ended the darkness.

Unreserved thanks goes to my mother Mrs Edith Kasonde for her love, support and making this prospect possible for me. For the personal sacrifices that she had to make and continues to make on my behalf so that I could have this opportunity. I will forever be indebted to her.

To the departed pillars in my life, my beloved father Mr Steven Chikondo Kasonde and Mr Edward Chikondo Kasonde, they are greatly missed and till we meet again.

Abstract

Malaria is a potentially fatal parasitic disease that is endemic in 109 countries and threatens over 2.4 billion people, representing 40% of the global population. While there has been a gradual decrease in the number of fatalities resulting from the disease in recent decades, this progress is now under serious risk of being reversed as a result of the parasite developing resistance to the currently available chemotherapies. This has led to a new impetus to look for new antimalarial drugs that have different modes of action to the ones that are currently available.

This thesis contains the following areas of research;

- 1) The design and synthesis of various compounds of the classes substituted benzyl- α -hydroxy phosphonates, substituted benzyl- α -methylene phosphonates, substituted benzyl- α -hydroxy phosphonic acids and substituted benzyl- α -amino phosphonic acids.

These compounds are intended to target one of the recently hypothesised antimalarial drug development targets, *Pf*-glutamate dehydrogenase (*Pf*GDH).

- 2) The synthesised compounds were then tested for their antimalarial activity against the *P. falciparum* strains 3D7 and Dd2. Furthermore, the synthesised compounds were tested against other parasitic organisms, *Trypanosoma brucei*, *Trypanosoma cruzi* and *Leishmania major*.

Chapter One describes the rationale for the research, why there is a need for new antimalarials, the pathogenesis of the disease and the current constraints to the development of new antimalarials. The chapter discusses why *Pf*-glutamate dehydrogenase (*Pf*GDH) would be a viable antimalarial target, from a biological point of view; the compounds designed to target this enzyme (*Pf*GDH), the rationale behind the design of such compounds and the novel synthetic targets that this project was interested in. This chapter also has a brief summary of current malaria chemotherapies that are in use and are currently being researched; the results

of the effectiveness of first generation LMU synthesised GDH inhibitors. The compounds that this research project synthesised became second generation or second series LMU GDH inhibitors.

Chapter two describes the detailed reaction mechanisms that drove the synthesis of the target compounds and detailed analyses of the analytical data of the synthesised compounds. Most of the data that was discussed in this chapter was the NMR and mass spectrometry data. Any anomalies in the synthetic procedures were discussed in this chapter, for example, the synthesis of the 1,2-benzyl- γ -lactone- diethyl phosphonate and the 1,2-Brook intramolecular phosphonate-phosphate rearrangement.

Chapter three describes how the synthesised compounds were tested against the *P. falciparum* 3D7 and Dd2 strains. Two antimalarial tests were performed, the fluorescence test and the growth inhibition test. The differences in the merits of the two tests were discussed in this chapter as well. The activity of the synthesised compounds was compared to that of the existing malaria chemotherapies, Chloroquine (CQ) and Dihydroartemisinin (DHA). Furthermore, the chapter describes how the synthesised compounds were tested against other parasitic organisms, *Trypanosomiasis brucei*, *Trypanosomiasis cruzi*, *Leishmania major* and HeLa cells. The activity of the compounds against these various parasites was discussed and compared to current chemotherapies that are in use against these parasites.

Chapter four describes alternate synthetic methods that could be utilised to generate substituted benzyl- α -methylene phosphonates, substituted benzyl- α -amino phosphonic acids thereby improving the yields of these compounds and minimising side reactions. Alternate methods of producing phosphonic acids from their precursors which could improve the purity and yields of these phosphonic acids were discussed in this chapter as well. This chapter also discussed the challenges of monophosphate and monophosphonate drug development and some of the prodrug strategies that are currently being utilised to improve the efficacy of the monophosphate and monophosphonate therapeutics. The different phosphate and phosphonate masking strategies were considered and the merits and demerits that arise from their uses. Of

particular interest was the ProTide prodrug strategy, this chapter discussed how ProTide prodrug strategy was developed, how it has been used to improve the efficacy of the compounds that the strategy was applied to. This chapter also considered how the ProTide prodrug strategy could be applied to the phosphonate esters synthesised in this project to improve their efficacy

Chapter five describes the methods (experimental) utilised for the synthesis of all the synthetic targets and their relevant analytical data. The protocols and procedures for the antimalarial evaluations and the evaluations for the other parasitic organisms, *T. brucei*, *T. cruzi*, *L. major* are described in this chapter as well. A total of twenty- seven (27) compounds were synthesised across five classes. The diethyl phosphonates and the dibenzyl phosphonates were considered to be precursors for the final target compounds, their respective phosphonic acids. The precursors were to be tested as well to determine if they would have any antimalarial activity.

The compounds that were produced in this study that showed significant antimalarial activity would provide the basis for lead compounds, that would be further studied and optimised for a new generation of antimalarial compounds. These compounds would then be utilised independently or alongside current chemotherapies as part of combination therapy in the fight against malaria. The research developed a new simpler method to substitute the hydroxyl functional group of the substituted benzyl- α -hydroxy phosphonates with hydrogen to generate the substituted benzyl- α -methylene phosphonates which worked on two compounds, **24** and **25**. This substitution method also resulted in the 1,2-Brook intramolecular phosphonate-phosphate rearrangement under basic conditions occurring, therefore, careful optimisation of reaction conditions is required in order to obtain the desired phosphonates and prevent the rearrangement reaction.

Abbreviations

Å	Angstrom (10^{-10} m)
AcOH	Acetic Acid
BF ₃ .OEt ₂	Boron trifluoride etherate
CD ₃ CN	Deuterated acetonitrile
CDCl ₃	Deuterated chloroform
COSY	Correlation spectroscopy
d	Doublet
D ₂ O	Deuterated water
DMSO	Dimethyl Sulfate
EC ₅₀	Concentration of a drug that produces half maximal response. (Effective Concentration)
ED ₅₀	Dose that produces the desired effect in 50 per cent of a population. (Effective Dose/median Effective Dose)
EI	Electron Impact
EtOAc	Ethyl Acetate
FTIR	Fourier transform infrared spectroscopy
GDH	Glutamate Dehydrogenase
He La	Henrietta Lacks
Hex	Hexane
Hz	Hertz
IC ₅₀	Concentration of inhibitor that produces half maximal inhibitory response. (Inhibitory Concentration)
<i>L. major</i>	Leishmania Major
LMU	London Metropolitan University
m	Multiplet
M.Wt	Molecular weight
m/z	Mass to charge ratio
MeOD	Deuterated methanol

MHz	Megahertz
MMV	Medicines for Malaria Venture
mp	melting point
NaH	Sodium Hydride
NaI	Sodium Iodide
<i>P. falciparum</i> (Pf)	Plasmodium falciparum
ppm	Parts per million
R _f	Retention factor
s	Singlet
SAR	Structure Activity Relationship
t	Triplet
<i>T. brucei</i>	Trypanosoma brucei
<i>T. cruzi</i>	Trypanosoma cruzi
TMSiBr	Trimethylsilyl bromide
TMSiCl	Trimethylsilyl chloride
TOF	Time Of Flight
δ	Chemical shift
$\nu_{\max} \text{ cm}^{-1}$	Wavenumber
Ala (A)	Alanine
Arg (R)	Arginine
Asn (N)	Asparagine
Asp (D)	Aspartic acid
Cys (C)	Cysteine
Glu (E)	Glutamic acid
Gln (Q)	Glutamine
Gly (G)	Glycine
His (H)	Histidine

Ile (I)	Isoleucine
Leu (L)	Leucine
Lys (K)	Lysine
Met (M)	Methionine
Phe (F)	Phenylalanine
Pro (P)	Proline
Ser (S)	Serine
Thr (T)	Threonine
Tyr (Y)	Tyrosine
Trp (W)	Tryptophan
Val (V)	Valine

CONTENTS

Acknowledgements.....	ii
Abstract.....	iv
Abbreviations.....	vii
Tables.....	xv
Figures.....	xv
1 INTRODUCTION.....	1
1.1 Rationale of the research project.....	1
1.2 Malaria pathogenesis	4
1.3 Sources of NADPH in erythrocytes and <i>P. falciparum</i>	11
1.4 Sequences and 3D structures of <i>H. sapiens</i> and <i>P. falciparum</i> GDH's compared.	15
1.5 <i>P. falciparum</i> GDH active site.....	16
1.6 Current malaria chemotherapies, strategies and modern developments	20
1.7 GDH inhibitors.....	36
1.8 Synthetic targets.....	39
2 RESULTS AND DISCUSSION	54
2.1 Substituted benzyl- α -hydroxy dibenzyl/diethyl phosphonates	54
2.1.1 Reaction mechanism	54
2.2 2-Fluorobenzyl- α -hydroxy dibenzyl phosphonate (6)	57
2.2.1 $^1\text{H-NMR000001}$	57
2.2.2 $^{13}\text{C-NMR000001}$	59
2.2.3 $^{31}\text{P-NMR00001}$	60
2.3 Mass Spectrometry (EIMS ⁺) (6)	60
2.4 Substituted benzyl- α -hydroxy diethyl phosphonates	61
2.4.1 Reaction mechanism for the synthesis of the 1,2-benzyl- γ -lactone diethyl phosphonate (18).....	62
2.5 2-Fluoro benzyl- α -hydroxy diethyl phosphonate (12)	63
2.5.1 $^1\text{H-NMR012A}$	63
2.5.2 $^{13}\text{C-NMR012A}$	64

2.5.3	³¹ P-NMR012A.....	67
2.6	Mass Spectrometry (EIMS ⁺) (12)	67
2.6.1	MS012A.....	67
2.7	1,2-Benzyl- γ -lactone-2-diethyl phosphonate (18)	68
2.7.1	¹ H-NMR022A1	68
2.7.2	¹³ C-NMR022A1	71
2.7.3	³¹ P-NMR022A1.....	73
2.8	Mass Spectrometry (TOF MS ES ⁺) (18).....	74
2.8.1	MS022A1	74
2.9	Infrared spectroscopy (18)	74
2.10	Conversion of the α -hydroxyl to the methylene group	75
2.10.1	Reaction mechanism	75
2.11	Possible side reactions for the substituted benzyl- α -methylene phosphonates	78
2.11.1	Possible side reaction 1	78
2.11.2	Possible side reaction 2.....	78
2.12	2-Fluorobenzyl-dibenzyl phosphate (19).....	84
2.12.1	¹ H-NMR001B2	84
2.12.2	¹³ C-NMR001B2	85
2.12.3	³¹ P-NMR001B2.....	86
2.13	Mass Spectrometry (EIMS ⁺) (19)	87
2.13.1	MS001B2	87
2.14	2-Fluorobenzyl-diethyl phosphate (20).....	87
2.14.1	¹ H-NMR012B3	87
2.14.2	¹³ C-NMR012B3	88
2.14.3	³¹ P-NMR012B3.....	90
2.15	Mass Spectrometry (EIMS ⁺) (20)	90
2.15.1	MS012B2.....	90
2.16	Synthesis of substituted benzyl- α -hydroxy phosphonic acids from their diethyl phosphonate precursors.....	90

2.17	Synthesis of substituted benzyl- α -hydroxy phosphonic acids from their diethyl phosphonate precursors by acid hydrolysis	92
2.17.1	Reaction mechanism	92
2.18	Synthesis of substituted benzyl- α -hydroxy phosphonic acid from their diethyl phosphonate precursors by bromotrimethylsilane (TMSiBr).	94
2.18.1	Reaction mechanism	94
2.19	NMR of 2-carboxy benzyl- α -hydroxy phosphonic acid (27).....	97
2.19.1	^1H -NMR022D2	97
2.19.2	^{13}C -NMR022D2	98
2.19.3	^{31}P -NMR022D2.....	99
2.20	Mass spectrometry (TOF MS ES $^-$) (27)	99
2.20.1	MS022D1	99
2.21	Synthesis of substituted benzyl- α -amino phosphonic acids.....	100
2.21.1	Reaction mechanism	100
2.22	NMR of 2-fluoro benzyl- α -amino phosphonic acid (34)	101
2.22.1	NMR0004B ^1H NMR.....	101
2.22.2	NMR0004B ^{13}C NMR.....	102
2.22.3	NMR0004B ^{31}P NMR	103
2.23	Mass spectrometry (EIMS $^+$) (34).....	103
2.23.1	MS004B	103
3	BIOLOGICAL EVALUATION RESULTS	104
3.1	Introduction.....	104
3.1.1	London Metropolitan University (LMU) compounds submitted for testing	107
3.1.2	'Protected' glutamic acid (glutamate) analogues	107
3.1.3	'Unprotected' glutamic acid (glutamate) analogues	108
3.1.4	Non-glutamic acid (glutamate) analogues	108
3.1.5	Malaria fluorescence tests	109
3.1.6	Malaria fluorescence tests	110
3.2	Malaria growth inhibition tests	112
3.2.1	Compounds that inhibited malaria growth.....	113

3.2.2	Compounds that did not have malaria growth inhibition	116
3.2.3	Activity of compounds against these parasites	118
4	CONCLUSION AND FUTURE WORK	123
5	EXPERIMENTAL	136
5.1	General experimental	136
5.2	Synthesis of substituted benzyl- α -hydroxy phosphonates	137
5.2.1	2-Fluorobenzyl- α -hydroxy dibenzyl phosphonate (6)	137
5.2.2	3-Cyanobenzyl- α -hydroxy dibenzyl phosphonate (7).....	138
5.2.3	3-Nitrobenzyl- α -hydroxy dibenzyl phosphonate (8).....	139
5.2.4	2-Nitrobenzyl- α -hydroxy dibenzyl phosphonate (9).....	139
5.2.5	4-Cyanobenzyl- α -hydroxy dibenzyl phosphonate (10) (data for this compound agreed with <i>Pawar, V., et al 2006</i>).	140
5.2.6	4-Nitrobenzyl- α -hydroxy dibenzyl phosphonate (11) (data for this compound agreed with <i>Pogatchnik, D., et al 1997</i>).	141
5.3	Synthesis of substituted benzyl- α -hydroxy diethyl phosphonates	141
5.3.1	2-Fluorobenzyl- α -hydroxy diethyl phosphonate (12).....	141
5.3.2	3-Cyanobenzyl- α -hydroxy diethyl phosphonate (13) (data for this compound agreed with <i>Pandi. M, et al 2012</i>), 99%.	142
5.3.3	4-Cyanobenzyl- α -hydroxy diethyl phosphonate (14) (data for this compound agreed with <i>Pandi. M, et al 2012</i>), 99%	143
5.3.4	3-Nitro benzyl- α -hydroxy diethyl phosphonate (15) (data for this compound agreed with <i>Goldeman. W, et al 2006</i>), 79%	143
5.3.5	4-Nitro benzyl- α -hydroxy diethyl phosphonate (16) (data for this compound agreed with <i>Pandi. M, et al 2012</i>), 98%.	144
5.3.6	2-Nitro benzyl- α -hydroxy diethyl phosphonate (17) (data for this compound agreed with <i>Pandi. M, et al 2012</i>), 97%.	144
5.3.7	Attempted synthesis of 2-cyanobenzyl- α -hydroxy diethyl phosphonate (18) (data for this compound agreed with <i>Menear. K. A, et al 2012, US008247416B2</i>). ...	145
5.4	Conversion of the substituted benzyl- α -hydroxy to the substituted benzyl- α - methylene-phosphonates and substituted benzyl-dialkyl-phosphates.....	146
5.4.1	2-Fluoro benzyl-dibenzyl phosphate (19).....	147

5.4.2	2-Fluoro benzyl-diethyl phosphate (20) (data for this compound agreed with <i>Pallikonda. G, et al 2015</i>), 92%.....	147
5.4.3	3-Cyanobenzyl-diethyl phosphate (21).....	148
5.4.4	4-Cyanobenzyl-diethyl phosphate (22).....	149
5.4.5	3-Nitrobenzyl-diethyl phosphate (23).....	149
5.5	Substituted benzyl- benzyl- α -methylene phosphonates.....	150
5.5.1	4-Nitro benzyl- α -methylene-dibenzyl phosphonate (24).....	150
5.5.2	4-Nitrobenzyl- α -methylene-diethyl phosphonate (25) (data for this compound agreed with <i>Döpp, D., (2000) (57%)</i>).	151
5.6	Synthesis of substituted benzyl- α -hydroxyl phosphonic acids from their diethyl phosphonates precursors.	152
5.7	Synthesis of substituted benzyl- α -hydroxy phosphonic acids from their diethyl phosphonates by acid hydrolysis.....	152
5.7.1	3-Carboxy benzyl- α -hydroxy phosphonic acid (26).....	152
5.7.2	2-Carboxyl benzyl- α - hydroxy phosphonic acid (27).....	153
5.7.3	4-Carboxyl benzyl- α -hydroxy phosphonic acid (28).....	153
5.8	Synthesis of substituted benzyl- α -hydroxy phosphonic acids by dealkylation of the substituted benzyl- α -hydroxy diethyl phosphonate precursors with bromotrimethylsilane	154
5.8.1	2-Fluoro benzyl- α -hydroxy phosphonic acid (29) (data for this compound agreed with <i>Murai. K, et al 2016</i>)......	154
5.8.2	2-Nitro benzyl- α -hydroxy phosphonic acid (30) (data for this compound agreed with <i>Uhlmann. E, et al 2000, US006028182A</i>).	155
5.9	Synthesis of substituted benzyl- α -amino phosphonic acids.....	156
5.9.1	2-Fluoro benzyl- α - amino phosphonic acids (34).....	156
5.10	Protocols and procedures for the antimalarial evaluations.....	157
5.10.1	<i>P. falciparum</i> drug assay method.....	157
5.11	Protocols and procedures for the testing against other parasites, (<i>T. brucei</i> , <i>T. cruzi</i> , <i>L. major</i> and HeLa).....	157
5.11.1	Cell lines and cell culture.....	157
5.11.2	Cytotoxicity EC ₅₀ assay.....	158

Tables

Table 1: Percentage inhibition of <i>P. falciparum</i> GDH by a series of glutamate analogue prepared at London Metropolitan University. Key: IPA-isophthalic acid, IBA-3-iodobenzoic acid, (1)- 2,6-pyridine-dicarboxylic acid, (2)- 6-methyl pyridine-2-carboxylic acid, (3) -1,5-dimethylpyrrole-2-carboxylic acid, (4)- 1-methyl-2,5-pyrrole dicarboxylic acid, (5)- 5-methyl-2-furanoic acid.	38
Table 2: Synthesized substituted benzyl-α-hydroxy dibenzyl phosphonates and their respective yields.....	56
Table 3: Distinguishing peaks of the substituted benzyl-α-hydroxy diethyl phosphonates	57
Table 4: Synthesized substituted benzyl-α-hydroxy diethyl phosphonates and their respective yields.....	61
Table 5: Distinguishing peaks of the substituted benzyl-α-hydroxy diethyl phosphonates	62
Table 6: Synthesized substituted benzyl-α-methylene dibenzyl phosphonates and their respective yields.....	79
Table 7: The observed J_{P-C7} coupling constants and ^{31}P δ-values for all of our synthesized targets (PA = phosphonic acids).	83
Table 8: Distinguishing peaks of the substituted benzyl-α-methylene dibenzyl phosphonates/phosphates	84
Table 9: Synthesized substituted carboxy benzyl-α-phosphonic acids and their respective yields.....	96
Table 10: Comparisons in yields between synthesis with TMSiCl and TMSiBr.....	96
Table 11: Distinguishing peaks of the substituted benzyl-α-hydroxy/amino phosphonic	97

Figures

Figure 1.2.1: Malaria life-cycle in human beings and in the parasite. www.CDC.gov	7
Figure 1.2.2: The biosynthesis of glutathione, essential for combating reactive oxygen species (ROS), is catalysed by glutathione disulfide reductase	10
Figure 1.3.1: The NADP+- dependant GDHs catalyses the reversible interconversion of L-glutamate to 2-oxoglutarate	15
Figure 1.5.1: The CLUSTALW sequence of <i>H. sapiens</i>, <i>C. symbiosum</i> and <i>P. falciparum</i> GDH. The nucleotide-binding fold is indicated in red, the N-terminal domain in blue. The residues highlighted in pink reveal those that bind NADP, while those in yellow bind	

the substrate L-glutamate. The unique N-terminal extension of <i>P. falciparum</i> GDH is shown in violet (Werner. C, et al (2005)).....	18
Figure 1.5.2: The 3D crystal structure of <i>P. falciparum</i> GDH.....	19
Figure 1.5.3: The 3D crystal structure of Human GDH.....	20
Figure 1.6.1: Examples of Dihydroorotate dehydrogenase (DHODH) inhibitors that have shown antimalarial activity, some of them in phase 1 and 2 clinical trials.....	22
Figure 1.6.2: Examples of imidazolopiperazines and Tafenoquine that have shown antimalarial activity.....	25
Figure 1.6.3: Examples of ozonides, tetraoxanes and trioxanes that have shown antimalarial activity, some of them now in Phase 1 and 2 clinical trials	28
Figure 1.6.4: Examples of quinoline analogues that have shown antimalarial activity, some of them in Phase 1 and 2 clinical trials	30
Figure 1.6.5: Examples of DHFR inhibitors and Spiroindolones that have shown antimalarial activity, some of them in Phase 1 and 2 clinical trials.	31
Figure 1.6.6: Examples of Phosphatidylcholine inhibitors that have shown antimalarial activity, some of them in Phase 1 and 2 clinical trials.....	32
Figure 1.6.7: Falcipain inhibitor and the marine natural product salinosporamide that have shown antimalarial activity	34
Figure 1.6.8: Active compounds derived from various approaches that have shown some antimalarial activity.....	35
Figure 1.7.1: A, The superimposed structures of isophthalate and glutarate. B, the superimposed structures of m-bromobenzoate, 5-bromofuroate and isophthalate (adopted from Caughey. W, et al 1957)	37
Figure 1.7.2: L-Glutamate analogues synthesised at London Metropolitan University and tested against PfGDH by the research group of Paul Engel at UCD (results shown in Table 1.0)	39
Figure 1.8.1: Naturally occurring phosphonic acids and phosphonates derived from protozoa, bacteria and other microorganisms (<i>Kafarski. B, 2019</i>).....	44
Figure 1.8.2: Substituted benzyl- α -hydroxyl phosphonates reaction scheme.....	47
Figure 1.8.3: Substituted benzyl- α -methylene phosphonates reaction scheme	47
Figure 1.8.4: Acid hydrolysis of the substituted benzyl- α -hydroxy diethyl phosphonates general reaction scheme	48
Figure 1.8.5: Reaction scheme for the dealkylation of the substituted benzyl- α -hydroxy diethyl phosphonates by TMSiBr	48
Figure 1.8.6: Synthesis of substituted benzyl- α -amino phosphonic acid reaction scheme	49

Figure 1.8.7: The structures of the second series of targeted protected and unprotected glutamate analogues synthesised in this research project. The lactone containing compound 18 was not the desired target; the 2-CN(and 2-CO₂H in the final hydrolysed product) compound was.	50
Figure 1.8.8: The structures of the second series of protected and unprotected non-glutamate analogues compounds synthesised in this research project.	51
Figure 1.8.9: The structures of the –α-methylene phosphate and phosphonate esters that were synthesised in this research project. The –α-methylene phosphate esters were not the desired targets	52
Figure 1.8.10: The structures of the desired α-methylene phosphonates synthetic targets that were not attained.	53
Figure 2.1.1: General reaction mechanism for the synthesis of substituted benzyl-α-hydroxy dibenzyl/diethyl phosphonates	54
Figure 2.1.2: substituted benzyl-α-hydroxy phosphonates reaction scheme	56
Figure 2.2.1: 2-Fluorobenzyl-α-hydroxy dibenzyl phosphonates with numbered carbons.	57
Figure 2.2.2: ¹H-NMR 2-fluorobenzyl-α-hydroxy dibenzyl phosphonate aliphatic region expanded	58
Figure 2.2.3: ¹H-NMR 2-fluorobenzyl-α-hydroxy dibenzyl phosphonate aromatic region expanded	59
Figure 2.2.4: ¹³C-NMR 2-Fluorobenzyl-α-hydroxy dibenzyl phosphonate aliphatic region expanded	59
Figure 2.2.5: ¹³C-NMR 2-fluorobenzyl-α-hydroxy dibenzyl phosphonate aromatic region expanded	60
Figure 2.3.1: General reaction mechanism for the synthesis of 1,2-benzyl-γ-lactone diethyl phosphonates	62
Figure 2.4.1: 2-fluorobenzyl-α-hydroxy diethyl phosphonates with numbered carbons	63
Figure 2.4.2: ¹H-NMR 2-fluorobenzyl-α-hydroxy diethyl phosphonate aliphatic region expanded	63
Figure 2.4.3: ¹H-NMR 2-fluorobenzyl-α-hydroxy diethyl phosphonate aromatic region expanded	64
Figure 2.4.4: ¹³C-NMR 2-fluorobenzyl-α-hydroxy diethyl phosphonate aliphatic region expanded	65
Figure 2.4.5: ¹³C-NMR 2-fluorobenzyl-α-hydroxy diethyl phosphonate aliphatic region expanded	65

Figure 2.4.6: ¹³ C-NMR 2-fluorobenzyl- α -hydroxy diethyl phosphonate aromatic region expanded	66
Figure 2.4.7: ¹³ C-NMR 2-fluorobenzyl- α -hydroxy diethyl phosphonate aromatic region expanded	67
Figure 2.5.1: 1,2-benzyl- γ -lactone diethyl phosphonates with numbered carbons	68
Figure 2.5.2: ¹ H-NMR 1,2-benzyl- γ -lactone diethyl phosphonates aliphatic region expanded	68
Figure 2.5.3: ¹ H-NMR 1,2-benzyl- γ -lactone diethyl phosphonates aliphatic region expanded	69
Figure 2.5.4: ¹ H-NMR 1,2-benzyl- γ -lactone diethyl phosphonates aliphatic region expanded	70
Figure 2.5.5: ¹ H-NMR 1,2-benzyl- γ -lactone diethyl phosphonates aromatic region expanded	71
Figure 2.5.6: ¹ H-NMR D ₂ O shake 1,2-benzyl- γ -lactone diethyl phosphonates aliphatic region expanded	71
Figure 2.5.7: ¹³ C-NMR 1,2-benzyl- γ -lactone diethyl phosphonates aliphatic region expanded	72
Figure 2.5.8: ¹³ C-NMR 1,2-benzyl- γ -lactone diethyl phosphonates aliphatic region expanded	72
Figure 2.5.9: ¹³ C-NMR 1,2-benzyl- γ -lactone diethyl phosphonates aliphatic region expanded	73
Figure 2.5.10: ¹³ C-NMR 1,2-benzyl- γ -lactone diethyl phosphonates aromatic region expanded	73
Figure 2.9.1: General reaction mechanism for the synthesis of substituted benzyl- α -methylene phosphonates.....	75
Figure 2.9.2: Possible side reaction mechanism for the substituted benzyl- α -methylene phosphonates 1	78
Figure 2.9.3: Possible side reaction mechanism for the substituted benzyl- α -methylene phosphonates 2	78
Figure 2.9.4: substituted benzyl- α -methylene phosphonates reaction scheme	79
Figure 2.9.5: A possible phosphonate to phosphate rearrangement, via an epoxy-phosphono-intermediate, that occurs in the attempted conversion of the α -OH compounds into their benzyl phosphate derivatives. (EWG: electron-withdrawing group).....	82
Figure 2.10.1: 2-fluorobenzyl-phosphate with numbered carbons.....	84
Figure 2.10.2: ¹ H-NMR 2-fluorobenzyl-dibenzyl phosphate aliphatic region expanded	85

Figure 2.10.3: ¹H-NMR 2-fluorobenzyl-dibenzyl phosphate aromatic region expanded	85
Figure 2.10.4: ¹³C-NMR 2-fluorobenzyl-dibenzyl phosphate aliphatic region expanded	86
Figure 2.10.5: ¹³C-NMR 2-fluorobenzyl-dibenzyl phosphate aromatic region expanded	86
Figure 2.11.1: 2-fluorobenzyl-diethyl phosphate with numbered carbons	87
Figure 2.11.2: ¹H-NMR 2-fluorobenzyl-diethyl phosphate aliphatic region expanded	88
Figure 2.11.3: ¹H-NMR 2-fluorobenzyl-diethyl phosphate aromatic region expanded	88
Figure 2.11.4: ¹³C-NMR 2-fluorobenzyl- diethyl phosphate aliphatic region expanded	89
Figure 2.11.5: ¹³C-NMR 2-fluorobenzyl- diethyl phosphate aliphatic region expanded	89
Figure 2.11.6: ¹³C-NMR 2-fluorobenzyl-diethyl phosphate aromatic region expanded	90
Figure 2.15.1: General reaction mechanism for the dealkylation of substituted benzyl-α-diethyl phosphonates by acid hydrolysis	92
Figure 2.15.2: General reaction mechanism for the acid hydrolysis of nitrile groups	93
Figure 2.16.1: Reaction mechanism for the dealkylation of Benzyl-α-diethyl phosphonates by bromotrimethylsilane (TMSiBr)	95
Figure 2.17.1: 2-carboxybenzyl-α-hydroxy phosphonic acid with numbered carbons	97
Figure 2.17.2: ¹H-NMR 2-carboxybenzyl-α-hydroxy phosphonic acid aliphatic region	98
Figure 2.17.3: ¹H-NMR 2-carboxybenzyl-α-hydroxy phosphonic acid aromatic region	98
Figure 2.17.4: ¹³C-NMR 2-carboxybenzyl-α-hydroxy phosphonic acid aliphatic region	99
Figure 2.17.5: ¹³C-NMR 2-carboxybenzyl-α-hydroxy phosphonic acid aromatic region	99
Figure 2.19.1: General reaction mechanism for the synthesis of substituted benzyl-α-amino phosphonic acids	100
Figure 2.20.1: 2-fluorobenzyl-α-amino phosphonic acid with numbered carbons	101
Figure 2.20.2: ¹H-NMR 2-fluorobenzyl-α-amino phosphonic acid aromatic region	102
Figure 2.20.3: ¹³C-NMR 2-fluorobenzyl-α-amino phosphonic acid aromatic region	103
Figure 3.1.1: ‘Protected’ Glutamic acid analogues	107
Figure 3.1.2: ‘Unprotected’ Glutamic acid analogues	108
Figure 3.1.3: Non-Glutamic acid analogues	108
Figure 3.1.4: LMU compounds that had similar fluorescence reduction profiles of the P. falciparum strains 3D7 and Dd2 to the control compounds Chloroquine (CQ) and Dihydroartemisinin (DHA)	109
Figure 3.1.5: LMU compounds that did not show similar fluorescence reduction profiles of the P. falciparum strains 3D7 and Dd2 to the control compounds Chloroquine (CQ) and Dihydroartemisinin (DHA)	111

Figure 3.2.1: LMU compounds that had malaria growth inhibition of the <i>P. falciparum</i> strains 3D7 and Dd2 compared to the control compound Chloroquine (CQ).....	113
Figure 3.2.2: LMU compounds that did not have malaria growth inhibition for the <i>P. falciparum</i> strains 3D7 and Dd2.....	116
Figure 3.2.1: Proposed alternate reaction mechanism to synthesise substituted benzyl-α-amino phosphonic acid	125
Figure 3.2.2: The structures of ProTide and phosphate ester prodrugs that have been discussed in this section(Thornton. P, et al 2016, Mehellou. Y, et al 2017).....	133
Figure 3.2.3: Proposed reaction scheme for the synthesis of PfGDH-inhibitor ProTides	134
Figure 3.2.4: 1-amino-cyclopropane-1,2-dicarboxylic acid reaction scheme.....	135
Figure 5.2.1: Synthesis of substituted benzyl-α-hydroxy phosphonates general reaction scheme	137
Figure 5.4.1: Synthesis of substituted benzyl-dialkyl phosphonates general reaction scheme	146
Figure 5.5.1: Synthesis of substituted benzyl- phosphates general reaction scheme ...	150
Figure 5.6.1: Acid hydrolysis of the substituted benzyl-α-hydroxy diethyl phosphonates general reaction scheme	152
Figure 5.8.1: Reaction scheme for the dealkylation of the substituted benzyl-α-hydroxy diethyl phosphonates by TMSiBr	154
Figure 5.9.1: Synthesis of substituted benzyl-α-amino phosphonic acid reaction scheme	156

1 INTRODUCTION

1.1 Rationale of the research project

Malaria is a potentially fatal parasitic disease that is endemic in 109 countries and threatens over 2.4 billion people, representing 40% of the global population (*WHO malaria reports 2008, 2009, and 2010*). Malaria transmission occurs in regions of Africa, Latin and South America, Asia, the Middle East, the South Pacific and the Caribbean. Current statistics show that in the years from 2000-2013 the global death rates have decreased from around 1 million, (mostly in children under the age of 5) to somewhere between 584,000-660,000 deaths in 2013. The number of global malaria deaths has been steadily declining with 416,000 estimated deaths in 2017 and 405,000 estimated deaths in 2018 (*WHO malaria reports 2019*). The incidence rate of malaria has also been declining globally between 2010 and 2018, from 71 to 57 cases per 1000 population at risk. However, from 2014 to 2018, the rate of change has slowed dramatically, reducing to 57 cases per 1000 in 2014 and remaining at similar levels through to 2018 (*WHO malaria reports 2019*). Although it is believed that the number of deaths could still be as high as 1.1 million when undiagnosed or untreated malaria cases are considered (*Miller. H. L, et al 2013*), *Diagana. T. T, 2015*). Malaria remains among the top 5 causes of death of children under the age of 5, these make up between 67%-78% of the total annual deaths (*WHO malaria reports 2019*). Malaria has 231-278 million reported clinical cases each year with 1% of those cases progressing to severe malaria (*WHO malaria reports 2019*). About 125 million pregnancies are at risk each year from malaria and as a result, an estimated 10,000 pregnant women and 200,000 babies die from the disease (*Biamonte. M. A, et al 2013*).

Malaria poses a major global health threat because of environmental changes, particularly climate change, population movements and biological changes to the parasite and the mosquito vector. Health systems in most countries to which malaria is endemic have weak drug management and supply systems. This results in a growing problem of resistance to the available antimalarial drugs as a result of mutations in the parasites or as a result of irrational

use of antimalarial drugs. This increase in the parasite's resistance to the available antimalarial drugs has led to an increase in the morbidity and mortality of the group at the highest risk which is African children (*Snow. R. W, et al 2001*), thus the need to develop new antimalarial agents. Antimalarial drug development can follow several different strategies, which range from minor modifications to existing compounds to design of novel agents that act on new targets, and combining available agents to improve antimalarial regimens (*Rosenthal. P, 2003*).

Antimalarial drug development is affected by the same constraints that affect any other drug development program. In addition to the general considerations such as the new agent being safe and demonstrate high efficacy, additional important properties specific to the disease must be accounted for. In the case of malaria, the drug development process must consider that the drug be available for major widespread use in developing countries. Due to the limited resources in these areas the drug should be dosed orally and be effective with single daily dosing with a full treatment regimen lasting between 1-3 days in length. However, the most important consideration in antimalarial drug development is economical. Financial considerations are important in two crucial areas. First, for antimalarial drugs to be widely used, they have to be cheaply priced for the populations that need them in developing countries, as such, a cost of \$1 USD per treatment regimen may be too expensive and unacceptable given the degree of poverty in malaria infested areas.

To this end, any new anti-malaria agents must have a similar cost to that of currently available drugs such as chloroquine which cost \$0.1 USD per treatment regimen. The second financial consideration is that since malaria is prevalent in poor countries, there are limited funding opportunities, and investment in antimalarial drug research, discovery and development is small. With the estimated funds available for malaria control from international sources peaking at US\$2 billion in 2011, this remains well short of US\$5 billion that is required to meet global malaria targets between 2010-2015 (*WHO world malaria report 2011*). This has resulted in research in antimalarial drug discovery to rely on simple synthetic routes and

shortcuts to minimize excess costs (Rosenthal. P, 2003). As a result, anti-malaria drug discovery is dependent on financial support outside large pharmaceutical companies. This financial support comes mainly from grants to academics and industry groups from philanthropic organisations such as the Wellcome Trust and the Bill and Melinda Gates Foundation, research agencies and new public-private partnerships such as the Medicines for Malaria Venture (MMV) formed to address the imbalance in funding between developed and developing world diseases (Rosenthal. P, 2003), Diagana. T. T, 2015).

The current challenge is whether malaria can be completely eliminated on a global scale. Several countries have put forward and or begun implementing malaria elimination programmes, but it is clear that the targets for these programmes will neither be achieved nor successful with the currently available drugs. From 1950 to 2011, Paraguay systematically developed policies and programmes to control and eliminate malaria, a significant public health challenge for a country that reported more than 80,000 cases of the disease in the 1940s. As a result, Paraguay registered its last case of *P. falciparum* malaria in 1995, and *P. vivax* malaria in 2011. This was followed by a five-year plan to consolidate the gains, prevent re-establishment of transmission and preparation for elimination certification. The plan involved robust case management, engagement with communities, and education to make people more aware of ways to prevent malaria transmission, and about diagnosis and treatment options. Paraguay was certified malaria free by WHO in 2016 (WHO newsletter June 2018).

Whilst the current artemisinin based combination therapies are still viable, they require multiple daily doses and there is a looming threat of the parasite becoming resistant to them, this makes the currently available artemisinin based combination therapies unsuitable for malaria elimination programmes (Diagana. T. T, 2015). Sequencing of the parasite's genome and a greater understanding of the parasite's biology has resulted in the identification of new targets for drug development which could be used to defeat the disease (Sahu. N, et al 2008). The sequencing of the plasmodium genome and the application of modern genetic tools has also led to the identification of numerous potential targets, which include glutathione disulfide

reductase and glutamate dehydrogenase, that could be useful in the development of novel antimalarials. However, only a few of these targets have been adequately validated chemically and even fewer of those fully validated have proved to be viable targets (*Biamonte. M. A, et al 2013*). A major part of the problem is that no antimalarial with a novel mechanism of action has entered phase 2 clinical trials since hydroxy-1,4-naphthoquinone atovaquone in 1992 (*Diagana. T. T, 2015*).

Most of the available antimalarial drugs target the blood stages of the parasite's lifecycle, at present, the only antimalarials present that are effective against the liver stages of the parasite are the combination therapy atovaquone/proguanil and primaquine. Although atovaquone/proguanil affects the blood stages of the parasite, it is also effective at clearing parasites from the liver. The main obstacle in the search for liver stage drugs is the unavailability of efficient and effective culture techniques and models. This means that trials for liver stage antimalarials have to utilise primate animal models that are cumbersome and unreliable. Current theories suggest an effective antimalarial prophylactic will have to target the liver stage and not the blood stage of the life cycle. As of 2015, there are no known antimalarials that successfully target the transmission stage of the parasite's lifecycle (*Biamonte. M. A et al (2013)*). Enzymes such as glutathione disulfide reductase and glutamate dehydrogenase (GDH), among others, are important to the survival and development of the plasmodium inside the host. Synthesis of novel compounds that mimic the structures of these enzymes' substrates could potentially have antimalarial properties. This Ph.D. project focused on the development of potentially new antimalarials based on substrates of the parasite's glutamate dehydrogenase (GDH), which would then act as inhibitors to the enzyme.

1.2 Malaria pathogenesis

The malaria parasite is a small single-celled protozoan micro-organism that lives as a parasite in man and in the female anopheles' mosquito. There are five different types of plasmodium parasites *P. vivax*, *P. ovale*, *P. falciparum*, *P. malariae* and *P. knowlesi*. *Plasmodiums ovale*, *vivax* and *malariae* cause more benign forms of malaria, *P. falciparum* being the most severely

malignant and can be potentially fatal. *P. vivax* and *P. falciparum* cause most of the infections worldwide. *P. falciparum* accounts for much of the burden in sub-Saharan Africa, whilst *P. vivax* accounts for half of the burden in South and East Asia and up to 80 % of the burden in the Americas. *P. knowlesi* was a species that was previously thought to just infect non-human primates but has now emerged as a zoonotic malaria parasite and is now an important, sometimes, lethal cause of human malaria in parts of South East Asia, in particular Malaysia, Indonesia, Thailand, Singapore and the Philippines. *P. knowlesi* is now a potential cause of malaria among travellers returning from this region. There is a limited understanding of the pathogenesis of malaria. The knowledge that is available has been provided by studying animal models and human malaria. The pathogenicity that is provided by animal models, as valuable as it is, does not give an accurate pathogenic process of *P. falciparum*, therefore, observations made in humans are of central importance (Miler. H. L, et al 1994).

The plasmodium lifecycle consists of two stages, the first stage is in the mosquito and the second stage of the lifecycle is in humans. In the human stage of the plasmodium lifecycle, the plasmodium sporozoites develop, mature and multiply in the liver hepatocytes for about a week. Tens to hundreds of hepatocytes are targeted by the sporozoites and this stage of the infection is not responsible for the disease. (Miler. H. L, et al 1994). The mature sporozoites, known as merozoites, rupture the hepatocytes, migrate to, and complete the remainder of their lifecycles in the red blood cells. This erythrocytic cycle of the infection is when parthenogenesis begins. The parasite remodels the erythrocyte within 12 hours of invasion to facilitate a large periodic amplification of the size of the parasite population to increase the probability of the merozoites developing into gametocytes (Miler. H. L, et al 1994). Infected erythrocytes bind to the endothelium through *P. falciparum* Erythrocyte Membrane Protein-1 (*Pf*EMP-1) to avoid clearance in the spleen. Attachment of the infected erythrocytes to the endothelium damages the endothelial cells and disrupts blood flow which leads to tissue hypoxia and lactic acidosis. This is the same mechanism that contributes to organ specific

syndromes such as cerebral malaria and placental malaria when the attachment of the infected erythrocytes happens in the brain and/or the placenta.

The rupture of the infected red blood cells (haemolysis) and near-by bystander red blood cells causes anaemia which is worsened by impaired erythropoiesis. Haemolysis also worsens the endothelial damage and dysfunction due to the free haemoglobin (Hb) catalysing oxidative damage and consumes nitric oxide (NO) a key regulator of endothelial cells. The rupture of infected erythrocytes also causes fevers and rigours (*Miller. H. L, et al 2013*). Merozoites often invade uninfected erythrocytes and circulate as ring stage parasites but a few develop into schizonts, trophozoites and finally into male and female gametocytes. The gametocytes continue to circulate in the bloodstream without being treated by the current antimalarials at the asexual blood stages. The male and female gametocytes are then transported by the mosquito *Anopheles gambiae* when it bites and draws blood from the human host. Discovering effective, safe therapies to kill gametocytes will go a long way to combat *P. falciparum* (*Miller. H. L, et al 2013*). The clinical manifestations of the disease are as a result of the multiplication and differentiation of the protozoan parasites in the erythrocytes (*Wagner. J. T, et al (1998)*). In the erythrocytes, the parasite digests the host's haemoglobin freeing the reactive haem groups. The release of haem groups from the rupture of erythrocytes leads to the formation of reactive oxygen species through Fenton like reactions (*Buffington G.D. et al 1986*).

Malaria
(*Plasmodium spp.*)

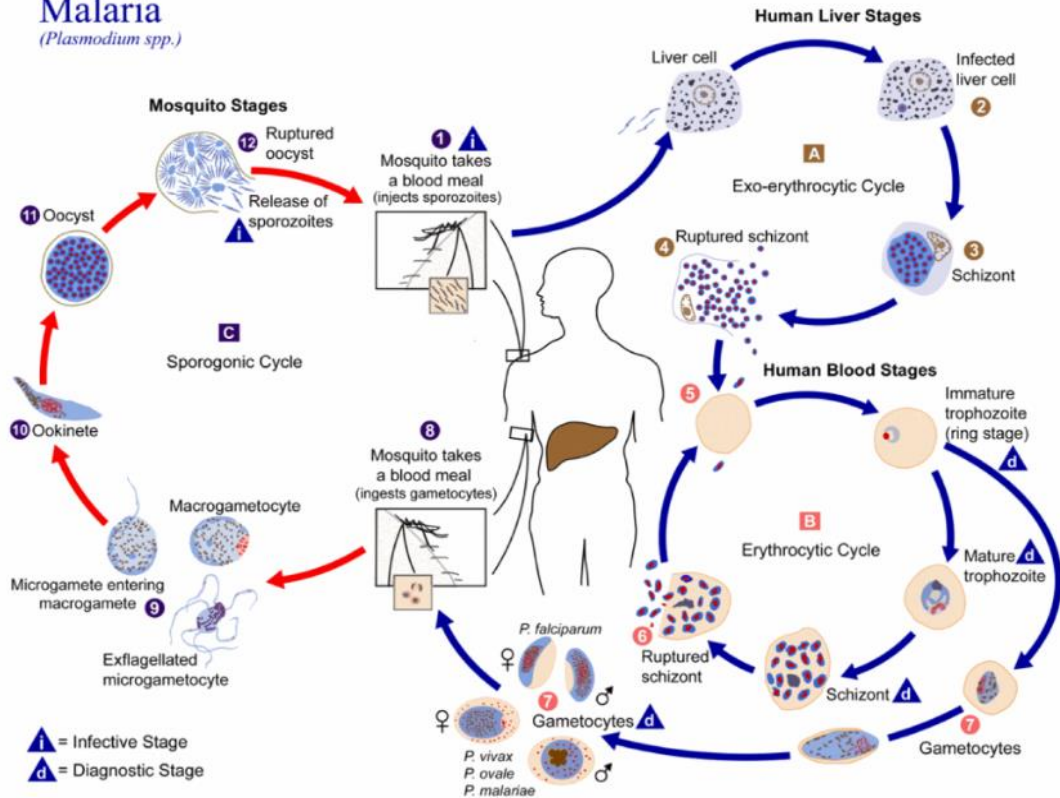


Figure 1.2.1: Malaria life-cycle in human beings and in the parasite. www.CDC.gov

All aerobic life requires the maintenance of a homeostatic intracellular redox environment that minimizes the production of reactive oxygen species and allows for the essential metabolic functions to progress. (Muller. S, et al 2004). These aerobic organisms are exposed to reactive oxygen species (ROS) such as superoxide anions (O_2^-), hydrogen peroxide (H_2O_2) and hydroxyl radicals (OH^\cdot) that are generated by their metabolism. These ROS, if left to accumulate, can lead to the damage of nucleic acids, proteins, lipids and cell membrane which leads to the loss of cellular structure and function. The plasmodium merozoites do not only have to contend with, and be able to effectively remove their endogenous toxic metabolites, but have to be able to cope with the oxidative or respiratory burst from the host's immune system. The host's respiratory burst is the sum of the ROS that are produced during the host's defence against pathogens. This includes the optimal anti-microbial action of the neutrophils and other phagocytes which involves the rapid production of more reactive oxygen species leading to the production of superoxide anions (O_2^-) by activated NADPH oxidases. The superoxide anions (O_2^-) are then processed to produce hydrogen peroxide (H_2O_2), hydroxyl

radical (OH^\cdot), hypochlorous acid (ClO^\cdot) and oxidising derivatives of nitric oxide (NO^\cdot) such as peroxynitrite (ONOO^\cdot) (Muller. S, et al 2003). In addition to this, during the erythrocytic cycle of the infection, the parasite digests haemoglobin resulting in the formation of more ROS and the toxic ferriprotoporphyrin (IX) through Fenton like reactions. The parasite is sensitive to the reactive oxygen species that are produced by the Fenton like reactions so its survival in the erythrocyte is dependent on the parasite having good defences against these oxidising entities.

To combat these stresses, the plasmodium has to have powerful and efficient antioxidant and detoxification systems that are based on superoxide dismutases and thioredoxin-dependent peroxidases but lack catalase and glutathione peroxidases that function alongside its other systems which maintain the homeostatic redox conditions (Muller. S, et al 2004). The first line of defences of the parasites against these ROS involves several of these superoxide dismutases, peroxidases and thiol-dependant reductases (Werner. C, et al 2005). Critical to the maintenance of a stable cellular redox state are the ratios of reduced and oxidised pyridine nucleotide NADP^+ and NADPH and thiols such as glutathione/glutathione disulfide and thioredoxin/thioredoxin disulfide. The amounts of ROS present in a cell at any given time can be directly monitored by the amounts of the NADP^+ and NADPH pools that will be present in the cells at that given time. The thioredoxin and glutathione redox cycles both use NADPH as a reducing agent that is used as an electron source for the anti-oxidative enzymes glutathione reductase and thioredoxin reductase resulting in the transfer of electrons through a series of peroxidases to an acceptor molecule. This occurs through a number of redox active enzymes and cofactors which neutralise the harmful ROS to less harmful products; for example, hydrogen peroxide is converted to water and oxygen, thereby protecting the parasite from oxidative damage (Werner. C, et al 2005). These NADPH dependent enzymes such as thioredoxin reductase glutathione reductase are critical to the survival of the intraerythrocytic *P. falciparum* (Muller. S, et al 2004). The plasmodium uses some enzymatic reactions absent in the red blood cells. These defences are driven by NADPH and the production of NADPH

is catalysed by the enzyme glutamate dehydrogenase (GDH), an enzyme that is abundantly expressed by the parasite but not by the host erythrocytes (*Chodhury. R, et al 2007*). Research has identified glutamate dehydrogenase is the main source for NADPH that is used by the parasite's antioxidant defence systems (*Werner. C, et al 2005*). This makes such enzymes and disruption of these redox cycles excellent drug targets to combat the disease. Additionally, inhibiting the enzyme glutamate dehydrogenase will deprive the parasite of a source of NADPH which will render it vulnerable to oxidative damage. The combination of such new inhibitors with either the artemisinin based therapies or even older quinoline-based alcohol therapies as prodrugs could lead to the successful cost effective management of the disease. The enzymes that are present in the red blood cells for the production of antioxidants to mop up excess reactive oxygen species ROS are glucose-6-phosphate dehydrogenase and glutathione reductase. Glutathione disulfide reductase is involved in the reaction;

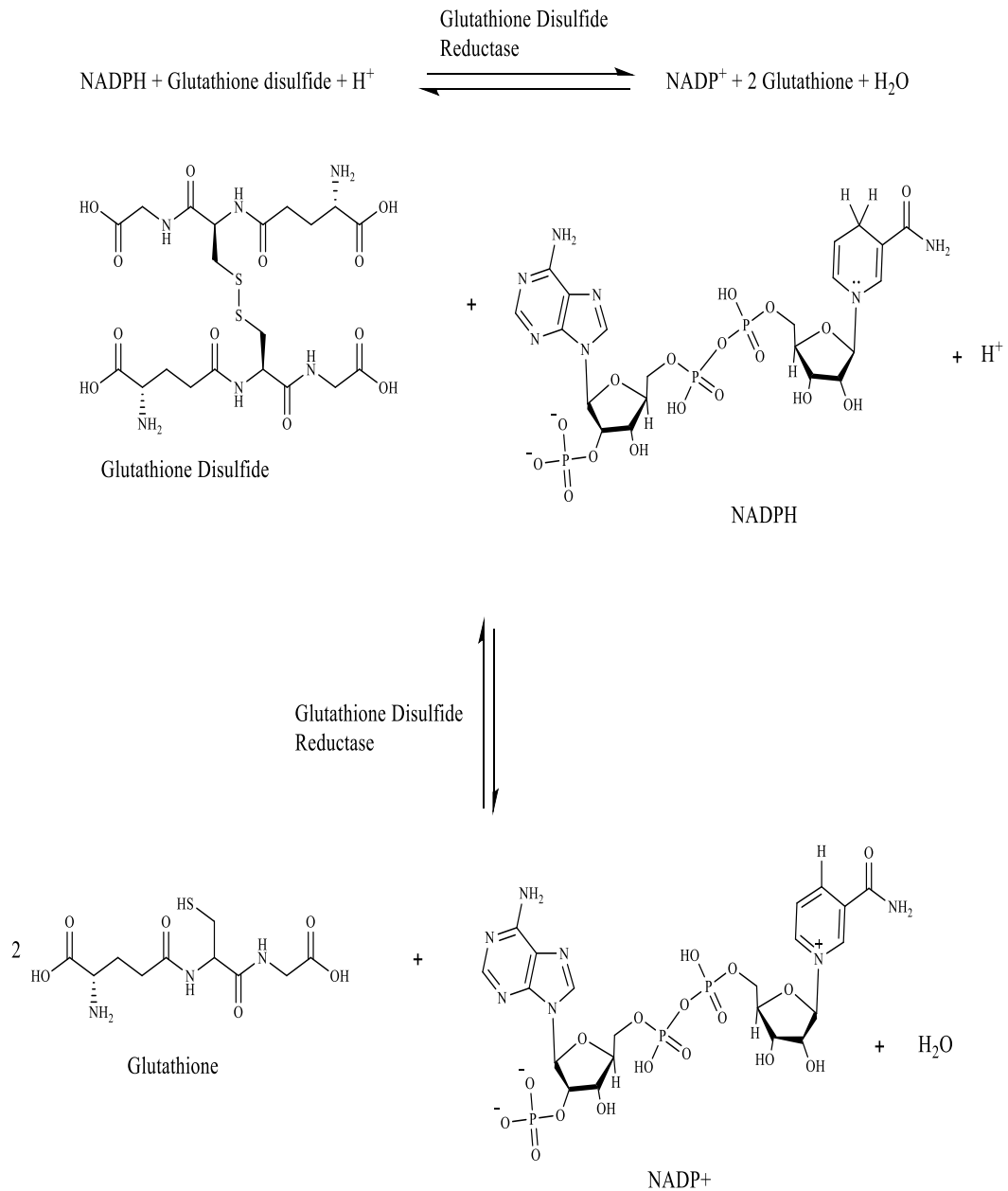


Figure 1.2.2: The biosynthesis of glutathione, essential for combating reactive oxygen species (ROS), is catalysed by glutathione disulfide reductase

Glutathione disulfide reductase is involved in the growth and differentiation of the *P. falciparum* parasite. Glutamate dehydrogenase (GDH) is an important enzyme that occupies an important junction between carbon and nitrogen metabolism. GDH catalyses the reversible oxidative deamination of L-glutamate, which yields 2-oxoglutarate and ammonia (Wagner. J. T, et al 1998).

1.3 Sources of NADPH in erythrocytes and *P. falciparum*

During the intra-erythrocytic stages of the lifecycle, the *P. falciparum*, like the host erythrocytes obtains its ATP from glycolysis. Unlike the erythrocytes, the *P. falciparum* does not have its own a source of NADPH which it requires for its biosynthetic processes and provides an electron source for its defence mechanism. Research has not shown evidence that the erythrocytes' NADPH is available for the parasite and thus, the parasite will need its own source of NADPH (Vander. D. L, et al 1989). The major source of NADP in the erythrocytes is the pentose phosphate pathway (PPP). This pathway mostly uses the enzyme glucose-6-phosphate dehydrogenase (G6PD) for the production of its NADPH. Research has shown that the *P. falciparum* has different sources of NADPH. These sources include the presence of NADP-specific GDH, which happens to be a key marker for the malarial parasite in the erythrocytes (Vander. D. L, et al 1989). The activity associated with this enzyme is only limited to the parasite, the erythrocytes do not exhibit any GDH activity.

It is for this reason that *P. falciparum* GDH presents itself as a viable target for novel antimalarial drugs or prodrugs. Genome sequencing has provided evidence that shows that the parasite encodes the homologs of the enzymes that are necessary for a complete citric acid cycle, these enzymes are expressed during the intra-erythrocytic stage of the plasmodium life cycle. The citric acid cycle plays a crucial role in cellular respiration which results in the production of the co-factors NADH and FADH₂. In eukaryotic cells there are mostly mitochondrial NAD-dependent, some mitochondrial NADP-dependent and some cytosolic NAD-dependent isocitrate dehydrogenase (IDH) enzymes which are utilised by the citric acid cycle for the production of these co-factors. The *P. falciparum* encodes for mostly mitochondrial NADP- dependent enzymes which means that the citric acid cycle in the *P. falciparum* will mostly produce NADPH, however, some NAD-dependent isocitrate dehydrogenase (IDH) has been identified in parasite extracts (Olszewski. K. L, et al 2011).

Due to the *P. falciparum* mostly undergoing anaerobic respiration in the earlier stages of its carbohydrate metabolism instead of glycolysis, there are not enough substrates to sufficiently

contribute to its citric acid cycle, therefore, alternate sources of substrates are required. The *P. falciparum* has been shown to be able to undergo carbon dioxide fixing in the cytoplasm through the enzyme PEP carboxylase leading to the production of two of the citric acid cycle intermediates oxaloacetate and malate. Another source of the citric acid cycle intermediate 2-oxoglutarate is obtained by converting glutamine to glutamate by the enzyme glutamate synthetase; glutamate is then converted to 2-oxoglutarate by the enzyme glutamate dehydrogenase, and this stage results in the production of NADPH (*Olszewski. K. L, et al 2011*). *P. falciparum* encodes for three distinct GDH enzymes, all of the three enzymes that are produced have been shown to be NADP-dependant. The first one GDHa, is thought to be predominantly found in the apicoplast of the parasite and is thought to be responsible for supplying NADPH for biosynthetic reactions in that compartment. The second NADP-dependant GDHb which lacks a cleavable signal sequence and is thus believed to be a cytosolic enzyme that is responsible for the redox control and the parasites defence mechanisms. Available theories suggest that cytosolic GDH is the most abundant and is the major source NADPH for the parasite but this has not been confirmed. The third is a large fungal type NAD-dependant GDHc which does not have any signal sequence and whose purpose is really not understood at the moment (*Olszewski. K. L, et al 2011*).

Presented research has also provided evidence of the presence of a *P. falciparum* pentose phosphate pathway (PPP) which uses the enzyme glucose-6-phosphate dehydrogenase (G6PD) for the production of NADPH in the parasite. The erythrocyte's and the *P. falciparum* glucose-6-phosphate dehydrogenase (G6PD) enzyme have both been sequenced and have been noted to be significantly different to each other, making the plasmodium glucose-6-phosphate dehydrogenase another viable anti-malaria target. The pentose phosphate pathway (PPP) is an essentially conserved pathway that is present in more or less every cell that is capable of metabolising carbohydrates (*Olszewski. K. L, et al 2011*). Its main purpose is the production of five-carbon sugars that are used in nucleotide synthesis and the production of NADPH. The pentose phosphate pathway (PPP) is the foremost source of NADPH in human erythrocytes

but it is not clear if it is a major source of NADPH in the *P. falciparum* since the main enzyme for this pathway, glucose-6-phosphate dehydrogenase has been observed as having modest activity inside the parasite (Wagner. J. T, et al 1998).

The importance of the effects of the glutamate dehydrogenase (GDH) and glutathione disulfide reductase in the defence against reactive oxidative species is evidenced by the fact that glucose-6-phosphate dehydrogenase (G6PD) deficiency, an enzyme used in the host erythrocytes that undergoes similar reactions as the glutamate dehydrogenase (GDH), had a potent antimalarial effect (Werner. C, et al 2005). It has been observed that several haemoglobinopathies such as thalassemia, sickle cell disease, glucose-6-phosphate dehydrogenase (G6PD) deficiency and other red cell defects provide protection against malaria (Katja. B, et al 2003). Sickle cell disease is the haemoglobinopathy that is currently known to offer the best protection against malaria (Katja. B, et al 2003). Interestingly, these haemoglobinopathies are most prevalent among people inhabiting malaria-infested regions; Africa, South Asia and the Middle East, possibly indicating an evolutionary response to malarial stress. Understanding how these conditions provide protection against malaria will help us better understand how the parasite can be eliminated during the intra-erythrocytic stage of the plasmodium life cycle by disruption of the parasite's redox balance. In these conditions, the erythrocytes membrane fluidity is altered due to changes in the erythrocyte's membrane lipid composition and protein cross-linking. These changes to the erythrocyte result in enhanced oxidative stress in the erythrocytes and therefore making the erythrocytes defective. Existing theories suggest that the underlying mechanisms of these disorders are as a result of the enhanced oxidative stress which the defective erythrocytes are under (Shavlev, et al 1995). It is believed that the oxidative environments in the defective erythrocyte impair the growth rate and multiplication of the parasite. Another theory suggests that the defective erythrocytes are recognised by the host's immune system early due to the early occurrence of band 3 auto-antibodies and are phagocytized much more efficiently (Muller. S, et al 2004). This is especially effective as it means that the parasite is removed from the body at an early stage of

the infection before it has the opportunity to cause parasitaemia and the symptomatic phase of the infection can take hold.

The importance of these enzymes, glutathione disulfide reductase and GDH were noted in research which showed that the concentration of the antimalarial drugs chloroquine and amodiaquine needed to kill the parasites was inversely proportional to the glutathione levels in the cells (*Ginsburg. H, et al (1998), Becker. K, et al (2004)*). This correlation was confirmed by a research finding, which showed the correlation between the levels of Glutathione in the cells and the degree of chloroquine resistance which was exhibited by different *P. falciparum* strains (*Meierjohann. S, et al (2002); Muller et al (2002); Biot. C, et al (2004)*). This research pointed to the importance of glutathione in the development of chloroquine resistance. The current protocols for control of malaria involves preventive measures such as the use of insecticides to eliminate the mosquito vectors, and the use of long lasting insecticidal nets, early diagnosis, followed by the prompt and effective pharmacological intervention (*WHO report 2010*). The use of a combination of antimalarial drugs, particularly the use of artemisinin-based combination therapy is the most important pharmacological tool in use today in the fight against malaria (*WHO report 2008*). However, the emergence of *P. falciparum* strains that are resistant to the pharmacological interventions that are in use today, the lack of a vaccine and the threat of malaria spreading to new areas as a result of failure of vector elimination and control programs, global warming and human travel patterns has led to the urgent need for new antimalarial drugs (*Biot. C, et al (2004); WHO report 2010*).

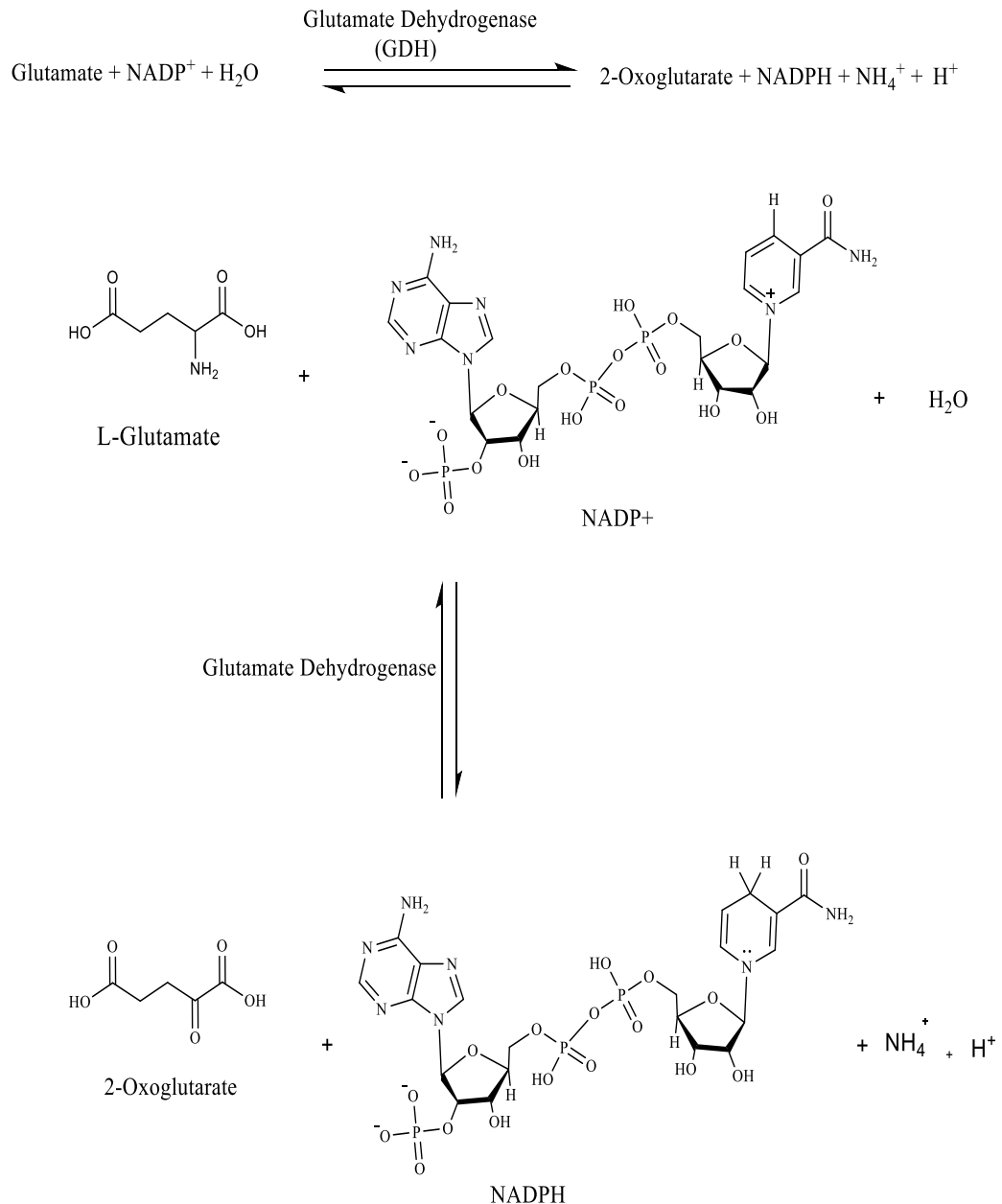


Figure 1.3.1: The NADP⁺- dependant GDHs catalyses the reversible interconversion of L-glutamate to 2-oxoglutarate

1.4 Sequences and 3D structures of *H. sapiens* and *P. falciparum*

GDH's compared

There are two different types of GDH, the NADP⁺- dependant GDHs which are concerned with ammonium fixation, and the NAD⁺- dependant GDHs associated with glutamate catabolism. Higher eukaryotes have a dual- coenzyme specificity GDH which suggests that it may be involved in both metabolic pathways, catabolism and anabolism, whereas bacterial and fungal GDH is just NADP⁺ dependant (*Wagner. J. T, et al 1998*). When NADP-dependant

GDH was extracted from a *P. falciparum* infected erythrocyte, the protein represented a marker for the parasite as the enzyme is absent in the host erythrocytes. When the protein was cloned it was determined that the gene for NADP - dependant GDH encodes for a protein that has 470 residues which was a 50% match for GDHs from lower eukaryotes and eubacteria but, was significantly different from mammalian GDH, with a sequence identity of about 23%, indicating a long evolutionary distance between the two (Werner. C, et al 2005), (Wagner. J. T, et al 1998). The parasite GDH is inhibited by D-glutamate and glutarate but it is not inhibited by chloroquine. Unlike mammalian GDH, the parasite GDH is not affected by either GTP or ADP. The parasite GDH is a homohexamer with a subunit Mr of about 49,500 Dalton which is similar to the GDH of other NADP dependant bacteria and invertebrates, the subunits are linked together by salt bridges whilst in the human GDH, the subunits are linked together by hydrophobic interactions (Werner. C, et al 2005). The GDH of *P. falciparum* has a unique N-terminal extension that is about 20 residues long and is not observed in any other GDHs that have been characterised to-date from other protozoa or bacteria (Werner. C, et al 2005).

1.5 *P. falciparum* GDH active site

The active site of the parasite GDH is similar to that of *Clostridium symbiosum*. The part of the active site that is in contact with the substrate is perfectly conserved and the amino acid residues occupy the exact same spots. There is an assumption that there are residues within the active site that bind to both the α - and γ -carboxylates of the glutamate substrate. Thus, amino acid residues Lys112 and Ser401 are believed to bind to the γ -carboxylate of the substrate while Gln133 and Lys136 similarly bind to the α -carboxylate. Just two of these active-site residues are different in the human GDH: Gln133 is replaced by Met115, and the amino group ligand Gly187 is substituted by Pro171. In addition to the differences in the primary structure of the amino acids, there may be further differences in the way the substrate binds to the active site. Human GDH and liver bovine GDH share a 96% sequence identity but bovine GDH has a different binding mode to *Clostridium symbiosum* GDH (Peterson P. E, et al 1999). This close relationship between human and bovine GDH makes bovine GDH a good

analogue for human GDH in biological studies. The coenzyme binding site of the *P. falciparum* GDH is similar to that of dual-specific mammalian GDH in that they are both NADP dependant. This is different from the coenzyme binding site of the *Clostridium symbiosum* GDH which is NAD dependant and therefore has different amino acid residues. The amino acids that are present in the coenzyme binding site of the *Clostridium symbiosum* GDH are Arg285, Asn133 and Pro262, these amino acid residues restrict the access to the coenzyme binding site of the *Clostridium symbiosum* GDH resulting in a theoretically, less positively charged coenzyme binding site compared to that of *P. falciparum* GDH (Werner. C, et al 2005). The NADP-specific GDH coenzyme binding site of the *plasmodial* GDH and mammalian GDH have the amino acid residues Ser284, Lys156 and Lys306. These residues allow for charge compensation of the 2'-phosphate group of the ribose moiety (Werner. C, et al 2005).

<i>P. falciparum</i>	MSALKDKTGRFVVLKDNASNYESLVDQEMNNVYERVMKLDPNQVDFLQAFHEILYSLKPL	60
<i>C. symbiosum</i>	-----SKYVDRVIAAEVEKKYA-----DEPEFVQTVEEVLSLGLPV	35
<i>H. sapiens</i>	-----SEAVADRIEDDPNFFKMVEGPFDRGASIVEDKLVEDLRTRE	40
<i>P. falciparum</i>	FMEEPKY--LPIIETLSEPERAIQFRVCWLDINGVQRKNRCFRVQYNSALGPPYKGLLPH	118
<i>C. symbiosum</i>	VDAHPEYEEVALLERMVIPERVIEFRVWEDDNGKVVHNTGYRVQFNGAIGPYKGLLFA	95
<i>H. sapiens</i>	SEEQKRNRVRGILRIIKPCNHVLSLSFPIRRDDSSWEVIEGYEAGHSQHRTECKGGIRYS	100
<i>P. falciparum</i>	PSVNLSTIVFIFGFRIFKNSLTGLSMGGGHSDFDPIGKSDNEILKFCOAFVNLVYRH-	177
<i>C. symbiosum</i>	PSVNLSTIVFIFGFRIFKNSLTGLSMGGGHSDFDPIGKSDNEILKFCOAFVNLVYRH-	154
<i>H. sapiens</i>	TDVSVDEVKALASLWTKCAVVDVPPGJAJAIVKINPKNYTNELEKITRRTTMLAKKG	160
<i>P. falciparum</i>	-IGPCTDVPAGGIGVGGREIGYLYGQKKIIVN---SFNGTLTGHNVKWGGSNLVEATG	232
<i>C. symbiosum</i>	-IGPDIIDVPAGGLGVGAREIGYMYGQRRKIIVGG---FYNGVLTGHRARSPGSLVRPEATG	210
<i>H. sapiens</i>	FIPGGIDVPAQPMSTGEREMSWIADTIASTIGHYDINAHACVTGPIISQGGIHRISATG	220
<i>P. falciparum</i>	YGLVYFVLEVLKSLNIP-----VEKQTAVVSGSENVALYCVQKILHLNVKVLTLSDS	284
<i>C. symbiosum</i>	YGSVYYVEAVMKHENDT-----LVGKIVALAGFENVAVGAAKLAELGAKAVTLSPG	262
<i>H. sapiens</i>	RGVFHGIENFINEASYMSILGMTPGFGDKLFFVQSPFENVGLHSMRYLHRFPAKCIAVGES	280
<i>P. falciparum</i>	NGYVYENGFTHEN-LEFLIDLKEEKGRIKEYLNHSSTAKYFENEKPPWG-----VPCTL	338
<i>C. symbiosum</i>	DGYIYDDEGLITTEEKINYMLEMASGRNKVQDYADKFG-VQFFPGEKPPWG-----QKVDI	316
<i>H. sapiens</i>	DGSIWNDDIDPKE---LEDPLQHGSIILG-----FKKAKPYEGSILREACDI	325
<i>P. falciparum</i>	AFFCATQNEINLEDAKLLQKNGCILVGGANMESTVDNIN-LFKSNIIYCSKAANAGG	397
<i>C. symbiosum</i>	IMPCATQNDVDLEQAKKIVANNVKKYIEVANMETNEALRFLMQQPNMVAASKAVNAGG	376
<i>H. sapiens</i>	LIEAASEKQLTKSNAPRVKAK---IIARGANGETTPEADKIFLER-NIMVIEDLYLNAGG	381
<i>P. falciparum</i>	VAISGLEMSQNFQFSHWI-----	415
<i>C. symbiosum</i>	VLVSGFEMSCNSERLSWT-----	394
<i>H. sapiens</i>	MTVSYPFWLKNLNHVSYGRLTFKYERDSNYHLLMSVQESLERKFGKHGGTIPIVPTASFO	441
<i>P. falciparum</i>	-----RETVDEKIKKEMRNIPIACSENLKTKNKYDIQAGANIAGFLKVAESYIEQ	467
<i>C. symbiosum</i>	-----REEVDSKLIHQVMTDIHDGSAAAAERYGLG-YNEVAGANIYVGFQKIDAMMAQ	445
<i>H. sapiens</i>	DRISGASEKDIYHSGLAYTMEARSARQIMRTAMKYNLG-LDERTAAVYVNAIEKVFVKVYNEA	500
<i>P. falciparum</i>	CF--	470
<i>C. symbiosum</i>	IAW-	449
<i>H. sapiens</i>	VTFT	505

Figure 1.5.1: The CLUSTALW sequence of *H. sapiens*, *C. symbiosum* and *P. falciparum* GDH. The nucleotide-binding fold is indicated in red, the *N*-terminal domain in blue. The residues highlighted in pink reveal those that bind NADP, while those in yellow bind the substrate L-glutamate. The unique *N*-terminal extension of *P. falciparum* GDH is shown in violet (Werner, C, et al (2005)).

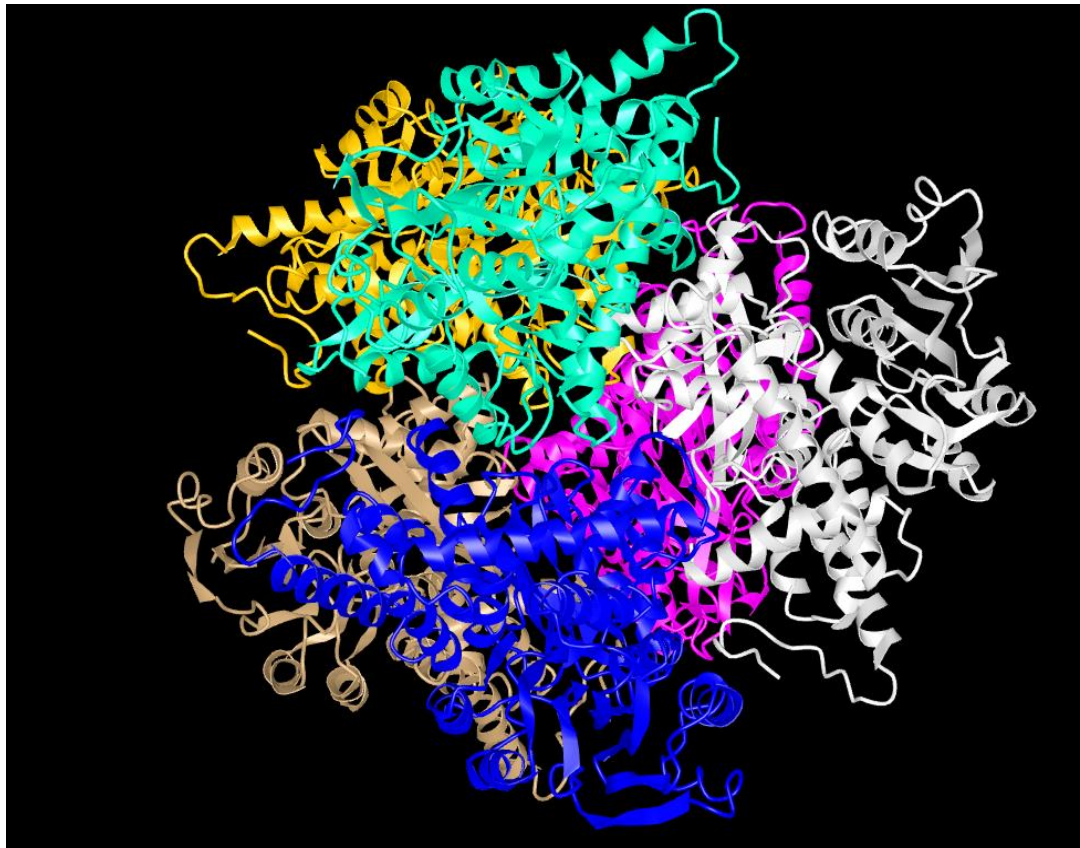


Figure 1.5.2: The 3D crystal structure of *P. falciparum* GDH

The main difference between the human and *P. falciparum* GDH subunit contacts is structurally significant enough for the difference to be exploited in drug development. In the *P. falciparum* GDH, the Arg10 which adjoins the C-terminal part of the helix 447-465 is hydrogen bonded to the Gln94 of the neighbouring subunit, this arrangement causes spatial arrest due to the multiple interactions contributing to the overall packing of the terminal domain. The N-terminal peptide approaches the C-terminal helix shielding it from solvent. The inter-subunit contact formed by the Arg10 and the Gln94 could contribute to the hexameric structure of the *P. falciparum* GDH. Peptides and peptidomimetics have been shown to be able to disrupt the different protein sub-units' interfaces and can be potentially developed as drug candidates. Peptidomimetics with negative charges could interact specifically with positively charged Arginine residues in the *P. falciparum* GDH subunit interfaces. This could be significant because parasitized red blood cells are known to exhibit permeability to negatively charged compounds (Werner. C, et al 2005).

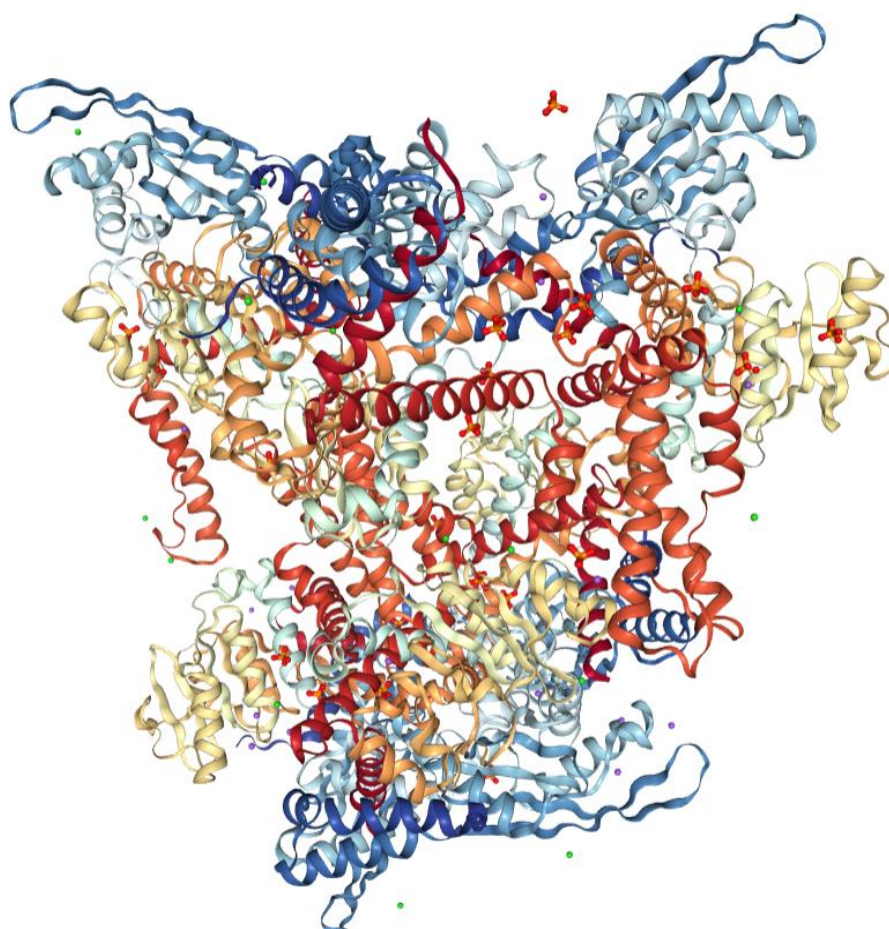


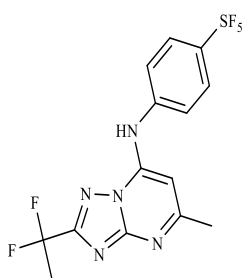
Figure 1.5.3: The 3D crystal structure of *Human* GDH

1.6 Current malaria chemotherapies, strategies and modern developments

The *P. falciparum* is incapable of salvaging pyrimidines, which is the conversion of pyrimidine bases into nucleotides, unlike its human host and is therefore dependent on the de novo biosynthesis pathways to recoup these pyrimidines. This biosynthetic pathway utilises the enzyme dihydroorotate dehydrogenase (DHODH). The project that attempted to synthesise (*pf*DHODH) inhibitors was named project of the year (2010) by the Medicines for Malaria Venture (MMV) and was carried out in conjunction with GlaxoSmithKline, the University of Texas Southwestern, the University of Washington and the University of Monash (*Biamonte. M. A, et al (2013)*). A search for a selective inhibitor for the enzyme dihydroorotate dehydrogenase (DHODH) has led to the clinical candidate DSM265, which represents the first attempt to clinically validate a genetically identified target. DSM265 was very selective for

PfDHODH with an IC_{50} of 33 nM for *PfDHODH* and an IC_{50} of 2500 nM for human *DHODH* (Diagana. T. T, 2015). This compound is 57%-68% orally bioavailable in rats and has a $t_{1/2}$ of 12-28 hours. DSM265 was entered into phase 1 trials in 2013; an initial two-part phase 1 trial was run, with part one being run between 12/04/2013 and 14/07/2015 involving 73 participants (DSM265, n=55; placebo, n=18). Part two of the phase 1 trial was run between 30/09/2013 and 25/11/2013 involving 9 participants (150 mg DSM265, n=7; 10 mg/kg mefloquine, n=2), with the results from the trials being reported in 2017. The first test of the trial reported 117 adverse effects events, no drug-related serious or severe events were reported. The main drug related event that was reported for these trials were headaches. The two phase 1 trials concluded that DSM265 had a good safety profile, long elimination half-life and an antimalarial effect that supported its further development as a partner drug in a single-dose antimalarial combination treatment (McCarthy. J. S, et al 2017).

A similar *pfDHODH* inhibitor which was obtained by the Medicines for Malaria Venture (MMV) 2010 project is the triazolopyrimidine derivative DSM190, was observed to be less potent in vitro with an IC_{50} of 190 nM and an EC_{50} of 1.1 μ M in mouse but is 100% bioavailable in rats. IC_{50} being a measure of the in vitro potency of a compound and EC_{50} being a measure of the concentration of a compound that gives a quantal dose response curve for a given ligand or receptor – (Gleeson. M. P, et al 2011). Genzyme Biotechnology company is investigating some benzimidazole derivatives which could potentially be *pfDHODH* inhibitors, the properties of such compounds are being further explored as these benzimidazole derivatives have also been observed to inhibit parasite growth. The best candidate benzimidazole derivative has been shown to inhibit *pfDHODH* (IC_{50} = 40 nM) and it inhibits parasite growth (EC_{50} = 7-10 nM), and has a 49% bioavailability in rats and a 19% bioavailability in dogs. It is eliminated with a $t_{1/2}$ of 0.85 hours in rats and 0.52 hours in dogs. Genzyme is also investigating the compound Genz-668764 a single enantiomer whose configuration has not been published. This compound is believed to inhibit *P. falciparum* in vitro EC_{50} of 28 nM (3D7) and 65 nM (Dd2) (Biamonte. M. A, et al (2013).



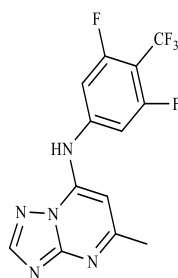
DSM265

IC₅₀= 33 nM

EC₅₀= 43 nM (3D7 strain)

ED₅₀=2.8 mg/kg/day

Preclinical and Phase 1 trials

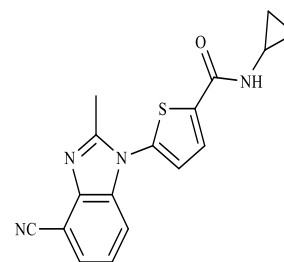


DSM190-TRIAZOLOPYRIMIDINE-DERIVATIVE

IC₅₀= 190 nM (3D7 strain)

EC₅₀= 1100 nM (3D7 strain)

ED₅₀=10 mg/kg/day

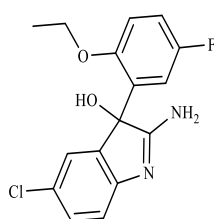


BENZIMIDAZOLE-DERIVATIVE

IC₅₀=40 nM (3D7 strain)

EC₅₀=7-10 nM (3D7 strain)

ED₅₀=13 mg/kg/day



GENZ-668764

EC₅₀= 28 nM (3D7 strain)

EC₅₀=65 nM (Dd2 strain)

ED₉₉=approx.100 mg/kg/day

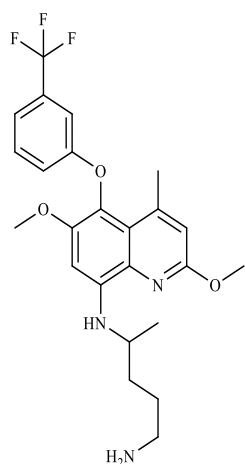
Figure 1.6.1: Examples of Dihydroorotate dehydrogenase (DHODH) inhibitors that have shown antimalarial activity, some of them in phase 1 and 2 clinical trials

P. vivax hypnozoites can remain dormant in the liver of the host for a number of years which may result in relapses of the infection later on. This makes the liver residency a very crucial stage of the parasite lifecycle. The potential hypnozoiticidal compound tafenoquine (WR-238905) has successfully completed phase 3 clinical trials and was approved for use in July 2018. (*Diagana. T. T, 2015, MMV, 2020*). Tafenoquine is a novel 8-aminoquinoline which is an analogue of primaquine and pamaquine. Primaquine is one of the few compounds that target the liver stages of the parasite's lifecycle but has the disadvantage of being slow acting and is therefore administered in combination with other drugs, most commonly chloroquine. Primaquine causes haemolytic anaemia in people with glucose-6-dehydrogenase (G6PD) deficiencies. Glucose-6-dehydrogenase (G6PD) deficiencies occur in 10% of the population in malaria prevalent populations. Another disadvantage of primaquine is that studies have shown that compliance with the 14-day regimen is not followed as rigorously as it should be; tafenoquine has the same glucose-6-dehydrogenase (G6PD) deficiency liabilities that

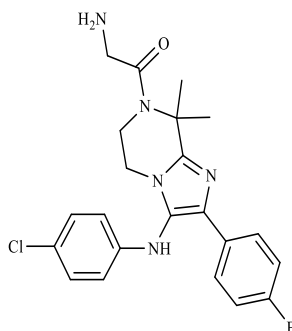
primaquine has, but it is a single dose treatment which makes compliance easier. Due to tafenoquine's long elimination half-life, it has the potential to kill all forms of the parasite and be utilised as malaria chemoprophylaxis in geographic areas that chloroquine resistant strains of the *P. falciparum* parasite have been identified (Dhanawat. M, et al 2009). Between September 19, 2011, and March 25, 2013, 329 patients were randomly assigned to a treatment group (chloroquine plus tafenoquine) in phase 2a and 2b clinical trial. The study concluded that a single-dose tafenoquine 300 mg co-administered with chloroquine for *P vivax* malaria relapse prevention was more efficacious than chloroquine alone, with a similar safety profile as chloroquine. As a result, (chloroquine plus tafenoquine) combination therapy was selected for further clinical assessment in phase 3 trials and approved for use in July 2018 (Llanos-Cuentas. A, et al 2013; MMV, 2020).

The Scripps Research Institute and Novartis led a drug discovery programme in 2009 that intended to identify non-8-aminoquinoline compounds that were effective against the asymptomatic stages of the parasite's lifecycle and will eliminate the sporozoites and/or the hypnozoites in the liver stages without any glucose-6-dehydrogenase (G6PD) liabilities. These two establishments managed to develop a new high-throughput screening imaging assay technique for the determination of live cell parasite (*Plasmodium* sporozoites) traversal into the liver cells. The assay measures fluorescence that occurs, when the hepatocyte plasma membrane is disrupted by the traversing dye-labelled sporozoites. The assay was then used to screen 4000 compounds that were known to have blood stage activity with the hope of obtaining liver stage inhibitors that could prevent sporozoite migration through cells, therefore, preventing the invasion of hepatocytes, and inhibiting the development of sporozoites in the liver cells (Derbyshire. E. R, et al 2011); (Biamonte. M. A, et al 2013). This technique identified a class of compounds called imidazolopiperazines, whose mode of action is currently unknown, which had GNF-pf-5069 as the lead compound. This compound was optimised to give compounds GNF179 and GNF156. GNF156 also known as KAF156 has completed phase 2 clinical trials, GNF156/KAF156 has an EC₅₀ of 6 nM against *P. falciparum*.

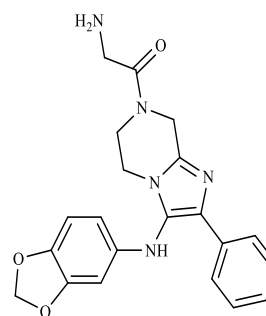
GNF156/KAF156 is orally bioavailable in mouse 72%, $t_{1/2}$ =2.2 hours and has a bioavailability of 20-57%, $t_{1/2}$ =4.7-8.4 hours in rats. GNF156 inhibits the liver stages of the parasite and also prevents transmission of the parasite. The potency figures of GNF156/ KAF156 in *plasmodium yoelli* have not been disclosed. From March to August 2013, a phase 2, KAF156/GNF156/lumefantrine open-label two-part study was done to evaluate the efficacy and safety of the compound. A total of 21 adults with acute uncomplicated malaria (11 with *P. vivax* malaria (cohort 1) and 10 with *P. falciparum* malaria (cohort 2) were enrolled in the multiple-dose study, and 22 patients with uncomplicated *P. falciparum* malaria were enrolled in the single-dose study (cohort 3). 400 mg of KAF156 was given once daily for 3 days to patients with uncomplicated *P. vivax* malaria (cohort 1) or *P. falciparum* malaria (cohort 2). Patients in cohort 3, which was a separate group of patients with *P. falciparum* malaria, were treated with a single 800-mg dose of KAF156 in order to assess the cure rate at 28 days and the potential for a single-dose cure. 1 patient in cohort 1 and another in cohort 2 experienced nausea and vomiting. 4 patients in cohort 3 experienced nausea and 6 patients in cohort 3 experienced vomiting (Nicholas. W. J, 2016). GNF179 is reported to have similar EC₅₀ figures as GNF156, it is not known if these compounds are active against the *P. vivax* and *P. ovale* hypnozoites (Diagana. T. T, 2015).



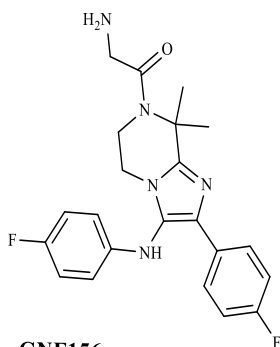
**TAFENOQUINE/
WR-238605**
Now in use



GNF179
EC₅₀= 6 nM (3D7)
EC₅₀=6 nM (*p. yoelli* liver stages)
ED₉₉=2.2 mg/kg/day



GNF-pf-5069
EC₅₀= 462 nM (3D7)
EC₅₀=221 nM (*p. yoelli* liver stages)
Poor exposure in animal models



GNF156
EC₅₀= 6 nM (3D7)
EC₅₀=N/A (*p. yoelli* liver stages)
ED₉₉=2.2 mg/kg/day
Phase 1 and 2 trials

Figure 1.6.2: Examples of imidazolo[1,2-a]piperazines and Tafenoquine that have shown antimalarial activity.

The malaria parasite is rich in haem-iron that is derived from the proteolysis of the host cell haemoglobin which possibly accounts for artemisinin's selective toxicity to the parasite. Haemoglobin is digested within a specialised, acidic, lysosome-like compartment of the parasite also known as a food vacuole, resulting in the formation of free haem. As free haem is toxic to the parasite, it is rendered inert as it is produced, by combining one of the peripheral carboxyl groups with the Fe(III) iron of an adjacent haem to form the insoluble bio-mineral haemozoin (*Krishna. S, et al 2008*). Haemozoin is a parasite specific pigment also known as the 'malaria-pigment' that is deposited within the food vacuole after digestion of haemoglobin, it has long been proposed as a target of artemisinin and artemisinin like compounds (*Fong. K.*

Y, et al 2013). The antimalarial mode of action of artemisinin is believed to involve the cleavage of the endoperoxide bridge in the parasite vacuole. The cleavage of the endoperoxide bridge of artemisinin is activated by ferrous Fe(II) iron in the haemozoin generating oxygen free radicals which are rearranged to produce more stable carbon-centred free radicals. This is then followed by the alkylation of certain malaria proteins and lipid peroxidation by the carbon free radicals thereby resulting in lethal damage to the malaria parasite (Egan. T. J, et al (2003); Dhanawat, M et al 2009). This has led to the idea that there could be alternative synthetic peroxides that could be effective with a similar mode of action as artemisinin; these compounds are called 1,2,4-trioxolanes or secondary ozonides.

The first compound of this first-generation of ozonide peroxides is OZ277 arterolane which has proven to be effective against chloroquine-resistant and chloroquine-sensitive parasite strains (K1) with an IC₅₀ of 1.6-1.8 nM. This compound has been launched by Ranbaxy as a 3-day combination therapy of arterolane maleate and piperaquine in India 2012. A second generation ozonide peroxide OZ439 which has EC₅₀ of 3.4-4.0 nM is now in phase 2a clinical trials. The arrangement of the O-O bond in this ozonide makes the compound 50 fold more stable towards Fe(II), presumably because of steric reasons, which translates to a longer half-life and make it possible for the treatment with this compound to have a shorter dosage regimen (Biamonte. M. A, et al 2013). OZ439 has also shown to have a prophylactic effect when administered in rats 48 hrs before parasite inoculation. From October 2010 to May 2012, a phase 2a, OZ439/Artefenomel open-label exploratory study was done to evaluate the efficacy and safety of the compound. This study involved a total of 82 adults with acute uncomplicated *P. falciparum* or *P. vivax* malaria (20 in each of the 200 mg, 400 mg, and 800 mg cohorts, and 21 in the 1200 mg cohort). One patient withdrew consent before administration of artefenomel. All doses were equally effective in both *P. falciparum* and *P. vivax* malaria, with median parasite clearance half-lives of 4.1 hours to 5.6 hours for *P. falciparum* and 2.3 hours to 3.2 hours for *P. vivax*. Maximum plasma concentrations for doses proportional to 800 mg, occurred at 4 hours (median). The estimated elimination half-life was

46–62 hours. No serious drug-related adverse effects were reported; other adverse effects were generally mild and reversible, with the highest number in the 1200 mg cohort (17) patients with at least one adverse event. The most frequently reported adverse effect was an asymptomatic increase in plasma creatine phosphokinase concentration. Artefenomel has been generally well tolerated in volunteers at doses up to 1600 mg and is being developed as a partner drug in an antimalarial combination treatment. (*Phyo. A. P, et al (2016)*).

Further exploration of the idea of stabilizing the O-O bond has led to a new class of compounds called tetraoxanes for which one of the leading candidate is RKA182 which has displayed an IC₅₀ of 4.9 nM against the chloroquine-resistant *P. falciparum* K1 strain and an IC₅₀ of 1.9 nM for the chloroquine-sensitive parasite strain 3D7. This compound inhibits parasite growth with an ED₅₀ of 1.8mg/kg/day and the tosylate salt of this compound has a bioavailability of 42% in mouse and 38% in rats. However, RKA182 has been reported thus far to not be curative in a single dose. The central Drug Institute, Lukow, India is investigating the trioxane CDRI-97/98 which has concluded phase 1 studies, furthermore, the trials that have been conducted on other artemisinin derivatives, ozonides and 1,2,4-trioxanes have been reported to have similar potencies as the artemisinin derivative artemether but were not shown to possess any additional obvious advantage (*Biamonte. M. A, et al (2013)*). CDRI 97/78 has shown efficacy in animal models with *falciparum* malaria. The first in-human phase I trial in healthy volunteers were carried out in July 2012. The study was conducted in 50 healthy volunteers in a single, ascending dose, randomized, placebo-controlled, double-blind design. The dose ranges evaluated were from 80 mg to 700 mg. After evaluation of safety study results, another cohort of 16 participants were administered as a single oral dose of 200 mg of the drug and a detailed pharmacokinetic analysis was undertaken. The compound was found to be well tolerated. The few adverse events noted were of grade 2 severity (Moderate; minimal intervention indicated; some limitation of activities), not requiring intervention and not showing any dose response relationship. The electrocardiographic parameters showed statistically significant differences, but all were within the predefined normal range. The novel

1,2,4 trioxane CDRI 97/78 is safe and will be an asset in malarial therapy if results are replicated in multiple dose studies and its benefit are shown in confirmatory trials.

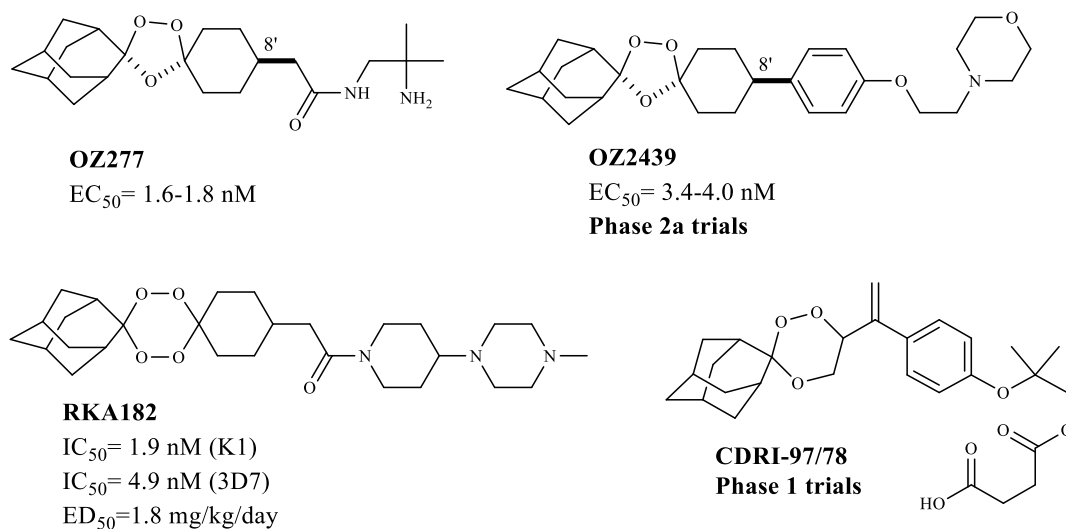


Figure 1.6.3: Examples of ozonides, tetraoxanes and trioxanes that have shown antimalarial activity, some of them now in Phase 1 and 2 clinical trials

Modifications are being made to existing antimalarials derived from 4-aminoquinolines with the hope that variations of these compounds could be effective against the chloroquine resistant malarial strains. Early candidates for such alternatives are Ferroquine which is in phase 2 clinical trials and other related compounds in which the ferrocene has been replaced by a benzene ring. Both compounds have shown to be effective against chloroquine-resistant and chloroquine-sensitive parasite strains (K1 and W2). *N-tert-Butyl* isoquine (GSK369796) is in phase 1 clinical trials, has been shown to be effective against the chloroquine-resistant (K1) with an EC₅₀ of 13 nM both in vivo and in vitro, had a similar mode of action to amodiaquine but proved to be no safer than chloroquine, and was therefore discontinued. Mefloquine is composed of four isomers, which are divided into two groups (diastereomers) each consisting of two enantiomers (namely a [+] -enantiomer and a [-] -enantiomer) within the groups but not across groups. The first group is called threo-mefloquine (WR177602) defined by the R, R and S, S configurations (known as group: R*, R*). The second group is called erythro-mefloquine (WR142490) defined by the R, S and S, R configurations (known as group: R*, S*) (Bermudez. L. E, et al (2014); Maaswinkel. H, et al (2015)). Erythro-mefloquine as a racemic mixture [(R, S) -(±)-α-2-piperidinyl-2, 8-bis(trifluoromethyl)-4-

quinolinemethanol hydrochloride] or [(±)-erythro-mefloquine] is the drug that has been clinically used as an effective antimalarial since 1985 (*Bermudez. L. E, et al (2012)*). It has now been found that the (+)-erythro-mefloquine, [11R, 2S)- (+)-α-2-piperidinyl-2, 8-bis(trifluoromethyl)-4-quinolinemethanol] enantiomer is effective as an antimalarial and has reduced side-effects compared to the racemic [(±)-erythro-mefloquine] (*Fletcher. A, et al (2003) US0066643971B1*). The (-)-enantiomer of erythro-mefloquine, [(-)-erythro-mefloquine], [(11S, 2R) (-)-α-2-piperidinyl-2, 8-bis(trifluoromethyl)-4-quinolinemethanol hydrochloride] has a half-life of 430 hours and is believed to cause side effects that include depression, psychosis and nightmares. (*Schlagenhauf. P, et al (1999)*; *Biamonte. M. A, et al (2013)*).

A series of second generation quinoline methanol derivatives that have similar potency as mefloquine but without the side effects are being investigated. The Walter Reed Army Institution has a lead compound in this class that has lower brain penetration, WR621308. Cycloguanil and pyrimethamine are Dihydrofolate reductase inhibitors (DHFR) which have developed widespread resistance. Structure based drug design has led to the development of WR99210 and P218, DHFR inhibitors which have flexibility within their structure's design that allow them to tolerate all existing clinically relevant DHFR mutations, resulting in these compounds being effective for longer. Sulfadoxine-pyrimethamine combinations have long been used as intermittent preventative treatment (IPT) for pregnant women, this treatment has become less effective in recent years owing to the parasite developing resistance to this drug combination. A combination of azithromycin-chloroquine has been used as a combination treatment against chloroquine-resistant *P. falciparum* in clinical trials. Azithromycin on its own is a slow acting antimalarial and finding azithromycin analogues that are fast acting and efficient has been challenging (*Biamonte. M. A, et al 2013*).

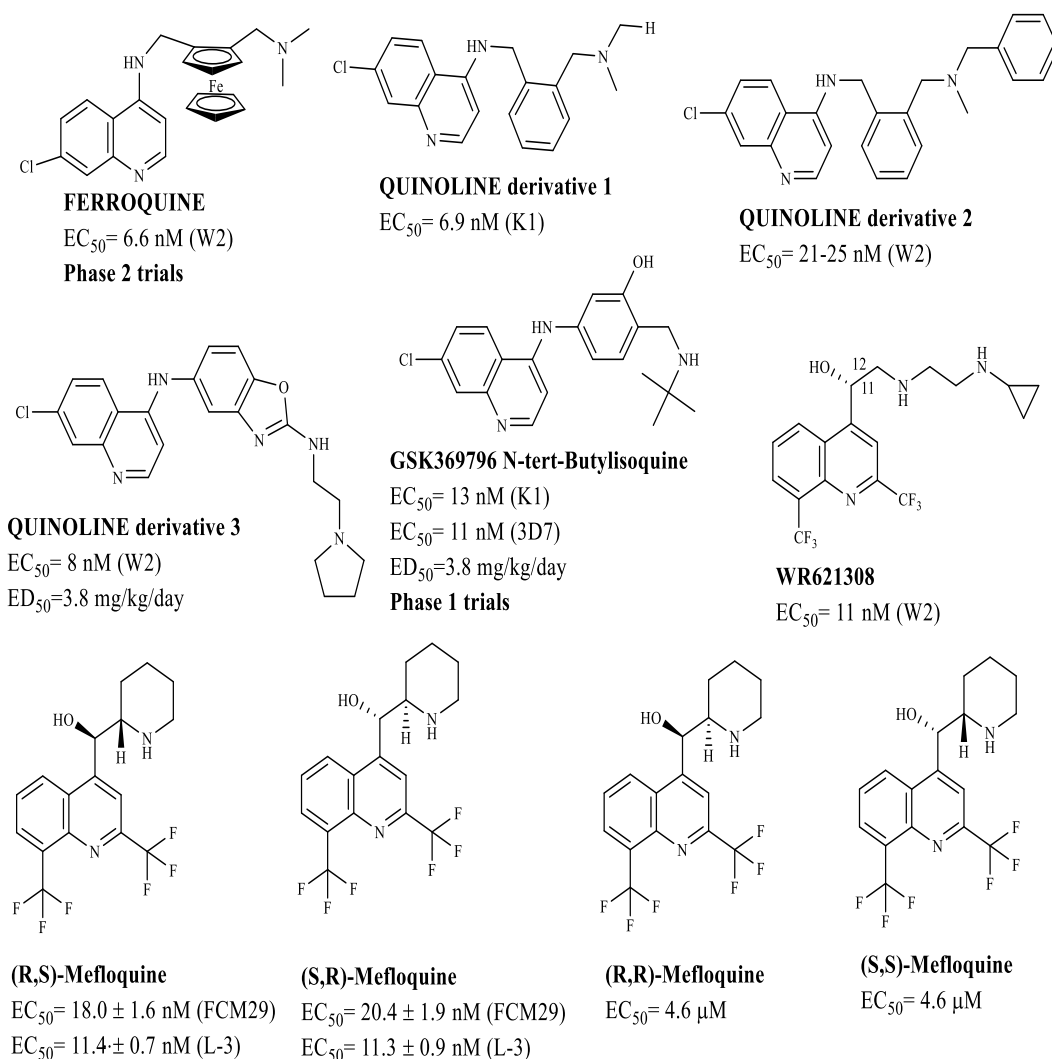


Figure 1.6.4: Examples of quinoline analogues that have shown antimalarial activity, some of them in Phase 1 and 2 clinical trials

Novartis has identified the compound NITD-609/KAE609, a spiroindolone, which has undergone phase 2 trials and is very potent with a reported EC_{50} of 0.7 nM; it has a bioavailability of 100% in mice and rats and has an oral $t_{1/2}$ of 10 hours in mice and 27 hours in rats. NITD-609/KAE609 has been shown to be a potent inhibitor of gametocytogenesis and blocks the transmission of the gametes to the parasite. The spiroindolones project was named project of the year (2009) by the Medicines for Malaria Venture (MMV). Novartis published the results of phase 2 clinical trials of the leading compound NITD-609/KAE609 in 2014 for this prospective novel antimalarial with a new mode of action and representing a new class of antimalarials (*Diagana. T. T, 2015*). As of February 2018 NITD-609/KAE609, also known as cipargamin, is in phase 2 in-patient studies and is also undergoing parenteral GLP safety

studies. Novartis is also in the process of developing compounds that are phosphatidylinositol-4-OH kinase inhibitors [PI(4)K] that are effective in all of the major lifecycle stages of the parasite in its host (*Biamonte. M. A et al (2013), Diagana. T. T, 2015*).

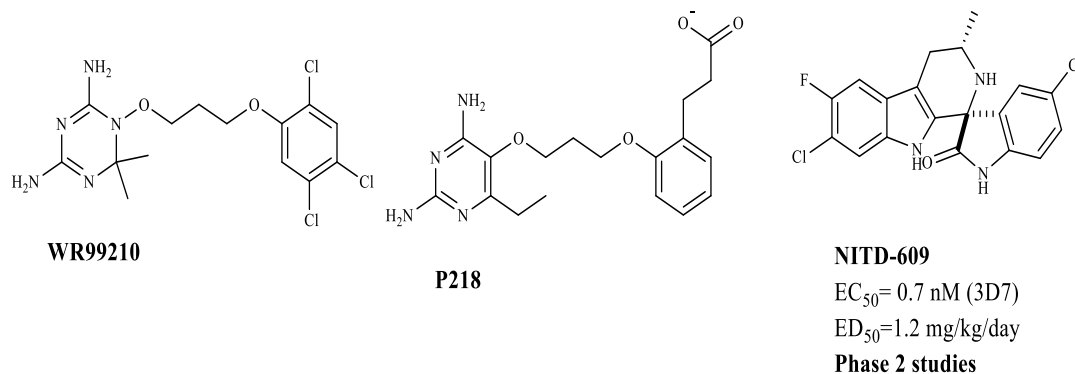


Figure 1.6.5: Examples of DHFR inhibitors and Spiroindolones that have shown antimalarial activity, some of them in Phase 1 and 2 clinical trials.

Albitiazolium also known as T3 or SAR97276(A) is being researched by the University of Montpellier/Sanofi and CNRS is in phase 2 clinical trials. Albitiazolium inhibits the transport of choline in the parasite which disrupts the synthesis of phosphatidylcholine, the main lipid in the cell membranes when it replicates to form new membranes. This compound is very potent and has an EC₅₀ of 2 nM. It is efficacious when administered as an oral dose which would be preferable as well, but has a very low oral bioavailability. The clinical trials conducted in two separate studies between August 2008 and July 2009 and another in October 2011 and January 2012 have so far been carried out with intravenous and intramuscular injections. These studies showed that monotherapy with SAR97276A up to twice daily for 3 days is not an efficacious treatment for *P. falciparum* malaria. SAR97276A will not be further developed for the treatment of malaria (*Held. J, et al 2017*). The pro-drug of Albitiazolium, TE3 has an improved oral bioavailability of 15% in mice, reported in 2004-2005, any further attempt to improve the bioavailability of such bis-cations has not been successful. Actelion, ACT-213615 is fast-acting against all asexual erythrocytic stages of the infection. It is also 30 times more potent against *P. falciparum* than *P. berghei*. Against the *P. falciparum*, ACT-213615 has a potency comparable to chloroquine with no acute toxicity observed in mouse models. Anacor pharmaceuticals has identified benzoxaborole through structure activity

relationships (SAR) as a viable starting point for further optimisation (*Biamonte. M. A, et al 2013*). Investigating various configurations of these molecules indicated acidic side chains were favoured for high potency antimalarials. Several compounds with an $EC_{50} < 100$ nM have been identified for further screening and optimisation.

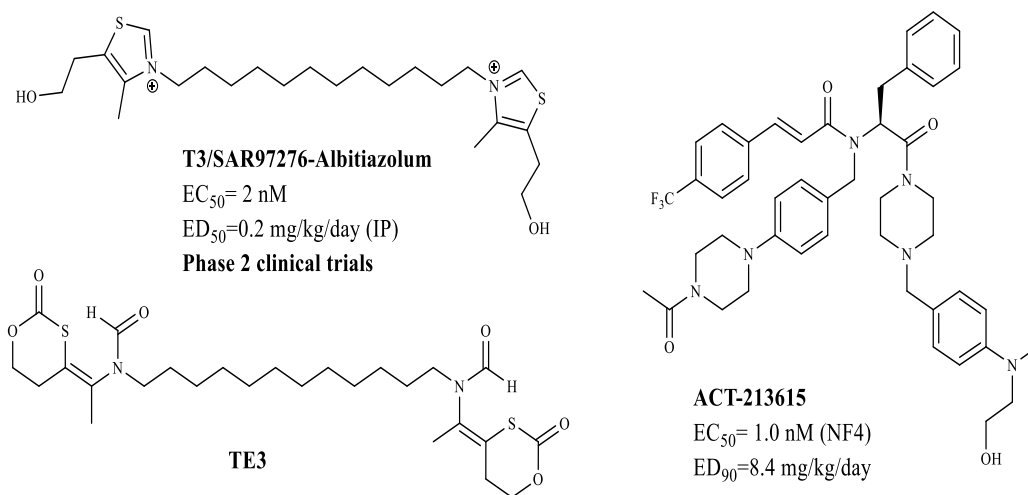
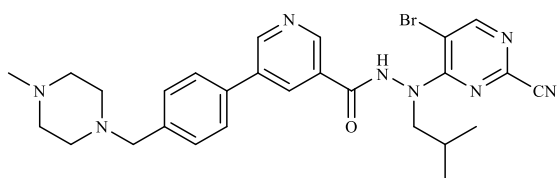


Figure 1.6.6: Examples of Phosphatidylcholine inhibitors that have shown antimalarial activity, some of them in Phase 1 and 2 clinical trials.

The screening network funded by the WHO Special Programme for Research and Training in Tropical Diseases (TDR) screened 10000 compounds against pathogenic organisms for tropical diseases including intraerythrocytic forms of *P. falciparum*. The most potent hit was TDR84420 with an EC_{50} of 326 nM against chloroquine-resistant (K1) strain. Several kinase inhibitors screened by GlaxoSmithKline (GSK) have been evaluated as weak inhibitors with an $EC_{50} > 100$ nM. Continued structure activity relationships (SAR) screening carried out by GlaxoSmithKline (GSK) identified 47 high quality screening hits for further investigation and modification. This SAR screening process has led to the compound TCMDC-134142. GlaxoSmithKline (GSK) is developing a potentially potent new class of compounds called 2-pyrimidinecarbonitriles that will act as inhibitors for the proteins falcipain-2 and falcipain-3. Falcipains are a group of cysteine proteases that hydrolyse the host's haemoglobin to provide amino acids for the parasite's protein synthesis. Heat shock protein 90 (hsp90) inhibitors have traditionally been pursued as anti-cancer drugs. Harmine is a beta-carboline alkaloid that has a variety of pharmacological properties such as anti-microbial, anti-fungal, anti-tumor, anti-

plasmodial, anti-oxidant, anti-mutagenic, anti-genotoxic and is also hallucinogenic. The alkaloid Harmine has been found to selectively inhibit *plasmodium* hsp90 with an $EC_{50} = 50$ nM. The Chinese plant Chang Shan (*Dichroa febrifuga*) has the active component febrifugine which is a potent antimalarial that has rapid effect and bioavailability. However, the compound was observed to be very hepatotoxic and that has precluded it from clinical use. Modifications to the febrifugine have led to the compound SSJ-183 which is as effective against malaria as artesunate and has a better hepatotoxicity profile. Several natural products are being investigated as some of these natural products have had some potent antimalarial activity. These include the natural marine product salinosporamide A, prodiginine, tsitsikammamine C, a berberine analogue, quindolone, propafenone, a sulfonamide analogue [Nitrophenyl-(4-(furanyl-thiocarboxy)-piperazyl-sulfonamide/NP(FTC)-PSA], a diamine 1,1'-[1,6-Hexanediylbis(imino-3,1-propanediyl)]bis((3-phenylurea) and an iridoid extract obtained from the African herb iThemba's. The O'Neill group at the University of Liverpool are looking at alternative antimalarials that target the electron transport chain of the *P. falciparum* as Atovaquone does. The enzyme NADH: ubiquinone reductase (*pf*NDH2) is believed to be involved in the *P. falciparum*'s electron transport chain. Investigations of (*pf*NDH2) inhibitors have led to the compound CK-2-25 which is specific for (*pf*NDH2) and has shown potent in vivo antimalarial activity in studies carried out in mice with an ED_{50} of 1.8mg/kg/day (Biamonte, M. A, et al 2013).



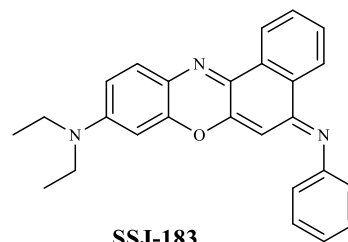
FALCIPAIN INHIBITOR

5-Bromo pyrimidine carbonitrile N-isobutyl-5,4,4-methyl-1-piperazynyl methyl phenyl nicotinohydrazide

IC₅₀= 0.5 nM

EC₅₀=1 nM (W2)

ED₉₉=2.2 mg/kg/day



SSJ-183

EC₅₀=7.6 nM (K1)

ED₅₀=20 mg/kg/day

Figure 1.6.7: Falcipain inhibitor and the marine natural product salinosporamide that have shown antimalarial activity

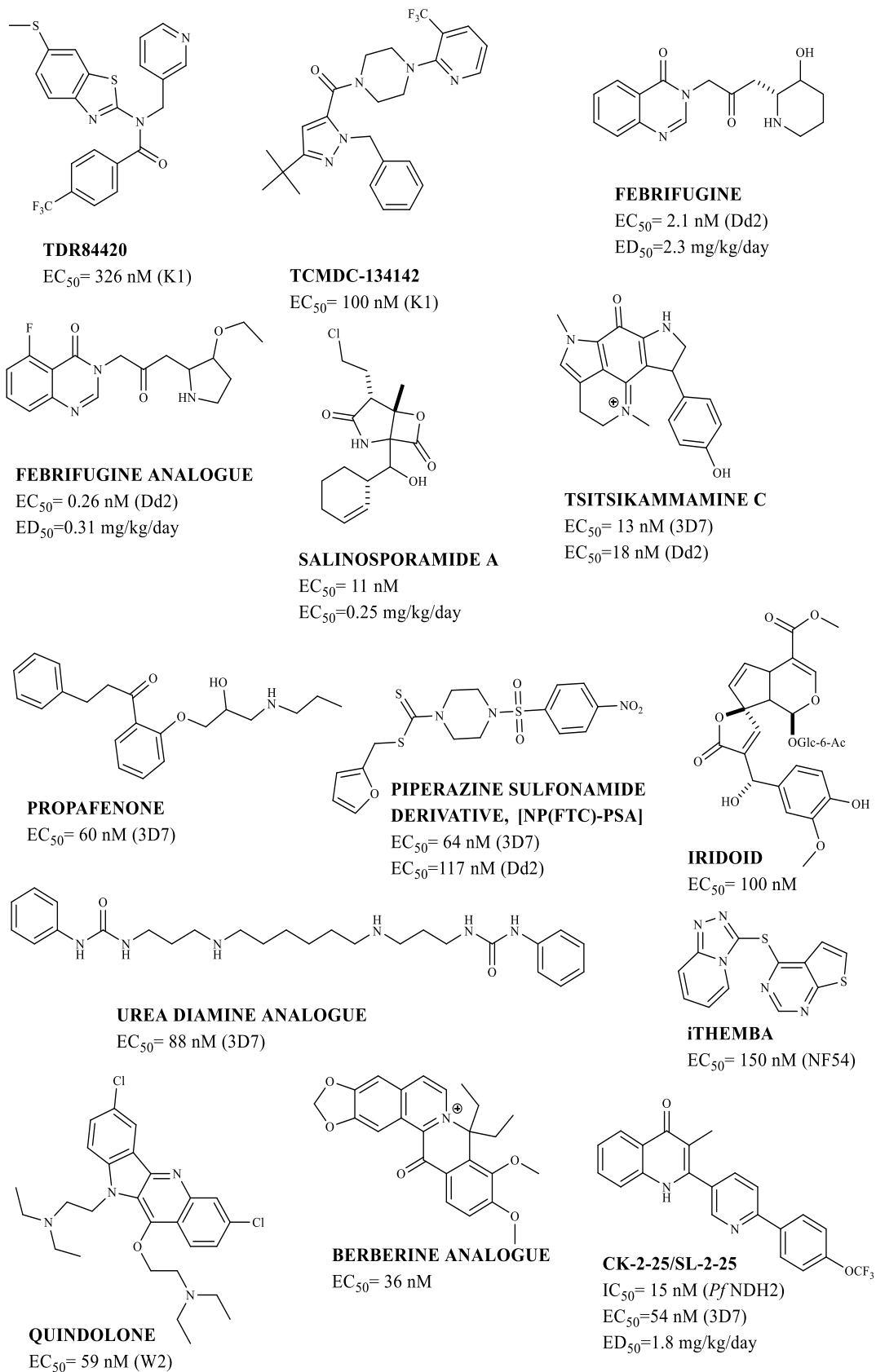


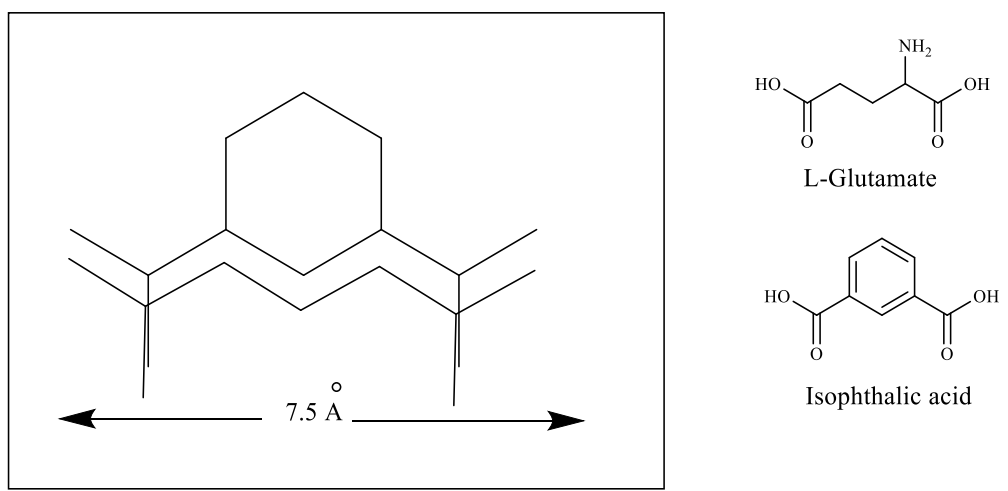
Figure 1.6.8: Active compounds derived from various approaches that have shown some antimalarial activity

1.7 GDH inhibitors

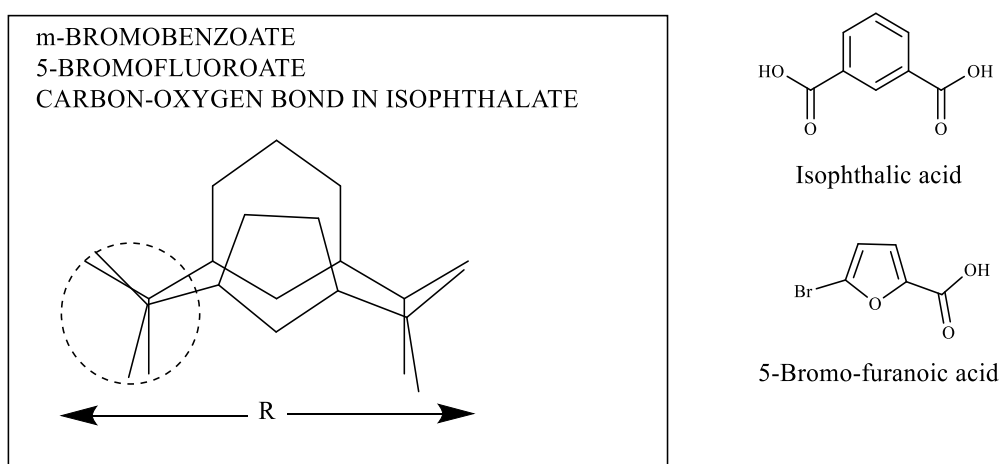
The research project aims to:

- 1) Design and synthesise novel and selective *P. falciparum* GDH inhibitors as potential antimalarial agents.
- 2) The GDH inhibitors will be based on molecules similar in structure and size to the substrate glutamate, hence, will compete for the active site on the GDH, thus minimising its activity.
- 3) Utilize simple inexpensive synthetic routes to obtain the intermediates and the final products.
- 4) Find out if any of the synthesised compounds had any activity against other parasitic agents.

Early research done with bovine GDH determined that the best inhibitors were compounds containing an analogous glutamate structure, like isophthalic acid, or electronically similar molecules, like 3-nitro and 3-halogeno-benzoates, and 5-bromofuroic acid. These compounds were selected based on stereochemical considerations such as similar intramolecular distances between the two carboxyl groups of the glutamate and its analogues (*Caughey. W, et al. 1957*).



A



B

Figure 1.7.1: A, The superimposed structures of isophthalate and glutarate. B, the superimposed structures of m-bromobenzoate, 5-bromofuroate and isophthalate (adopted from Caughey, W, et al 1957)

Studies on competitive inhibitors by the Engel group at University College Dublin (UCD), Ireland, showed remarkable differences in affinity constants (K_i) between *Clostridium symbiosum* GDH and bovine liver GDH, which were used as surrogates for *P. falciparum* and *human* GDHs respectively (Song Y, 2005). Isophthalic acid and 3-nitrobenzoic acid were shown to be 10 and 7 times, more selective, respectively, for *Clostridium symbiosum* GDH over bovine GDH.

The same group later carried out a comparison of the inhibitory effects of isophthalic acid and a series of related compounds (supplied by our group at London Metropolitan University:

Milek A and Ubosowu D 2008) on *P. falciparum* GDH and bovine GDH (Aparicio I. M, 2010). Isophthalic acid (IPA) was shown to be the most active compound tested, and was shown to be ~70 fold more active against the parasite GDH. The Engel group confirmed the effect of IPA and the related compounds on the native NADP (H)-dependent GDH activity of the parasite. Once again, IPA was shown to be the most efficacious, giving ~87% and ~98% inhibitions at 0.1 mM and 1.0 mM concentrations, respectively. Of all the other compounds tested, only 2, 6-pyridine dicarboxylic acid (a pyridine analogue of IPA), showed good activity, giving ~38% and 90% inhibitions at 0.1 mM and 1.0 mM respectively (Table 1 below).

Table 1: Percentage inhibition of *P. falciparum* GDH by a series of glutamate analogue prepared at London Metropolitan University. Key: IPA-isophthalic acid, IBA-3-iodobenzoic acid, (1)- 2,6-pyridine-dicarboxylic acid, (2)- 6-methyl pyridine-2-carboxylic acid, (3) -1,5-dimethylpyrrole-2-carboxylic acid, (4)- 1-methyl-2,5-pyrrole dicarboxylic acid, (5)- 5-methyl-2-furanoic acid.

Compound	Concentration /mM	% Inhibition of <i>Pf</i> GDH
IPA	0.1	87
IPA	1.0	98
IBA	0.1	30
IBA	1.0	49
1	0.1	38
1	1.0	90
2	0.1	27
2	1.0	50
3	0.1	33
3	1.0	50
4	0.1	28
4	1.0	40
5	0.1	33
5	1.0	45

While the results of these compounds are interesting and show promise it is important to note that the compounds are effective in the micromolar range as based on the values of the EC₅₀. Any viable anti-malaria drug that will go into wide spread use must have EC₅₀ that are comparable to those of well-established antimalarial drugs such as chloroquine and artemisinin which have EC₅₀ in the low nanomolar range. This is important due to the fact that the emergence of clinically significant resistant parasites occurs when the ED₅₀ for the drug

increases by approximately 10 fold pushing the concentration required for ED₅₀ into the macro molar range (*Gelb. Michael. H. 2007*).

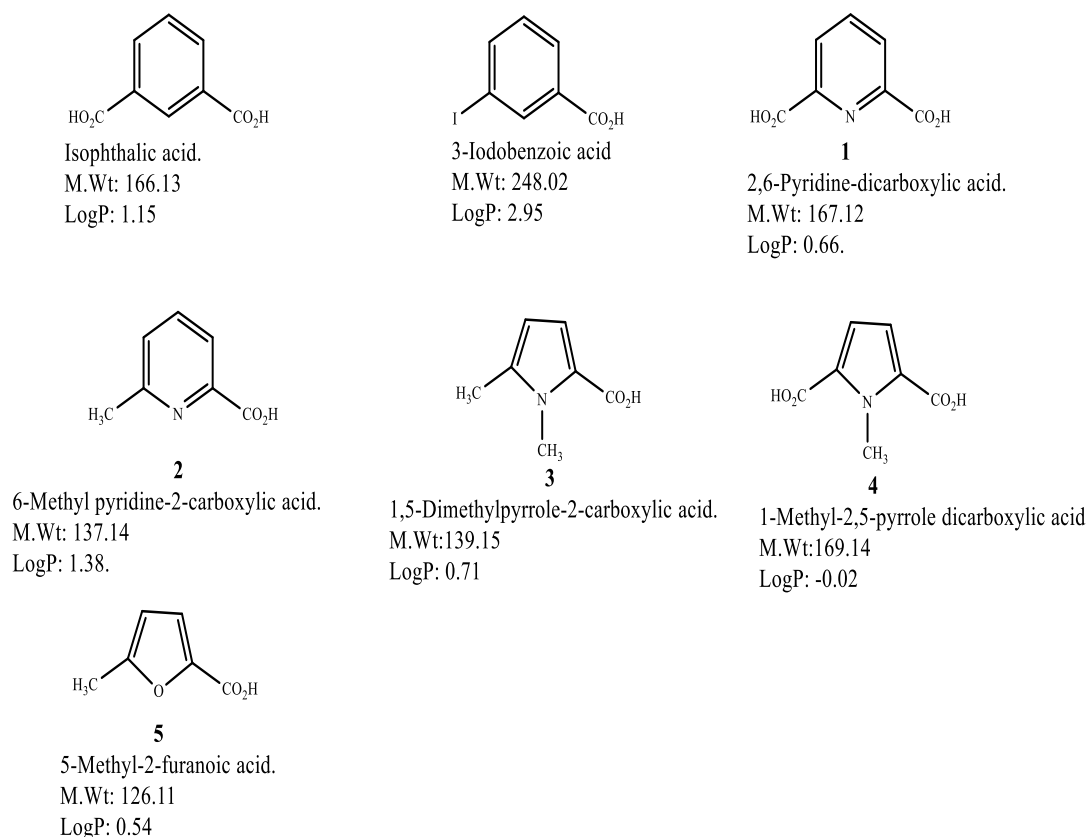


Figure 1.7.2: L-Glutamate analogues synthesised at London Metropolitan University and tested against *Pf*GDH by the research group of Paul Engel at UCD (results shown in Table 1.0)

1.8 Synthetic targets

In recent decades there has been a decline in the pharmaceutical industry's drug discovery research innovation and productivity as a result of decreased efficiency in pharmaceutical research (*Lipinski. C. A, et al 2001*). As a result, pharmaceutical companies have focussed on the development of drug-like property strategies during the drug discovery process to promote the drug discovery process and pharmaceutical industry's productivity in the hope of reducing the attrition rates of compounds and projects during the early discovery process. This will enable a rapid selection of high quality compounds and also decrease the number of iterations it will take to get to the successful compound. The selection, design and chemical optimisation of high quality compounds is done by using one or a combination of metrics to aid in the decision making process (*Mignani. S, et al 2018*). The 'drug-like' filters and strategies aid

with the processing and handling of the large amounts of data that is now available in both computational and experimental approaches. The main weaknesses of these filters include:

- 1) They act as cut-off point for a cardinal decision on whether or not a drug candidate should be developed further.
- 2) They are not well related to the many complex efficacy and safety properties of drugs.
- 3) It is difficult to choose which approach to use given the differences in the mathematical approaches that are used to determine the physiochemical parameter evaluation or the in-vivo parameters and that every approach has its own compounds that are exceptions.

Lipinski's rule or the rule of 5 (RO5) is a set of computational approaches that help determine and predict if a compound will have the desired physical and chemical properties that will allow it to be taken orally (*Lipinski. C. A, et al (2001)*). The RO5 is one of the many multi-parametric computational approaches that is now being used to act as a simple and or complex filter to increase the probability of rapidly finding and developing high quality compounds. Other such filters include the extended RO5 (eRO5), beyond RO5 (bRO5), Quantitative Estimated Drug-likeness QED, ligand-binding thermodynamic and kinetic profiles and the Ligand-Efficiency indices (LE indices) also known as the (LE matrices) and 2D Maps (*Mignani. S, et al 2018*). Modern approaches such as Quantitative Estimated Drug-likeness (QED) outperformed most of the other simpler scoring systems and approaches including the RO5 because of the extra parameters that it uses in its calculation, and because it uses a set of approved oral drugs as the basis of its methodology (*Ritchie. T. J, et al 2014*).

The RO5 predicts with high probability that compounds with good absorption and permeability, have a molecular weight less than or equal to 500, not more than 5 hydrogen bond donors, not more than 10 hydrogen bond acceptors and a calculated Log P (CLog P) less than 5 or a Moriguchi Log P (MLog P) less than 4.15. Lipophilicity is the most important physiochemical property that is used in quantitative structure activity relationship (QSAR) analysis. Lipophilicity is an important tool that is used to describe the pharmacodynamics,

pharmacokinetics and toxic aspects of drug activity. The lipophilic nature of a compound is most commonly defined by the partition coefficient, P , or its decimal logarithm, $\log P$ (*Bakht. M. A, et al, 2014*). The $\log P$ value only applies for neutral, uncharged molecules and provides an indication of whether a substance will be absorbed by living tissue (organic phase) or will be easily carried away and disseminated by water (aqueous phase). A negative value for $\log P$ means the compound has a higher affinity for the aqueous phase (hydrophilic). When $\log P = 0$ the compound is equally partitioned between the lipid and aqueous phases and a positive value for $\log P$ denotes a higher concentration in the lipid phase (lipophilic). Highly lipophilic compounds ($\log P > 5$) have low aqueous solubility thereby compromising their bioavailability. Such highly lipophilic compounds will be sequestered by the fatty tissue making them difficult to excrete, resulting in accumulation of the compound leading to systemic toxicity. However, since the majority of compounds investigated in pharmaceutical research contain ionizable sites, the $\log D$ would be a better descriptor of lipophilicity. The $\log D$ is the distribution of the various ionized species at any given pH. $\log D$ would be a particularly useful descriptor for the lipophilicity of phosphonates and phosphates which are charged at physiological pH (pK_{a1} 1.1-2.3 and pK_{a2} 4.0-7.2) (*Sevrain. M. C, et al, 2017*). Compounds with large molecular weights have poor blood brain barrier and intestinal wall penetration. Increased compound molecular weight also leads to rapid decline in permeation time of the phospholipid bilayer. Compounds with a smaller number of hydrogen bond donors have a higher probability of having better permeability. Higher number of hydrogen bond acceptors have been shown to hinder phospholipid bi-layer permeability (*Lipinski. C. A, et al 2001*).

There are orally active compounds that exist outside the RO5, these include antibiotics, antifungals, vitamins and cardiac glycosides. This is because members for these classes of compounds have features that make them act as substrates for naturally occurring transporters. Compounds that fail to meet the RO5 criterion are considered to likely have poor bioavailability and as a result, only one violation can be tolerated. The RO5 does not predict whether a compound is pharmacologically active, it predicts whether compounds can be orally

delivered and be absorbed by passive mechanisms (*Lipinski. C. A, et al 2001*). If the compounds synthesized meet the criteria as determined by the RO5 or have one violation, that means such compounds would have the desired physical and chemical properties that will allow them to be taken orally and are therefore acceptable.

Fluorine containing compounds are very important and are usually at the forefront of new developments in the life sciences industries. In 1990, there were approximately 220 fluorine containing compounds representing 8% of all synthetic pharmaceutical compounds that came to the market. By 1997 they were 1500 fluorine containing compounds under development in the pharmaceutical industry. In the agricultural industry, the number of fluorine containing compounds has increased from 4% to 17% of all the currently used crop protection agents since 1978. This increase in popularity of fluorinated compounds is due to the fact that selectively fluorinated compounds have exhibited dramatically improved potency when compared to their non-fluorinated analogues. The incorporation of fluorine into a biologically active compound alters the electronic, lipophilic, steric parameters and can increase the intrinsic activity, the chemical and metabolic stability and the bioavailability of the compound. One of the most common bioisosteric replacement is the substitution of a hydrogen atom with fluorine. This is possible because fluorinated compounds have a similar size and shape (Van der Waals radius; 1.47 Å for F and 1.20 Å for H) to their non-fluorinated analogues allowing the fluorinated compounds to fit in the same target site. Replacement of the C-H bond with the C-F enhances the lipophilicity of a compound with functional groups such as CF₃, CF₃O and CF₃S being amongst the most lipophilic groups currently known. Compounds containing such groups having different pharmacokinetic behaviour such as enhanced passive diffusion across membranes. This is evidenced by the fact that most compounds that act on the central nervous system (CNS) contain a fluoro-phenyl group or a CF₃ group which contribute to the pharmacological activity by increasing the CNS penetration. The strength of the C-F bond (485KJmol⁻¹ compared to 416KJmol⁻¹ for the C-H bond) makes the fluorinated compounds resistant to metabolic degradation. The high electronegativity of fluorine (4.0 against 2.1 for

H) alters the electronic effects and chemical reactivity of the compound resulting in an enhanced intrinsic activity as well as different chemical behaviour (*Maienfisch. P, et al 2004*).

Phosphonates and phosphonic acids are organic phosphorus compounds that are common in different organisms such as prokaryotes, eubacteria, fungi, molluscs and insects and have been shown to have anti-fungal, anti-bacterial and anti-cancer activity. The first naturally occurring phosphonate was isolated in 1959 from the ciliated protozoa in the rumen of sheep, which is where this β -alanine and taurine analogue derives its name from, ciliatine. Methyl phosphonates and 2-hydroxyethylphosphonates have been mainly found in *Nitrosopumilus maritimus*, one of the most abundant organisms on the planet, that is resident in oxygen rich environments of the open oceans (*Kafarski. B, 2019*). Despite the different structural and electronic functionalities in terms of size, shape, acidity and geometry, phosphonates are however, considered to be bioisosteres of the carboxylic group (*Kamel. A, et al 2015*).

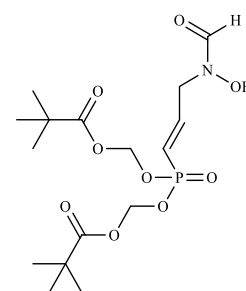
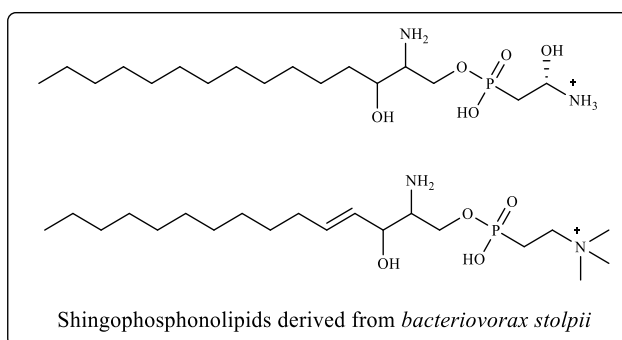
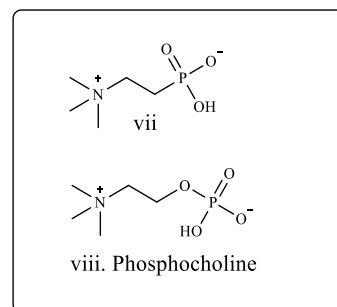
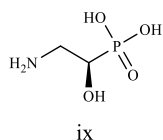
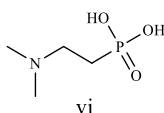
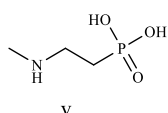
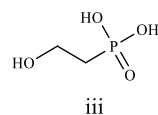
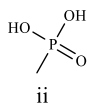
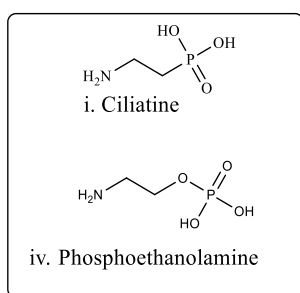


Figure 1.8.1: Naturally occurring phosphonic acids and phosphonates derived from protozoa, bacteria and other microorganisms (Kafarski, B, 2019)

An estimated one-third of all cellular proteins are modified through phosphorylation, making it the second most prevalent post translation modification after glycosylation. This makes phosphorylation a pivotal modulator of cellular function through its regulation of signal transduction pathways. Phosphorylation and dephosphorylation of target molecules are carried out by the large numbers of kinases and phosphatases respectively, that are present in large numbers within the human cell cytoplasm and nucleus. Phosphorylation pathways on lipid and carbohydrate based substrates play a fundamental role in metabolic processing and in protein, carbohydrate and lipid recognition. Due to the ubiquitous nature of substrate phosphorylation in cell signalling networks, these pathways are important to physiological processes such as

cellular differentiation, migration, metabolism, and apoptosis. When these processes go errand, this may result in conditions such as cancer, diabetes and Alzheimer's disease among others. As a result of these wide ranges of effects, general strategies for the design of improved inhibitors and probes of these classes of inhibitors that have substrates that can be phosphorylated or dephosphorylated is of continued interest to medicinal chemists (*Downey, A, et al 2014*).

As the phosphonates are hydrolysed to the desired phosphonic acids at the target site there is a change in the charge state of the compound making a salt bridge and hydrogen bonding more favourable. The nature of the enzymes that are involved in the transformation of phosphate and phosphonate esters require their natural substrates to have one or more negative charges. As a result, the drug molecules that target these enzymes, generally, must be charged as well. This creates an interesting dilemma where the phosphate and phosphonate small drug molecules are charged and have great difficulties crossing cell membranes by any means other than endocytosis. The resulting contradiction has stimulated abundant effort to develop effective prodrugs, these are compounds that are uncharged to enable them to transit biological membranes but are then able to release the charged parent drug once inside the target cell. For example, the Hepdirect prodrug pradefovir achieved better oral bioavailability (42%) compared to the parent drug adefovir (31%) (*Wiemer, A, et al 2016*). Phosphonates and phosphate esters may be lipophilic enough to cross cell membranes where they will be hydrolysed to the charged molecules that are active compounds. As such, phosphonates and phosphate esters have become central in advancing prodrug forms for their application in the development and improvements of drugs.

The principal synthetic targets of this project were novel analogues of glutamic acid that contain the same intramolecular arrangement of carboxylic and/or phosphonic acid functionalities (*Yokomatsu, T, et al 1997*). Synthesis of the 1-hydroxyphosphonic acid derivatives has been achieved via the well-established Pudovik reaction (*Green, D, et al 1996; Pudovik, A, N, et al 1950*). The synthetic targets for the *P. falciparum* GDH were the 2- nitro-

benzyl- and the 2-carboxyl-benzyl analogues These compounds are glutamate analogs as they have the same number of carbon atoms between the acid/acid-isostere functional groups. The 3-nitro-benzyl, 4-nitro benzyl, 3-carboxyl benzyl and 4-carboxy benzyl analogues are not expected to be active as they have one or more extra carbons in-between. These compounds are not expected to be active against *P. falciparum* glutamate dehydrogenase. These compounds were synthesised as a proof concept, that it is the stereochemical considerations of the 2- nitro benzyl phosphonic acids (**30**) and the 2- carboxyl-benzyl phosphonic acids (**27**) that make the compounds effective inhibitors. The 1-hydroxy phosphonic acids were obtained as racemic mixtures as the α -hydroxy carbon is a chiral centre. After testing, any compounds that showed significant activity and were considered promising targets for further development as lead compounds would have to be resolved to their pure enantiomers. In a research environment, chiral compounds can be resolved in a number of ways including chiral chromatography, however, for large scale synthesis, the racemic intermediate or phosphonic acid mixture would be converted to a diastereoisomer. This is achieved by converting the hydroxyl group to an ester with a pure enantiomer of either R/S-lactic acid or mandelic acid which will give the a diastereoisomeric mixture. The two diastereoisomers will have different chemical and physical properties consequently enabling them to be separated by recrystallization or simple chromatography. The diastereoisomers will then be hydrolysed yielding the pure 1-hydroxy phosphonate enantiomers.

The target compounds were obtained by initially using the well-established Pudovik reaction to synthesize the substituted benzyl- α -hydroxy diethyl phosphonates and the substituted benzyl- α -hydroxy dibenzyl phosphonates.

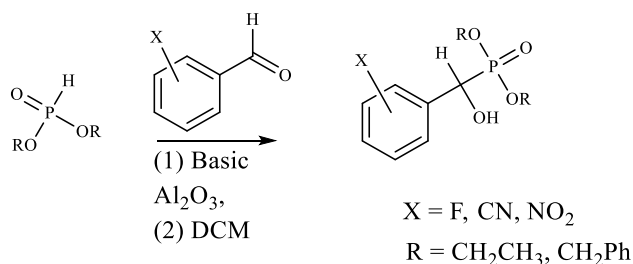


Figure 1.8.2: Substituted benzyl- α -hydroxyl phosphonates reaction scheme

Substitution of the α -hydroxyl group to the α -methylene was also achieved. This was done to determine if the non-chiral compound at this position would have any activity against *P. falciparum*.

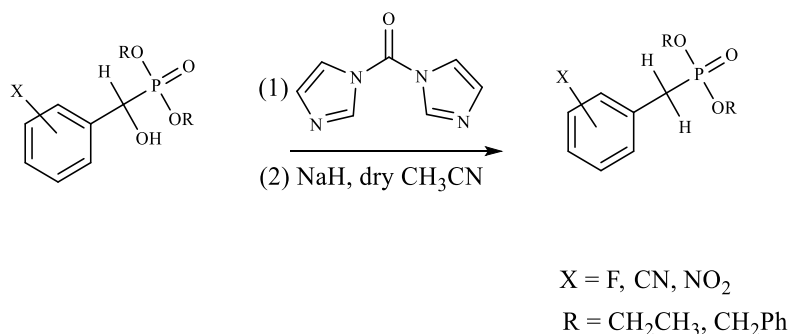


Figure 1.8.3: Substituted benzyl- α -methylene phosphonates reaction scheme

These substituted benzyl- α -hydroxy diethyl phosphonates and the substituted benzyl- α -hydroxy dibenzyl phosphonates and their respective substituted benzyl- α -methylene diethyl phosphonates and the substituted benzyl- α -methylene dibenzyl phosphonates were used as precursors to get to their respective phosphonic acid compounds. The substituted benzyl- α -hydroxy diethyl phosphonates and the substituted benzyl- α -methylene diethyl phosphonates were easier to hydrolyse because they required simple acidolysis whereas the substituted dibenzyl phosphonates required catalytic hydrogenolysis. The substituted benzyl- α -hydroxy diethyl phosphonates and the substituted benzyl- α -methylene diethyl phosphonates were converted to their respective phosphonic acids in two main ways:

- 1) Acid hydrolysis with 6M hydrochloric acid or concentrated acetic acid
- 2) Dealkylation with bromotrimethylsilane (TMSiBr)/chlorotrimethylsilane (TMSiCl) in the presence of a metal halide.

Two methods were required for hydrolysis because **29** and **30** could not be obtained by acid hydrolysis in which case dealkylation with TMSiBr/TMSiCl was used to obtain these phosphonic acids. The F- and NO₂ functional groups are unaffected by the TMSi-X reagents hence, the dealkylation of the 2-fluoro and the 2-nitro derivatives work well with these reagents. The compounds 3-carboxybenzyl- α -hydroxyl phosphonic acid **26**, 4-carboxybenzyl- α -hydroxyl phosphonic acid **28** and 2-carboxybenzyl- α -hydroxyl phosphonic acid **27**, could not be obtained by dealkylation with TMSiBr/TMSiCl as these reagents failed to react with the CN groups. Therefore, acid hydrolysis was used to obtain these phosphonic acids as it cleaved the alkyl groups and hydrolysed the CN and the lactone to COOH simultaneously.

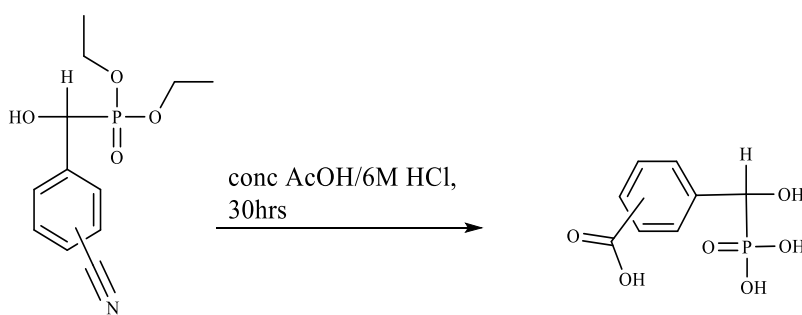
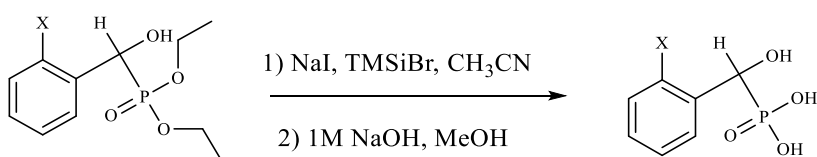


Figure 1.8.4: Acid hydrolysis of the substituted benzyl- α -hydroxy diethyl phosphonates general reaction scheme



X=NO₂, F

Figure 1.8.5: Reaction scheme for the dealkylation of the substituted benzyl- α -hydroxy diethyl phosphonates by TMSiBr

The substitution of the α -hydroxyl group to the α -amino was also attempted. This was done to synthesise the substituted benzyl- α -amino phosphonic acids. Amino acids are very important biochemical compounds that have a plethora of important tasks within the cell. These tasks include but are not limited to catalysing chemical reactions, providing substrates for chemical reactions, providing structural elements of a cell, transport of vital materials into the cell and

controlling gene activity. If the proposed synthesised substituted benzyl- α -amino phosphonic acids inhibitors have a closer structural relationship to the amino acid substrate glutamate, they are more likely to be better competitive inhibitors for the enzyme as they will have similar interactions with the enzyme *pf* GDH as the substrate has.

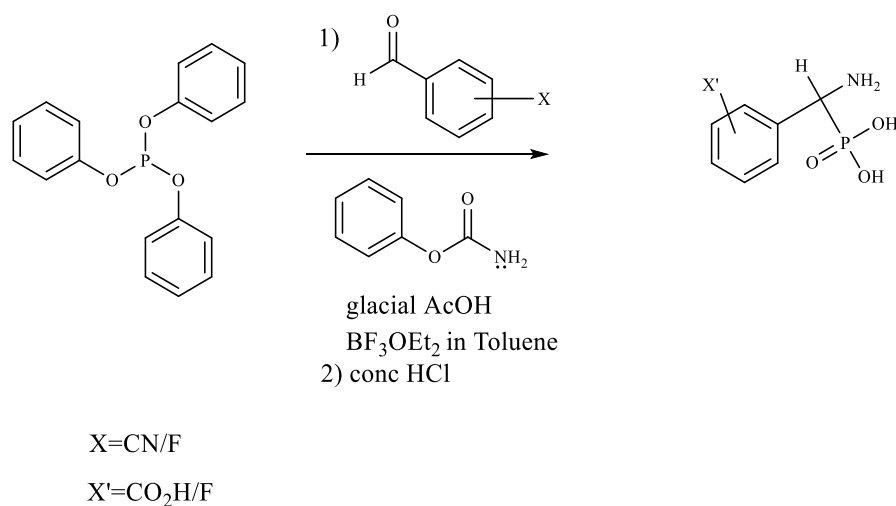
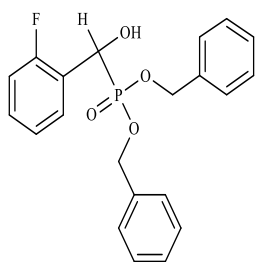


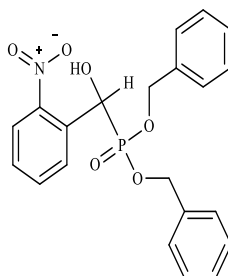
Figure 1.8.6: Synthesis of substituted benzyl- α -amino phosphonic acid reaction scheme

All of the target molecules were tested against assays of *P. falciparum* (*Pf*) parasites strains 3D7 and Dd2 to determine differences in their relative inhibitions of both strains of the parasite at Sanger institute at Cambridge University. The biological results are discussed in chapter 3.



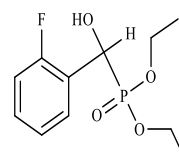
6

2-Fluoro benzyl- α -hydroxy-dibenzyl phosphonate
M.Wt: 386.36
LogP: 5.34



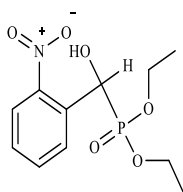
9

2-Nitro benzyl- α -hydroxy-dibenzyl phosphonate
M.Wt: 413.37
LogP: 3.2



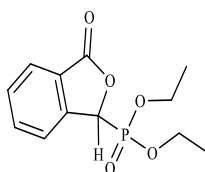
12

2-Fluoro benzyl- α -hydroxy-diethyl phosphonate
M.Wt: 262.22
LogP: 2.47



17

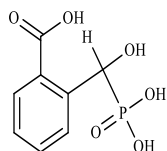
2-Nitro benzyl- α -hydroxy-diethyl phosphonate
M.Wt: 289.22
LogP: 1



18

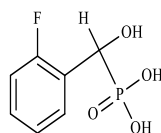
1,2-Benzyl- γ -lactone-2-diethyl phosphonate.
M.Wt: 270.22
LogP: 2.33

PROTECTED GLUTAMATE ANALOGUES



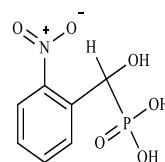
27

2-Carboxy benzyl- α -hydroxy-phosphonic acid.
M.Wt: 232.13
LogP: 1.28



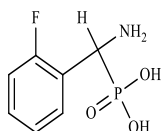
29

2-Fluoro benzyl- α -hydroxy-phosphonic acid.
M.Wt: 206.11
LogP: 1.72



30

2-Nitro benzyl- α -hydroxy-phosphonic acid
M.Wt: 233.12
LogP: -0.8

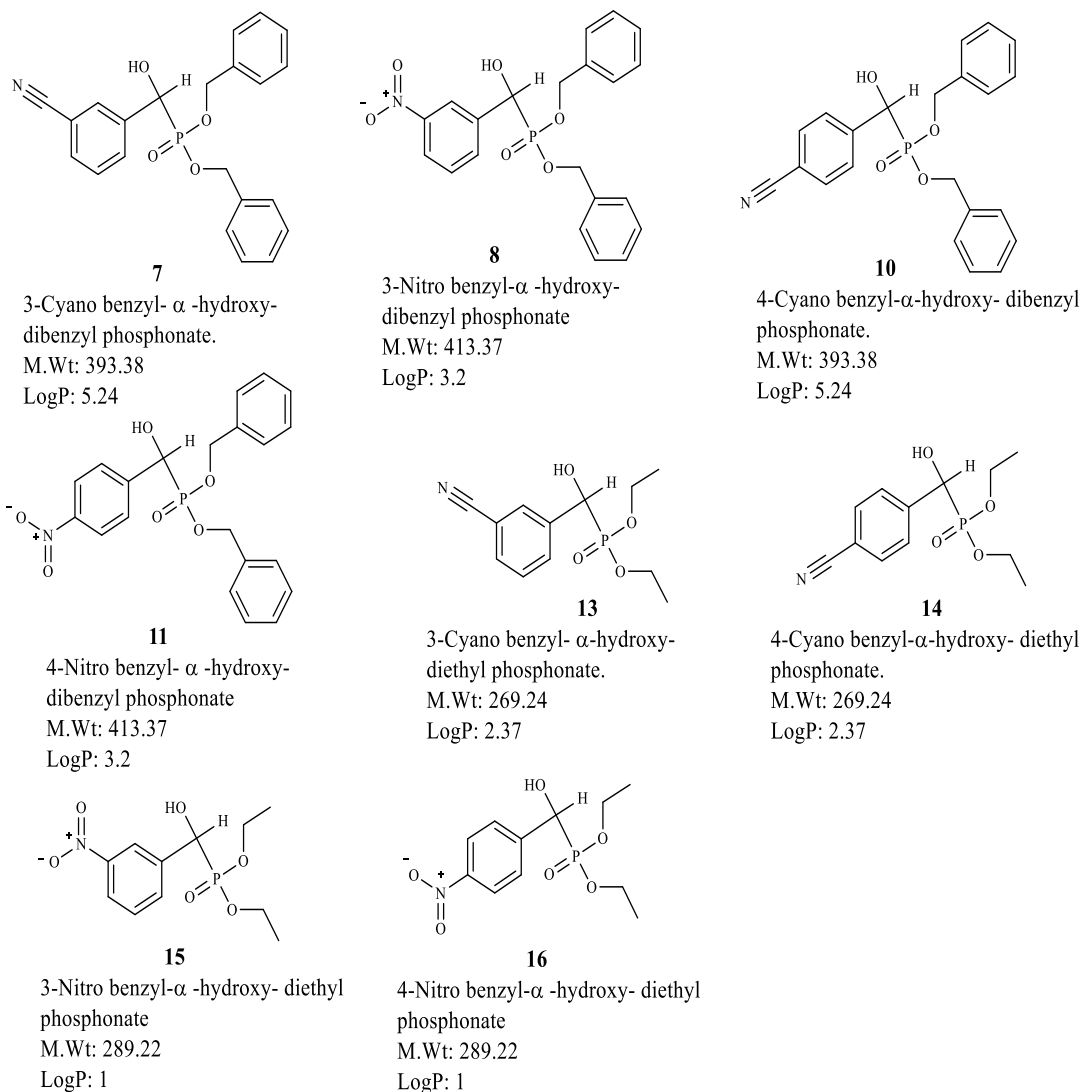


34

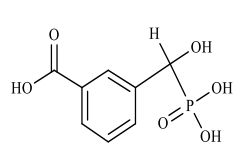
2-Fluoro benzyl- α -amino-phosphonic acid
M.Wt: 205.13
LogP: 1.38

UNPROTECTED GLUTAMATE ANALOGUES

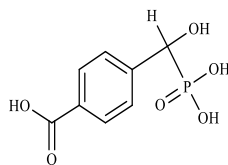
Figure 1.8.7: The structures of the second series of targeted protected and unprotected glutamate analogues synthesised in this research project. The lactone containing compound 18 was not the desired target; the 2-CN (and 2-CO₂H in the final hydrolysed product) compound was.



PROTECTED NON-GLUTAMATE ANALOGUES



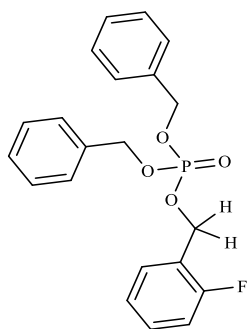
26
3-Carboxy benzyl- α -hydroxy-phosphonic acid.
M.Wt: 232.13
LogP: 1.28



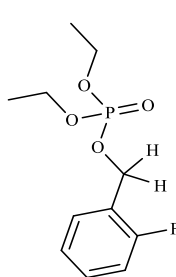
28
4-Carboxy benzyl- α -hydroxy-phosphonic acid.
M.Wt: 232.13
LogP: 1.28

UNPROTECTED NON-GLUTAMATE ANALOGUES

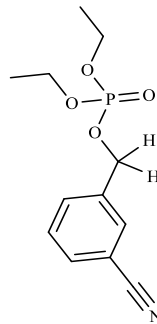
Figure 1.8.8: The structures of the second series of protected and unprotected non-glutamate analogues compounds synthesised in this research project.



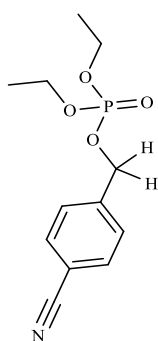
19
2-Fluoro benzyl- dibenzyl
phosphate.
M.Wt: 386.36
LogP: 6.02



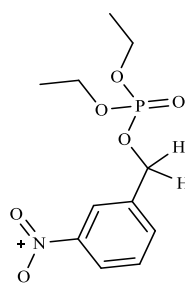
20
2-Fluoro benzyl-diethyl
phosphate.
M.Wt: 262.22
LogP: 3.16



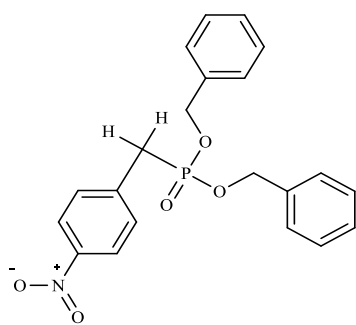
21
3-Cyano benzyl- diethyl
phosphate.
M.Wt: 269.24
LogP: 3.05



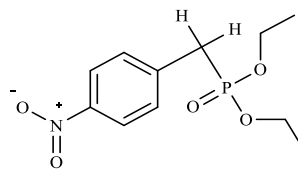
22
4-Cyano benzyl- diethyl
phosphate.
M.Wt: 269.24
LogP: 3.05



23
3-Nitro benzyl-diethyl
phosphate.
M.Wt: 289.22
LogP: 1.59



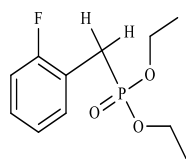
24
4-Nitro benzyl-α -methylene-
dibenzyl phosphonate.
M.Wt: 397.37
LogP: 3.92



25
4-Nitro benzyl-α -methylene-
diethyl phosphonate,
M.Wt:273.22
LogP: 1.88

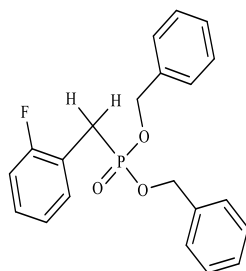
PHOSPHONATE ESTERS

Figure 1.8.9: The structures of the α -methylene phosphate and phosphonate esters that were synthesised in this research project. The α -methylene phosphate esters were not the desired targets



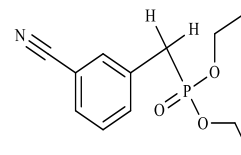
35

2-Fluoro benzyl- α -methylene-diethyl phosphonate.
M.Wt: 246.08
LogP: 2.58



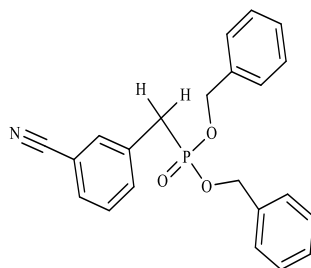
36

2-Fluoro benzyl- α -methylene-dibenzyl phosphonate.
M.Wt: 370.36
LogP: 5.45



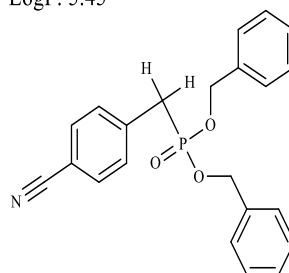
37

3-Cyano benzyl- α -methylene-diethyl phosphonate.
M.Wt: 253.24
LogP: 2.47



38

3-Cyano benzyl- α -methylene-dibenzyl phosphonate.
M.Wt: 377.12
LogP: 5.34



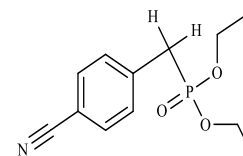
39

4-Cyano benzyl- α -methylene-dibenzyl phosphonate.
M.Wt: 377.12
LogP: 5.34



40

3-Nitro benzyl- α -methylene-diethyl phosphonate.
M.Wt: 273.22
LogP: 1.88



41

4-Cyano benzyl- α -methylene-diethyl phosphonate.
M.Wt: 253.24
LogP: 2.47

Figure 1.8.10: The structures of the desired α -methylene phosphonates synthetic targets that were not attained.

2 RESULTS AND DISCUSSION

2.1 Substituted benzyl- α -hydroxy dibenzyl/diethyl phosphonates

2.1.1 Reaction mechanism

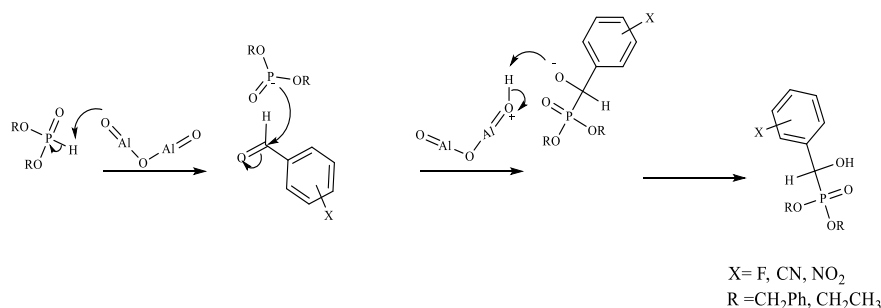


Figure 2.1.1: General reaction mechanism for the synthesis of substituted benzyl- α -hydroxy dibenzyl/diethyl phosphonates

The bioactivity of α -hydroxy phosphonates has made their synthesis a topic of continued interest in organophosphorus chemistry (Rădai, Z, *et al* 2018). The bioactivity of α -hydroxy phosphonates has been acknowledged in their use as antibacterial agents, herbicides, anti-HIV agents and inhibitors of many different enzymes. They have played a significant role as precursors for the synthesis of many other biologically significant molecules such as α -keto phosphonates, α -acetoxy phosphonates and α -amino phosphonates to name a few (Pandi, M, *et al* 2012). There are several approaches to the synthesis of α -hydroxy phosphonates, the most common being the addition of a dialkyl phosphite to an oxo (an oxygen atom linked to a carbon or another element by a double bond) compound in the presence of a base catalyst. The high efficiency of the reaction, (Good atom economy- the percentage of reactants that are converted to useful or desired products resulting in high yields.) makes this the most appealing way to synthesise these compounds although a few acid catalysed variations are known. An alternative route for the synthesis of these compounds is the condensation of an oxo compound and a trialkylphosphite, this method is usually catalysed by acids. In the literature, these reactions are called by a variety of names which include the Pudovik and Abramov reactions and phospho-aldol reaction. Other methods that can be utilised to get α -hydroxy phosphonates include the reaction of α -keto phosphonates with Grignard reagents or other similar

organometallic compounds followed by hydrolysis (*Rădai. Z, et al 2018*). The reaction for obtaining α -hydroxy phosphonates from dialkyl phosphonates and oxo compounds which is catalysed by alkali alcoholates was first reported by Pudovik, but since then, variations involving different catalysts and conditions have been elaborated. Recent methods have targeted the production of these α -hydroxy phosphonates using inexpensive and simple catalysts and mild reaction conditions in the spirit of green chemistry and sustainable research development. In most cases, this approach has targeted the production of α -hydroxy phosphonates without any solvent present. It is worth noting that obtaining α -hydroxy phosphonates from ketones is much more challenging than obtaining them from aldehydes. This is due to ketones being less reactive because of both steric and electronic effects (*Rădai. Z, et al 2018*).

The reaction begins with the deprotonation of the phosphorus of the dibenzyl phosphite by the basic alumina catalyst thereby generating a negative charge and increasing the nucleophilicity of the dibenzyl phosphite (*Abell. J. P, et al 2008*). The nucleophilic dibenzyl phosphite attacks the electrophilic carbonyl of the aldehyde (*Merino P, et al 2008*). This carbonyl transfers its electrons to the oxygen of the C=O generating an alkoxide. The alkoxide is then protonated by the alumina-hydride to turn it into a hydroxyl group and regenerating the basic alumina. The basic alumina acts as a base in the deprotonation of the dibenzyl phosphite and as an acid when it is regenerated in the protonation of the alkoxide. This mechanism forms a catalytic cycle which results in the formation of the α - amino and α - hydroxy phosphonic esters (*Merino P, et al 2008*). This is the same reaction that occurs for the diethyl phosphonates below. The yields for the diethyl phosphonates are higher than that of the dibenzyl phosphonates, this is due to the steric hindrances from the dibenzyl groups. The increase in the size of the alkyl group in the dibenzyl phosphites may have the effect of reducing the nucleophilicity of the phosphite ion that is formed thereby decreasing its reactivity (*Abell. J. P, et al 2008*).

These compounds were straight forward to synthesise. The main source of impurity in the product was the starting aldehyde which was easily removed by washing the product

repeatedly with a 1:1 hexane diethyl ether mixture. The 3-nitrobenzyl- α -hydroxy dibenzyl phosphonate and 4-nitrobenzyl- α -hydroxy dibenzyl phosphonate needed recrystallization (hexane: ethyl acetate, 1:1) in order to obtain them as pure compounds.

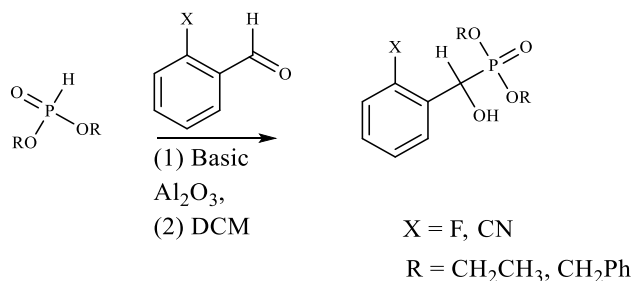


Figure 2.1.2: substituted benzyl- α -hydroxy phosphonates reaction scheme

Table 2: Synthesized substituted benzyl- α -hydroxy dibenzyl phosphonates and their respective yields

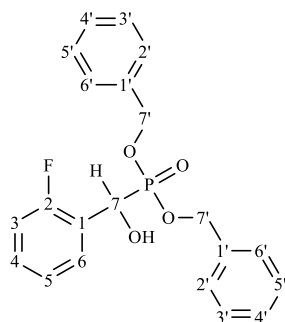
Compounds	Yield %
2-Fluorobenzyl- α -hydroxy dibenzyl phosphonate (6)	98
3-Cyanobenzyl- α -hydroxy dibenzyl phosphonate (7)	54
3-Nitrobenzyl- α -hydroxy dibenzyl phosphonate (8)	64
2-Nitrobenzyl- α -hydroxy dibenzyl phosphonate (9)	65
4-Cyanobenzyl- α -hydroxy dibenzyl phosphonate (10)	96
4-Nitrobenzyl- α -hydroxy dibenzyl phosphonate (11)	58

Since all the synthesised compounds have a similar structure, the data they produce will have a similar pattern. The distinct section of the ^1H and ^{13}C -NMR for these compounds was the asymmetric section [$-\alpha\text{-CH(OH)-P-}$]; (C-7). The peaks in this region experienced deshielding from the adjacent electron-withdrawing groups and were observed down field. The (C-7) carbon is directly bonded to the phosphorus and as a result, there is splitting that is observed with these peaks due to (P-H) and (P-C) phosphorus coupling. Compounds in which the aryl group contained fluorine resulted in the asymmetric section experiencing additional splitting from long range fluorine coupling, hence the peaks were observed as multiplets. The $-\alpha\text{-C-OH}$ peak disappeared from the ^1H -NMR spectra on D_2O shake.

Table 3: Distinguishing peaks of the substituted benzyl- α -hydroxy diethyl phosphonates

Compound	δ_{H} CH-OH (ppm)	δ_{H} CH-OH (ppm)	δ_{C} CH-OH (ppm)	δ_{P} (ppm)	$^1J_{31\text{P}-13\text{C}}$ (Hz) (C-7)
6	5.52-5.56	5.52-5.56	63.94	22.19	163.5
7	5.08	5.44	70.02	21.39	160.02
8	4.78	5.15	70.21	21.17	158.76
9	6.32	4.63	66.14	21.59	158.76
10	5.10	4.18	70.49	21.20	157.50
11	5.15	4.60	70.45	21.03	157.50

2.2 2-Fluorobenzyl- α -hydroxy dibenzyl phosphonate (6)

**Figure 2.2.1: 2-Fluorobenzyl- α -hydroxy dibenzyl phosphonates with numbered carbons.**

2.2.1 $^1\text{H-NMR}$

The peaks in the region from 4.90-5.06 ppm represent the two CH_2 groups of the 7' carbons (C-7'). The peak in the region 5.52-5.56 ppm are from the C-H and the CH-OH of the asymmetric carbon (C-7);

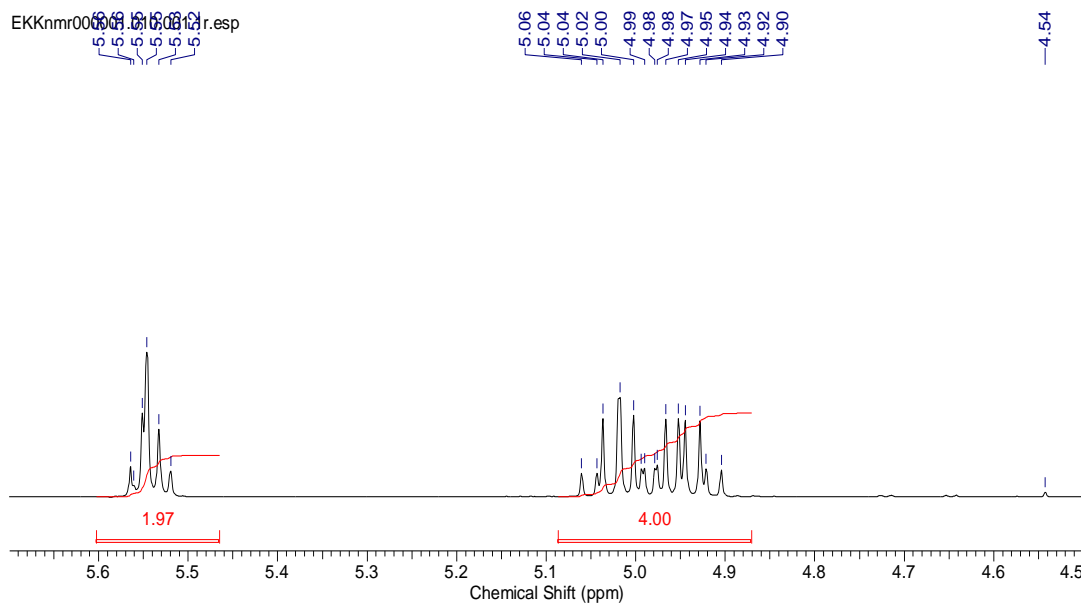


Figure 2.2.2: ¹H-NMR 2-fluorobenzyl- α -hydroxy dibenzyl phosphonate aliphatic region expanded

The peaks in the region 6.95-7.73 ppm represent the hydrogens bonded to the two types of aromatic rings; the two identical phenyl groups and the 2-fluoro benzyl ring. The two phenyl groups are symmetrical so will only give three signals each. The peaks for the phenyl rings should correspond to ten hydrogens that resonate in the same region. The peaks in this region will overlap, therefore, they cannot be identified individually.

The peaks of the 2-fluoro benzyl ring will experience fluorine coupling which results in the splitting of the peaks, generating multiplets. The multiplet at 7.69-7.73 ppm ($^3J_{19F-1H-o} = 7.4$ Hz) is the hydrogen that is adjacent to the C-F group. This peak experiences the strongest fluorine coupling which generates the complex multiplet, which is observed. This peak is observed in this region because of the electron-withdrawing effects of the adjacent electronegative fluorine which pulls the H-3 hydrogen further downfield. The effects of the fluorine coupling become weaker the further away the peaks are from the C-F bond resulting in smaller longer range coupling. The remaining peaks of the 2-fluoro benzyl ring will overlap with the ten hydrogens from the two phenyl rings, therefore, they cannot be identified individually.

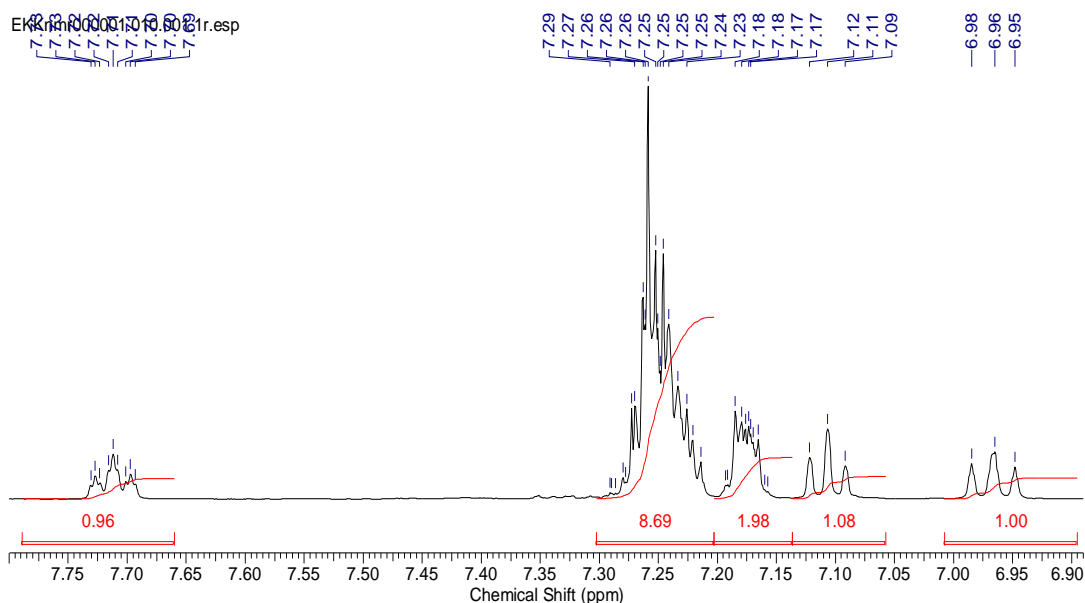


Figure 2.2.3: ^1H -NMR 2-fluorobenzyl- α -hydroxy dibenzyl phosphonate aromatic region expanded

2.2.2 ^{13}C -NMR000001

The doublets at 68.27-68.33 ppm ($^2J_{31\text{P}-^{13}\text{C}} = 7.6$ Hz) and 68.72-68.77 ppm ($^2J_{31\text{P}-^{13}\text{C}} = 6.3$ Hz) are from the CH_2 (C-7') from the dibenzyl group. The peaks at 63.28-63.30 ppm and 64.58-64.60 ppm ($^1J_{31\text{P}-^{13}\text{C}} = 163.5$ Hz); ($^3J_{19\text{F}-^{13}\text{C}} = 2.7$ Hz) are from the asymmetric carbon (C-7).

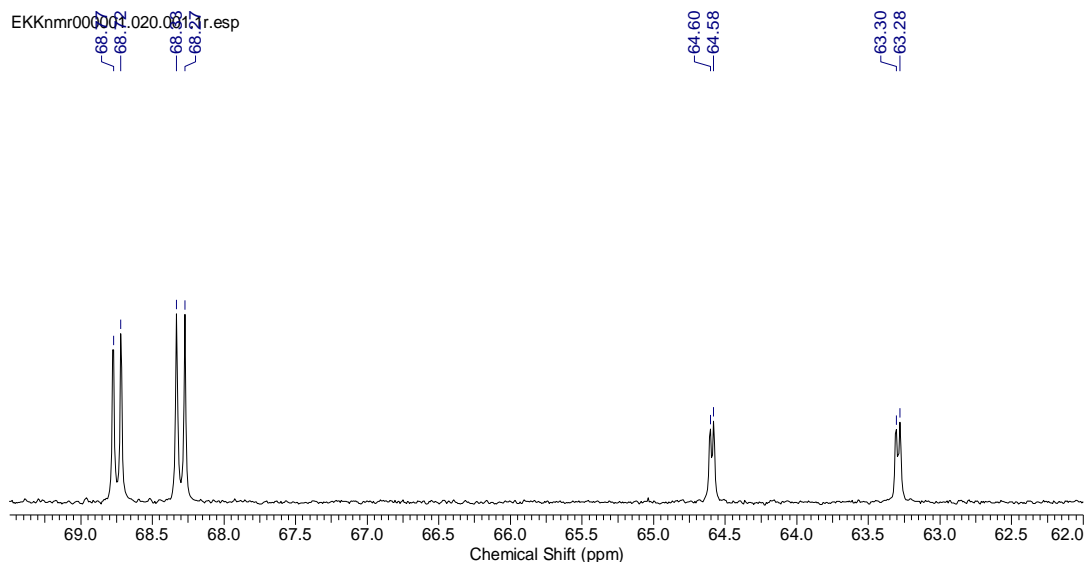


Figure 2.2.4: ^{13}C -NMR 2-Fluorobenzyl- α -hydroxy dibenzyl phosphonate aliphatic region expanded

The peaks between 114.92 ppm and 160.65 ppm represent the two phenyl groups and the 2-fluoro benzyl ring. The similar phenyl groups will produce 4 peaks each which will resonate in the same region. The 2-fluorobenzyl group produces 6 peaks, the peak at 158.62-158.68

ppm and 160.60-160.65 ppm are from the C-F in the 2-fluorobenzyl ring. This peak appears as a doublet of a doublet due to the coupling effect from the phosphorus (${}^4J_{31\text{P}-13\text{C}} = 6.3$ Hz; ${}^4J_{31\text{P}-13\text{C}} = 7.6$ Hz) and fluorine (${}^1J_{19\text{F}-13\text{C}} = 255.78$ Hz) resulting in splitting of the peaks. This peak resonates furthest downfield because it is directly attached to the electronegative fluorine. The peaks in the region 115.09-136.01 represent the remaining peaks of both the two phenyl rings and the 2-fluorobenzyl ring.

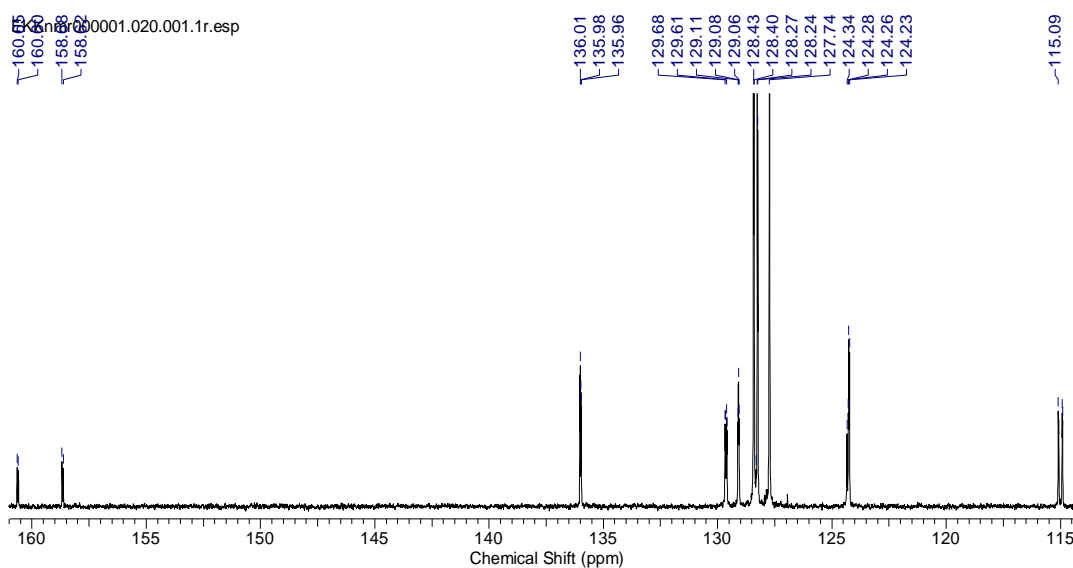


Figure 2.2.5: ${}^{13}\text{C}$ -NMR 2-fluorobenzyl- α -hydroxy dibenzyl phosphonate aromatic region expanded

2.2.3 ${}^{31}\text{P}$ -NMR00001

The phosphorus NMR shows one peak, a doublet, in the region 22.18-22.22 ppm. No other phosphorus containing compounds are present in the sample.

The NMR peaks of the remaining compounds in the same class had similar patterns.

2.3 Mass Spectrometry (EIMS⁺) (6)

2.3.1.1 MS0001

There is no molecular ion present therefore fragments from the molecular ions will be used to indicate the presence of the molecular ion. The Mr of the ion is 386. The peak at m/z 262 indicates the loss of 125 amu from the molecular ion. This peak represents the dibenzyl phosphate ion $(\text{PhCH}_2\text{O})_2\text{PO}$ fragment. The peak at m/z 180 is from the $\text{C}_6\text{H}_4\text{CHPO}_3\text{C}^+$

fragment. The peak at m/z 171 is from the $\text{FC}_6\text{H}_4\text{CPO}_2^+$ fragment ion. The peak at m/z 123 is from the 2-fluoro benzyl ring $\text{FC}_6\text{H}_4\text{CO}^+$. The peak at m/z 91 is from the $\text{C}_6\text{H}_5\text{CH}_2^+$ fragment.

2.4 Substituted benzyl- α -hydroxy diethyl phosphonates

The synthesis of these compounds was straightforward and produced very clean solid compounds except for 2-cyano benzyl- α -diethyl phosphonate. The compound 2-cyano benzyl- α -diethyl phosphonate showed four spots which corresponded to four different products on the TLC plates (hexane: ethyl acetate; 1:1 and 2:8), one of which was the starting aldehyde, 2-cyanobenzaldehyde. Upon purification of the product by column chromatography, NMR determined that instead of the 2-cyano benzyl- α -diethyl phosphonate being formed, the 1,2-benzyl- γ lactone- diethyl phosphonate had been formed. Column chromatography separated the fractions clearly and any remaining impurities were washed off with a mixture of 1:1 hexane diethyl ether. NMR of this resultant product showed that the product was pure but it confirmed that a different reaction had occurred. The proximity of the α -hydroxyl group with the 2-cyano group resulted in the basic alumina catalysing the conversion of the two groups into a lactone. This was confirmed by infra-red spectroscopy which showed the presence of a C=O peak, and this confirmed that the 2-cyano group had been converted to the lactone.

Table 4: Synthesized substituted benzyl- α -hydroxy diethyl phosphonates and their respective yields

Compounds	Yield %
2-Fluorobenzyl- α -hydroxy diethyl phosphonate (12)	47
3-Cyanobenzyl- α -hydroxy diethyl phosphonate (13)	82
4-Cyanobenzyl- α -hydroxy diethyl phosphonate (14)	85
4-Nitrobenzyl- α -hydroxy diethyl phosphonate (16)	98
3-Nitrobenzyl- α -hydroxy diethyl phosphonate (15)	95
2-Nitrobenzyl- α -hydroxy diethyl phosphonate (17)	74
1,2-Benzyl- γ -lactone diethyl phosphonate (18)	26

2.4.1 Reaction mechanism for the synthesis of the 1,2-benzyl- γ -lactone diethyl phosphonate (18)

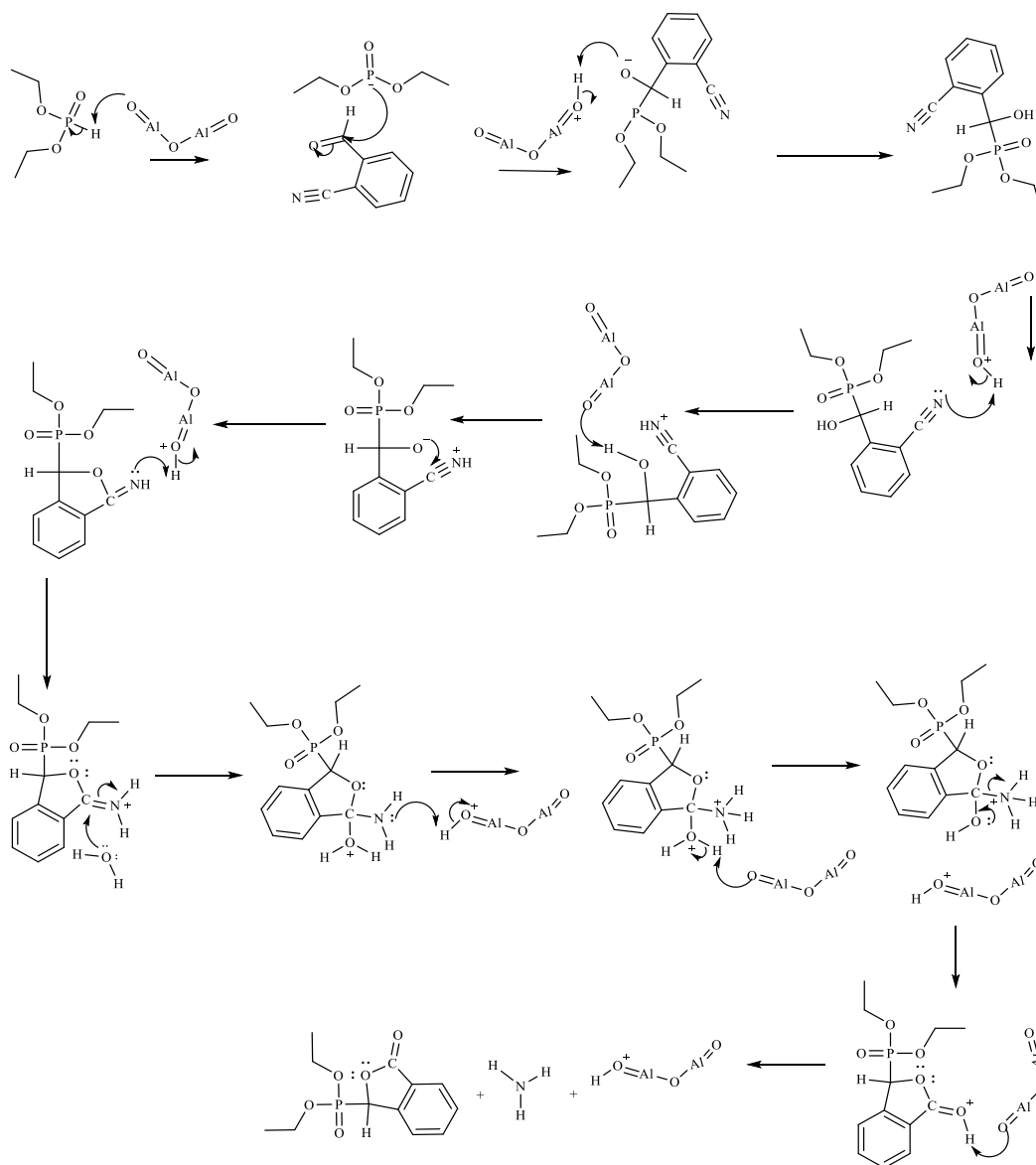


Figure 2.4.1: General reaction mechanism for the synthesis of 1,2-benzyl- γ -lactone diethyl phosphonates

Table 5: Distinguishing peaks of the substituted benzyl- α -hydroxy diethyl phosphonates

Compound	δ_{H} CH-OH (ppm)	δ_{H} CH-OH (ppm)	δ_{C} CH-OH (ppm)	δ_{P} (ppm)	$^1J_{31\text{P}-13\text{C}}$ (Hz) (C-7)
12	5.40	4.65	63.87	21.35	162.54
13	5.09	5.55	69.74	20.56	161.28
14	5.06	5.11	70.15	20.43	157.50
15	5.18	5.55	69.86	20.36	160.02
16	5.18	5.11	70.11	20.20	157.50
17	6.29	5.40	65.62	20.58	161.28
18	5.69	-	75.56	13.80	165.06

2.5 2-Fluoro benzyl- α -hydroxy diethyl phosphonate (12)

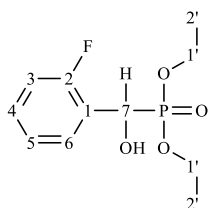


Figure 2.5.1: 2-fluorobenzyl- α -hydroxy diethyl phosphonates with numbered carbons

2.5.1 $^1\text{H-NMR}$ 012A

The multiplet at 1.20-1.36 ppm represent the two CH_3 groups of the C-2' carbon. The two peaks are observed as two triplets that overlap generating a multiplet. The peaks in the region 4.00-4.21 ppm represent the two CH_2 groups of the C-1' carbon. The two peaks are observed as two quartets that overlap creating a multiplet. The peak in the region 5.38-5.42 ppm ($^2J_{31\text{P}-1\text{H}} = 15$ Hz; $^4J_{19\text{F}-1\text{H}} = 10$ Hz) is from the CH of the asymmetric carbon (C-7). The peak of the hydroxyl group of the CH-OH asymmetric carbon resonates in the region 4.64-4.66 ppm ($^2J_{31\text{P}-1\text{H}} = 10$ Hz; $^4J_{19\text{F}-1\text{H}} = 10$ Hz).

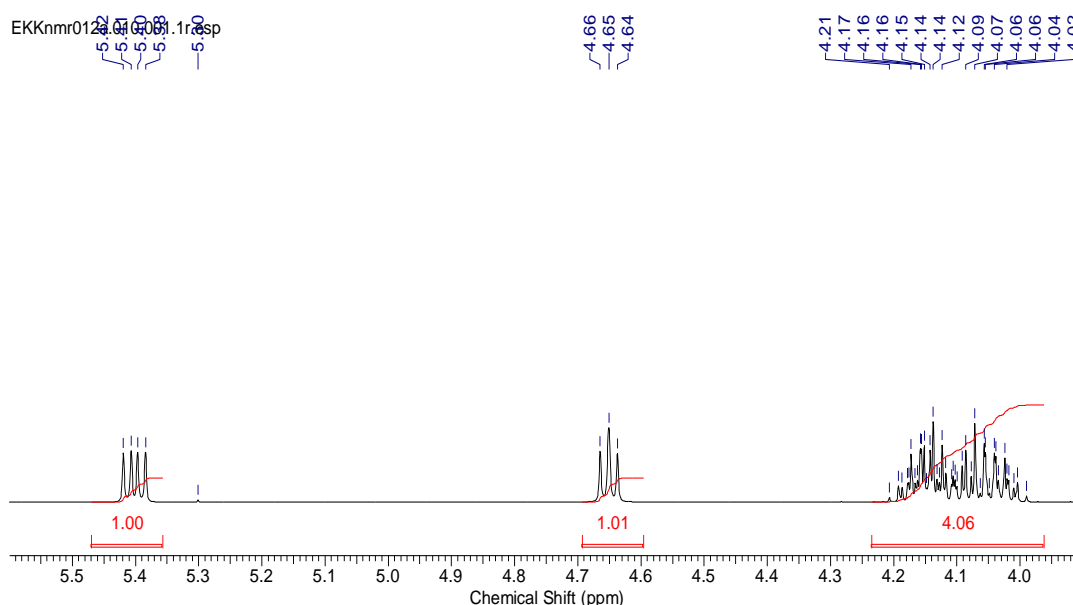


Figure 2.5.2: $^1\text{H-NMR}$ 2-fluorobenzyl- α -hydroxy diethyl phosphonate aliphatic region expanded

The peaks in the regions 7.02-7.71 ppm are from the hydrogens in the 2-fluoro-benzyl ring. The hydrogens in the aromatic region are observed as multiplets due to the fluorine coupling which leads to splitting of the peaks. The multiplet at 7.67-7.71 ppm ($^3J_{19\text{F}-1\text{H-o}} = 10.0, 5.0$ Hz) is the hydrogen that is in closest proximity to the C-F group. This peak experiences fluorine

coupling, generating a multiplet, which is observed. The effects of the fluorine coupling become weaker the further away the peak is from the C-F bond on carbon C-2 resulting in smaller longer range coupling. This peak resonates in this region because of the electron-withdrawing effects of the adjacent electronegative fluorine which pulls the H-3 hydrogen downfield. The peaks in the region 7.02-7.32 ppm shift upfield and are from the remaining hydrogens in the 2-fluoro benzyl ring.

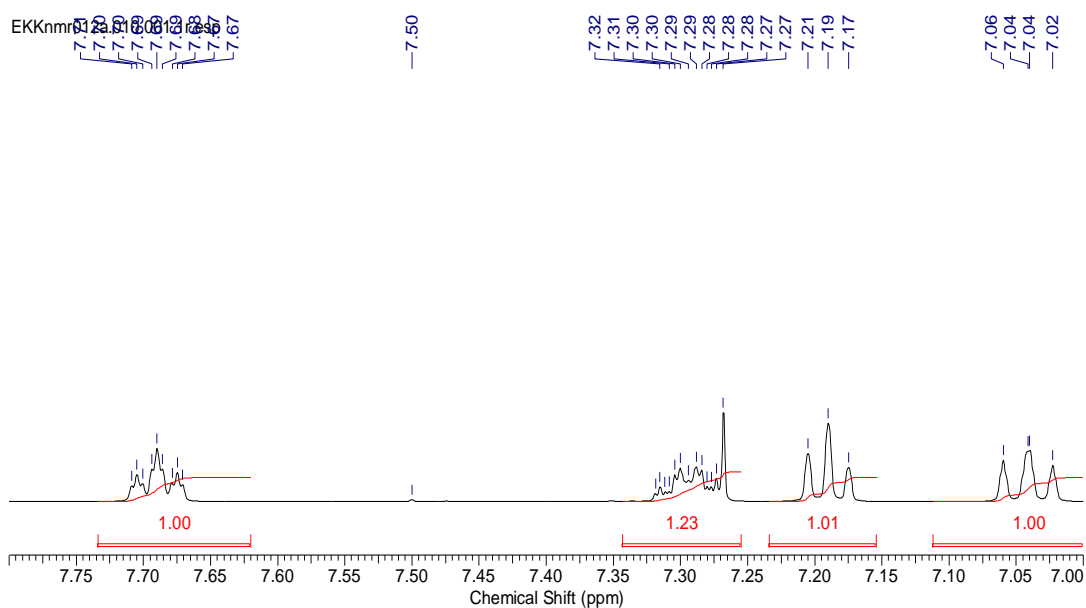


Figure 2.5.3: $^1\text{H-NMR}$ 2-fluorobenzyl- α -hydroxy diethyl phosphonate aromatic region expanded

2.5.2 $^{13}\text{C-NMR}$ 012A

The multiplet at 16.30-16.37 ppm represent the two CH_3 groups of the C-2' carbon.

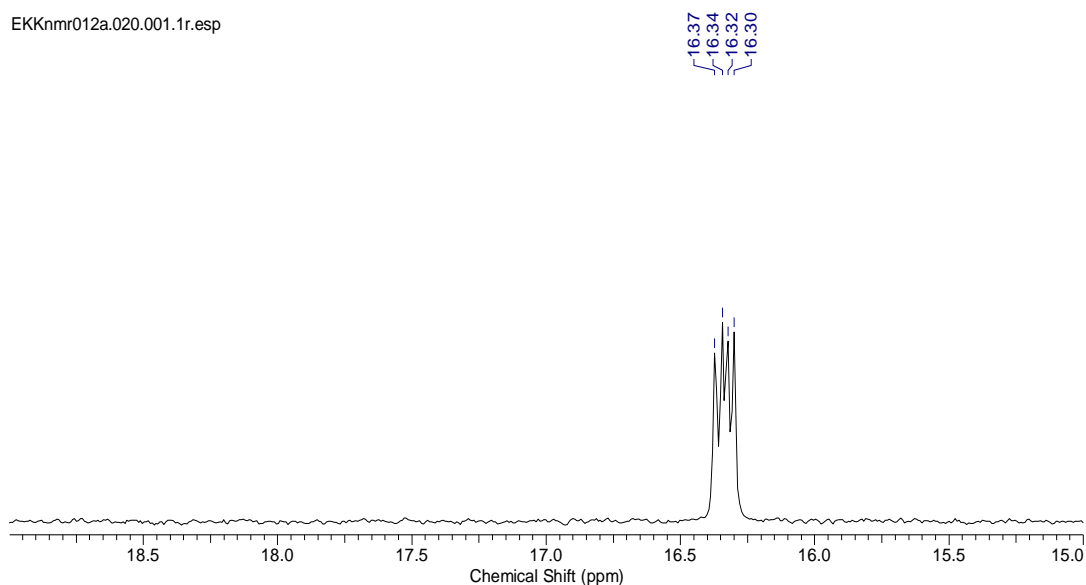


Figure 2.5.4: ^{13}C -NMR 2-fluorobenzyl- α -hydroxy diethyl phosphonate aliphatic region expanded

The doublets at 63.12-63.18 ppm ($^2J_{31\text{P}-^{13}\text{C}} = 7.6$ Hz) and 63.56-63.62 ppm ($^2J_{31\text{P}-^{13}\text{C}} = 7.6$ Hz) represent the two CH_2 groups from the carbon C-1'. The doublet of a doublet at 63.21-63.24 ppm and 64.50-64.53 ppm ($^1J_{31\text{P}-^{13}\text{C}} = 162.54$, $^3J_{19\text{F}-^{13}\text{C}} = 3.8$ Hz) represent the asymmetric carbon C-7.

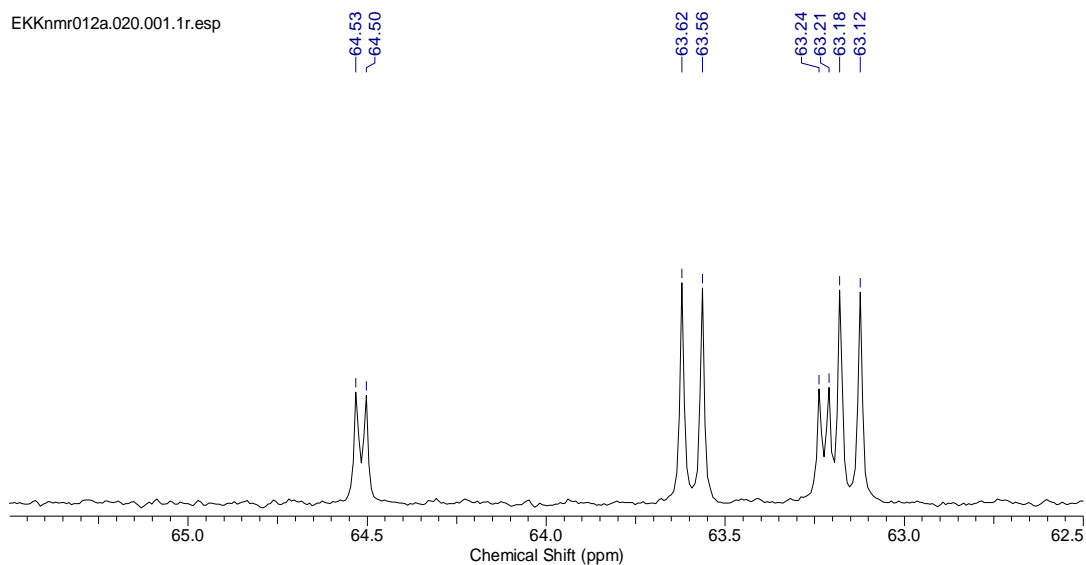


Figure 2.5.5: ^{13}C -NMR 2-fluorobenzyl- α -hydroxy diethyl phosphonate aliphatic region expanded

The peaks in the region 114.93-160.74 ppm are from the carbon atoms of the aromatic 2-fluoro-benzyl ring which produce 6 unique peaks. All of the peaks of the 2-fluoro-benzyl ring will experience C-F coupling and will be split hence they are observed as doublets. The doublet of a doublet at 158.72-158.78 and 160.68-160.74 ppm ($^4J_{31\text{P}-^{13}\text{C}} = 7.6$ Hz; $^1J_{19\text{F}-^{13}\text{C}} = 254.52$

Hz) are from the C-F, (C-2) in the 2-fluorobenzyl ring. This peak experiences phosphorus and fluorine coupling generating the doublet of a doublet.

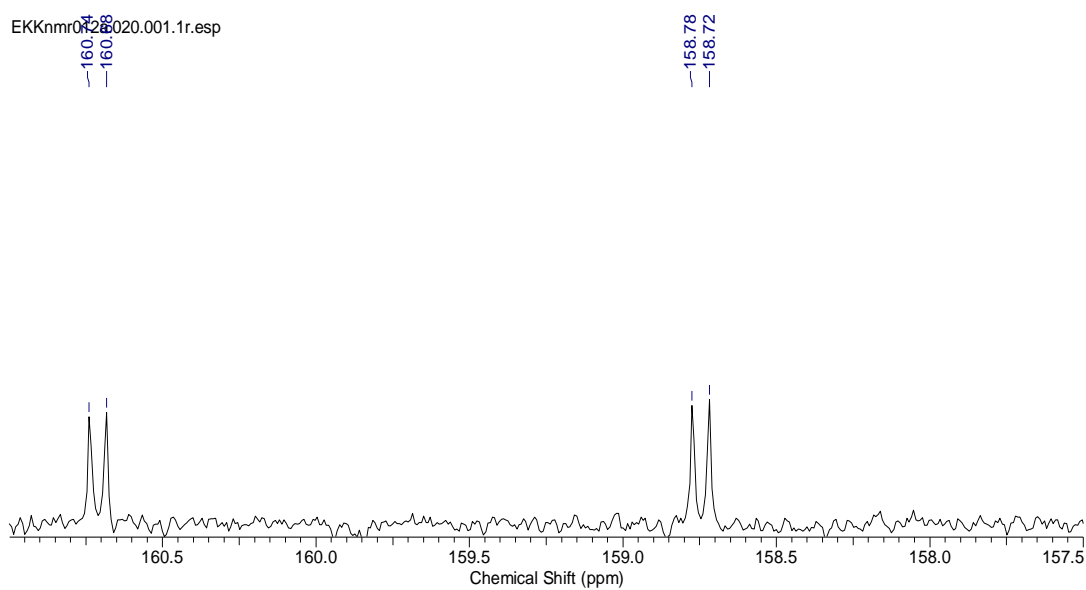


Figure 2.5.6: ¹³C-NMR 2-fluorobenzyl- α -hydroxy diethyl phosphonate aromatic region expanded

This peak is furthest downfield because it is directly attached to the electronegative fluorine. The effects of the fluorine coupling become weaker the further away the peaks are from the C-F bond on carbon C-2, resulting in smaller longer range C-F coupling.

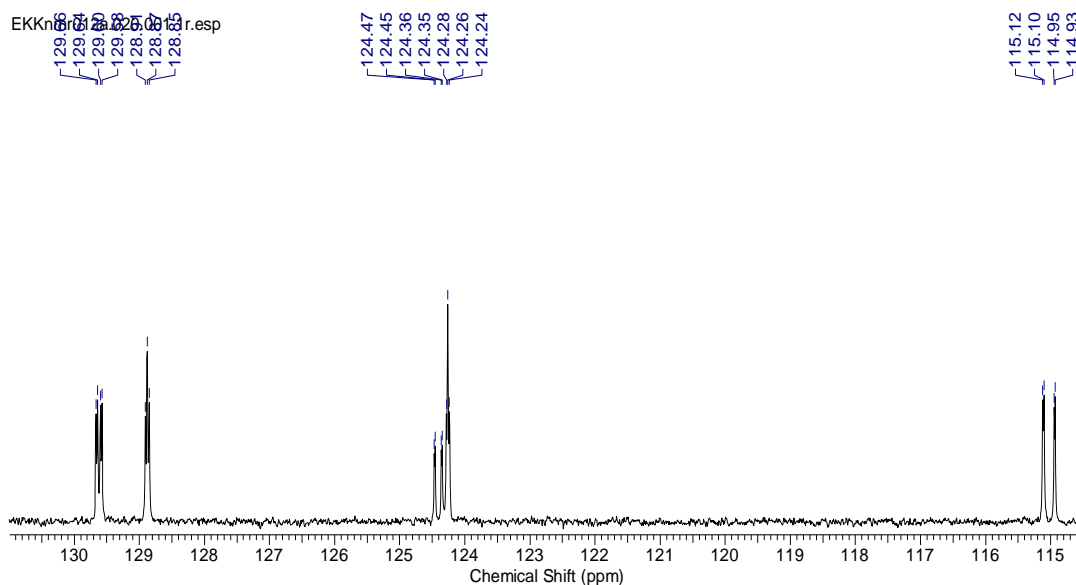


Figure 2.5.7: ^{13}C -NMR 2-fluorobenzyl- α -hydroxy diethyl phosphonate aromatic region expanded

2.5.3 ^{31}P -NMR012A

There is one peak present, a doublet, which is in the region 21.35-21.39 ppm. No other phosphorus containing compounds can be observed in the spectra.

2.6 Mass Spectrometry (EIMS⁺) (12)

2.6.1 MS012A

The Mr of the ion is 262. The peak at m/z 262 is the molecular ion. The peak at m/z 245 represents a loss of 17 amu, which indicates a loss of the hydroxyl group. The peak at m/z 233 is a loss of 29 amu which is a loss of CH_3CH_2^+ from the molecular ion. The CH_3CH_2^+ is from one of the ethyl groups from the diethyl group. The peak at m/z 217 arises from the loss of 45 amu, which is one of the $\text{OCH}_2\text{CH}_3^+$ groups, from the molecular ion. The fragment at m/z 186 is from the loss of 76 amu, which is the phenyl ring. The peak at m/z 172 is a fragment arising from the loss of both $\text{OCH}_2\text{CH}_3^+$ from the molecular ion. The fragment at m/z 153 represent the fragment $\text{CHPO}(\text{OCH}_2\text{CH}_3)_2$. The peak at m/z 138 is an $\text{F-C}_6\text{H}_4\text{CP}$ fragment that has cleaved off from the molecule. The peak at m/z 97 is a fragment representing the ion $\text{C}_6\text{H}_4\text{F}$. The peak at m/z 76.93 is from the fragment C_6H_4 phenyl ring.

2.7 1,2-Benzyl- γ -lactone-2-diethyl phosphonate (18)

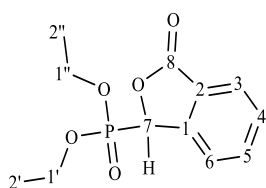


Figure 2.7.1: 1,2-benzyl- γ -lactone diethyl phosphonates with numbered carbons

2.7.1 $^1\text{H-NMR}$ 022A1

The triplets at 1.07-1.10 ppm and 1.40-1.43 ppm represent the two CH_3 groups of the C-2' and C-2'' carbons. The peaks are observed as two distinct separate peaks due to the presence of the γ -lactone ring, which confers a certain amount of rigidity and steric hindrances within the structure, therefore, the two diethyl groups are unable to rotate freely around the structure. As a result, each of the diethyl groups is in different environments and the hydrogens will appear in different areas of the spectra. The hydrogens of the C-2'' carbon are closer to the electronegative oxygen atoms of the γ -lactone ring, therefore, the peaks will resonate further downfield. The hydrogens of the C-2' carbon are closer to the benzyl ring which is less electron-withdrawing than the cyclic ester, hence will resonate further upfield in the region.

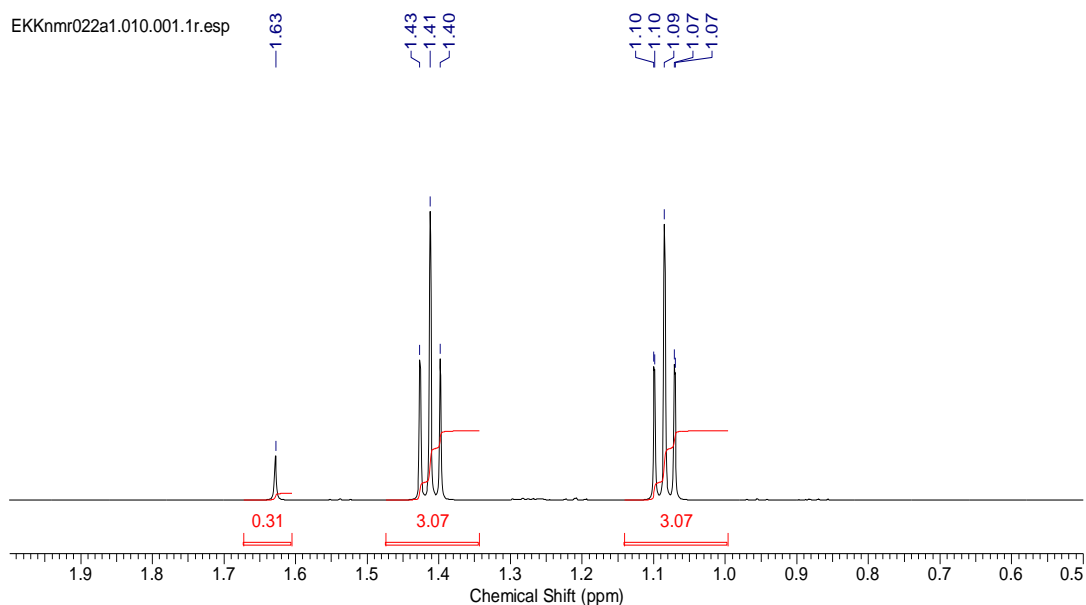


Figure 2.7.2: $^1\text{H-NMR}$ 1,2-benzyl- γ -lactone diethyl phosphonates aliphatic region expanded

The multiplets at 3.85-3.90 ppm, 3.99-4.04 ppm and 4.28-4.32 ppm represent the two CH_2 groups of the C-1' and C-1'' carbons. The hydrogens of the C-1'' carbon are closer to the

electronegative cyclic ester which will pull the peaks further downfield. Both hydrogens of the C-1'' carbon are represented within this multiplet. The hydrogens of the C-1' carbon are closer to the benzyl ring which is less electron-withdrawing than the cyclic ester, therefore they will resonate further upfield in the region 3.85-3.90 ppm and 3.99-4.04 ppm. These peaks experience phosphorus coupling which results in splitting of the peaks, generating a multiplets. Due to the 3D spatial arrangement of the C-1' carbon's hydrogens, one of the hydrogens will be closer to the γ -lactone ring than the other and that hydrogen will be pulled slightly further downfield than the other hydrogen on the same carbon which is why the peaks of these hydrogens are observed as two separate peaks.

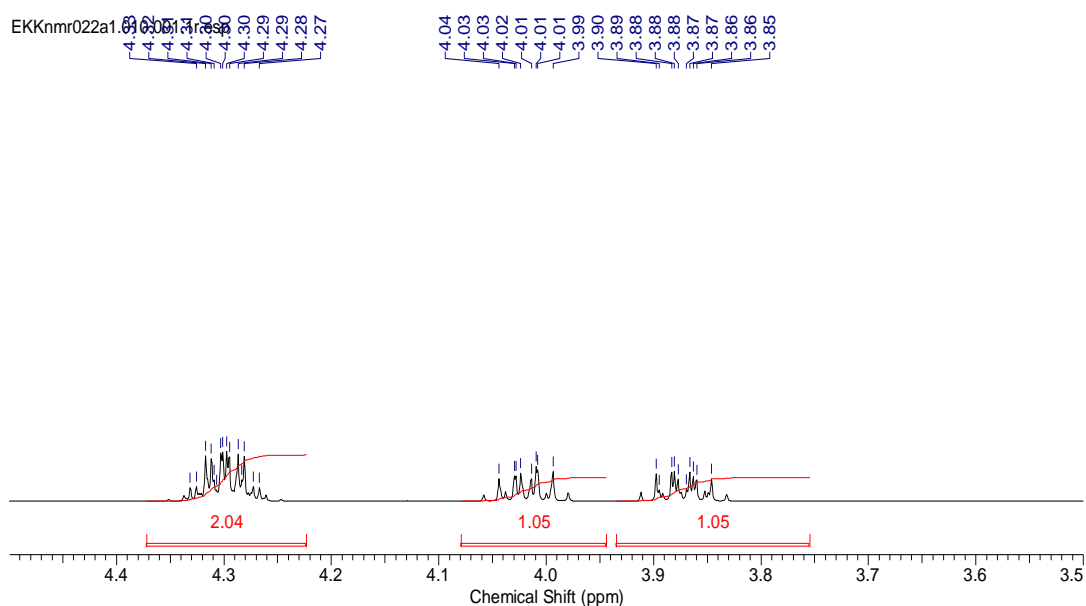


Figure 2.7.3: $^1\text{H-NMR}$ 1,2-benzyl- γ -lactone diethyl phosphonates aliphatic region expanded

The doublet at 5.68-5.71 ppm ($^2J_{31\text{P}-1\text{H}} = 15$ Hz) is from the CH of the asymmetric carbon (C-7); this C-H is observed further downfield because of the electron-withdrawing effects of the adjacent cyclic ester. The peak of the hydroxyl group is not available in this compound as it is now part of the cyclic ester. This peak is from a hydrogen that is attached to a carbon (C-7) which is directly bonded to the phosphorus and therefore, there is splitting that is observed as a result of P-H phosphorus coupling.

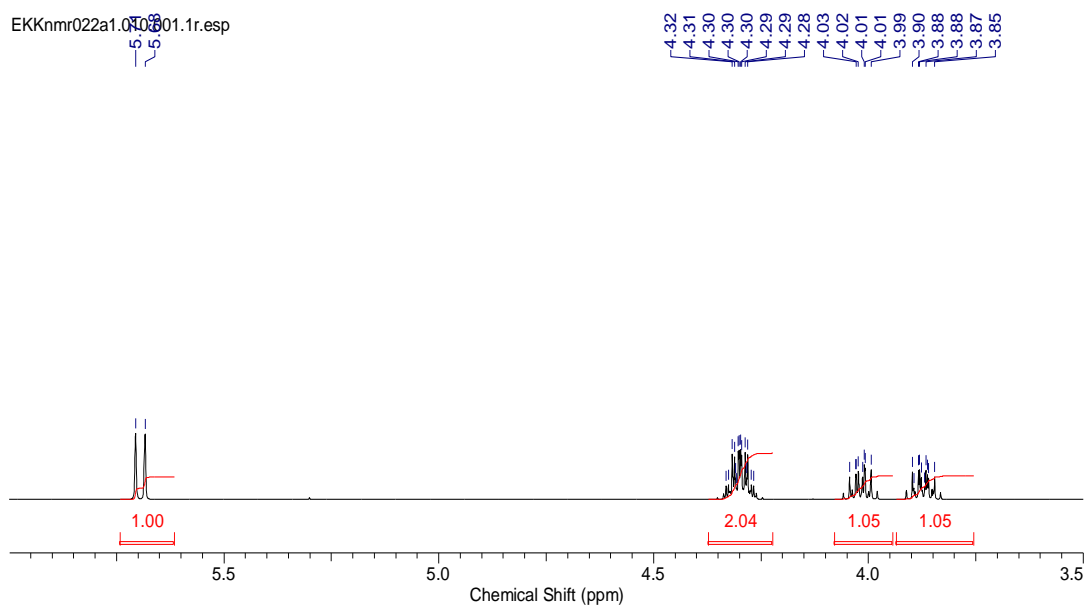


Figure 2.7.4: $^1\text{H-NMR}$ 1,2-benzyl- γ -lactone diethyl phosphonates aliphatic region expanded

The peaks in the regions 7.27-7.96 ppm are from the hydrogens in the 1,2- γ -lactone-benzyl ring. The peak that is at 7.94-7.96 ppm is the hydrogen that is closest to the C-O group of the cyclic ester which is H-3 in the benzyl ring. The nuclei of this hydrogen; H-3 is 'deshielded' due to the electron-withdrawing effects of the adjacent electronegative cyclic ester carbonyl group and therefore experiences greater influence from the external magnetic field and hence the chemical shifts resonate downfield. The rest of the peaks shift upfield as the hydrogens move further away from the electron-withdrawing groups.

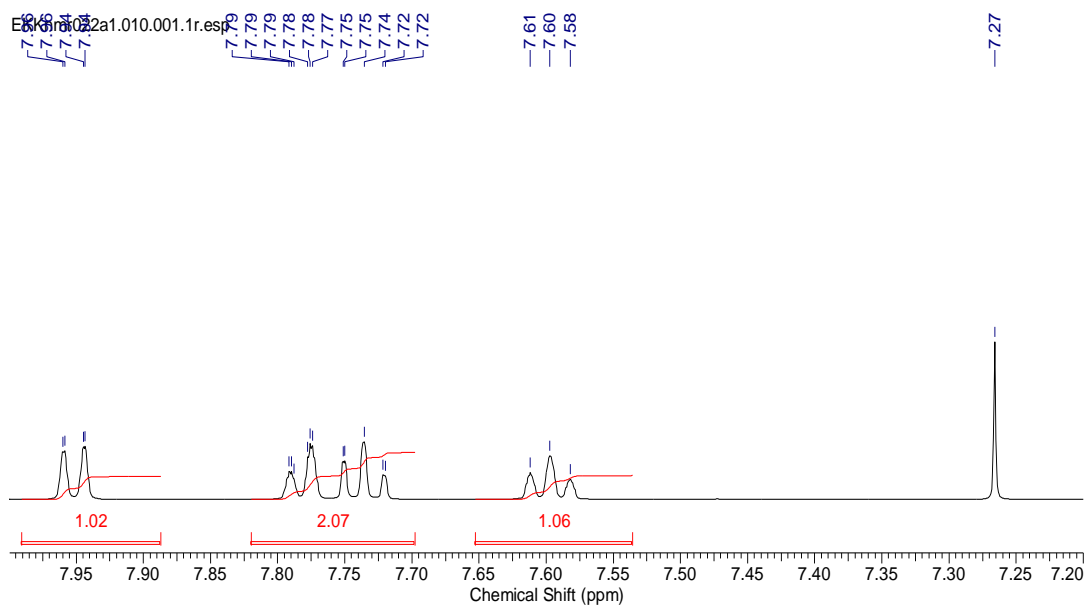


Figure 2.7.5: $^1\text{H-NMR}$ 1,2-benzyl- γ -lactone diethyl phosphonates aromatic region expanded

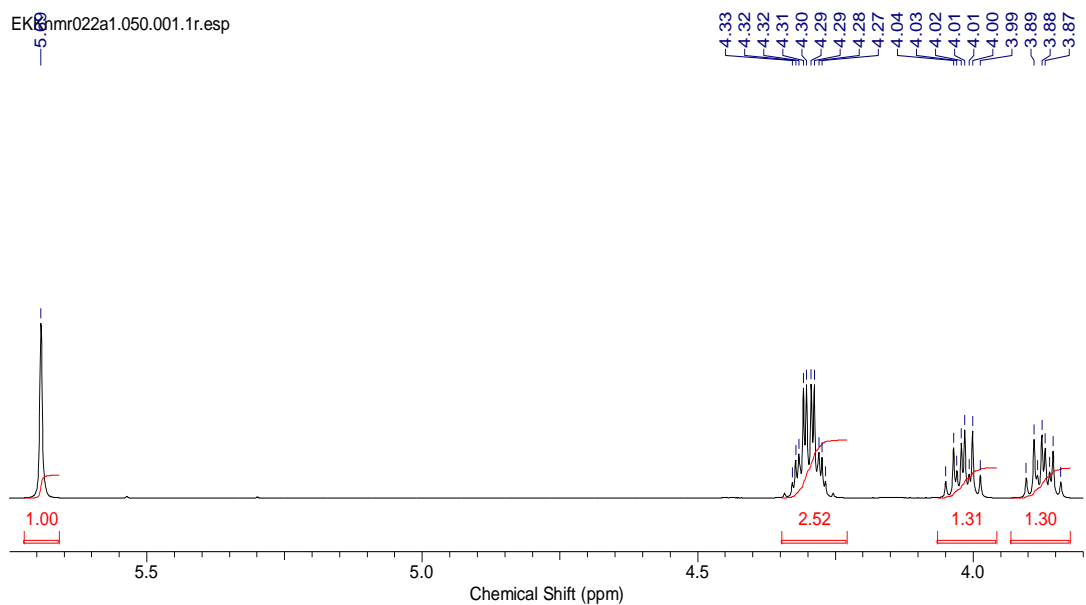


Figure 2.7.6: $^1\text{H-NMR}$ D_2O shake 1,2-benzyl- γ -lactone diethyl phosphonates aliphatic region expanded

2.7.2 $^{13}\text{C-NMR022A1}$

The doublets at 16.17-16.49 ppm ($^3J_{31\text{P}-^{13}\text{C}} = 6.3$ Hz) represent the two CH_3 groups of the C-2' and C-2'' carbons.

EKKnmr022a1.020.001.1r.esp

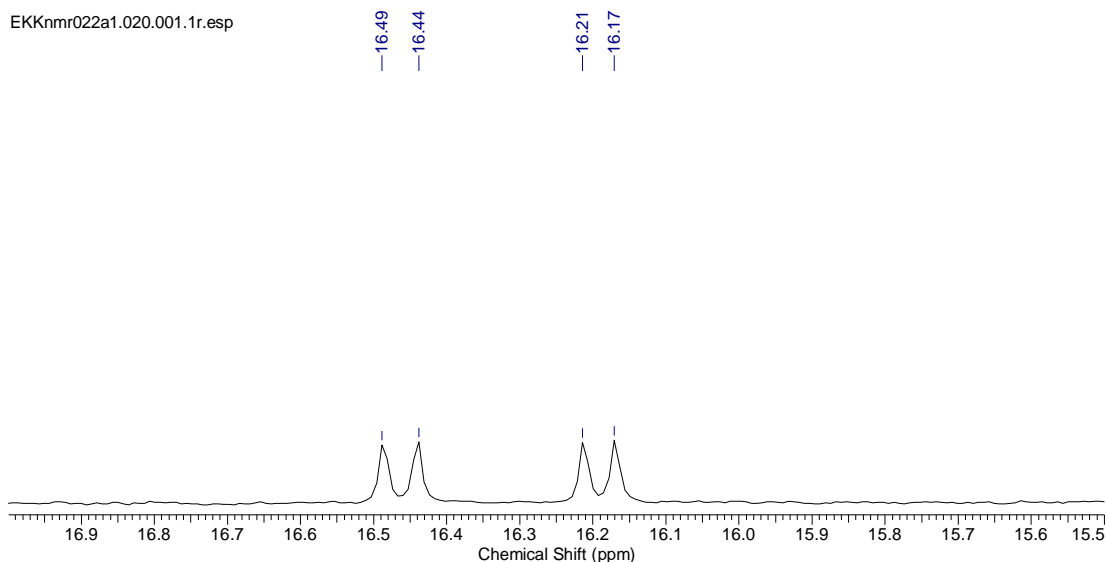


Figure 2.7.7: ^{13}C -NMR 1,2-benzyl- γ -lactone diethyl phosphonates aliphatic region expanded

The doublets at 63.96-64.35 ppm ($^2J_{31\text{P} - ^{13}\text{C}} = 6.3$ Hz) represent the two CH_2 groups from the carbon C-1' and C-1''. The peaks experience phosphorus coupling which results in splitting of the peaks, generating the doublets that are observed.

EKKnmr022a1.020.001.1r.esp

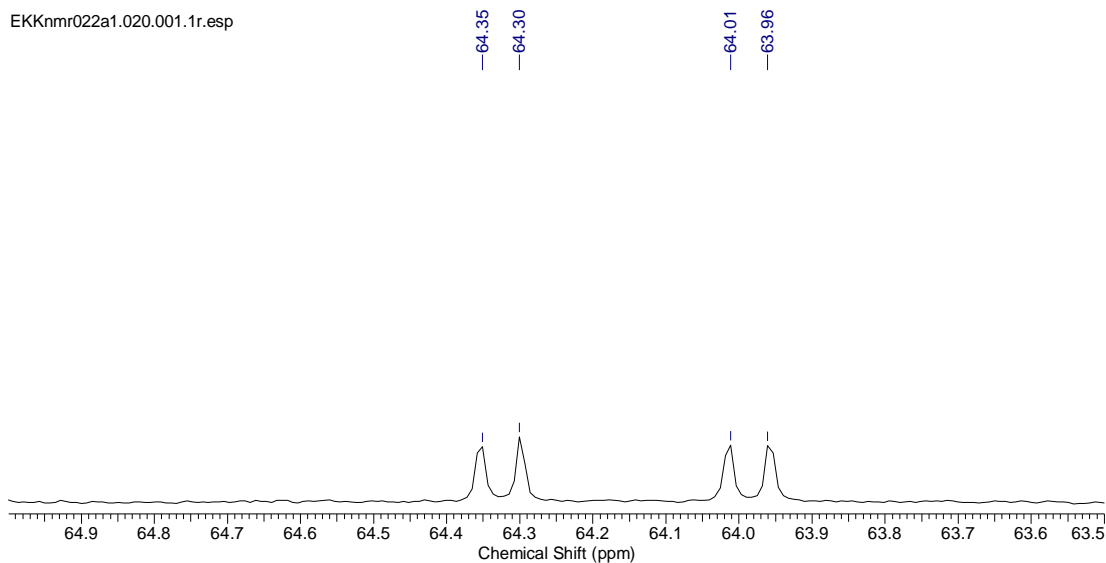


Figure 2.7.8: ^{13}C -NMR 1,2-benzyl- γ -lactone diethyl phosphonates aliphatic region expanded

The doublet at 74.91-76.22 ppm ($^1J_{31\text{P} - ^{13}\text{C}} = 165.06$ Hz) represent the asymmetric carbon C-7.

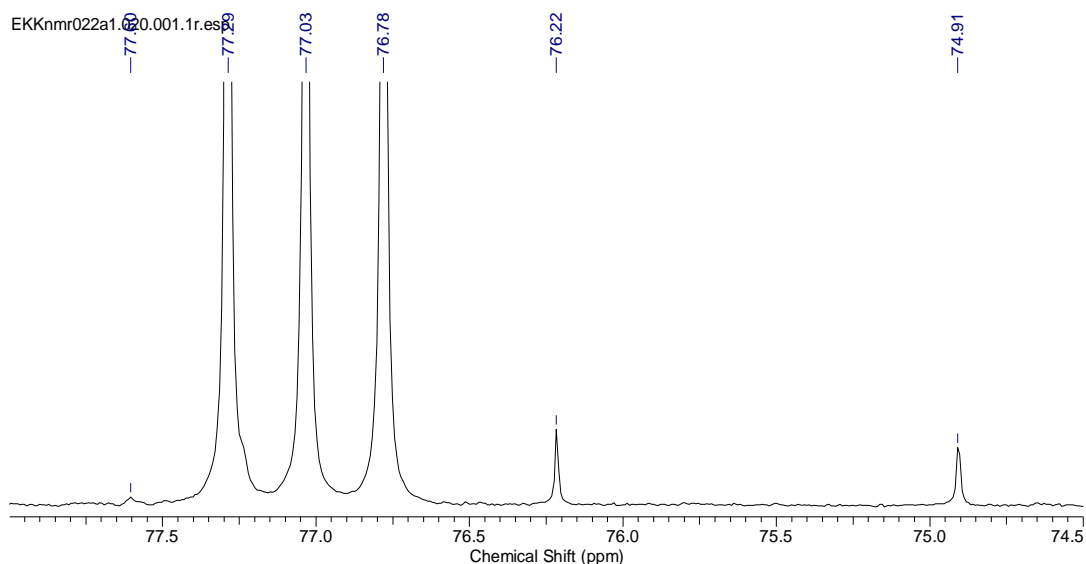


Figure 2.7.9: ^{13}C -NMR 1,2-benzyl- γ -lactone diethyl phosphonates aliphatic region expanded

The peaks in the region 123.65-169.77 ppm are from the carbon atoms of the aromatic 1,2- γ -lactone-benzyl ring which give 7 peaks. The peak in the region 143.83-143.86 ppm is from the C-C=O, (C-2) carbon. The peak at 169.77 ppm is from the carbonyl; C=O of the (C-8) carbon of the 1,2- γ -lactone ring.

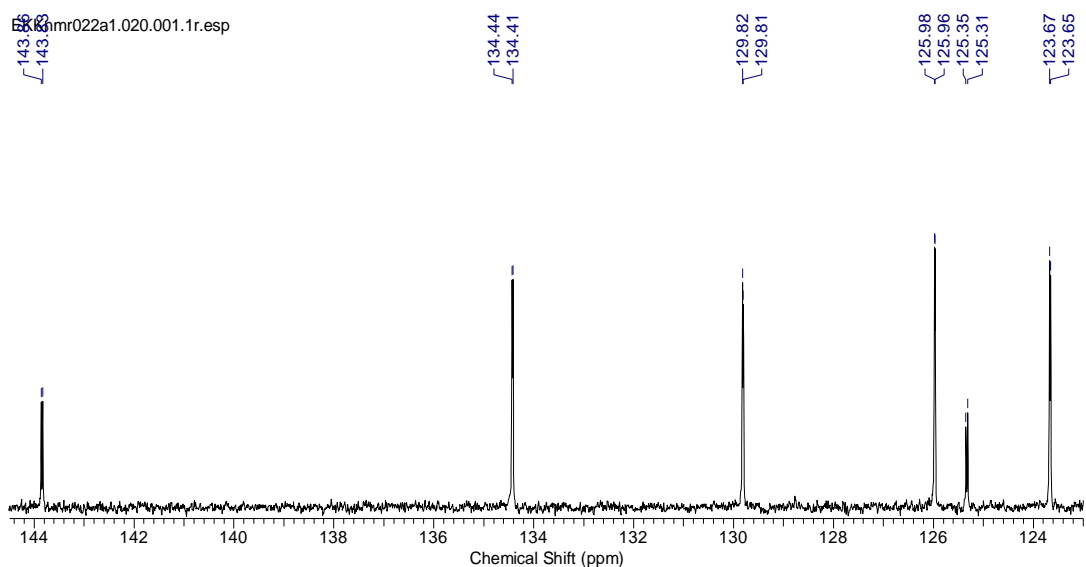


Figure 2.7.10: ^{13}C -NMR 1,2-benzyl- γ -lactone diethyl phosphonates aromatic region expanded

2.7.3 ^{31}P -NMR022A1

There is one peak present, which occurs at 13.80 ppm. No other phosphorus containing compounds can be observed in the spectra.

2.8 Mass Spectrometry (TOF MS ES⁺) (18)

2.8.1 MS022A1

The Mr of the ion is 270. The peak at m/z 271 which is the molecular ion, $[M+H]^+$. The peak at m/z 243 is a loss of 29 amu indicating a loss of one of the diethyl group from the molecular ion. The peak at m/z 215 is a loss of 56 amu which represents a loss of two of the $CH_3CH_2^+$ groups from the molecular ion. The peak at m/z 133 is from the fragment $C_8H_5O_2$ which is the isobenzofuranone (benzyl-lactone ring). The lactone ring is susceptible to heterolytic cleavage, leading to the opening of the five-membered ring and formation of the acylium ion. The peak at m/z 293 arises from the addition of a sodium ion to the molecular ion, $[M+Na]^+$.

2.9 Infrared spectroscopy (18)

The IR spectrum of 1,2-benzyl lactone-2-diethyl phosphonate was obtained and confirmed the presence of the lactone ring. The absence of the nitrile stretch in the 2229 cm^{-1} region confirmed that the nitrile group had reacted. That in combination with the presence of the C=O peak in the 1771 cm^{-1} region suggested the formation of the lactone ring. The C=O peak is not observed in the IR spectra of all the other R-benzyl- α -hydroxyl diethyl phosphonate compounds. The O-H stretch is absent in the IR spectrum of this compound.

2.10 Conversion of the α -hydroxyl to the methylene group

2.10.1 Reaction mechanism

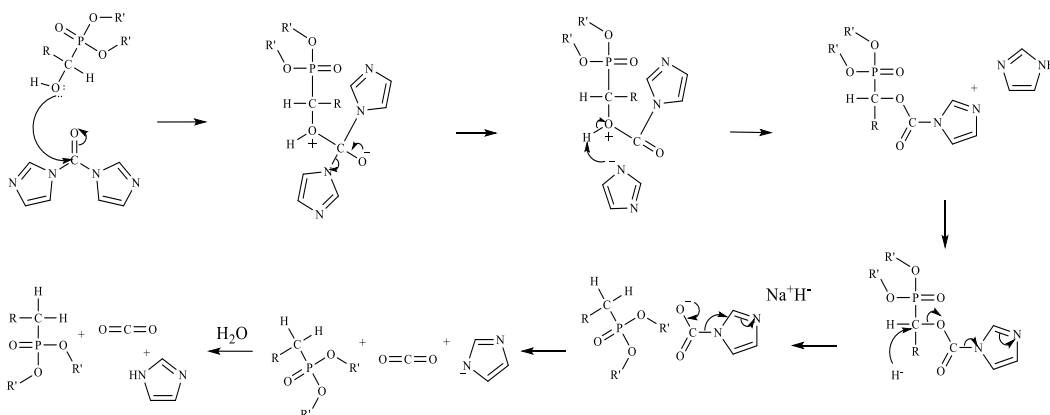


Figure 2.10.1: General reaction mechanism for the synthesis of substituted benzyl- α -methylene phosphonates

These reactions were adapted from the one step conversion of alcohols into alkyl halides through oxycarbonylimidazolium intermediates (Kamijo, T, et al 1983). It seemed feasible to replace the hydroxyl group of the α -carbon with hydride anion by making a slight alteration to the original procedure. The lone pair of electrons of the oxygen of the starting hydroxyl group acts as a nucleophile and attacks the carbonyl group of the carbonyl diimidazole group to give an imidazolium ester, following deprotonation of the resulting intermediate by the displaced imidazole anion. The formation of this complex is very crucial for the substitution of the hydroxyl group. This step must occur in dry conditions because any moisture will stop the reaction from occurring. As such, water and all protic solvents must be avoided as they react with the hydride anion. This esterification process makes the α -carbon a good electrophile and therefore an excellent target for a hard nucleophile such as a halide. For the purposes of our reaction, the hard nucleophile was the hydride anion (H^-). The H^- attacks the δ^+ α -carbon which results in the breaking of the C-O bond to form a carbon dioxide molecule and another imidazole anion. The imidazole anion is then deprotonated during the work up to generate imidazole. This step completes the final substitution from the α -hydroxyl carbon to the α -methylene carbon. The final products are the α -methylene compound, carbon dioxide and imidazole. The reaction is cost effective when compared to similar methods that are used in organic substitution reactions which convert a C-OH to a C-H. Since substitution is a crucial

method for functional groups interconversion, it is important to continually find ways to make the reaction as environmentally friendly and non-toxic as possible. This is not currently possible with current reducing agents such as lithium aluminium hydride, borane and hydrogen which are all hazardous (*Lawrence. J. N, et al 1999*).

All the attempted reactions were observed to proceed to completion through TLC, and, following aqueous work-up and column chromatography, the products were obtained as oils in moderate to good yields. Most of the starting α -hydroxyl phosphonates compounds dissolved in dry acetonitrile with the exception of 3-nitrobenzyl- α -hydroxy dibenzyl phosphonate and 4-nitrobenzyl- α -hydroxy dibenzyl phosphonate which were dissolved in dry THF. The compounds 3-nitrobenzyl- α -methylene dibenzyl phosphonate, 2-nitrobenzyl- α -methylene dibenzyl phosphonate and 2-nitrobenzyl- α -methylene diethyl phosphonate were synthesised but could not be purified due to the presence of competing reactions. The TLC profiles of these compounds showed two spots which corresponded to two different products with similar R_f values, therefore, eluted from the column at the same time. These two products could not be resolved by either changing the eluent systems, column size or the amount of silica gel used. Some of the solvent systems that were attempted were hexane: ethyl acetate 2:8, 1:1 and 4:6. Diethyl ether: ethyl acetate 1:1 and 2:8. Hexane: ethyl acetate: dichloromethane 2:6:2. Alternative purification methods such as the use of Prep TLC plates were unsuccessfully attempted. It is assumed, at the moment, that the reason that these three compounds are forming more by-products is due to hydride abstraction of the relatively acidic hydrogen on the asymmetric carbon.

The synthesis of these substituted benzyl- α -methylene phosphonates suggested that there is a possibility for the hydroxyl group to be substituted with various functional groups to give different compounds. The rationality being that an activated imidazolium ester of the substituted benzyl- α -hydroxy phosphonate could turn the hydroxyl into a good leaving group that could be replaced easily by a good nucleophile. Consequently, it seems feasible to convert the hydroxyl group to an amine and or amide functional group by using sodium azide which

could then be reduced to the amine by catalytic hydrogenation or by sodium borohydride (NaBH_4) in methanol.

2.11 Possible side reactions for the substituted benzyl- α -methylene phosphonates

2.11.1 Possible side reaction 1

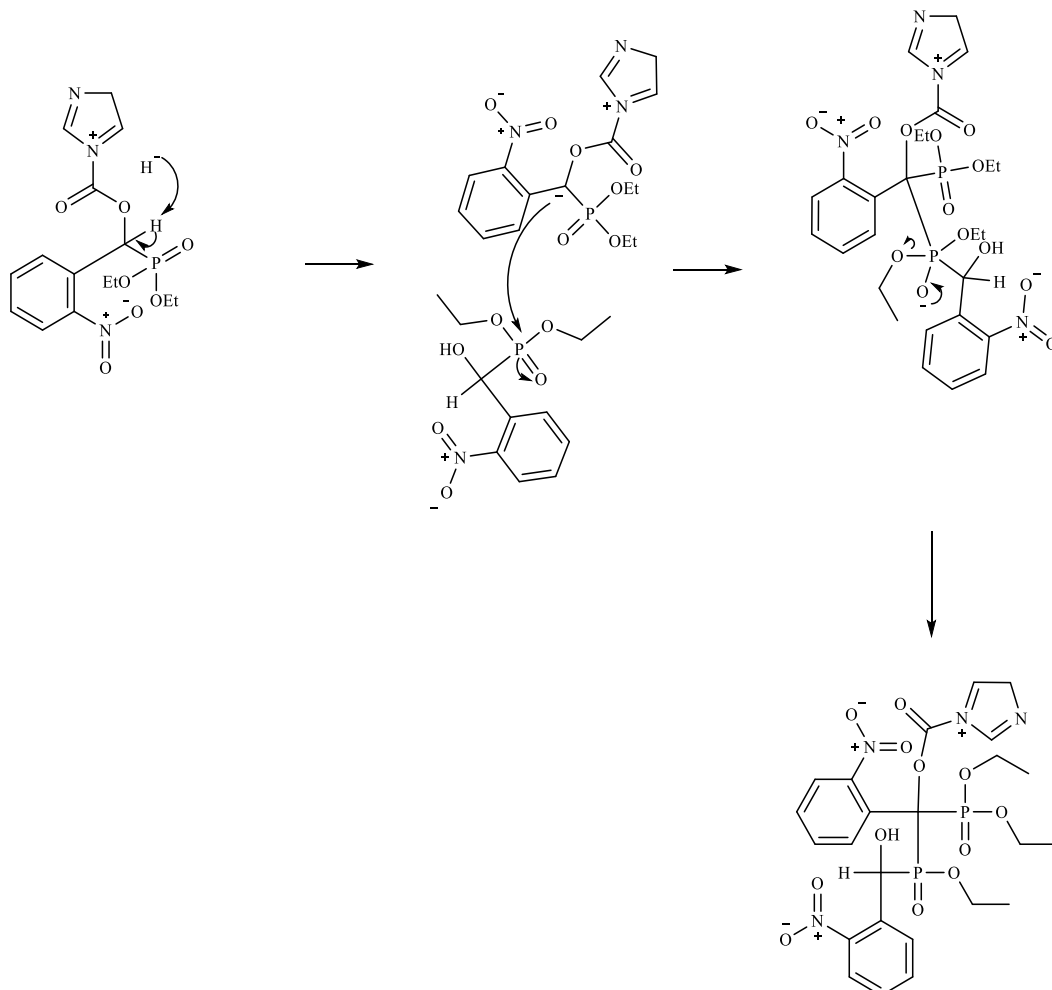


Figure 2.11.1: Possible side reaction mechanism for the substituted benzyl- α -methylene phosphonates 1

2.11.2 Possible side reaction 2

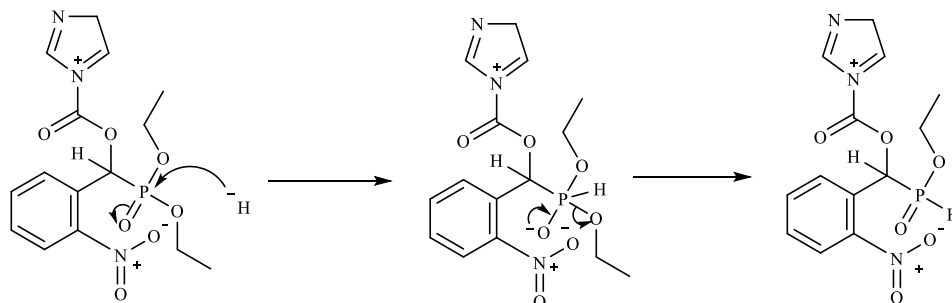


Figure 2.11.2: Possible side reaction mechanism for the substituted benzyl- α -methylene phosphonates 2

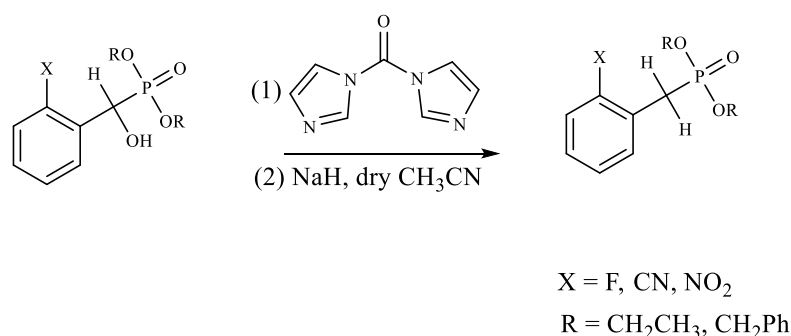


Figure 2.11.3: substituted benzyl- α -methylene phosphonates reaction scheme

Table 6: Synthesized substituted benzyl- α -methylene dibenzyl phosphonates and their respective yields

Compounds	Yield %
2-Fluorobenzyl-dibenzyl phosphate (19)	24
2-Fluorobenzyl-diethyl phosphate (20)	93
4-Cyanobenzyl-diethyl phosphate (22)	59
3-Cyanobenzyl-diethyl phosphate (21)	14
3-Nitrobenzyl-diethyl phosphate (23)	47
4-Nitrobenzyl- α -methylene diethyl phosphonate (25)	20
4-Nitrobenzyl- α -methylene dibenzyl phosphonate (24)	25

The α -CH₂ hydrogens of the desired α -methylene phosphonate esters should resonate at 3.00ppm and not 5.00ppm in the ¹H-NMR spectra. With the exception of the 4-nitro derivative (**24** and **25**), all of the α -CH₂ hydrogens of the synthesised methylene compounds resonated at 5.00ppm. A closer examination of the ³¹P-NMR and ¹³C-NMR spectra also highlighted a few substantial irregularities;

- 1) The phosphorus resonances and the observed phosphorus- α -carbon (C-7) coupling constants. With the exception of the 4-nitro derivative, all of the benzyl-phosphonates had J_{P-C7} coupling constants of 5.0 Hz instead of the expected values, which are in the region of 150 Hz.
- 2) The ³¹P-NMR δ -values were all in the 0.35 to -0.60 ppm range, which is expected for phosphates, but not phosphonates, whose ³¹P-NMR δ -values occur in the 15 to 30 ppm region.

- 3) Closer examination of the electron-impact mass spectra of the benzyl-phosphonates, clearly show the presence of the relevant substituted benzyl carbocations in very high relative abundances, which is not expected for phosphonates but very commonly observed in phosphates. The 2-fluoro derivatives **19** and **20** show the expected carbocation $C_7H_6F^+$ (m/z 109.0) in 60% and 100% relative abundances respectively. The 3-nitro derivative **23** shows the expected carbocation $C_7H_4NO_2^+$ (m/z 134.0) at 100% but the 4-nitro derivatives **24** and **25** display this carbocation at 35% and 12% relative abundances, respectively. The 3- and 4-cyano derivatives **21** and **22** all show the expected carbocation $C_8H_6N^+$ (m/z 116.0) at 100% abundances. Furthermore, peaks that correspond to the molecular ion peak for the phosphate ester products have been observed in the electron-impact mass spectra for the compounds **19**, **20**, **21**, **22** and **23**.
- 4) All attempted hydrolysis reactions of the benzyl-phosphonate esters did not yield the expected phosphonic acids or their salts. Using either of the procedures mentioned in the hydrolysis section of this thesis below, in all cases the attempted hydrolysis of these compounds produced solid residues that were insoluble in all NMR solvents or solvent mixtures (DMSO, DMSO- D_2O , D_2O -NaOD, methanol) and as a result we were unable to obtain any NMR data.

This data suggests strongly that our modified *Kamijo* reaction has possibly yielded phosphate ester products rather than our desired phosphonates, with the exception of the 4-nitro derivatives (**24** and **25**). This occurs by means of a 1,2- Phospha-Brook rearrangement, which is an intramolecular phosphonate-phosphate rearrangement under basic conditions. This rearrangement has been well studied but, has shown to have limited applicability to substrates having α -H (*Khan. S, et al 2016*). The Phospha-Brook rearrangement is mechanistically analogous to the Brook rearrangement, which comprises the anionic migration of a silyl group from a carbon atom to an oxygen atom, thereby converting an oxyanion (typically a lithium alkoxide) to a carbanion (an organolithium) in the presence of catalytic base such as NaOH,

NaOEt, NaH, Na-K, Et₂NH and DBU (*Smith. A, et al 2006; Prechelmacher. S, et al 2018*). The simplest Brook rearrangement being the 1,2- Brook rearrangement, has been shown to proceed intramolecularly, via a hypervalent pentacoordinate silicon species with retention of configuration at silicon and inversion of configuration at carbon (*Brook. A. G, et al 1974*). The Phospha-Brook intramolecular rearrangement proceeds via a pentacoordinate phosphorus species with retention of configuration at phosphorus and inversion of configuration at carbon (*Pudovik. A. N, et al 1980*). An alternate method to make the hydroxyl a good leaving group is to convert it into a sulfonate ester [methanesulfonates (mesylates)] which can then take part in a substitution reaction.

The rearrangement under the reaction conditions could arise from the failure of the reaction with carbonyl diimidazole, presumably for steric reasons, and then reaction with hydride anion which deprotonates the alcohol, leading to the formation of a charged epoxy phosphono-intermediate, which then ring opens to yield the benzyloxy carbanion, which is resonance stabilized by the presence of the electron-withdrawing substituents, in particular CN and NO₂ on carbons 2 and 4. This does not fully explain why the C-3 derivatives also presumably undergo this rearrangement, nor why, in the case of the 4-nitro derivatives (**24** and **25**), the desired products have been formed. The failure of the hydrolyses reactions carried out on the putative benzyl-phosphonate esters (**19-25**) may be explained by the rapid hydrolyses of the phosphates to yield phosphoric acid which was then converted into insoluble polyphosphates upon workup, in particular during rotary evaporation of the highly acidic 6M HCl solutions employed.

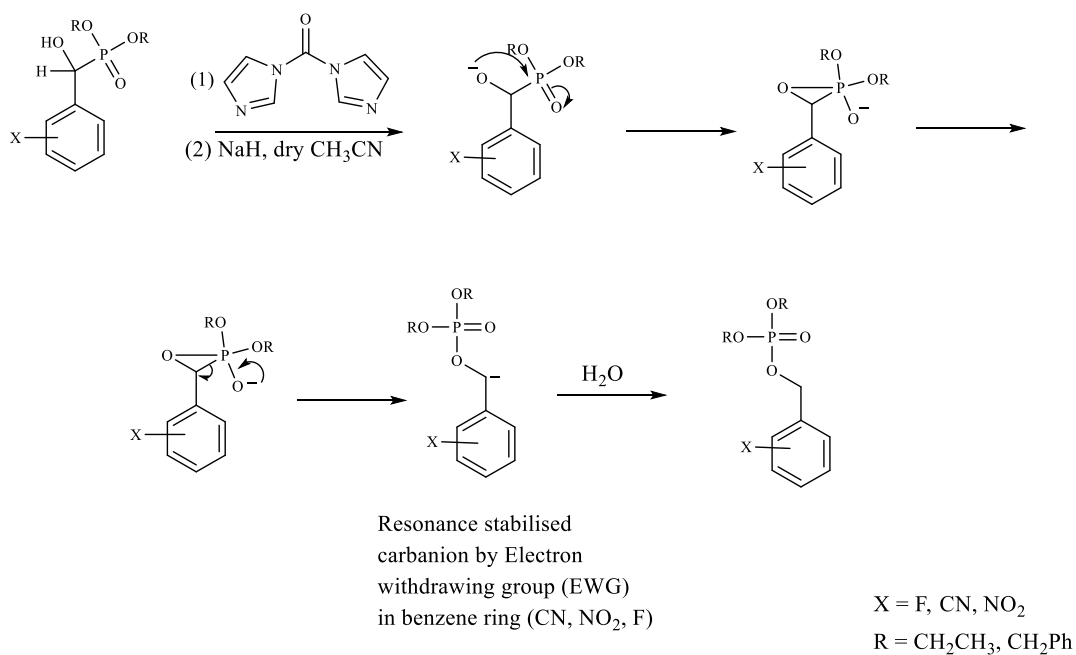


Figure 2.11.4: A possible phosphonate to phosphate rearrangement, via an epoxy-phosphono-intermediate, that occurs in the attempted conversion of the α -OH compounds into their benzyl phosphate derivatives. (EWG: electron-withdrawing group).

Table 7: The observed J_{P-C7} coupling constants and ^{31}P δ -values for all of our synthesized targets (PA = phosphonic acids).

Compound No	Benzyl derivative (X)	Phosphonate ester	C ₇ -X'	J_{P-C7} /Hz	^{31}P / δ
6	2-F	PhCH ₂	OH	163.50	22.19
9	2-NO ₂	PhCH ₂	OH	158.76	21.59
18	2-CO ₂ -lactone	PhCH ₂	OH	165.06	13.80
29	2-F	PA	OH	152.50	16.55
30	2-NO ₂	PA	OH	142.38	15.57
27	2-CO ₂ -lactone	PA	OH	158.58	12.86
34	2-F	PA	NH ₂	165.06	13.80
26	3-CO ₂ H	PA	OH	163.80	20.68
28	4-CO ₂ H	PA	OH	161.28	20.38
20	2-F	CH ₃ CH ₂	H	5.0	-0.60
19	2-F	PhCH ₂	H	5.0	-0.51
21	3-CN	CH ₃ CH ₂	H	5.0	-0.49
7	3-CN	CH ₃ CH ₂	OH	160.02	21.39
13	3-CN	PhCH ₂	OH	161.28	20.56
10	4-CN	PhCH ₂	OH	157.50	21.20
14	4-CN	CH ₃ CH ₂	OH	157.50	20.43
8	3-NO ₂	PhCH ₂	OH	158.70	21.17
11	4-NO ₂	PhCH ₂	OH	157.50	21.03
12	2-F	CH ₃ CH ₂	OH	162.54	21.35
15	3-NO ₂	CH ₃ CH ₂	OH	160.02	20.36
16	4-NO ₂	CH ₃ CH ₂	OH	157.50	20.20
17	2-NO ₂	CH ₃ CH ₂	OH	161.28	20.58
22	4-CN	CH ₃ CH ₂	H	6.30	-0.49
23	3-NO ₂	CH ₃ CH ₂	H	5.0	-0.46
25	4-NO ₂	CH ₃ CH ₂	H	137.34	24.61
24	4-NO ₂	PhCH ₂	H	137.34	25.85

The distinct section of the 1H and ^{13}C -NMR for these compounds was the asymmetric section [- α -CH₂-P-]; (C-7). As with the - α -hydroxy phosphonates, the peaks in this region experience phosphorus coupling therefore splitting is observed with these peaks due to (P-H) and (P-C) phosphorus coupling. Compounds in which the aryl group contained fluorine resulted in the

asymmetric section experiencing additional splitting from long range fluorine coupling hence the peaks were observed as multiplets. The absence of the $-\alpha\text{-C(OH)}$ confirmed the conversion to $-\alpha\text{-CH}_2$ had occurred for the compounds **24** and **25**, the rest the rearrangement reaction had occurred.

Table 8: Distinguishing peaks of the substituted benzyl- α -methylene dibenzyl phosphonates/phosphates

Compound	$\delta_{\text{H}} \text{CH}_2$ (ppm)	$\delta_{\text{C}} \text{CH}_2$ (ppm)	δ_{P} (ppm)	$J_{31\text{P}-13\text{C}}$ (Hz) (C-7)
19	5.09	63.14	-0.51	5.0
20	5.14	62.88	-0.60	5.0
21	5.09	67.49	-0.49	-
22	5.13	67.64	-0.49	6.3
23	5.17	67.42	-0.46	5.0
24	3.21	34.33	25.85	137.34
25	3.25	34.01	24.61	137.34

2.12 2-Fluorobenzyl-dibenzyl phosphate (19)

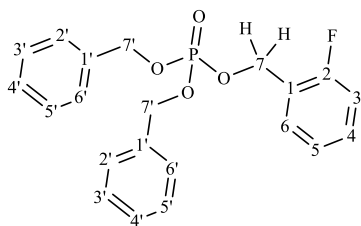


Figure 2.12.1: 2-fluorobenzyl-phosphate with numbered carbons

2.12.1 $^1\text{H-NMR001B2}$

The doublet at 5.02-5.04 ppm ($^3J_{31\text{P}-1\text{H}} = 10$ Hz) represent the two CH_2 groups of the 7' carbons (C-7'). The peaks at 5.08 ppm and 5.09 ppm are from the α -methylene CH_2 , of the C-7 carbon.

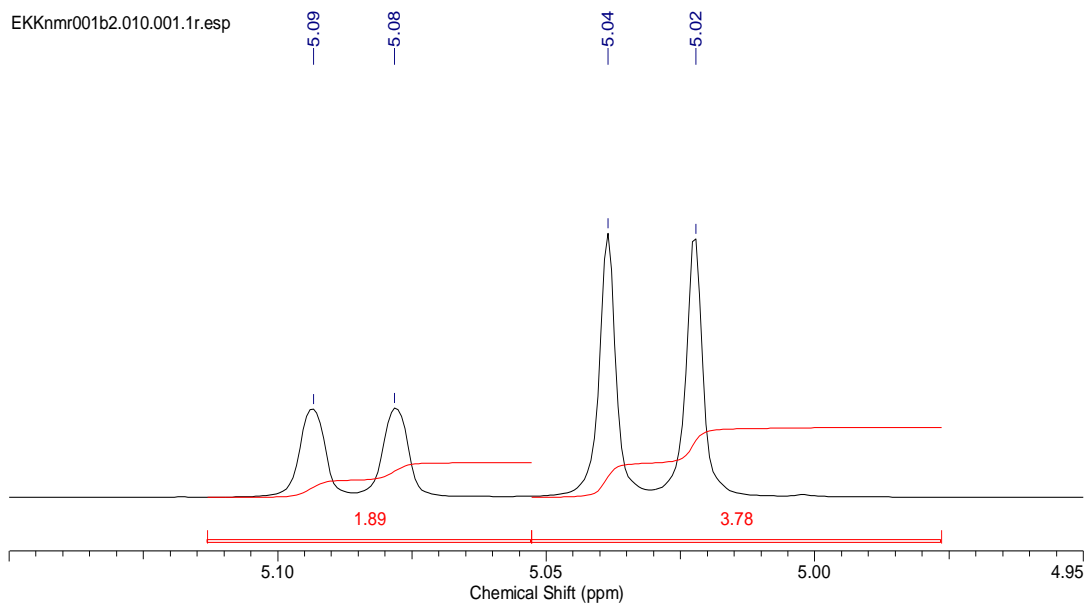


Figure 2.12.2: $^1\text{H-NMR}$ 2-fluorobenzyl-dibenzyl phosphate aliphatic region expanded

The peaks in the region 7.02-7.37 ppm represent the hydrogens of the two types of aromatic rings; the two identical phenyl rings and the 2-fluoro benzyl ring. The multiplicities of these peaks will interfere with each other therefore, cannot be identified individually.

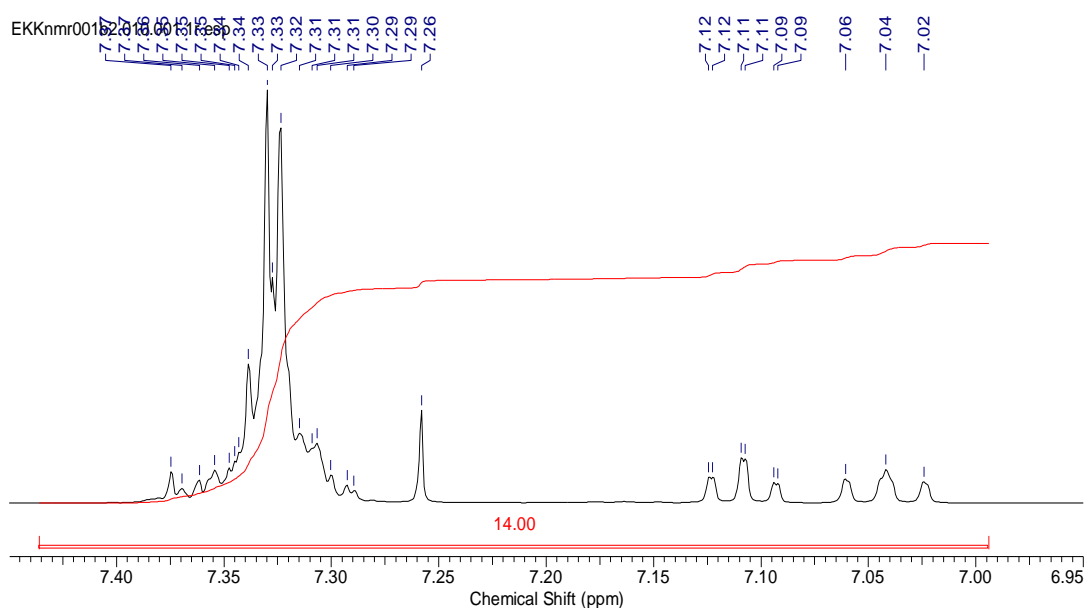


Figure 2.12.3: $^1\text{H-NMR}$ 2-fluorobenzyl-dibenzyl phosphate aromatic region expanded

2.12.2 $^{13}\text{C-NMR001B2}$

The multiplet at 63.11-63.19 ppm ($^2J_{31\text{P} - 13\text{C}} = 5.0$ Hz) represent the α - methylene carbon (C-7). The doublets at 69.32-69.37 ppm ($^2J_{31\text{P} - 13\text{C}} = 6.3$ Hz) are from the two CH_2 groups of the C-7' carbon.

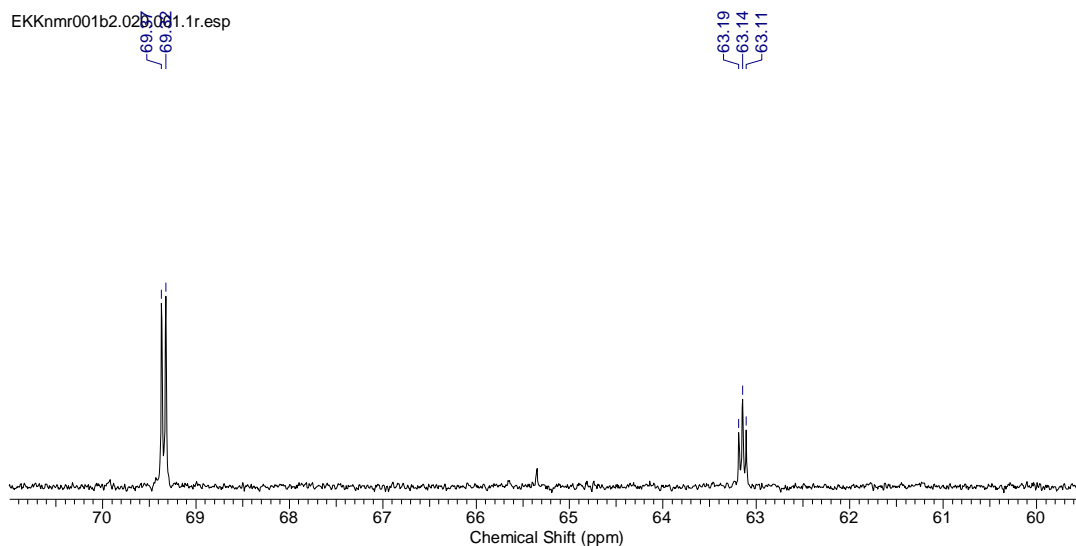


Figure 2.12.4: ^{13}C -NMR 2-fluorobenzyl-dibenzyl phosphate aliphatic region expanded

The peaks in the region 115.31-161.58 ppm represent the two phenyl groups and the 2-fluoro benzyl ring. The doublet at 159.61-161.58 ppm ($^1J_{^{19}\text{F} - ^{13}\text{C}} = 249.48$ Hz) is from the C-F bond in the 2-fluorobenzyl ring. The peaks of the carbons in the 2-fluoro benzyl ring will overlap with the peaks of the carbons of the two benzyl rings.

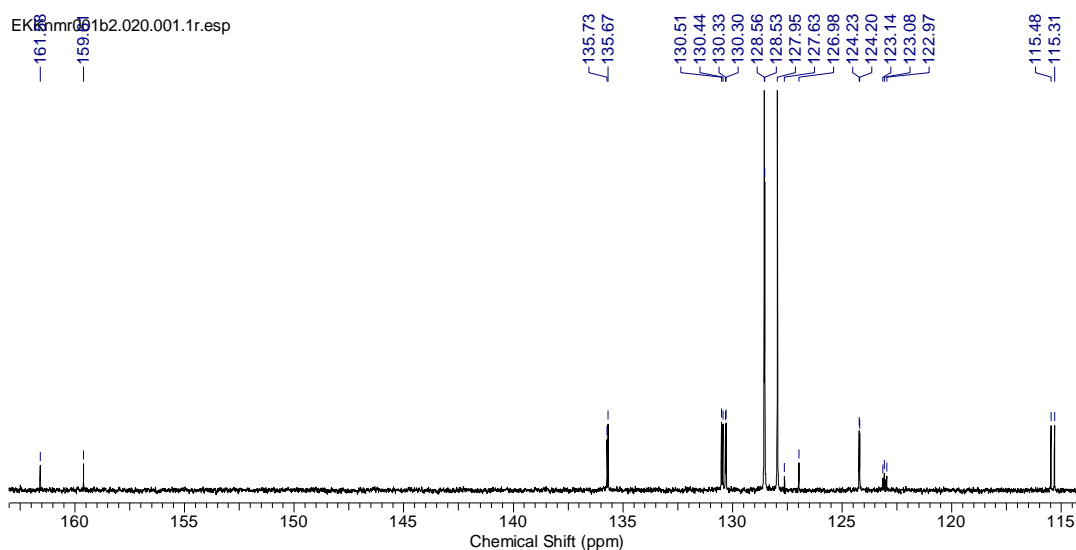


Figure 2.12.5: ^{13}C -NMR 2-fluorobenzyl-dibenzyl phosphate aromatic region expanded

2.12.3 ^{31}P -NMR001B2

The phosphorus NMR shows one peak, which occurs at -0.51 ppm. No other phosphorus containing compounds can be observed in the spectra. This is expected for the rearranged phosphates, but not for the desired phosphonates.

2.13 Mass Spectrometry (EIMS⁺) (19)

2.13.1 MS001B2

The Mr for the expected phosphonate ion is 370. There is no phosphonate molecular ion peak in the mass spectra. The peak at m/z 387 represents the molecular ion peak for the phosphate compound. The peak at m/z 277 represents a loss of 110 amu which is a loss of $C_6H_4F(CH_2)^+$ from the molecular ion. The peak at m/z 199 represents the $[(C_6H_5CH_2O)(OCH_2)PO-CH_2-]^+$ fragment that has been cleaved from the molecular ion. The peak at m/z 109 represents the $[FC_6H_4CH_2]^+$ fragment that has cleaved from the molecule. The peak at m/z 91 represents the $[C_6H_4CH_2]^+$ fragment that has cleaved from the molecule.

2.14 2-Fluorobenzyl-diethyl phosphate (20)

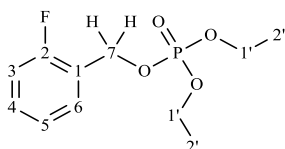


Figure 2.14.1: 2-fluorobenzyl-diethyl phosphate with numbered carbons

2.14.1 ¹H-NMR012B3

The multiplet at 1.30-1.33 ppm represent the two CH_3 groups of the C-2' carbons of diethyl phosphate. The multiplet at 4.09-4.14 ppm represent the two CH_2 groups of the C-1' carbon. The peaks in the region 5.13-5.15 ppm are from the α - CH_2 of the carbon (C-7).

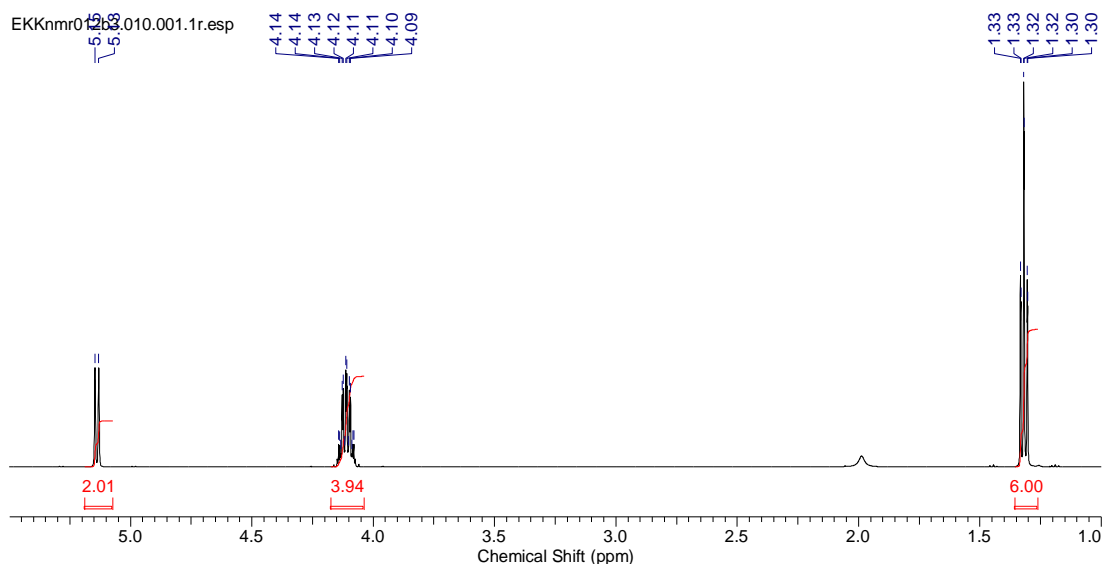


Figure 2.14.2: $^1\text{H-NMR}$ 2-fluorobenzyl-diethyl phosphate aliphatic region expanded

The peaks in the region 7.06-7.47 ppm are from the 4 hydrogens of the in the fluoro benzyl ring. The multiplet at 7.45-7.48 ppm is the hydrogen that is in closest proximity to the C-F group. The peaks in the region 7.06-7.35 ppm shift upfield as the hydrogens resonate further away from the electronegative fluorine group.

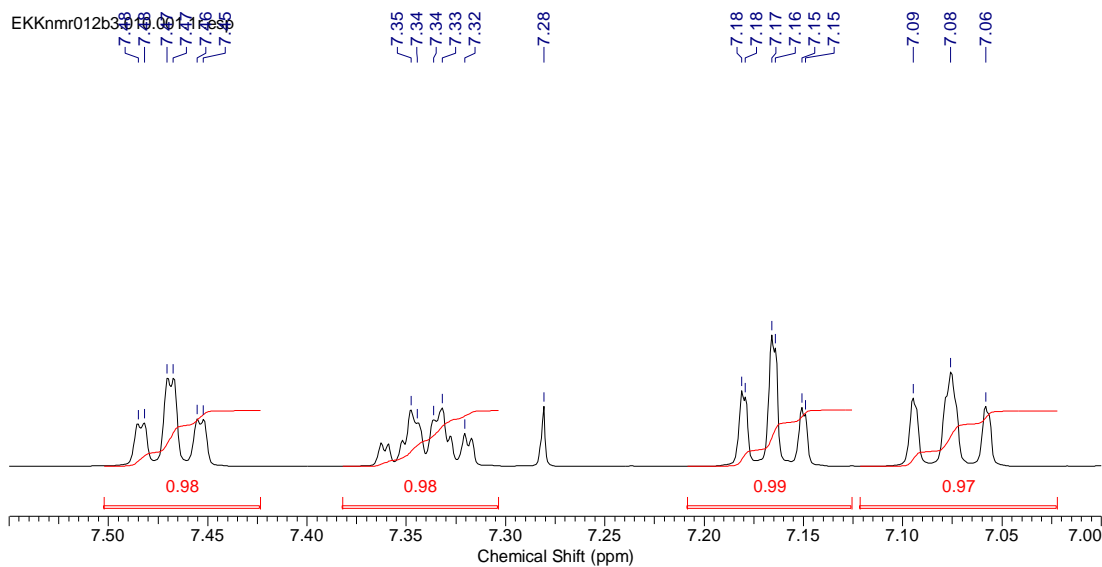


Figure 2.14.3: $^1\text{H-NMR}$ 2-fluorobenzyl-diethyl phosphate aromatic region expanded

2.14.2 $^{13}\text{C-NMR012B3}$

The peaks at 16.01-16.07 ppm is from the two CH_3 from the diethyl phosphate of the C-2' carbon.

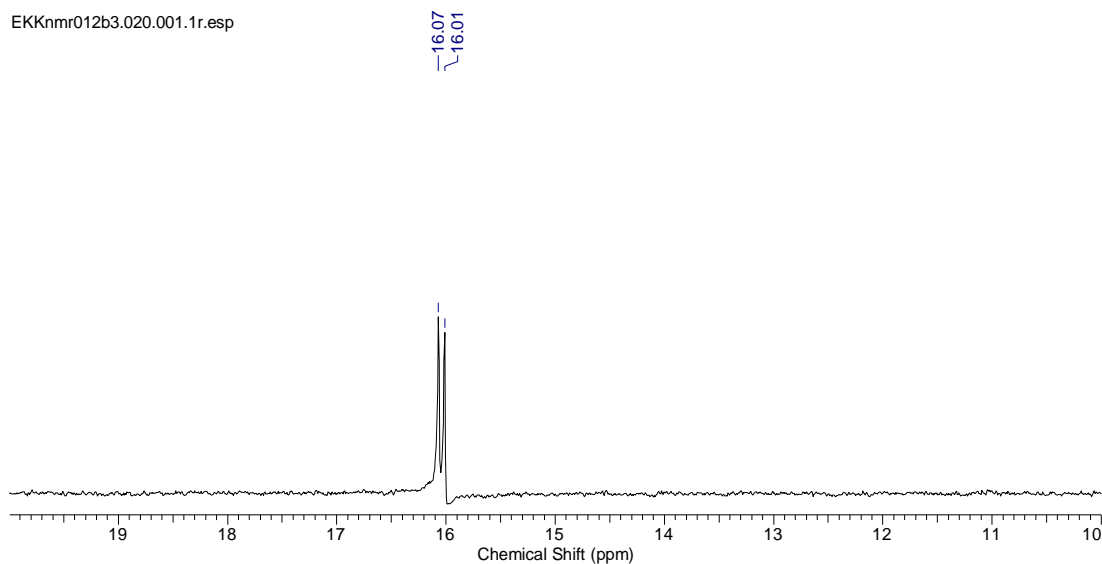


Figure 2.14.4: ^{13}C -NMR 2-fluorobenzyl- diethyl phosphate aliphatic region expanded

The peak at 63.88-63.93 ppm is from the two CH_2 groups from the diethyl phosphate from the carbon C-1'. The multiplet at 62.84-62.92 ppm is from the α -methylene CH_2 carbon C-7.

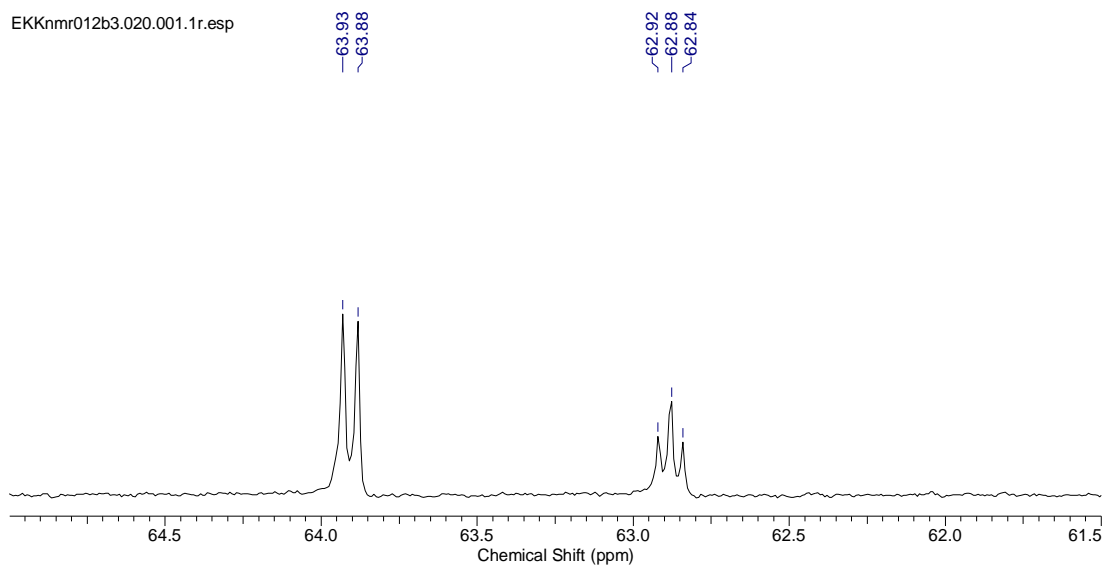


Figure 2.14.5: ^{13}C -NMR 2-fluorobenzyl- diethyl phosphate aliphatic region expanded

The peaks in the region 115.31-130.46 ppm are from the carbon atoms of the 2-fluoro-benzyl ring which produces 6 unique peaks. All the peaks of the 2-fluoro-benzyl ring will experience C-F coupling and will hence be split. The doublet at 159.66-161.64 ppm ($^1J_{^{19}\text{F}-^{13}\text{C}} = 249.48$ Hz) is from the C-F in the 2-fluorobenzyl ring.

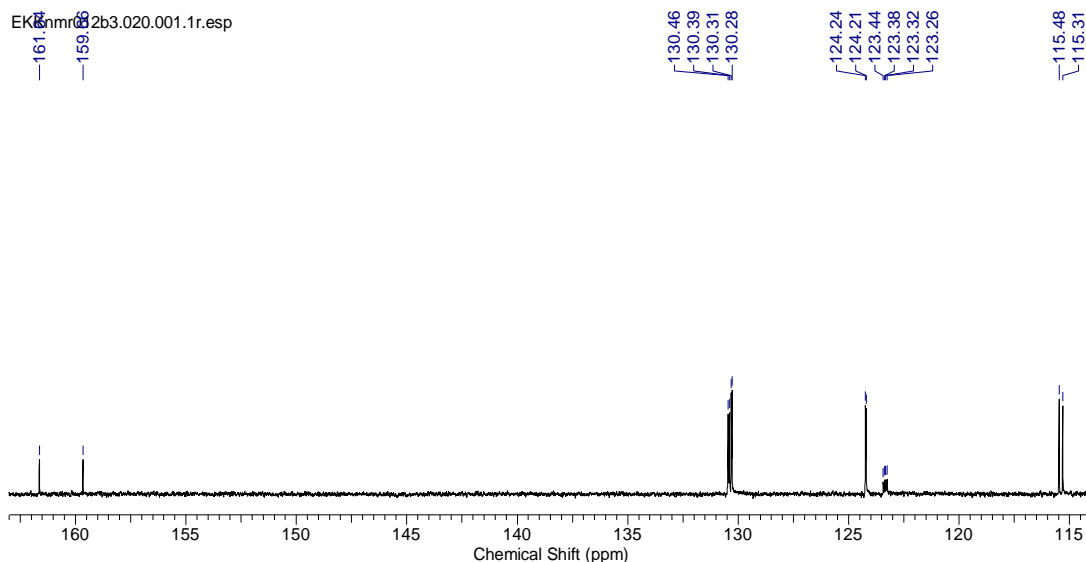


Figure 2.14.6: ^{13}C -NMR 2-fluorobenzyl-diethyl phosphate aromatic region expanded

2.14.3 ^{31}P -NMR012B3

The phosphorus NMR shows one peak, which occurs at -0.60 ppm, no other phosphorus containing compounds can be observed in the spectra. This is expected for the rearranged phosphates, but not for the desired phosphonates.

2.15 Mass Spectrometry (EIMS⁺) (20)

2.15.1 MS012B2

The Mr for the expected phosphonate ion is 246. There is no phosphonate molecular ion peak present in the mass spectra. The peak at m/z 262 represents the molecular ion peak for the phosphate compound. The peak at m/z 233 is a loss of 29 amu which is a loss of CH_3CH_2^+ from the molecular ion. The peak at m/z 214 represents a loss of 19 amu from the fragment m/z [233]⁺ which is the loss of the fluorine. The peak at m/z 186 represents the $\text{FC}_6\text{H}_4\text{CPO}_3^+$ fragment that has been cleaved from the molecular ion. The peak at m/z 109 represents the $\text{FC}_6\text{H}_4\text{CH}_2^+$ fragment.

2.16 Synthesis of substituted benzyl- α -hydroxy phosphonic acids from their diethyl phosphonate precursors.

The substituted benzyl- α -hydroxy diethyl phosphonates and substituted benzyl- α -methylene diethyl phosphonates were selected for hydrolysis to their respective phosphonic acids instead of the corresponding substituted R-benzyl- α -hydroxyl dibenzyl phosphonates and substituted

benzyl- α -methylene dibenzyl phosphonates. The diethyl phosphonates were hydrolysed in two main ways:

- 1) Hydrolysis by the use of strong acid, in this instance, 6M HCl and concentrated acetic acid (AcOH).
- 2) Dealkylation with chlorotrimethylsilane or bromotrimethylsilane/metal halide (*Morita, T, et al 1981*) for compounds that could not be successfully hydrolysed to their phosphonic acids by acid hydrolysis.

This is a milder method for dealkylation which involves the conversion of the dialkyl phosphonate into their silyl esters and hydrolysing the silyl ester with a strong base, 1M sodium hydroxide (NaOH). Bromotrimethylsilane and iodotrimethylsilane have been considered to be the most efficient reagents for this dealkylation process but they are much more expensive. Chlorotrimethylsilane, on the other hand, is much cheaper but has been considered to be an inefficient dealkylation agent (*Morita, T, et al 1981*).

AcOH, 6M and concentrated HCl were not strong enough to hydrolyse the 2-fluorobenzyl- α -hydroxy diethyl phosphonate (**12**) and the 2-nitrobenzyl- α -hydroxy diethyl phosphonate (**17**), these acids did not produce the required phosphonic acids for the respective compounds when the reflux was carried out for 48-72 hours. As a result, chlorotrimethylsilane was used to dealkylate compounds **12** and **17** to their respective phosphonic acids. There were concerns that utilising concentrated HCl to hydrolyse the diethyl phosphonates would decompose them therefore, 6M HCl was used. The melting point of compound **29** was >300 °C which was beyond the limits of the instruments that were utilised. The melting point of compound **30** was difficult to attain because the compound decomposed at 155-158 °C.

2.17 Synthesis of substituted benzyl- α -hydroxy phosphonic acids from their diethyl phosphonate precursors by acid hydrolysis

2.17.1 Reaction mechanism

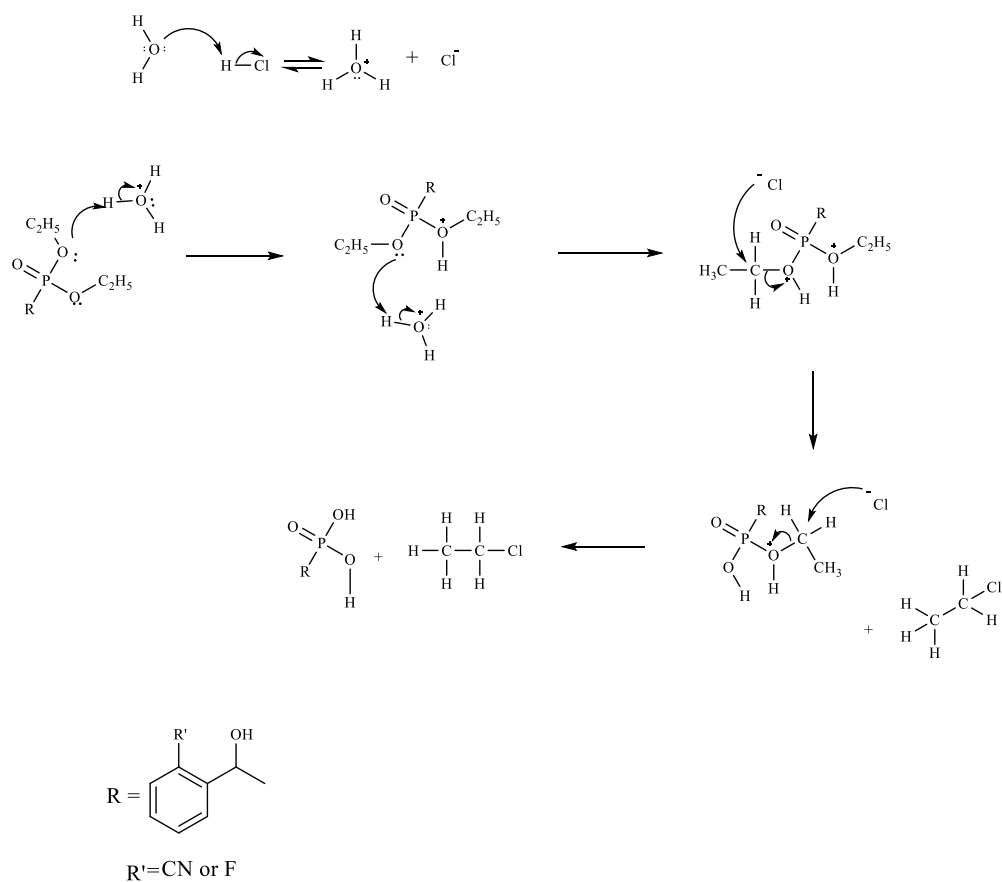


Figure 2.17.1: General reaction mechanism for the dealkylation of substituted benzyl- α -diethyl phosphonates by acid hydrolysis

The acid will protonate the oxygen atom of the ethoxy group which is then followed by an S_N2 attack on the adjacent CH_2 by the chloride anion and the displacement of phosphonate generating the phosphonic acids.

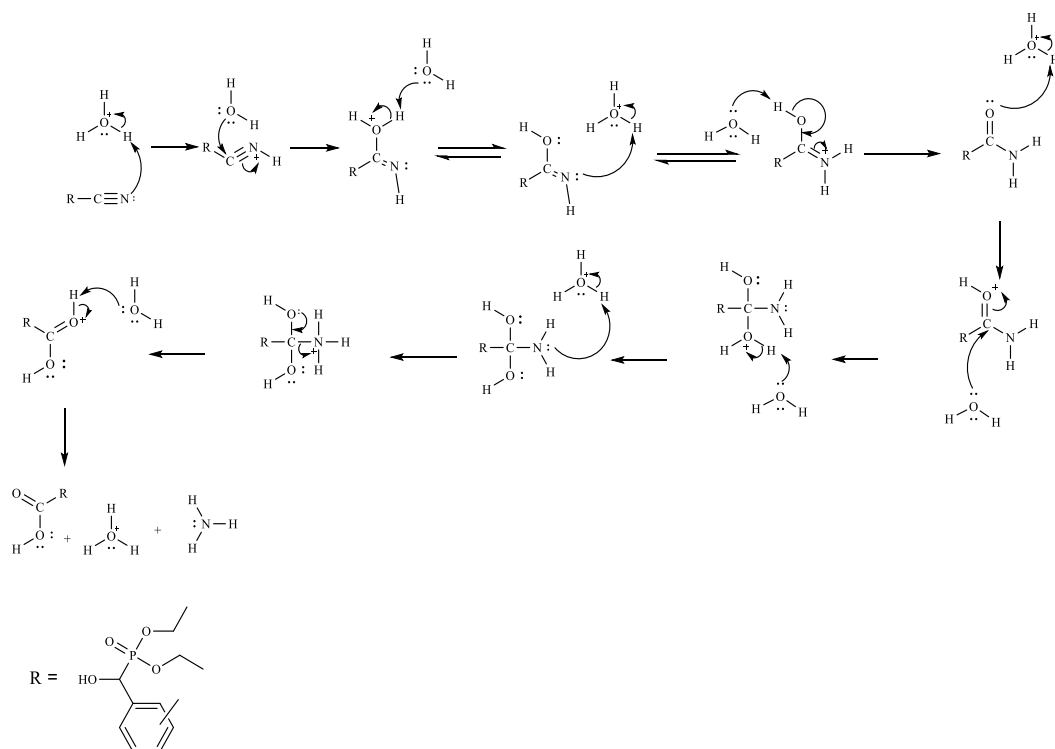
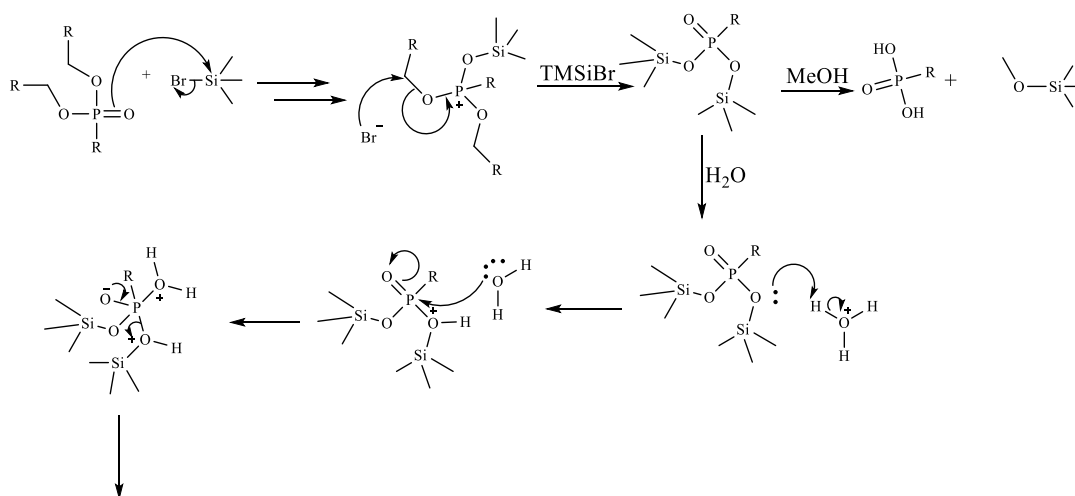
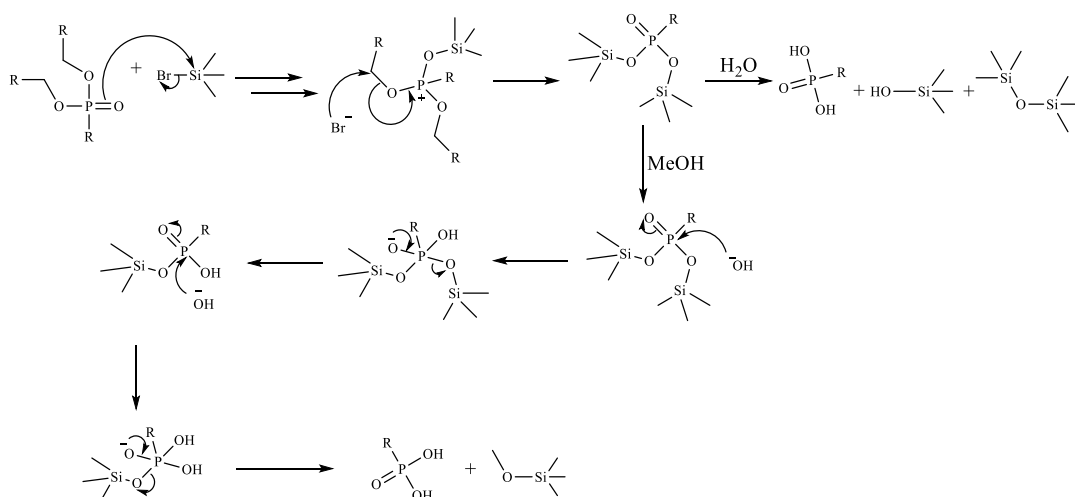
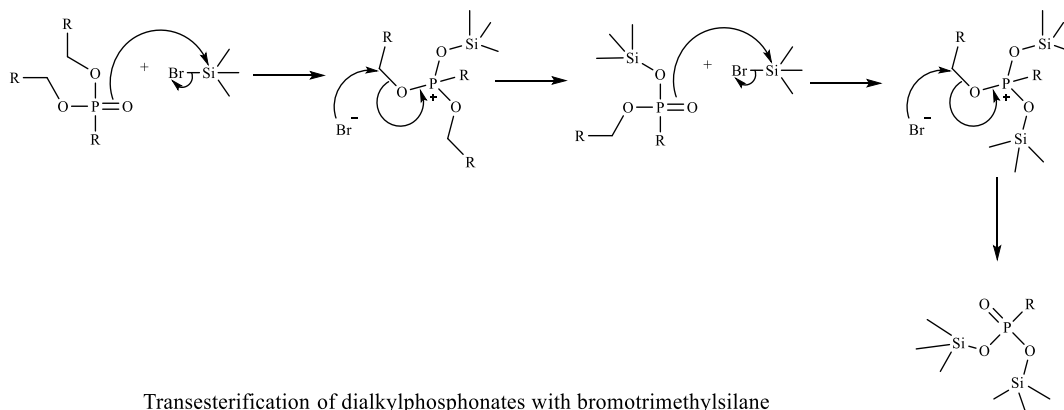


Figure 2.17.2: General reaction mechanism for the acid hydrolysis of nitrile groups

The nitrile group has two pi triple bonds and a lone pair of electrons on the nitrogen. The nitrogen of the nitrile group is protonated by the H_3O^+ resulting in the formation of an activated nitrile which has a positively charged nitrogen. This is then followed by the addition of water to the carbon of the nitrile to give a primary amide. The carbonyl of the primary amide is then protonated by the H_3O^+ , the positive charge that is generated makes that carbon more electrophilic making the addition of another water molecule on to the carbon possible resulting in a neutral tetrahedral intermediate. The amine is much more basic than the oxygen and is therefore protonated making it a very good leaving group, and the carboxylic acid product is formed.

2.18 Synthesis of substituted benzyl- α -hydroxy phosphonic acid from their diethyl phosphonate precursors by bromotrimethylsilane (TMSiBr).

2.18.1 Reaction mechanism



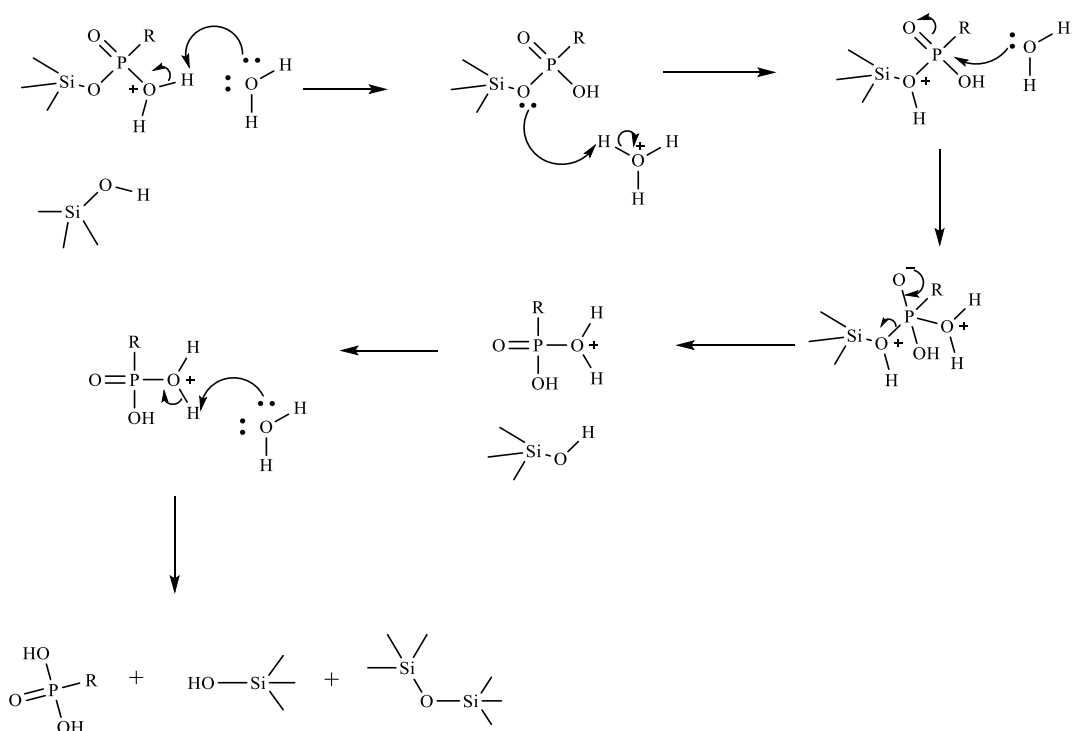


Figure 2.18.1: Reaction mechanism for the dealkylation of Benzyl- α -diethyl phosphonates by bromotrimethylsilane (TMSiBr)

McKenna's method reported in 1977 occurs by oxophilic substitution on the silicon atom whereby the bromide ion acts as a leaving group to produce the di-silylated ester. The hydrolysis of this di-silylated ester produces the phosphonic acid. The P=O double bond acts as a nucleophile that attacks the electropositive silicon atom resulting in silicon giving up its electrons to the bromide leaving group (*Sevrain. M. C, et al, 2017*). The next stage of the reaction will progress as an $\text{S}_{\text{N}}2$ reaction resulting in the removal of the alkyl group. This reaction is repeated resulting in the formation of the di-silylated ester. The final products at this stage in the reaction are two bromoethane molecules and a disilyl phosphonate.

The last stage of the mechanism is the removal of the silyl esters by either, methanolysis with a strong base, sodium hydroxide, or hydrolysis with water to give the final phosphonic acids, this occurs again as an $\text{S}_{\text{N}}2$ reaction. The hydroxyl (OH^-) is drawn toward the phosphorus creating a new P-OH bond, this results in the generation of an oxyanion followed by a concerted electron pair shift from the oxyanion to the silyl ester leaving group. The final products from this reaction are the volatile methoxy trimethylsilane and the phosphonic acid. The by-products that are generated if the removal of the silyl esters is carried out by hydrolysis

with water are trimethylsilanol and hexamethyldisiloxane. This milder method to prepare phosphonic acids by the transesterification of dialkyl phosphonates reaction mechanism has been confirmed (Sevrain. M. C, et al (2017), Bartlet. P. A, et al (1991) and the experimental proof was obtained by using ^{17}O and ^{18}O enriched benzyl diethyl phosphonate. These experiments showed that the terminal P=O was the nucleophile that attacked the silicon (Sevrain. M. C, et al (2017). The nucleophilicity of the bromide only works for alkyl chain phosphonates but was not very efficient for dibenzyl phosphonates (Pohjala, E. et al, (1993).

Table 9: Synthesized substituted carboxy benzyl- α -phosphonic acids and their respective yields

Compounds	Yield %
2-Fluorobenzyl- α -hydroxy phosphonic acid (29)	19
3-Carboxybenzyl- α -hydroxy phosphonic acid (26)	97
4-Carboxybenzyl- α -hydroxy phosphonic acid (28)	85
2-Carboxybenzyl- α -hydroxy phosphonic acid (27)	14
2-Nitrobenzyl- α -hydroxy phosphonic acid (30)	68

The compounds that were synthesised by dealkylation with TMSiCl were resynthesised with TMSiBr to find out if the yields could be improved. The yields of the compounds synthesised via the TMSiCl route improved on using TMSiBr. This is due to the fact that TMSiBr is more reactive and Br⁻ is a better leaving group than Cl⁻.

Table 10: Comparisons in yields between synthesis with TMSiCl and TMSiBr

Compound	TMSiCl synthesis yield %	TMSiBr synthesis yield %
2-Fluorobenzyl- α -hydroxy phosphonic Acid (29)	19	88
2-Nitrobenzyl- α -hydroxy phosphonic Acid (30)	68	75

The main distinguishing peaks for the phosphonic acids was the absence of the phosphonate ester derivatives in the $^1\text{H-NMR}$ and the $^{13}\text{C-NMR}$. Additionally, the presence of peaks corresponding to the -COOH resonating in the region 169-173 ppm of the $^{13}\text{C-NMR}$ (for

compounds which previously had a -CN group). The benzonitrile -CN peak resonates in the region 118 ppm. The spectra were run in methanol or D₂O, which will exchange with OH and NH₂ groups.

Table 11: Distinguishing peaks of the substituted benzyl- α -hydroxy/amino phosphonic

Compound	δ_{H} CH-OH (ppm)	δ_{C} CH-OH (ppm)	δ_{P} (ppm)	$^1J_{31\text{P}-13\text{C}}$ (Hz) (C-7)
26	3.62	71.87	20.68	163.8
27	5.80	78.55	12.86	158.8
28	5.02	72.13	20.28	161.28
29	5.13	66.52	16.55	152.5
30	5.76	69.05	15.57	142.38
34	4.13	51.00	18.20	132.30

2.19 NMR of 2-carboxy benzyl- α -hydroxy phosphonic acid (27)

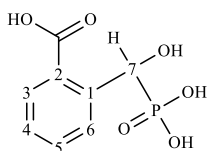


Figure 2.19.1: 2-carboxybenzyl- α -hydroxy phosphonic acid with numbered carbons

2.19.1 ¹H-NMR022D2

The doublet at 5.79-5.81 ppm ($^2J_{31\text{P}-1\text{H}} = 10.0$ Hz) is from the CH of the asymmetric carbon (C-7).

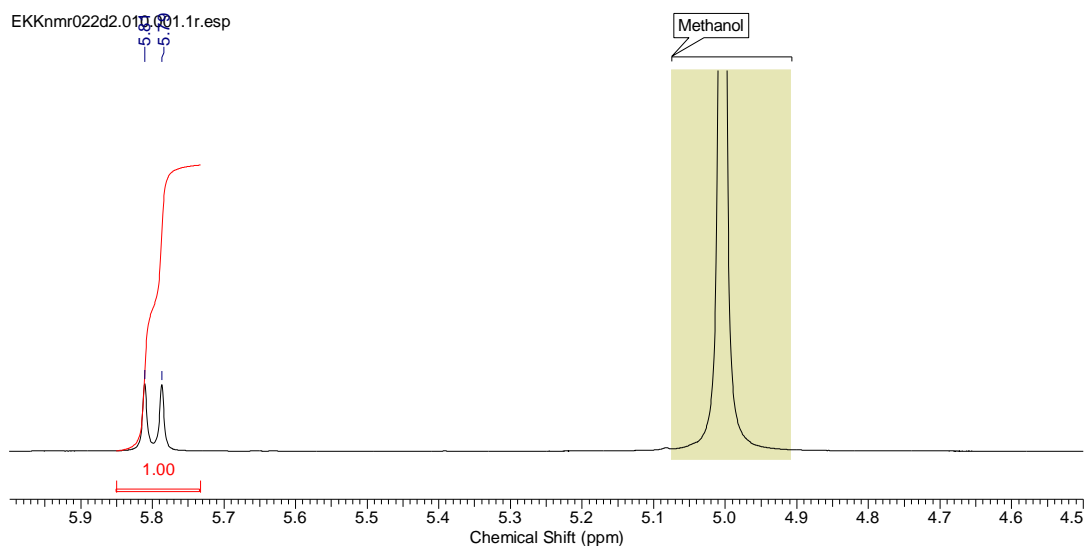


Figure 2.19.2: $^1\text{H-NMR}$ 2-carboxybenzyl- α -hydroxy phosphonic acid aliphatic region

The peaks in the regions 7.61-7.90 ppm are from the 4 hydrogens in the 2-carboxyl benzyl ring.

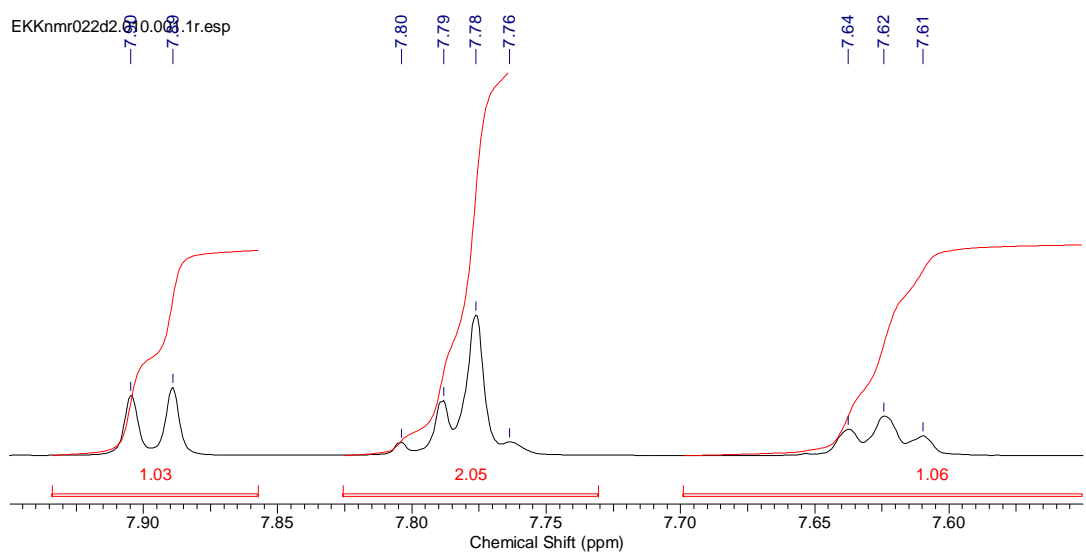


Figure 2.19.3: $^1\text{H-NMR}$ 2-carboxybenzyl- α -hydroxy phosphonic acid aromatic region

2.19.2 $^{13}\text{C-NMR}$ 022D2

The doublet at 77.92-79.18 ppm ($J_{31\text{P}-^{13}\text{C}} = 158.76$ Hz) is from the asymmetric carbon C-7.

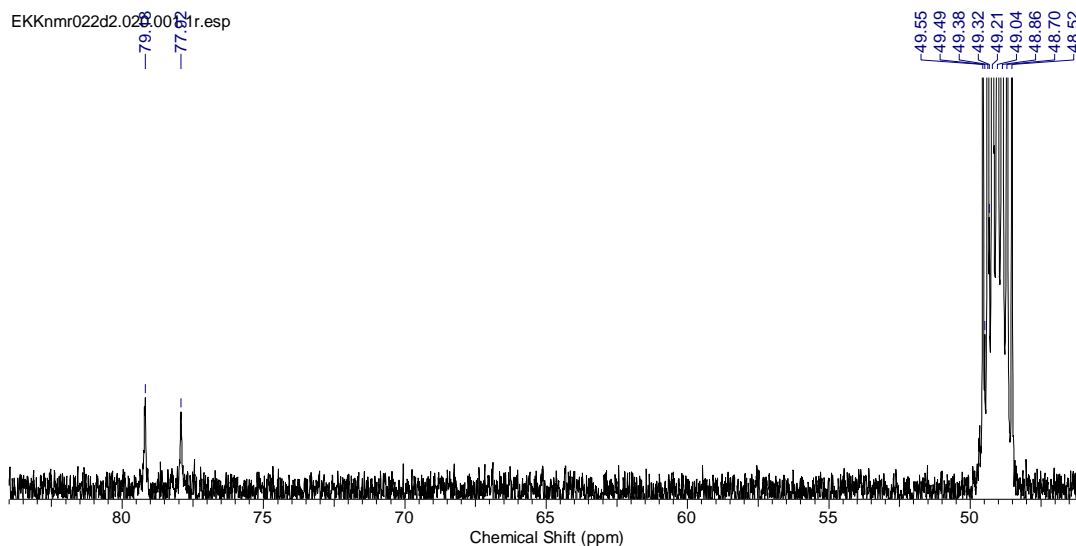


Figure 2.19.4: ^{13}C -NMR 2-carboxybenzyl- α -hydroxy phosphonic acid aliphatic region

The peak at 172.48 ppm is from the -COOH bond. The peaks in the region 124.76-146.90 ppm are from the carbon atoms of the phenyl ring. All the peaks of the 2-carboxy benzyl ring are accounted for in this region.

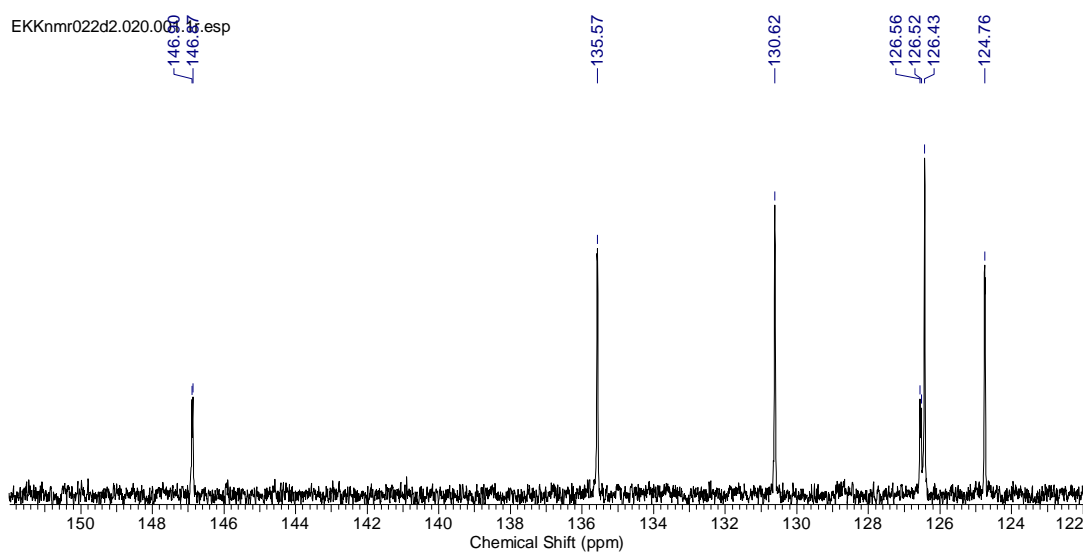


Figure 2.19.5: ^{13}C -NMR 2-carboxybenzyl- α -hydroxy phosphonic acid aromatic region

2.19.3 ^{31}P -NMR022D2

The phosphorus NMR shows one peak, which occurs at 12.86 ppm, no other phosphorus containing compounds can be observed in the spectra.

2.20 Mass spectrometry (TOF MS ES⁻) (27)

2.20.1 MS022D1

The peak at m/z 232 [M- H]⁻ is from the molecular ion.

2.21 Synthesis of substituted benzyl- α -amino phosphonic acids

2.21.1 Reaction mechanism

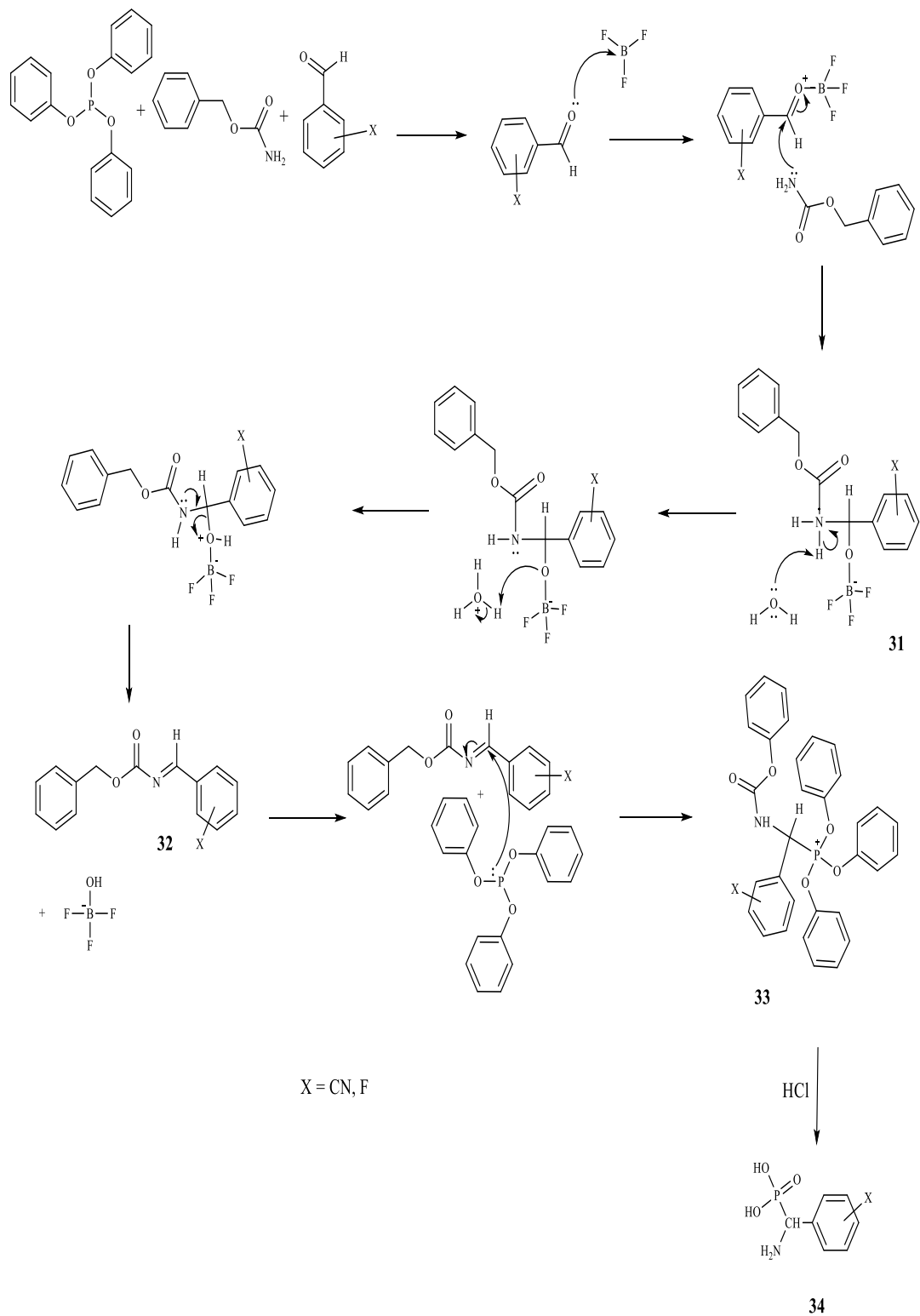


Figure 2.21.1: General reaction mechanism for the synthesis of substituted benzyl- α -amino phosphonic acids

The amine attacks the aldehyde to form a hemiaminal intermediate **31**. An acid catalyst is not necessary for this step, an acid catalyst at this stage would only slow the reaction as the nucleophilic amine would be removed as a salt. Dehydration of the hemiaminal gives the imine **32**, the iminium ion loses a proton and becomes a neutral imine, this step requires an acid catalyst, the catalyst will make the hydroxyl group a better leaving group. The ideal pH for the formation of the imine should be between 4-6, at a lower pH too much of the amine is protonated and the rate of the first step is too slow. At a pH above 4-6, the proton concentration is too low to allow for the protonation of the hydroxyl leaving group in the dehydration step. As a result, a boron trifluoride catalyst is used to activate the aldehyde and make it a better electrophile. This compound **33** is then hydrolysed by a strong acid to produce the required aminophosphonic acid **34**.

The NMRs of the compounds 2-carboxybenzyl- α -amino phosphonic acid, 3-carboxybenzyl- α -amino phosphonic acid and 4-carboxybenzyl- α -amino phosphonic acid showed extra peaks in the ^{31}P NMRs indicating the presence of more than one phosphorus containing compound, hence, the compounds were impure. The 2-fluoro benzyl- α -amino phosphonic acid **34** was isolated as a pure compound

2.22 NMR of 2-fluoro benzyl- α -amino phosphonic acid (**34**)

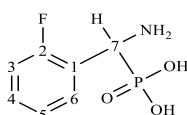


Figure 2.22.1: 2-fluorobenzyl- α -amino phosphonic acid with numbered carbons

2.22.1 NMR0004B ^1H NMR

The peak in the region 4.11-4.15 ppm ($^2J_{^{31}\text{P}-^1\text{H}} = 20.0$ Hz) is from the CH of the asymmetric carbon (C-7).

The peaks in the regions 7.10-7.48 ppm are from the hydrogens in the 2-fluoro-benzyl ring, these peaks will experience fluorine coupling as the other fluorine containing compounds. The multiplet at 7.45-7.48 ppm is the hydrogen that is adjacent to the C-F group. The peaks in the

region 7.10-7.33 ppm shift upfield as the hydrogens are located further away from the electronegative fluorine group.

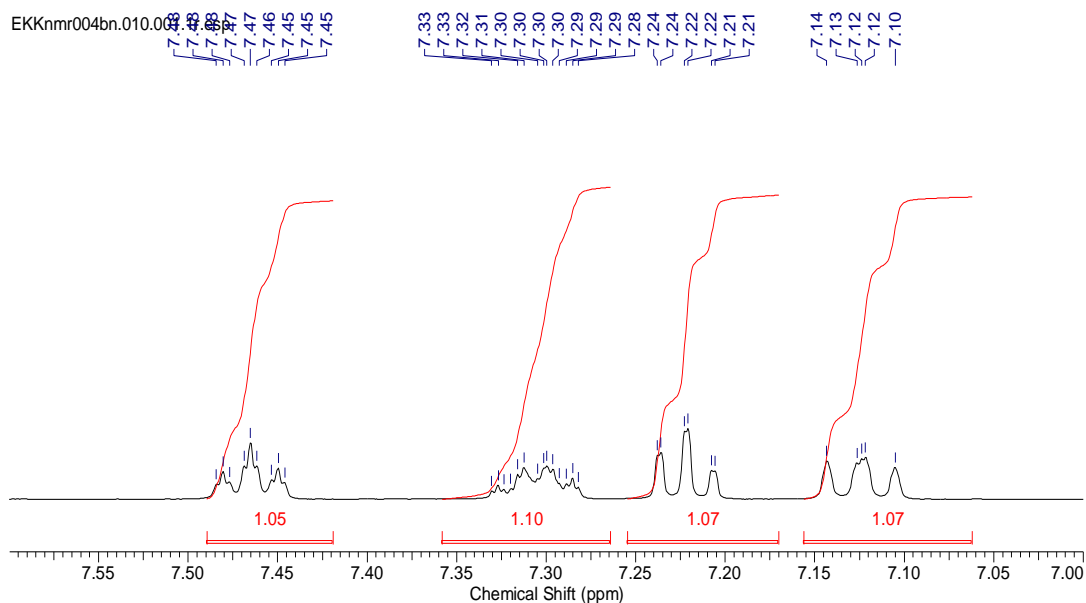


Figure 2.22.2: ^1H -NMR 2-fluorobenzyl- α -amino phosphonic acid aromatic region

2.22.2 NMR004B ^{13}C NMR

The doublet at 50.48-51.53 ppm ($^1J_{31\text{P}-^{13}\text{C}} = 132.30$ Hz) is from the asymmetric carbon (C-7). The peaks in the region 117.51-163.50 ppm are from the carbon atoms of the aromatic 2-fluoro-benzyl ring which produce 6 unique peaks. The doublet at 161.57-163.50 ppm ($^1J_{19\text{F}-^{13}\text{C}} = 243.18$ Hz) is from the C-F, (C-2) carbon. All the peaks of the 2-fluoro benzyl ring are accounted for in this region.

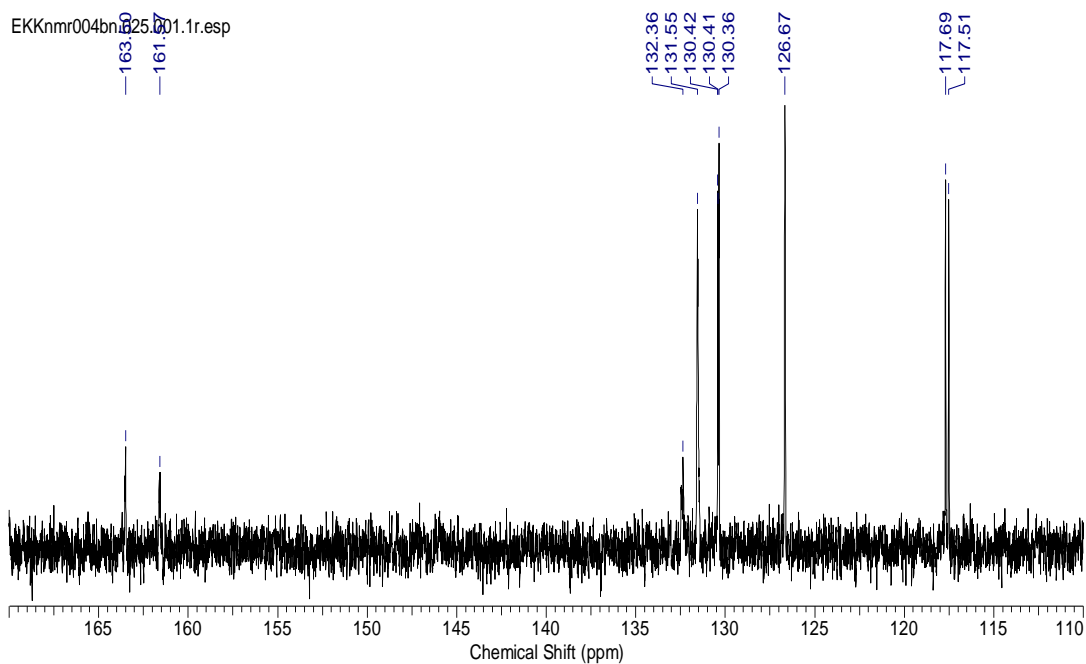


Figure 2.22.3: ^{13}C -NMR 2-fluorobenzyl- α -amino phosphonic acid aromatic region

2.22.3 NMR0004B ^{31}P NMR

There is one peak that is observed at 18.20 ppm region of this spectrum, no other phosphorus containing compounds can be observed in the spectra.

2.23 Mass spectrometry (EIMS⁺) (34)

2.23.1 MS004B

The Mr of the compound is 205, there is no peak for the molecular ion that can be observed in the spectrum. The peak at m/z 83 is from the fragment $[\text{PO}_3\text{H}_3]^+$. The peak at m/z 109 is from the fragment $[\text{FC}_6\text{H}_4\text{CH}]^+$. These are the two peaks that can be easily identified in the spectra.

3 BIOLOGICAL EVALUATION RESULTS

3.1 Introduction

The synthesised compounds were sent to St Andrews University and Cambridge University where they were tested against other protozoan parasitic diseases and the malaria parasite respectively. The St Andrews team tested the synthesised compounds against *Trypanosomiasis brucei*, *Trypanosomiasis cruzi*, *Leishmania major* and the *HeLa* cells. *HeLa* cells were used as surrogates for human cells, compounds that were active against the *HeLa* cells will be toxic against human cells as well. The compounds were tested against malaria *P. falciparum* parasite 3D7 and Dd2 strains at the Sanger Institute at Cambridge University.

Trypanosomiasis brucei is an extracellular flagellate protozoan parasite transmitted by the tsetse fly. The parasite has two subspecies that are responsible for two variants of the disease, Human African Trypanosomiasis (HAT) or sleeping sickness. *Trypanosomiasis brucei gambiense* causes the chronic form of the disease that is predominantly found in Central and West Africa which represents >95% of all cases (Brun. R, et al 2018). The disease affects primarily the poorest, rural parts of the least developed African Countries and has between 300,000-500,000 cases annually. The currently available treatments for the Human African Trypanosomiasis (HAT) or sleeping sickness are inadequate and the chemotherapies such as Melarsoprol (Mel B) which are used for the late stages of the disease are highly toxic to humans. Like most parasitic diseases there, are no prophylactic treatments and efforts for a viable vaccine have been unsuccessful to date (Berriman. M, et al 2005). *Trypanosomiasis brucei rhodesiense* is responsible for the more acute form of the disease that is found in East and Southern Africa and is predominantly found in animals such as horses and cattle but can be transmitted to humans. Both diseases are fatal to humans if they are left untreated (Brun. R, et al 2018).

Trypanosomiasis cruzi is the protozoan causative agent of the acute form of Chagas disease. This infection is primarily prevalent in South and Central America and can cause an acute

form of the disease that can be fatal, but, it can evolve into a debilitating chronic, systematic condition which results in death. It is estimated that Chagas disease has between 5-18 million cases and approximately 21,000 deaths annually. The number of cases of Chagas disease has been decreasing in recent years due to a concerted effort to remove the vector (triatomine bug) and improvements in health care management systems in areas that the disease is prevalent. However, since the levels of funding that have been available to enable this level of progress cannot be maintained indefinitely coupled with the high risk of political instability in the region the disease is prevalent, there are concerns that the progress that has been made will be reversed (*El-Sayed N. M, et al 2005*). Another factor that has resulted in the re-classification of Chagas disease by WHO as both a re-emerging and neglected tropical disease is the changing distribution of the disease in endemic and non-endemic countries because of migration. Human migration has resulted in the geographical expansion to the regions where the disease is now present (*Connors. E. E, et al 2016*). The protozoa are mainly transmitted through the blood sucking reduviid bugs, a sub-family of Triatominae by means of a blood meal. However, the disease can also be transmitted to humans by non-vectoral means such as blood transfusions and mother-infant transmissions (*Rassi Jr. A, et al 2010*). Attempts to find vaccines against parasitic diseases including Chagas diseases have been unsuccessful to date (*Rassi Jr. A, et al 2010*).

Leishmania is a neglected protozoan parasite species that causes a variety of human diseases that are predominantly found in the tropical and sub-tropical regions of the world with approximately 2 million reported new cases annually in 88-98 countries across five continents (*Sohrabi. Y, et al 2018*). *Leishmania major* is the causative agent of the cutaneous leishmaniasis which is characterised by painless ulcerous lesions which can appear as isolated lesions or as multiple lesions (*Zahirnia. A. H, et al 2018*). About 20 species of the parasite leishmania are responsible for infections in humans and the disease is transmitted by the Sand-fly which acts as the vector. Most of the lesions that result from leishmaniasis will self-heal over time but in rare cases, the lesions will not heal as a result of secondary bacterial infections.

The trypanosomatids family of parasitic protozoa have been shown to be sensitive to reactive oxygen species ROS and share some of the similar systems and enzymes that are involved in maintaining homeostasis regarding ROS and antioxidant balance (Leroux. A, et al 2016). The exact enzymatic pathways that are involved in the protection of trypanosomatids from ROS are not yet fully understood but, presently, it is believed that they combat oxidative stresses through a unique thiol redox system using trypanothione [T(SH)₂] which comprises of a spermidine moiety linked to two glutathione molecules. Compounds such as andrographolid result in the rise of ROS levels and rupture of the mitochondrial membrane, releasing EndoG which, together with other nucleases, form a DNA-degradation complex and fragmentizes the parasite's DNA leading to trypanosomatids apoptosis. Andrographolid has been shown to be active against the erythrocytic stages of *P. falciparum* with an IC₅₀ of 9.1µM and non-toxic in in-vivo systems. It is not yet understood how it exerts its anti-malaria effect but it is thought to involve inhibition of enzymes that combat oxidative stresses within the erythrocyte (Banerjee. M, et al 2017). All three parasites *Trypanosomiasis brucei*, *Trypanosomiasis cruzi* and *Leishmania major* have been observed to have GDH that closely resemble bacteria, fungi and plants respectively, therefore, are very distinct from mammalian GDH. *Leishmania major* has two different types of GDH, an NADP-linked and an NAD-linked. The NAD dependant enzymes are probably localized in the mitochondrion and it is possibly these enzymes that are inhibited by Andrographolid. The biochemical information and the roles of the GDH in the parasites *Trypanosomiasis brucei*, *Trypanosomiasis cruzi* and *Leishmania major* is still deficient (Nowicki. C, et al 2008).

The *HeLa* cell line is the first continuous human cancer cell line that was shown to be able to survive in a test tube and could be reproduced readily. Its aggressive growth rate and the high survivability of the cell line after numerous replications have made it very useful to medical research. It is used to study the effects of a disease, develop medications and vaccines (Rahbari. R. et al., 2009). The rapid growth and multiplication of the *HeLa* cells enabled

researchers at the University of Minnesota Hospital to grow the poliovirus and develop the vaccine (Scherer. W. F et al., 1953).

3.1.1 London Metropolitan University (LMU) compounds submitted for testing

3.1.1.1 Glutamic acid (glutamate) analogues

There are 8 glutamate analogues supplied; compounds **6**, **9**, **18**, **29**, **30**, **27** and **34**. **18** and **27** are direct analogues of glutamic acid which contain two acidic functional groups, a carboxylic acid (CO₂H) and a phosphonic acid (-PO(OH)₂) separated by three carbon atoms. Compounds **6**, **9**, **29**, **30** and **34** contain carboxylic acid analogues; the nitro (NO₂) group in compounds **9** and **30**, and a fluorine atom (F) in compounds **6**, **29** and **34**.

3.1.2 'Protected' glutamic acid (glutamate) analogues

The five compounds below contain esterified phosphonates; dibenzyl phosphonates in compounds **6** and **9**, and diethyl phosphonates in compounds **12** and **17**. These esterified glutamate analogues will have greater bioavailability than their phosphonic acid counterparts, and the two ester groups will be susceptible to hydrolysis by esterase enzymes. The 5-membered lactone ring in compound **18** will also be very susceptible to esterase hydrolysis, yielding the full glutamate analogue compound **27**, and hence could be considered to be a pro-drug of compound **27**.

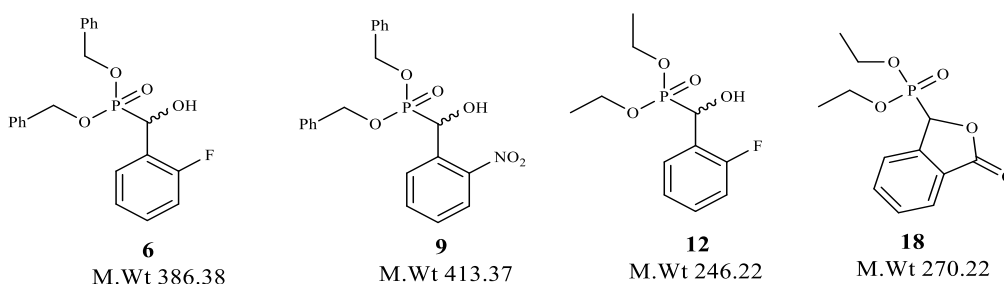


Figure 3.1.1: 'Protected' Glutamic acid analogues

3.1.3 'Unprotected' glutamic acid (glutamate) analogues

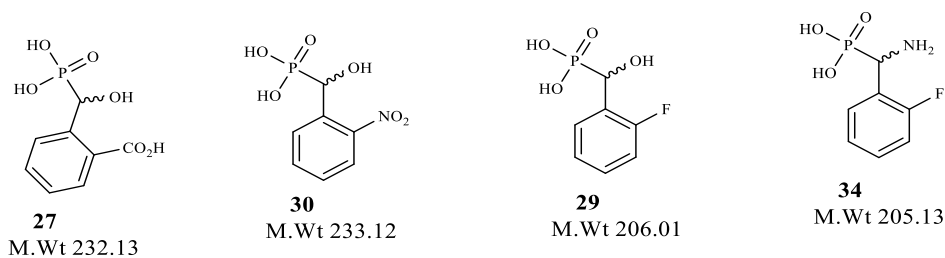


Figure 3.1.2: 'Unprotected' Glutamic acid analogues

3.1.4 Non-glutamic acid (glutamate) analogues

Compounds **26** and **28** are not direct glutamic acid analogues as they contain 4- and 5 carbon atoms between the acidic functional groups rather than 3 carbon atoms, therefore, compounds **26** and **28** are not expected to be active. Compounds **26** and **28** are isomers of compound **27** and hence possess the same molecular weights (M.Wt).

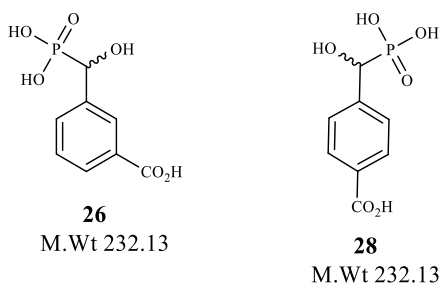


Figure 3.1.3: Non-Glutamic acid analogues

3.1.5 Malaria fluorescence tests

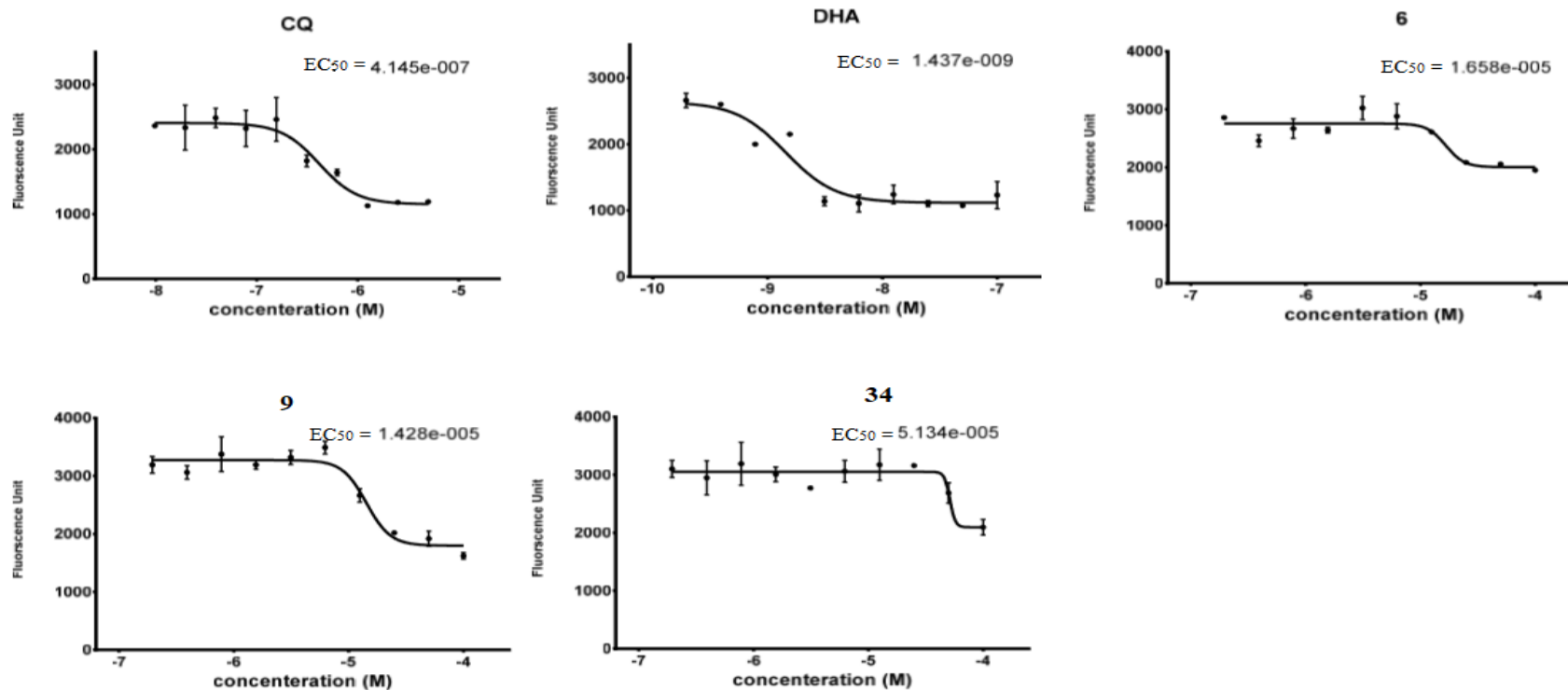


Figure 3.1.4: LMU compounds that had similar fluorescence reduction profiles of the *P. falciparum* strains 3D7 and Dd2 to the control compounds Chloroquine (CQ) and Dihydroartemisinin (DHA).

3.1.6 Malaria fluorescence tests

The fluorescence tests were carried out on both *P. falciparum* strains 3D7 and Dd2. The graphs of Chloroquine (CQ) and Dihydroartemisinin (DHA) which are known and currently utilised antimalarial chemotherapies were the controls of the experiment. The fluorescence unit decreased on addition of the drugs from around 3000 fluorescence units to about 1000 fluorescence units. This reduction in the fluorescence indicated the reduction of the levels of the parasite in the cells. The graphs also show the rate of decrease of the fluorescence and the concentration that the reduction in fluorescence occurs. The error bar indicates the variation of the corresponding coordinate of the point hence, showing the standard deviation of the data set.

Chloroquine(CQ) reduced the parasite levels from about 2500 to 1000 fluorescence units and had an $EC_{50} \approx 0.4 \mu\text{M}$, Dihydroartemisinin (DHA) reduced the parasite levels from about 2500 to 1000 fluorescence units and had an $EC_{50} \approx 1.5 \text{ nM}$.

The synthesised compounds **6**, **9** and **34** produced inhibition curves which had similar profiles to those of the control drugs, these profiles showed that there was a significant reduction in the parasites levels on addition of the compounds. These compounds clearly reduced the level of parasites in the cells. Compound **6** had an $EC_{50} \approx 17 \mu\text{M}$, the compound reduced the fluorescence units from about 3000 to 2000. Compound **9** had an $EC_{50} \approx 14 \mu\text{M}$, the compound reduced the fluorescence units from about 3000 to 1500. This compound showed the biggest reduction in fluorescence and had an inhibition curve that closely resembled the control drugs Chloroquine (CQ) and Dihydroartemisinin (DHA). Compound **34** had an $EC_{50} \approx 51 \mu\text{M}$, the compound reduced the fluorescence units from about 3000 to 2000. Compound **9** had the best reduction in fluorescence of the LMU tested compounds.

The compounds **18**, **29**, **30**, **27**, **26** and **28** did not significantly reduce the parasite fluorescence and the data from these compounds had large error bars indicating that any reduction was not significant and was within the margin of error

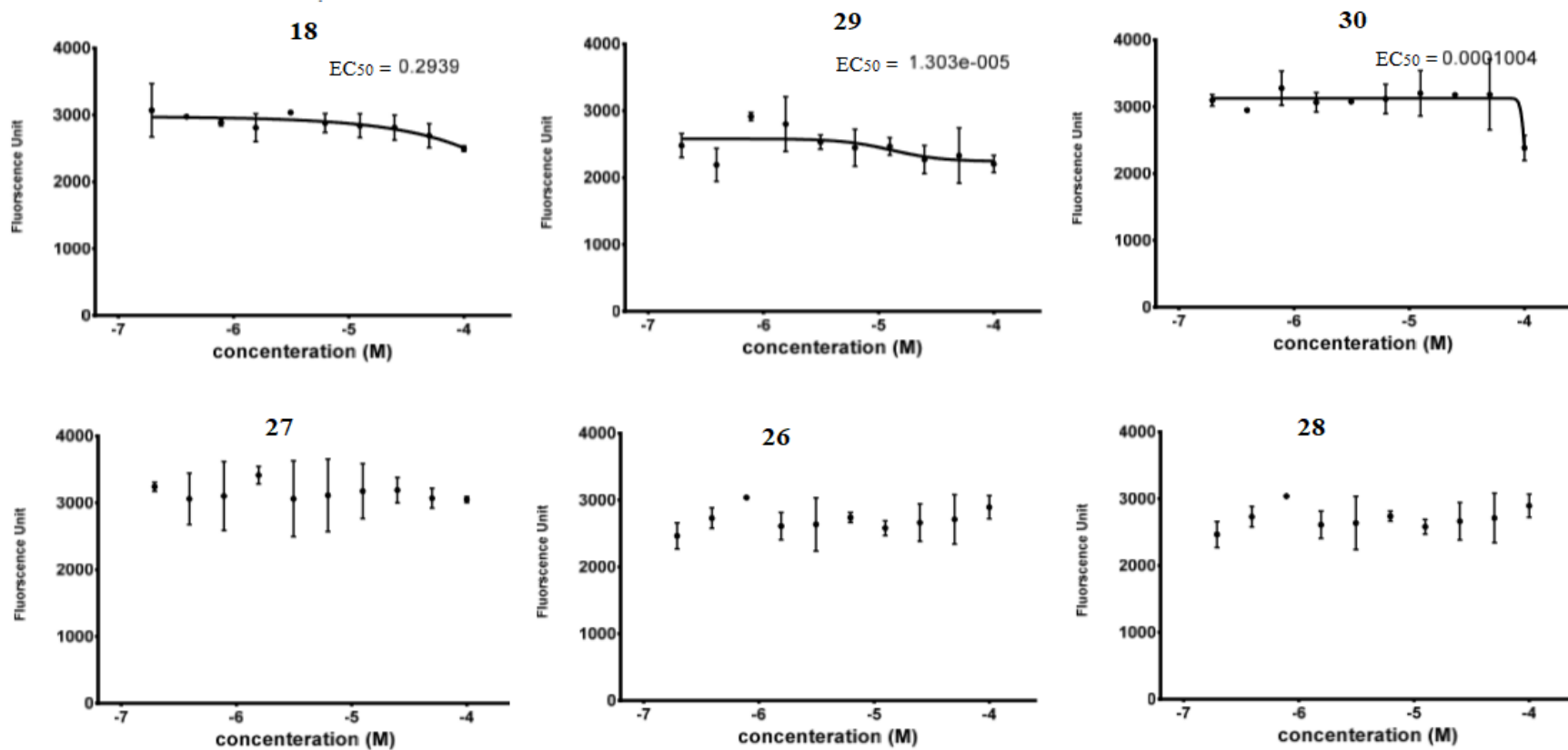


Figure 3.1.5: LMU compounds that did not show similar fluorescence reduction profiles of the *P. falciparum* strains 3D7 and Dd2 to the control compounds Chloroquine (CQ) and Dihydroartemisinin (DHA).

3.2 Malaria growth inhibition tests

The graphs below show the growth inhibition graphs for each compound, tested against two different parasite strains. These are *Pf* 3D7, which is sensitive to chloroquine and other antimalarials, and *Pf* Dd2, a Southeast Asian strain that is multidrug resistant (including chloroquine and pyrimethamine). The graphs also include DMSO titrations that reflect what the parasite growth would be in the presence of the equivalent amount of solvent. Most of the compounds were solubilised at high concentrations so that the highest DMSO level was 0.2%. However, the compounds **29**, **30** and **34** were not very soluble and required DMSO levels of 1% or 2%. At these DMSO concentrations, the DMSO inhibited the malaria parasites' growth.

3.2.1 Compounds that inhibited malaria growth

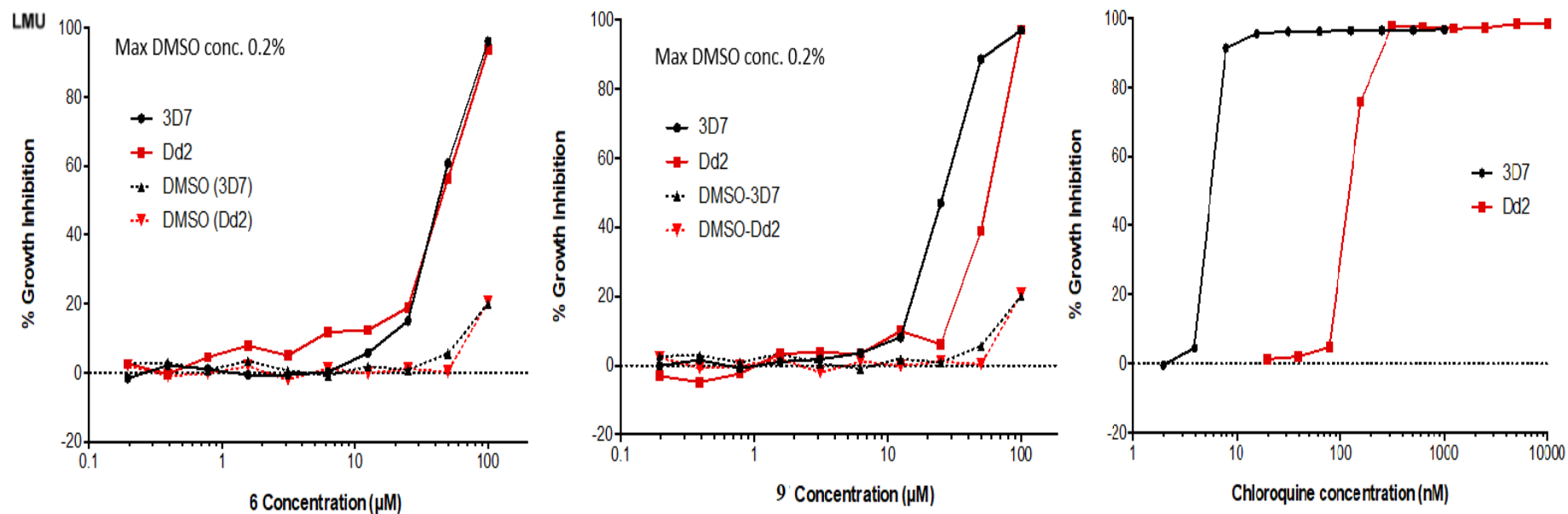


Figure 3.2.1: LMU compounds that had malaria growth inhibition of the *P. falciparum* strains 3D7 and Dd2 compared to the control compound Chloroquine (CQ).

The growth inhibition of both strains of malaria by the known antimalarials chloroquine and pyrimethamine was the control for the experiment for which the rest of the synthesised compounds were compared to. Chloroquine began inhibiting the growth of the *Pf* 3D7 strain at concentrations of ≈ 4 nM, the rate of growth inhibition was exponential and reached $\approx 100\%$ growth inhibition at a concentration of ≈ 7 nM. The drug concentration required to inhibit the *Pf* Dd2 strain was much higher than that required to inhibit the *Pf* 3D7 strain. Chloroquine began inhibiting the growth of the *Pf* Dd2 strain at concentrations of ≈ 90 nM, the rate of growth inhibition was exponential and reached $\approx 100\%$ growth inhibition at a concentration of ≈ 200 nM. Chloroquine had an $EC_{50} \approx 5$ nM for the *Pf* 3D7 strain and an $EC_{50} \approx 100$ nM for the *Pf* Dd2 strain. Compound **6** began inhibiting the growth of the *Pf* 3D7 strain at concentrations of ≈ 10 μ M, the growth inhibition increased at a steady rate until the concentration of the compound reached ≈ 20 μ M when the rate of growth inhibition became exponential and reached $\approx 100\%$ inhibition at a concentration of ≈ 90 μ M. Compound **6** began inhibiting the growth of the *Pf* Dd2 strain at a concentration of ≈ 1 μ M, the rate of growth inhibition increased with the increase in concentration of the compound up until the concentration of the compound reached ≈ 20 μ M when growth inhibition became exponential and reached $\approx 100\%$ inhibition at a concentration of ≈ 90 μ M. Compound **6** had an $EC_{50} \approx 40$ μ M for both the *Pf* 3D7 strain and the *Pf* Dd2 strain, from the ≈ 20 μ M, the growth inhibition profiles of the two strains were similar for this compound.

Compound **9** began inhibiting the growth of the *Pf* 3D7 strain at a concentration of ≈ 3 μ M, the rate of growth inhibition generally increased with increase in concentration of the compound until the concentration of the compound reached ≈ 11 μ M when growth inhibition became exponential up until $\approx 90\%$ inhibition was reached at a concentration of ≈ 30 μ M. The rate of growth inhibition began to level off and reached $\approx 100\%$ inhibition at a concentration of ≈ 90 μ M. Compound **9** began inhibiting the growth of the *Pf* Dd2 strain at a concentration of ≈ 2 μ M, the rate of growth inhibition generally increased with increase in concentration of the compound until the concentration of the compound reached ≈ 20 μ M, when rate of growth

inhibition became exponential and reached $\approx 100\%$ inhibition at a concentration of $\approx 90 \mu\text{M}$. Compound **9** had an $\text{EC}_{50} \approx 25 \mu\text{M}$ for the *Pf* 3D7 strain and an $\text{EC}_{50} \approx 50 \mu\text{M}$ for the *Pf* Dd2 strain. Compounds **6** and **9** were the compounds that showed the best malaria parasite growth inhibition activity. The strain *Pf* 3D7 is two times more sensitive to the compound **9** than the strain *Pf* Dd2. As a comparison with chloroquine, the difference in sensitivity between the *Pf* 3D7 strain and the *Pf* Dd2 strain is greater than 2-fold, which is not surprising due to the presence of the mutant *Pf* CRT (*P. falciparum* chloroquine resistance transporter) gene in malaria parasite strain *Pf* Dd2, which makes this strain (*Pf* Dd2) chloroquine resistant. The strains *Pf* 3D7 and *Pf* Dd2 had the same level of sensitivity to the compound **6** suggesting that the strain *Pf* Dd2 has not developed any resistance to this compound yet.

3.2.2 Compounds that did not have malaria growth inhibition

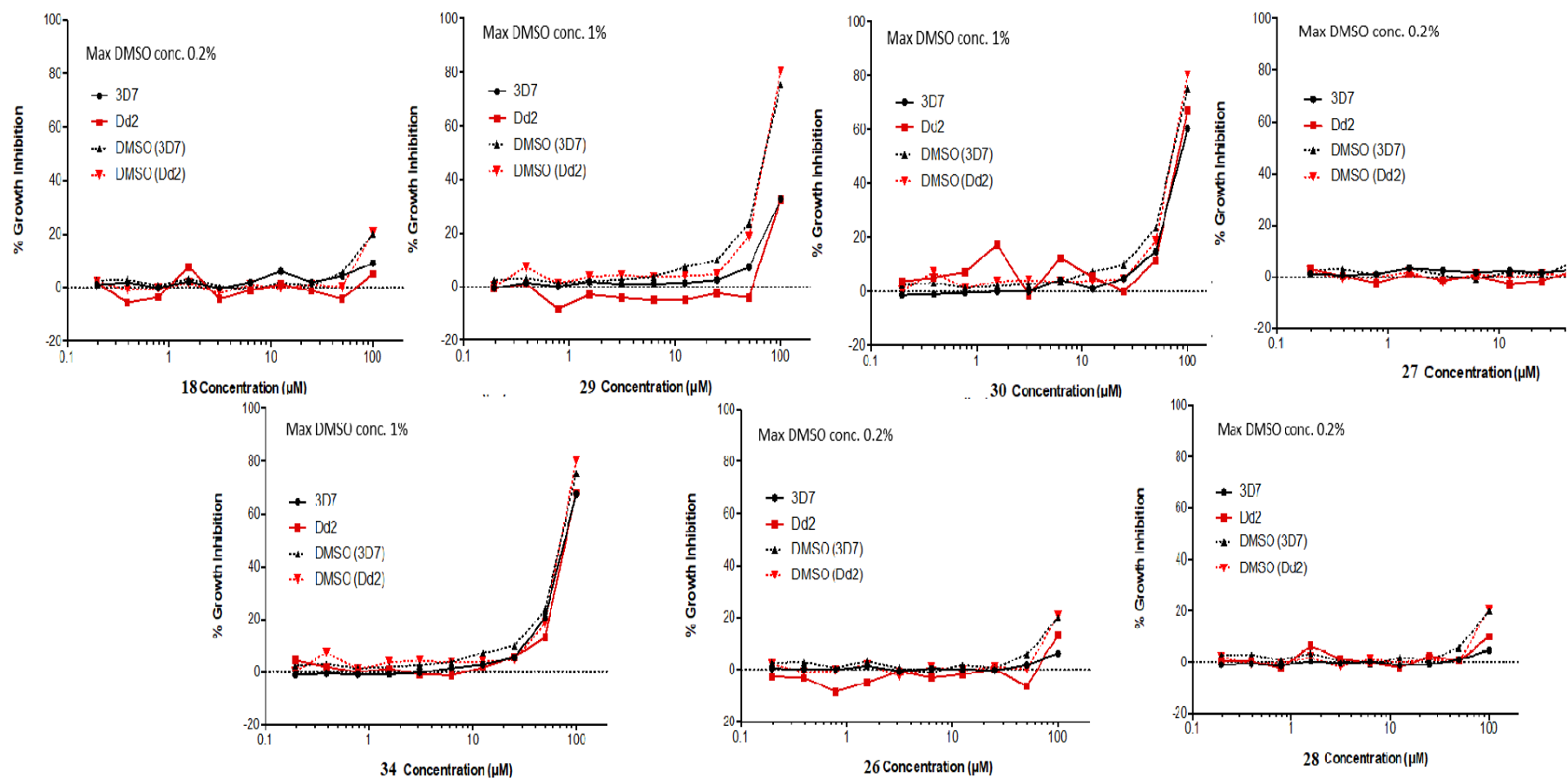


Figure 3.2.2: LMU compounds that did not have malaria growth inhibition for the *P. falciparum* strains 3D7 and Dd2.

The compounds **18**, **29**, **30**, **27**, **26** and **28** did not have any significant malaria parasite growth inhibition activity. The parasite growth inhibition rate for these compounds was similar to the parasite growth inhibition rate of DMSO therefore, the effects of the compounds cannot be distinguished from that of the DMSO control.

While both the parasite fluorescence and the parasite growth inhibition tests come to the same general conclusion with regards to the compounds with antimalarial activity, the growth inhibition tests contain more details and are more accurate. This is because the growth inhibition tests include the DMSO controls which are not included in the fluorescence tests. The DMSO controls helped eliminate compound **34**, since some of the compounds were readily soluble in DMSO, whereas others required a higher concentration of DMSO, and thus the final DMSO concentration in some cases is quite high (1-2%) at the highest drug concentration. At these levels of DMSO concentration (1-2%), the DMSO interfered with the tests. Compound **34** were considered active in the fluorescence test but the growth inhibition test results suggest that any activity these compounds had was due to the high DMSO concentrations rather than the compounds. Another advantage of the growth inhibition test was that it distinguished activity of the compounds between the two different parasite strains, the *Pf*Dd2 strain which is multidrug resistant (including chloroquine and pyrimethamine) and the *Pf*3D7 which is still drug-sensitive.

The compounds that showed activity against the malaria parasites were the substituted benzyl- α -hydroxy phosphonate dibenzyl esters compounds **6** and **9**. The dibenzyl esters enabled the compounds **6** and **9** to diffuse through the cell membranes and get into the cells. The corresponding unprotected phosphonic acids which are compounds **29** and **30** were not soluble in DMSO so they were unable to enter the cells and thus did not have any activity. The compounds that showed activity had the $-\alpha$ -hydroxyl group meaning the hydroxyl functional group in this position is important for the structure activity relationship (SAR).

3.2.3 Activity of compounds against these parasites

Table 12: Activity of tested compounds against *T. brucei*, *T. cruzi*, *L. major* and HeLa

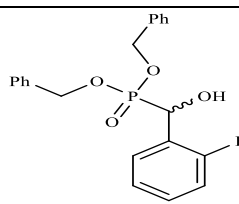
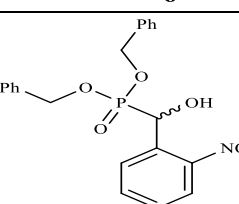
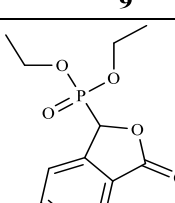
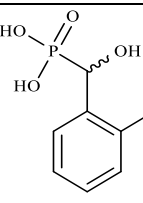
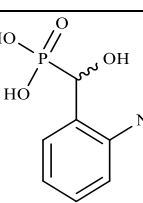
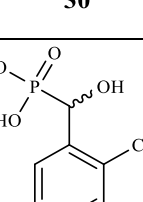
Compound Number & Structure	<i>T. brucei</i> EC ₅₀ (μM)	<i>T. cruzi</i> EC ₅₀ (μM)	<i>L. major</i> EC ₅₀ (μM)	HeLa EC ₅₀ (μM)
 <p>6</p>	30.4 ± 2.1	106.3 ± 5.3	30.4 ± 1.1	37.3 ± 2.1
 <p>9</p>	26.7 ± 1.7	>250	16.5 ± 1.0	112 ± 18
 <p>18</p>	>250	>250	>250	>250
 <p>29</p>	>250	>250	>250	>250
 <p>30</p>	>250	>250	>250	>250
 <p>27</p>	>250	>250	>250	161.2 ± 5.9

Table 13: Activity of tested compounds against *T. brucei*, *T. cruzi*, *L. major* and HeLa

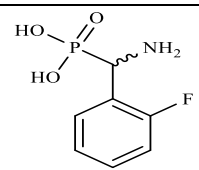
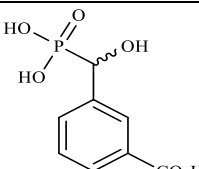
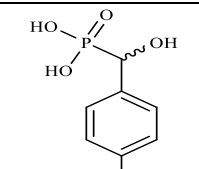
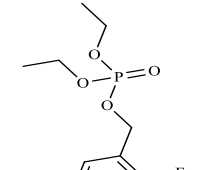
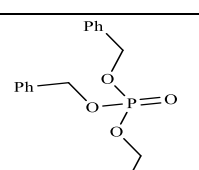
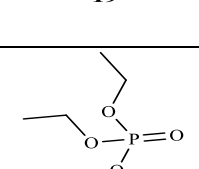
Compound Number & Structure	<i>T. brucei</i> EC ₅₀ (μM)	<i>T. cruzi</i> EC ₅₀ (μM)	<i>L. major</i> EC ₅₀ (μM)	HeLa EC ₅₀ (μM)
 <p>34</p>	>250	>250	>250	>250
 <p>26</p>	>250	>250	130.2 ± 6.8	148.6 ± 7.1
 <p>28</p>	>250	>250	124.8 ± 6.2	>250
 <p>20</p>	125.9 ± 13.5	110.6 ± 5.0	68.7 ± 2.7	91.7 ± 3.8
 <p>19</p>	57.4 ± 3.1	139.7 ± 6.2	81.9 ± 3.9	114.3 ± 5.9
 <p>21</p>	44.8 ± 1.8	112.8 ±	60.1 ± 2.6	70.6 ± 3.5

Table 14: Activity of tested compounds against *T. brucei*, *T. cruzi*, *L. major* and HeLa

cells, but, its low solubility limits its availability for absorption and therefore restricts its activity against all parasitic agents. The benzyl esters **6** and **9** have a high LogP values (3.2 and 5.34 respectively) indicating that they are lipophilic, allowing for the absorption of an adequate concentration of the compound to the site of action, stimulating a response in both the antimalarial tests and the tests against other parasites. The substituted benzyl-dialkyl-phosphates, **19**, **20** and **21** have logP values (2.58, 5.45 and 2.47 respectively) indicating that they are lipophilic allowing for the absorption of an adequate concentration of the compound to the site of action, but, these compounds had moderate or no action against the parasites *T. brucei*, *T. cruzi*, *L. major*. The inactivity of these compounds **19**, **20** and **21** against the parasite *T. cruzi* cannot be attributed to inadequate bioavailability of the compounds but to other factors such as but not limited to poor structure activity relationship (SAR). The compounds that showed activity had the α -hydroxyl group meaning the hydroxyl functional group in this position is important for the structure activity relationship (SAR). Compounds **19**, **20** and **21** have the α -methylene instead of the α -hydroxyl and they are the phosphates version instead of the phosphonate version of the compounds, thus, they are not direct glutamic acid analogues as they contain 5- and 6 bonds between the acidic functional groups rather than 3 bonds, therefore, such factors could contribute to the poor structure activity relationship (SAR) of these compounds.

Table 15: Summary of the tested compounds and the parasites they are active against

Compound Name	Compound Code	Parasite active against
2-Fluorobenzyl- α -hydroxy dibenzyl phosphonate	6	<i>T. brucei</i> , <i>L. major</i> , HeLa
2-Nitrobenzyl- α -hydroxy dibenzyl phosphonate	9	<i>T. brucei</i> , <i>L. major</i>
1,2-benzyl- γ -lactone diethyl phosphonate	18	None
2-carboxybenzyl- α -hydroxy phosphonic Acid	27	None
2-fluorobenzyl- α -hydroxy phosphonic Acid	29	None
2-nitrobenzyl- α -hydroxy phosphonic Acid	30	None
2-fluorobenzyl- α -amino phosphonic Acid	34	None
3-carboxybenzyl- α -hydroxy phosphonic Acid	26	None
4-carboxybenzyl- α -hydroxyl phosphonic Acid	28	None
2-fluoro benzyl-dibenzyl phosphate	19	<i>T. brucei</i> , <i>L. major</i>
2-fluoro benzyl-diethyl phosphate	20	<i>L. major</i> , HeLa
3-cyanobenzyl-diethyl phosphate	21	<i>T. brucei</i> , <i>L. major</i> , HeLa

4 CONCLUSION AND FUTURE WORK

The final substituted benzyl- α -hydroxy phosphonic acids; 3-nitrobenzyl- α -hydroxy phosphonic acid and 4-nitrobenzyl- α -hydroxy phosphonic acid had extremely poor yields (5.2% and 7.7%) respectively and both compounds were insoluble in different NMR solvents or solvent mixtures (DMSO, DMSO- D_2O , D_2O -NaOD, methanol). Attempts to dissolve these compounds in other alcohols; ethanol, isopropanol and butanol proved to be just as unsuccessful. These compounds were insoluble even when they were ionised with up to 11M deuterated sodium hydroxide. Synthesis of the substituted benzyl- α -methylene phosphonates must be repeated using carefully controlled conditions; various temperatures ($-20\text{ }^\circ\text{C}$, $0\text{ }^\circ\text{C}$, RT or $50\text{ }^\circ\text{C}$) and equimolar amounts of CDI and NaH. Careful controlling of the conditions would prevent the 1,2-Brook intramolecular phosphonate-phosphate rearrangement from occurring. The formation of the substituted benzyl- phosphates resulted in the failure of the hydrolysis reactions carried out on the compounds (**19-25**) which may be explained by the rapid hydrolyses of the phosphates to yield phosphoric acid which was then converted into insoluble polyphosphates upon workup, in particular, during rotary evaporation of the highly acidic 6M HCl solutions employed. An alternate method to make the hydroxyl a good leaving group, and enable substitution by hydride, requires the sulfonylation of the alcohol O-H with methanesulfonyl chloride (mesyl chloride) in the presence of pyridine (*Clayden. J, et al, Organic Chemistry, second edition 2001*). The resulting methanesulfonate esters are good leaving groups that are readily displaced by nucleophiles, including hydride anions.

Alternate methods of producing phosphonic acids from their precursors could improve the purity and yields of these phosphonic acids. These methods include, catalytic hydrogenolysis of the dibenzyl phosphonates precursors with a Palladium on charcoal catalyst. Hydrogenolysis of diallyl phosphonates with Wilkinson catalyst ($CIRh(PPh_3)_3$) has been reported to be an efficient way to produce phosphonic acids (*Sevrain. M. C, et al, 2017*).

Further work is needed to attempt to improve the solubility, purity and yields of the substituted benzyl- α -amino phosphonic acids. substituted benzyl- α -amino phosphonic acids were sparingly soluble in different NMR solvents therefore, the peaks in the ^{13}C -NMR for these compound were too small to be identified. Zooming the spectra led to the peaks being covered up by the NMR background or “noise”. The ^{31}P -NMRs for most of the synthesised benzyl- α -amino phosphonic acids showed more than one peak suggesting the products were impure.

Alternate synthetic routes to make these compounds have been proposed and are yet to be attempted. It is hoped that these synthetic routes will produce products with fewer intermediates and therefore improve the purity and yields of the final product. The proposed synthetic route would involve a modified version of the *Kamijo* method, using CDI and azide anion (N_3^-). The resulting substituted benzyl- α -azide diethyl phosphonate can then be converted to its respective substituted benzyl- α -amine diethyl phosphonate by reduction of the azide to an amine by catalytic hydrogenation over Palladium catalyst or by triphenylphosphines in what is known as the Staudinger reaction or by lithium aluminium hydride (LiAlH_4) or by sodium borohydride (NaBH_4) in methanol. Dealkylation of the diethyl phosphonate groups before reduction of the azide with NaBH_4 in methanol would prevent reactivity of the sensitive amine functional group. This method could be most optimal as the reduction of the azide to the amine will occur easily on the resulting azidophosphonic acids. The dealkylation of diethyl phosphonate groups containing amines, amino acids or peptides requires mild conditions to avoid reactivity with these functional groups. Me_3SiBr can also be used to dealkylate diethyl phosphonates with an amine or peptide functionalized groups. Other mild conditions, that may be able to dealkylate amine containing diethyl phosphonates include, the use of a combination of trimethylsilyl trifluoromethanesulfonate (TMS-OTf) as a silylating agent, trifluoroacetic acid (TFA) as the acidic reagent, and dimethylsulfide (DMS) and *m*-cresol to avoid side reactions associated with the generation of carbocations under the deprotecting conditions. The role of DMS is to encourage or ‘push’ the acidolytic cleavage of the protecting group, the cleavage reaction is driven by the addition of H^+ (a hard acid - Lewis

acids that are only weakly polarizable.) to the oxygen atom (a hard base) of the protecting ester group and the nucleophilic attack of the sulphur atom (a soft base) on the electron deficient carbon of the leaving group (soft acid). The reaction involves the cooperative action of the soft nucleophile and the hard electrophile on the substrate (push-pull mechanism). This reagent mixture is a milder form of acidic deprotection than using 6M HCl (*Kiso. Y, et al 1979*). The rate of reaction is depended on the nature of the attacking soft nucleophiles, hence, the cleavage reaction becomes more favourable in the order; thioanisole > dimethyl sulfide > ethanedithiol - phenol > anisole. More importantly, thioanisole has been found to be an alkylating agent at the moderate acidity of the S_N2 reaction conditions and thus may not be an optimal weak base (*Tam. J. P, et al, 1986*). Since dimethyl sulfide (DMS) does not possess this alkylating property, it is a more suitable choice as a weak base for the S_N2 studies. (*Kiso. Y, et al 1980*). This method has been reported as having the potential to generate phosphonic acids from sensitive amine, amino acids or peptides containing diethyl phosphonates (*Tam. J. P, et al, 1986, Sevrain. M. C, et al, 2017*).

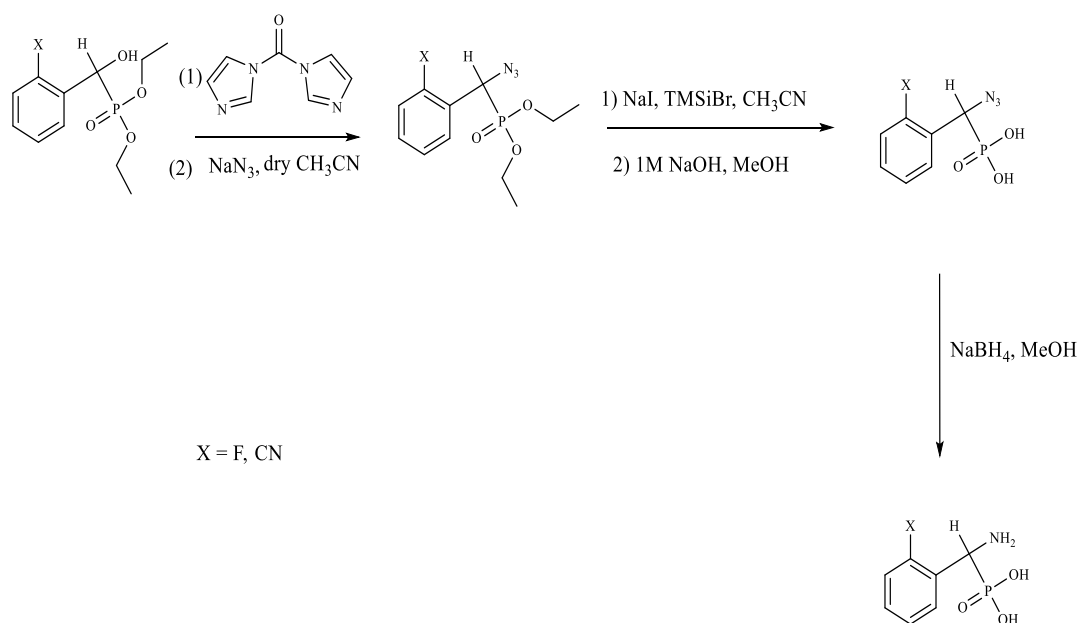


Figure 3.2.1: Proposed alternate reaction mechanism to synthesise substituted benzyl- α -amino phosphonic acid

Monophosphonates and monophosphates drug development has long been hindered by their inherent poor drug likeness properties and poor in vivo stability. This is due to

monophosphonates and monophosphates being negatively charged at physiological pH which results in them having poor bioavailability (*Hecker. S, et al 2008*). Consequently, these compounds have poor in vivo stability which increases the chances of their dephosphorylation in the blood stream and their inefficient transportation into the cells leading to these molecules having low concentrations at the target site (*Mehellou. Y, et al 2017*). The optimization of these compounds to include the application of prodrug strategies that have been successfully applied in the development of some anti-viral and anti-cancer drugs could improve their effectiveness (*Thornton. P, et al 2016*). Phosphonic acids are rarely found in drug candidate moieties, despite the potential that the functional group could provide unique binding interactions with a target enzyme or receptor. Similarly, organophosphonates are rarely incorporated into drug candidates despite the common appearance of phosphates in nucleosides, proteins, lipids and carbohydrates in nature.

Much of the reluctance to use these groups in pharmaceutical compounds stems from the reasons mentioned above which are;

- 1) Their negative charge at physiological pH
- 2) The inability for these molecules to achieve high concentrations at the target site due to poor oral bioavailability and or cell penetration
- 3) Their instability in most biological fluids.

Despite these shortcomings a number of nucleoside phosphates and their phosphonate analogues have proven to be extremely important anti-cancer and antiviral therapies. Consequently, phosphonate containing drugs are increasingly being explored in other therapeutic areas. In order to achieve adequate oral bioavailability and intracellular delivery of phosphonates and similar compounds, pro drug strategies have to be employed (*Hecker. S, et al 2008*). Theoretically, a diester is the simplest derivative of a phosphonic acid that is uncharged at physiological pH, that allows for the phosphonic acid to be transported into cells, the simplest diester being dimethylesters. Such dialkylesters are simple to synthesise and do not offer any stereogenic issues at the phosphorus position but, even with the emergence of

organophosphonate hydrolases in bacteria that have probably been driven by the widespread use of phosphorus-based insecticides, these dialkylesters are surprisingly stable in mammalian systems. Some phosphonate benzyl esters have shown more promise, but they tend to be cleaved and release their phosphonic acids too slowly to be of value. Simple dialkylesters are sometimes unrecognised by esterases and do not undergo the necessary bioconversion to their phosphonic acid therefore, simple dialkylesters could not function as prodrugs. However, diphenyl esters have performed better, being able to release the free phosphonic acid in vivo at high concentrations as well as having physiochemical properties that were more conducive to pharmaceutical formulation. (Wiemer. A, et al 2016). A successful phosphonate prodrug has to be able to:

- 1) Survive the gastrointestinal tract and be absorbed into the systemic circulation
- 2) Remain intact long enough for it to be distributed in specific cell tissues.

The lack of adequate aqueous and metabolic stability greatly limits the effectiveness of many prodrug classes (Hecker. S, et al 2008).

Prodrug strategies for phosphates and phosphonates seek to achieve passive diffusion through the cell membrane by masking the negative charges until the compounds are inside the cell. Therefore, the main considerations include what type of derivative will be used and what process or processes will be entrusted to remove the protecting groups once the prodrug is in the cell. The most common type of derivatives used to protect phosphates and phosphonates are esters and amides, yet, even after the initial choice, there are other concerns to be addressed and a variety of solutions and options that could be attempted. Some of these choices and options when attempting to mask two negative charges include using the same group (symmetrical diesters) or two different groups (unsymmetrical diesters). Different groups (unsymmetrical diesters) create a stereogenic centre at the phosphorus which brings its own challenges and benefits. Different groups may allow more flexibility in terms of the cleavage steps. These concerns have to be addressed in determining whether the ester or amide routes are taken. Another prodrug route that is gaining popularity is mixed ester-amides which have

shown to have an advantage in terms of both the cleavage step and organ or tissue targeting. Determination of the enzymes within the cells that will be involved in the regeneration of the desired drug adds to the complexity of the design as there are several different types of enzymes that could do the job. These include but are not limited to esterases, amidases, phosphatases, or even a redox process. Some reported prodrugs rely on thermal and photochemical cleavage and are available through photodynamic therapy approaches (Wiemer. A, et al 2016).

Work on the development of ProTides prodrug strategies began in the late 1980s with the objective of masking the oxygen atoms of phosphate groups in nucleoside monophosphate analogues so that they are neutral at physiological pH and hence have a better uptake into cells. ProTide prodrug strategy development process took at least two decades and was divided into six phases which began with utilising simple alkyl groups and evolved into utilising the intelligent masking of the phosphate with aryl groups and amino acid esters, which can be cleaved off inside the intact cells. The masking groups that were utilised in the phases of ProTide development strategies were (Mehellou. Y, et al 2017):

- 1) Simple alkyl groups
- 2) Alkyloxy and haloalkyloxy phosphoramidates
- 3) Phosphorodiamidates
- 4) Lactyl-Derived systems
- 5) Diaryl phosphates
- 6) Aryloxy phosphoramidates, referred to as ProTides

ProTide phosphoramidate prodrugs are an example of a prodrug strategy that has been successfully utilised to deliver monophosphates and monophosphonates which Prof. Chris McGuigan began developing at University College London, UK between 1987-1990 and continued later on at Cardiff University, UK (Mehellou. Y, et al 2009). This approach involves the masking of the negative charges of the phosphate or phosphonate with an aryl motif and an amino acid ester group. In the cell, the nucleoside monophosphates/monophosphonates

analogue is released in two enzymatic steps. The first step is initiated by esterases which cleave the ester motif. Under physiological pH (< 7.4), the unmasked, negatively charged carboxyl group carries out a nucleophilic attack on the phosphate or phosphonate group. The second enzyme is a phosphoramidase-type enzyme which cleaves the P-N bond of this metabolite resulting in the release of the nucleoside analogue monophosphate or monophosphonate. This particular prodrug approach has been utilised in the development of sofosbuvir and tenofovir alafenamide and is being applied to numerous other nucleoside ProTides entering clinical trials. ProTide approach has been applied to the experimental anti-cancer medicine NUC-1031, which is being developed by NuCana Biomed Ltd for treatment of lung, ovary, breast, colon and pancreatic cancers (*Thornton. P, et al 2016*). This ProTide, NUC-1031, was found to be effective against cancers that were resistant to the parent therapeutic nucleoside gemcitabine. The ProTide was more successful than the parent drug because:

- 1) It was able to overcome active cellular uptake mechanisms that limit the efficacy of gemcitabine as the prodrug is more lipophilic and enters cells through passive diffusion.
- 2) Overcame the dependency on the essential first activation step by deoxycytidine kinase, which is downregulated in some cancers.
- 3) The delivery of gemcitabine monophosphate limited the deamination of the cytosine nucleobase, which generates the inactive uracil nucleos(t)ide metabolite, a process that reduces the efficacy of gemcitabine.

Similar such improvements have been noticed in the efficacy of other compounds that this ProTide prodrug strategy has been applied to. This includes GS-5734, later renamed Remdesvir, an anti-HCV C-nucleotide ProTide developed by Gilead Science that has shown promising results as a potential treatment for the Ebola virus. GS-5734 (Remdesvir), has been reported to be a broad spectrum anti-viral agent that has exhibited potent activity against a variety of RNA viruses including COVID-19 (*Mehellou. Y, et al 2017; Eastman. R. T, et al 2020*). Improvements have been noticed to the efficacy of the ProTide stampidine, a prodrug

of the anti-HIV reverse transcriptase inhibitor nucleoside stavudine and thymectacin, a phenyl L-alanine methyl ester prodrug of the therapeutic nucleoside brivudine (BVdU) which is used to treat herpes zoster (shingles) (*Thornton. P, et al 2016*).

As with the diester, ProTides that consist of symmetrical diamidates avoid any phosphorus stereochemistry issues, diamidates have been shown to produce compounds that have good cellular activity. Additionally, preparation of symmetrical bisamidates from the symmetrical diesters has been reported (*Wiemer. A, et al 2016*). Another example of phosphate/phosphonate prodrug strategy would be to target a specific organ or tissue; such is the case of the HepDirect approach. The HepDirect aims to design prodrugs that will predominantly be metabolised in the liver via the cytochrome P450 (CYP450) enzymes, hence achieving liver-targeted drug delivery. In this approach, the two negative charges of the phosphate/phosphonate are masked by the formation of a phenyldioxaphosphinane oxide. This prodrug will then undergo oxidation in the liver by the CYP3A enzymes. This prodrug approach has been extensively utilised in the design of hepatitis infections therapeutics. HepDirect prodrug compounds include pradefovir used in the treatment of HBV and MB07133 which is used for the treatment of hepatocellular carcinoma.

There are some phosphate/phosphonate prodrugs that are based on monoesters. In these prodrugs, one of the negative charge is masked and the other is left free. These mono phosphonate/phosphate esters are a form of lipid phosphoconjugates that have been inspired by the natural occurring lysophosphatidylcholine. These conjugates have been shown to benefit from active uptake mechanisms in the intestine resulting in higher oral bioavailability (*Thornton. P, 2016*). Another useful variant of monoesters is the cyclic monoester which offers unique opportunities as a prodrug as it is based on upon an intramolecular cyclization (*Wiemer. A, et al 2016*). A case in point for this type of prodrug is the hexadecyloxypropyl (HDP) monoester prodrugs which are thought to be metabolised in vivo by phospholipases such as phospholipase C. This approach has led to the development of two nucleotide prodrugs in clinical development, brincidofovir a prodrug of the antiviral cidofovir referred to as CMX-

001 is dosed orally unlike its parent compound and is potent against a range of viruses that include adenoviruses, smallpox, cytomegalovirus (CMV), papillomavirus, polyomavirus and orthopoxviruses. CMX-157 is an alkoxyalkyl monoester of the clinically used nucleoside phosphonate tenofovir which is >300 times more active than the parent drug and is active against the major subtypes of the HIV-1 virus (*Thornton. P, 2016*). Work with azidothymidine (AZT) monophosphates reported that combining a monoester with a phosphoramidate led to unexpectedly good cellular potency. In the case of (AZT), the lactate derived aryloxy phosphoramidates led to a highly efficient prodrug (*Wiemer. A, et al 2016*).

As demonstrated by the HepDirect prodrugs, in addition to masking the phosphorus moieties to allow for diffusion across cell membranes, by careful selection of the protecting groups and the processes entrusted to remove the protecting groups, prodrugs can impart cell type and tissue type specificity which can impact the distribution of the free drug. This will determine where and when the free drug can be released. The majority of current prodrugs require enzymatic cleavage prior to release of the free drug that leads to biological function. This enzymatic cleavage especially one that relies on simple esterases and other simple chemical decomposition methods such as early cycloSal compounds or thermolytic prodrugs offer the least amount of control over tissue distribution. Ester based prodrugs are prone to non-specific esterases which are found in most cells as well as in the blood. Therefore, when attempting to use esters as the protecting groups in a prodrug, it might be more effective to prioritize esterase specificity over improved oral absorption. Phosphoramidates have proven to have more plasma stability than acyloxyalkyl ester compounds which allows them to have selectivity as to the enzymes that decompose them thereby giving them cell and or tissue specificity. Diamidates or aryloxy amino acid amidates appear to be released through an initial enzymatic hydrolysis of the amino acid carboxyl ester by the enzyme carboxypeptidase Y (cathepsin A) or carboxylesterase (I), hence, they will target cells and or tissues that express these enzymes. Improvements in the cell and tissue specificity of prodrugs would be greatly aided by a detailed

understanding of the chemistry and the biological systems and pathways involved (*Wiemer. A, et al 2016*).

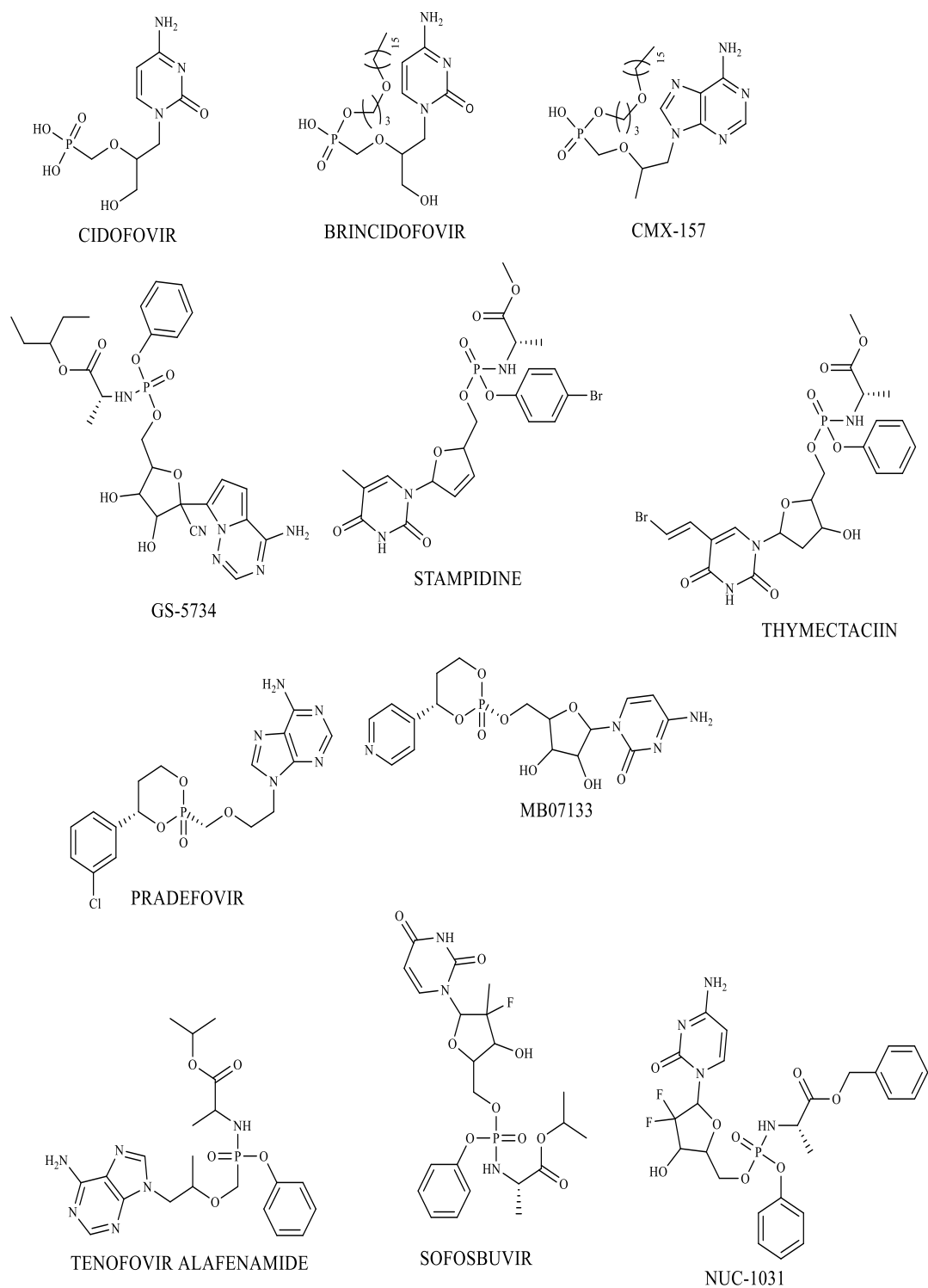
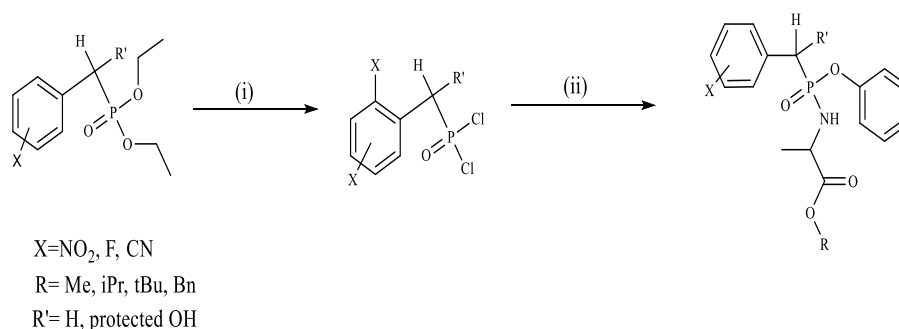


Figure 3.2.2: The structures of ProTide and phosphate ester prodrugs that have been discussed in this section (Thornton. P, et al 2016, Mehellou. Y, et al 2017).

ProTide versions of the synthesised target compounds could have improved efficacy. There are three different strategies that can be applied to generate ProTides which are:

- 1) The coupling of a nucleoside with a diarylphosphite followed by subsequent oxidative amination,
- 2) The coupling of the nucleoside with a phosphorochloridate reagent,
- 3) Coupling of an amino acid to a nucleoside aryl phosphate (Mehellou. Y, 2017)

The proposed synthetic route would be applied for the synthesis of *Pf*GDH inhibitor-ProTides. This synthetic route would work well with the α -methylene derivatives but the α -OH compounds would need protecting with a silyl protecting group like *t*-butyl-dimethylsilyl ((CH₃)₃C-Si-(CH₃)₂) which can be readily cleaved using tetrabutylammonium fluoride in acetonitrile (Bu₄N⁺F⁻/CH₃CN).



Reagents and conditions: (i) (a) TMSiBr, DCM, rt; (b) (COCl)₂, DMF cat, DCM, rt, 18hrs

(ii) (a) Phenol, Et₃N, DCM, -78 C for 30 mins then rt, 3hrs; (b) Substituted L-alanine ester hydrochloride, Et₃N, DCM, rt, 12hrs

Approx yields: 38-61%

Figure 3.2.3: Proposed reaction scheme for the synthesis of *Pf*GDH-inhibitor ProTides

Two promising future targets are 1-amino-cyclopropane-1,2-dicarboxylic acid and 4-methylene glutamic acid (Ezquerro. J, et al 1994), these are fascinating glutamate analogues with the potential to act as irreversible inhibitors of *Pf* GDH. The cyclopropane ring in the compound **46** and the alkene in the compound **44** are reactive and vulnerable to nucleophilic attack. The cyclopropane ring is highly strained due to the 60° bond angles within the ring (angle strain) which is not ideal; this weakens the C-C bonds in the ring making cyclopropane very reactive. As a result, the cyclopropane ring will be susceptible to being cleaved open by the *Pf* GDH in an attempt to relieve the angle strain, thereby, potentially making this analogue

an irreversible inhibitor of the *Pf*GDH enzyme. This is an interesting idea and hopefully it can be explored further by future projects. These compounds will then be submitted for anti-malarial testing to determine their activity.

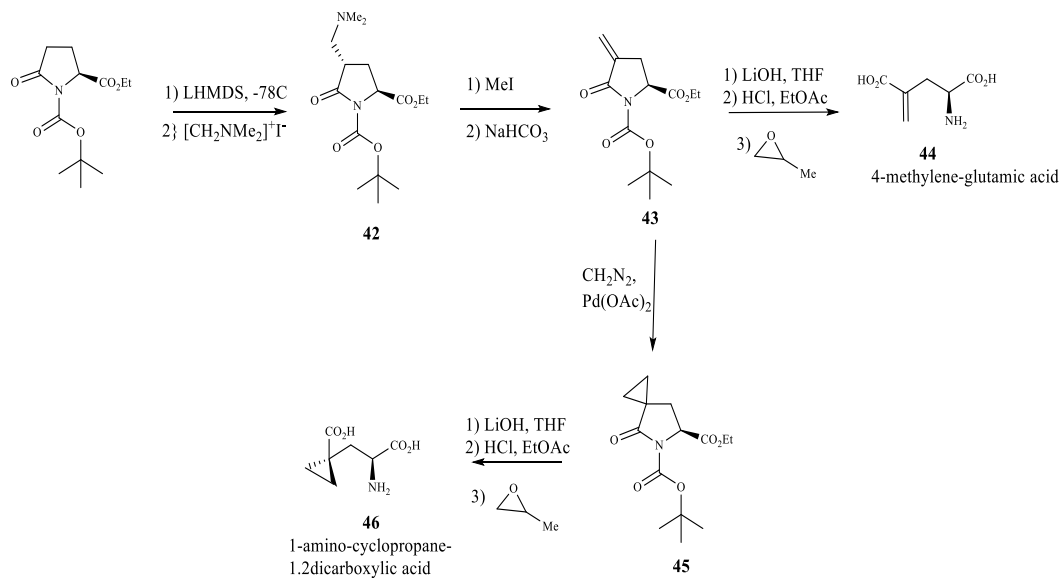


Figure 3.2.4: 1-amino-cyclopropane-1,2-dicarboxylic acid reaction scheme

5 EXPERIMENTAL

5.1 General experimental

All reactions requiring the use of dry conditions were carried out under an atmosphere of nitrogen. Stirring was by internal magnetic follower unless otherwise stated. All reactions were monitored by TLC and organic phases extracted were dried with either anhydrous magnesium sulfate or sodium sulfate. Thin layer chromatographic analysis was carried out using Merck aluminium-backed plates coated with silica gel 60 F254. Components were visualised using ultraviolet light/iodine staining. The compounds that needed further purification were purified by flash column chromatography, the silica gel used was Merck 60 (230-400 mesh). All solvents that needed to be dry such as acetonitrile and tetrahydrofuran (THF) were distilled from calcium hydride. The chemicals that were used in this project were acquired from Fisher Scientific, Sigma-Aldrich, British Oxygen Company (BOC) and Alfa Aesar. The purity of the compounds was not determined and thus unknown.

Infrared spectra were recorded on an Agilent Technologies Cary 630 FT-IR spectrophotometer. Elemental analysis was recorded on a Thermo Scientific Flash 2000 Organic Elemental Analyser. Mass spectra was carried out using Agilent Micromass Q-TOF premier Tandem Mass Spectrometer from Micromass utilising electrospray or a Thermo Electron Corporation DSQ utilising electron impact. Melting points were determined using open glass capillaries on a Stuart Scientific SMP3 apparatus and are uncorrected.

^1H -NMR, ^{13}C -NMR and ^{31}P -NMR were recorded on a Bruker Avance AV500 spectrometer operating at 500 MHz for proton, 126 MHz for carbon and 202 MHz for phosphorus. Chemical shifts (δ_{H} and δ_{C}) are quoted as parts per million downfield from 0. The multiplicity of a ^1H -NMR signal is designated by one of the following abbreviations: s = singlet, d = doublet, t = triplet, q = quartet, quin = quintet, sept = septet, br. = broad and m = multiplet. Coupling constants (J) are expressed in Hertz (Hz).

5.2 Synthesis of substituted benzyl- α -hydroxy phosphonates

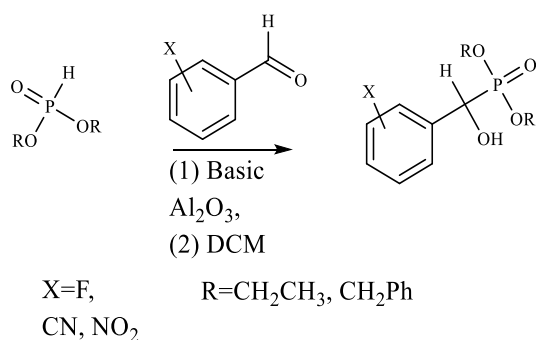
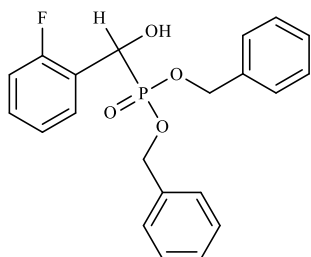


Figure 5.2.1: Synthesis of substituted benzyl- α -hydroxy phosphonates general reaction scheme

To a round bottomed flask, dibenzyl phosphite/diethyl phosphite was added to a solution of a substituted benzaldehyde dissolved in dichloromethane (15 cm³). Basic alumina (Al₂O₃) 10 molar excess was added to the reaction mixture and the resultant mixture was stirred and left to stand for 48 hours. The resultant mixture was washed with dichloromethane (120 cm³) and the basic alumina catalyst was removed under reduced pressure. The filtrate was concentrated under reduced pressure and the resultant residue was washed with a mixture of hexane/diethyl ether (1:1, 20 cm³) four times and dried under reduced pressure for an hour.

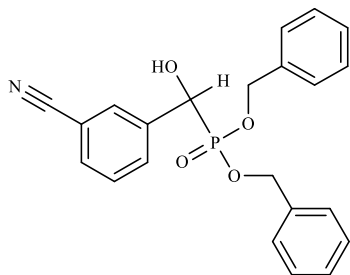
5.2.1 2-Fluorobenzyl- α -hydroxy dibenzyl phosphonate (6)



2-Fluorobenzaldehyde (1.0 cm³, 9.5 mmol), dibenzyl phosphite (2.1 cm³, 9.5 mmol) and 10 M basic alumina (Al₂O₃) (9.70 g, 95.1 mmol). Product; colourless solid (2.51 g, 98%). R_f = 0.64; (EtOAc:Hex; 8:2), mp 79-81°C; $\nu_{\text{max}}/\text{cm}^{-1}$ 3238 (O-H), 1212 (P=O), 963 (P-O), 996 (C-F); δ_{H} (500 MHz, CDCl₃) 4.94 – 5.06 (4 H, m, 2 × PhCH₂O), 5.52-5.56 (2 H, m, CH-OH, CH-OH), 6.96- 6.98 (1 H, m ArH), 7.11 (1 H, t, *J* 7.6, ArH), 7.17-7.18 (2 H, m, 2 × ArH), 7.21-7.28 (9 H, m, 9 × ArH), 7.71 (1 H, tt, *J* 5.0, ArH). δ_{C} (126 MHz, CDCl₃) 63.94 (1 C, dd, *J*, 163.5, 2.7, CH-OH), 68.24 (1 C, d, *J* 7.3, Ph-CH₂), 77.06 (1 C, d, *J* 6.4, Ph-CH₂-), 115.03 (1 C, dd, *J* 21.8, 8.8, ArC), 124.26–124.36 (2 C, m, 2 × ArC), 127.73 (4 C, d, *J* 1.8, 4 × ArC),

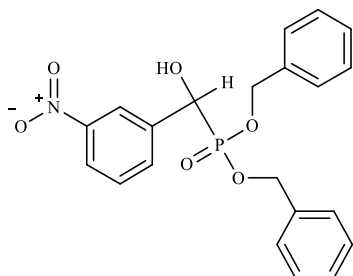
128.23-128.26 (3 C, m, 3 × ArC), 128.41 (4 C, d, *J* 3.6, 4 × ArC), 129.08 (1 C, t, *J* 3.6, ArC), 129.63 (1 C, dd, *J* 8.2, 2.7, ArC), 135.99 (1 C, dd, *J* 5.9, 2.3, ArC), 159.65 (1 C, dd, *J* 255.78, 7.3, ArCF). δ_P (202 MHz, CDCl₃) 22.19 (1 P, d, *J* 6.06). *m/z* (EI⁺): 262 [(PhCH₂O)₂PO]⁺, 34%), 180 ([C₆H₄CHPO₃C]⁺, 30), 171 ([FC₆H₄CPO₂]⁺, 73), 122.87 ([FC₆H₄CO]⁺, 38), 91 ([C₇H₇]⁺, 100).

5.2.2 3-Cyanobenzyl- α -hydroxy dibenzyl phosphonate (7)



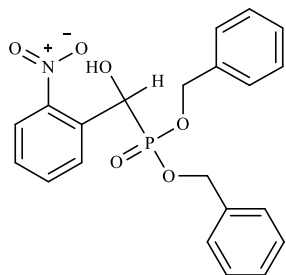
3-Formylbenzonitrile (0.51 g, 3.9 mmol), dibenzyl phosphite (0.86 cm³, 3.9 mmols). Basic alumina (Al₂O₃) (4.0 g, 39.2 mmol). Product; colourless solid (0.57 g, 54%). *R_f* = 0.46; (EtOAc:Hex; 8:2), mp 81-83 °C; $\nu_{\max}/\text{cm}^{-1}$ 3234 (OH), 2233 (CN), 1220 (P=O), 978 (P-O); δ_H (500 MHz, CDCl₃) 4.94-5.05 (4H, m, 2×PhCH₂), 5.08 (1 H, dd, *J* 10.0, 5.0, CH-OH), 5.44 (1 H, t, *J* 5.0, CH-OH-), 7.21-7.33 (10 H, m, 10 × ArH), 7.35 (1 H, d, *J* 10.0, ArH), 7.54 (1 H, dd, *J* 10.0, 5.0, ArH), 7.61 (1 H, d, *J* 10.0, ArH), 7.64 (1 H, s, ArH). δ_C (126 MHz, CDCl₃) 68.63 (1 C, d, *J* 7.6, PhCH₂), 69.14 (1 C, d, *J* 6.3, PhCH₂), 70.02 (1 C, d, *J* 160.02, CH-OH), 112.24 (1 C, d, *J* 2.5, ArC), 118.60 (1 C, s, ArCM), 128.04-128.76 (11 C, m, 11× ArC), 128.86 (1 C, d, *J* 5.0, ArC), 130.64 (1 C, d, *J* 5.0, ArC), 131.43 (1 C, d, *J* 3.8, ArC), 131.51 (1 C, d, *J* 2.5, ArC), 135.56 (1 C, t, *J* 8.8, ArC), 138.12 (1 C, s, ArC). δ_P (202 MHz, CDCl₃) 21.39 (1 P, s). *m/z* (EI⁺): 394 ([M]⁺, 17%), 302 ([M-C₇H₇]⁺, 100), 262 [(PhCH₂O)₂PO]⁺, 100), 222 ([CNC₆H₄CH(OH)PO₂(CH₂)₂]⁺, 5), 196 ([CNC₆H₄CH(OH)PO₂]⁺, 87), 180 ([CNC₆H₄CH(OH)PO]⁺, 100), 107 ([C₆H₄CH(OH)]⁺, 100), 92 ([C₇H₇]⁺, 100).

5.2.3 3-Nitrobenzyl- α -hydroxy dibenzyl phosphonate (8)



3-Nitrobenzaldehyde (1.51 g, 10.0 mmol), dibenzyl phosphite (2.2 cm³, 10.0 mmol), basic alumina (Al₂O₃) (10.2 g, 100 mmol). Product; colourless solid (2.64 g, 64%). $R_f = 0.33$; (EtOAc:Hex; 1:1), mp 115-117 °C; $\nu_{\max}/\text{cm}^{-1}$ 3190 (OH), 1529 (NO₂), 1290 (P=O), 1000 (P-O); δ_{H} (500 MHz, CDCl₃) 4.78 (1 H, t, J 5.0, CH-OH), 5.02-5.05 (4 H, m, 2 \times PhCH₂-), 5.15 (1 H, dd, J 10.0, 5.0, CH-OH), 7.23-7.32 (10 H, m, 10 \times ArH), 7.43 (1 H, t, J 7.5, ArH), 7.71 (1 H, d, J 5.0, ArH), 8.11 (1 H, d, J 10.0, ArH), 8.28 (1 H, d, J 5.0, ArH). δ_{C} (126 MHz, CDCl₃) 68.76 (1 C, d, J 7.6, PhCH₂), 69.16 (1 C, d, J 7.6, PhCH₂), 70.21 (1 C, d, J 158.76, CH-OH), 122.11 (1 C, d, J 5.0, ArC), 122.93 (1 C, d, J 2.5, ArC), 128.09-128.77 (10 C, m, 10 \times ArC), 129.03, (1 C, d, J 2.5, ArC), 133.03 (1 C, d, J 6.3, ArC), 135.55 (1 C, dd, J 8.8, 2.5, ArC), 138.51 (1 C, d, J 2.5, ArC), 148.13 (1 C, d, J 2.5, ArC). δ_{P} (202 MHz, CDCl₃) 21.17 (1 P, s). m/z (EI⁺): 414.11 ([M]⁺, 10%), 322 ([M-PhCH₂]⁺, 100), 262 ([PhCH₂O]₂PO]⁺, 100), 216 ([NO₂C₆H₄CH(OH)PO₂]⁺, 100), 91 ([C₇H₇]⁺, 100).

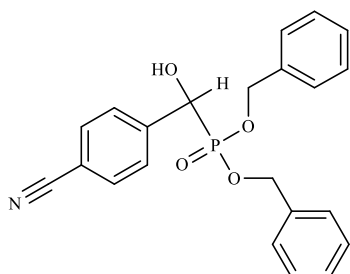
5.2.4 2-Nitrobenzyl- α -hydroxy dibenzyl phosphonate (9)



2-Nitrobenzaldehyde (1.51 g, 10.0 mmol) dibenzyl phosphite (2.2 cm³, 10.0 mmol). Basic alumina (Al₂O₃) (10.2 g, 100 mmol). Product; colourless solid (2.68 g, 65%). $R_f = 0.53$; (EtOAc:Hex; 1:1), mp 108-110 °C; $\nu_{\max}/\text{cm}^{-1}$ 3178 (OH), 1529 (NO₂), 1290 (P=O), 985 (P-O); δ_{H} (500 MHz, CDCl₃) 4.63 (1 H, t, J 5.0, CH-OH), 4.94-5.06 (4 H, m, 2 \times PhCH₂), 6.32 (1 H,

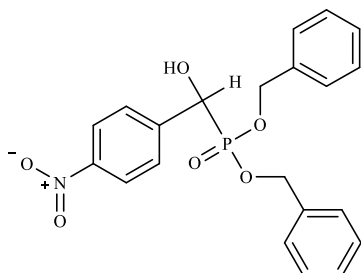
dd, J 15.0, 10.0, CH-OH), 7.16-7.31 (10 H m, $10 \times$ ArH), 7.40-7.44 (1 H, m, ArH), 7.61 (1 H, t, J 10.0, 5.0, ArH), 7.93 (1 H, d, J 10.0, ArH), 7.96 (1 H, d, J 5.0, ArH). δ_c (126 MHz, CDCl₃) 66.14 (1 C, d, J 158.76, CH-OH), 68.75 (1 C, d, J 6.3, PhCH₂), 69.06 (1 C, d, J 6.3, PhCH₂), 124.88 (1 C, d, 1.3, ArC), 127.91-128.60 (11 C m, $11 \times$ ArC), 128.97 (1 C, d, J 3.8, ArC), 132.51 (1 C, s, ArC), 133.45 (1 C, d, J 3.8, ArC), 135.70 (1 C, dd, J 5.0, 3.8, ArC), 147.49 (1 C, d, J 6.3, ArC). δ_p (202 MHz, CDCl₃) 21.59 (1 P, s). m/z (EI⁺): 414 ([M]⁺, 4%), 306 ([M-PhCH₂O]⁺, 3), 262 [(PhCH₂O)₂PO]⁺, 33), 216 (NO₂C₆H₄CH(OH)PO₂⁺, 57), 91 ([C₇H₇]⁺, 100).

5.2.5 4-Cyanobenzyl- α -hydroxy dibenzyl phosphonate (10).



4-Cyanobenzaldehyde (1.01 g, 7.7 mmol), dibenzyl phosphite (1.7 cm³, 7.7 mmol), Basic alumina (Al₂O₃) (7.9 g, 77.5 mmol). Product; colourless solid (3.15 g, 96%). (data for this compound agreed with Pawar, V., et al 2006) R_f = 0.41; (EtOAc:Hex; 1:1), mp 115-117 °C; $\nu_{\max}/\text{cm}^{-1}$ 3227 (OH), 2229 (CN), 1223 (P=O), 978 (P-O); δ_H (500 MHz, CDCl₃) 4.89-5.03 (4 H, m, $2 \times$ PhCH₂), 4.18 (1 H, br, CH-OH), 5.10 (1 H, d J 10.0, CH-OH-), 7.20-7.37 (10 H, m, $10 \times$ ArH), 7.47 (2 H, d, J 10.0, $2 \times$ ArH). 7.54 (2 H, d, J 10.0, $2 \times$ ArH). δ_c (126 MHz, CDCl₃) 68.69 (1 C, d, J 7.6, PhCH₂), 69.04 (1 C, d, J 7.6, PhCH₂), 70.49 (1 C, d, J 157.50, CH-OH), 111.72 (1 C, d, J 2.5, ArC), 118.70 (1 C, s, ArCN), 127.55-128.68 (10 C, m, $10 \times$ ArC), 128.76 (2 C, d, J 3.8, $2 \times$ ArC), 131.90 (2 C, d, J 2.5, $2 \times$ ArC), 135.55 (1 C, dd, J 5.0, 3.8, ArC), 141.43 (1 C, d, J 2.5, ArC). δ_p (202 MHz, CDCl₃) 21.20 (1 P, s). m/z (TOF ES⁺): 394 ([M+H]⁺, 30%).

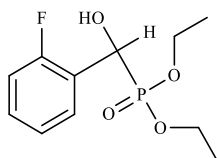
5.2.6 4-Nitrobenzyl- α -hydroxy dibenzyl phosphonate (11).



4-Nitrobenzaldehyde (1.51 g, 10.0 mmol), dibenzyl phosphite (2.2 cm³, 10.0 mmol). Basic alumina (Al₂O₃) (10.2 g, 100 mmol). Product; green solid (2.38 g, 58%). (data for this compound agreed with Pogatchnik, D., et al 1997). $R_f = 0.33$; (EtOAc:Hex; 1:1), mp 105-108 °C; $\nu_{\max}/\text{cm}^{-1}$ 3275 (OH), 1521 (NO₂), 1223 (P=O), 970 (P-O); δ_{H} (500 MHz, CDCl₃) 4.60 (1 H, br, CH-OH), 4.92-5.05 (4 H, m, 2 × PhCH₂), 5.15 (1 H, dd, J 10.0, 5.0, CH-OH), 7.21-7.34 (10 H, m, 10 × ArH), 7.52 (2 H, d, J 10.0, 2 × ArH), 8.09 (2 H, d, J 10.0, 2 × ArH). δ_{C} (126 MHz, CDCl₃) 68.78 (1 C, d, J 7.6, PhCH₂), 69.15 (1 C, d, J 7.6, PhCH₂), 70.45 (1 C, d, J 157.50, CH-OH), 127.69 (1 C, s, ArC), 127.73 (1 C, s, ArC), 128.10-128.70 (8 C, m, 8 × ArC), 128.78 (1 C, s, ArC), 128.83 (1 C, s, ArC), 135.55 (1 C, t, J 3.9, ArC), 143.45 (1 C, d, J 2.5, ArC), 147.58 (1 C, d, J 3.8, ArC). δ_{P} (202 MHz, CDCl₃) 21.03 (1 P, s). m/z (TOF ES⁺): 414 ([M+H]⁺, 18%).

5.3 Synthesis of substituted benzyl- α -hydroxy diethyl phosphonates

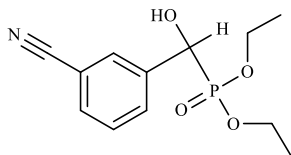
5.3.1 2-Fluorobenzyl- α -hydroxy diethyl phosphonate (12)



2-Fluorobenzaldehyde (2.0 cm³, 19.2 mmol) diethyl phosphite (2.4 cm³, 18.6 mmol) basic alumina Al₂O₃ (19.38 g, 190 mmol). Product; colourless solid (2.37 g, 47%). $R_f = 0.26$; (EtOAc:Hex; 8:2), mp 58-61 °C; $\nu_{\max}/\text{cm}^{-1}$ 3216 (OH), 2985 (C-H), 1205 (P=O), 1019 (C-F), 963 (P-O); δ_{H} (500 MHz, CDCl₃) 1.22 (3 H, t, J 7.5, CH₃), 1.31 (3 H, t, J 7.5, CH₃), 4.00-4.16 (4 H, m, 2 × CH₂O-), 4.65 (1 H, t, J 5.0, CH-OH), 5.40 (1 H, dd, J 15.0, 10.0, CH-OH), 7.04 (1 H, dd, J 10.0, 10.0, ArH), 7.19 (1 H, t, J 7.5, ArH), 7.27-7.30 (1 H, m, ArH), 7.69 (1 H, tt,

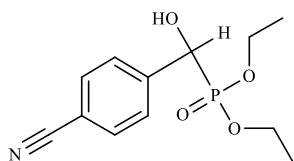
J 10.0, 5.0, ArH). δ_c (126 MHz, CDCl₃), 16.34-16.37 (2 C, m, 2 × CH₃), 63.15 (1 C, d, J 7.6, CH₂O), 63.59 (1 C, d, J 7.6, CH₂O-), 63.87 (1 C, dd, J 162.54, 3.8, CH-OH), 115.02 (1 C, dd, J 21.42, 2.5, ArC), 124.26 (1 C, t, 6.3, ArC), 124.41 (1 C, dd, 13.86, 2.5, ArC), 128.87 (1 C, t, J 16.4, ArC), 129.62 (1 C, dd, J 8.82, 2.5, ArC), 158.74 (1 C, d, J 7.6, ArC), 160.71 (1 C, dd, J 248.22, 7.6, ArC). δ_p (202 MHz, CDCl₃) 21.35 (1 P, d, J 6.06). m/z (EI⁺): 262 ([M]⁺, 66%), 245 ([M-OH]⁺, 2), 233 ([M-(CH₃)₂]⁺, 9), 217 ([M-OCH₂CH₃]⁺, 3) 186 ([FC₆H₄CHPO(OCH₂)]⁺, 7), 172 ([M-(OCH₂CH₃)₂]⁺, 2) 153 ([CH(OH)PO(OCH₂CH₃)(OCH₂)]⁺, 14) 138 ([FC₆H₄CP]⁺, 32), 97 ([C₆H₄F]⁺, 32) 77 ([C₆H₄]⁺, 25).

5.3.2 3-Cyanobenzyl- α -hydroxy diethyl phosphonate (13).



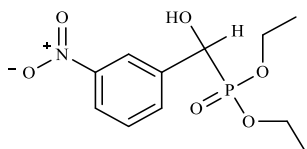
3-Cyanobenzaldehyde (0.5 g, 3.8 mmol) diethyl phosphite (0.5 cm³, 3.9 mmol), basic Alumina catalyst (Al₂O₃) (3.99 g, 39.1 mmol). Product; colourless solid (0.84 g, 82%). (data for this compound agreed with Pandi. M, et al 2012, 99%). R_f = 0.15; (EtOAc:Hex; 8:2), mp 68-72 °C; ν_{max} /cm⁻¹ 3208 (OH), 2985 (C-H), 2225 (CN), 1230 (P=O), 963 (P-O); δ_H (500 MHz, CDCl₃) 1.26 (3 H, t, J 5.0, CH₃), 1.30 (3 H, t, J 5.0, CH₃), 4.10- 4.16 (4 H, m, 2 × CH₂O-), 5.09 (1 H, dd, J 10.0, 5.0, CH-OH), 5.55 (1 H, t, J 5.0, CH-OH), 7.47 (1 H, t, J 10.0, ArH), 7.60 (1 H, dd, J 10.0, ArH), 7.72 (1 H, d, J 10.0, ArH), 7.84 (1 H, s, ArH). δ_c (126 MHz, CDCl₃) 16.36-16.43 (2 C, m, 2 × CH₃), 63.26 (1 C, d, J 7.6, CH₂O), 63.93 (1 C, d, J 7.6, CH₂O-) 69.74 (1 C, d, J 161.28, CH-OH), 112.30 (1 C, s, ArC), 118.76 (1 C, s, ArCN), 128.88 (1 C, d, J 2.5, ArC), 130.54 (1 C, d, J 5.0, ArC), 131.41-131.47 (2 C, m, 2 × ArC), 138.71 (1 C, d, J 2.5, ArC). δ_p (202 MHz, CDCl₃) 20.56 (1 P, s). m/z (EI⁺): 269 ([M]⁺, 10%), 241 ([M-(CH₃CH₂)]⁺, 5), 224 ([M-(OCH₂CH₃)]⁺, 8) 180 ([M-(OCH₂CH₃)₂]⁺, 5), 147 ([CNC₆H₄CHP]⁺, 5), 102 ([C₆H₄CN]⁺, 36).

5.3.3 4-Cyanobenzyl- α -hydroxy diethyl phosphonate (14).



4-Cyanobenzaldehyde (0.5 g, 3.8 mmol) diethyl phosphite (0.5 cm³, 3.9 mmol) basic alumina (3.9 g, 38.2 mmol). Product; colourless solid (0.872 g, 85%). (data for this compound agreed with Pandi. M, et al 2012, 99%). $R_f = 0.18$, (EtOAc:Hex; 8:2), mp 69-73 °C; $\nu_{\max}/\text{cm}^{-1}$ 3234 (OH), 2950 (C-H), 2229 (CN), 1255 (P=O), 1030 (P-O); δ_{H} (500 MHz, CDCl₃) 1.26 (3 H, t, J 7.5, CH₃), 1.28 (3 H, t, J 7.5, CH₃), 4.05-4.15 (4 H, m, 2 × CH₂O), 5.05-5.08 (1 H, m, CH-OH), 5.11 (1 H, dd, J 10.0, 5.0, 1 × CH-OH), 7.61 (2 H, d, J 5.0, 2 × ArH), 7.66 (2 H, d, J 10.0, 2 × ArH). δ_{C} (126 MHz, CDCl₃) 16.35-16.43 (2 C, m, 2 × CH₃), 63.25 (1 C, d, J 7.6, CH₂O), 63.89 (1 C, d, J 6.3, CH₂O-) 70.15 (1 C, d, J 157.5, CH-OH), 111.62 (1 C, d, J 2.5, ArC), 118.76 (1 C, d, J 1.3, ArCN), 127.55 (2 C, d, J 5.0, 2 × ArC), 131.92 (2 C, d, J 2.5, 2 × ArC). δ_{P} (202 MHz, CDCl₃) 20.43 (1 P, s). m/z (EI⁺): 269 ([M]⁺, 55%), 252. ([M-OH]⁺, 7), 241 ([M-(CH₃CH₂)⁺, 12), 224 ([M-(OCH₂CH₃)⁺, 57) 180 ([M-(OCH₂CH₃)₂]⁺, 15), 147 ([CNC₆H₄CHP⁺], 3).

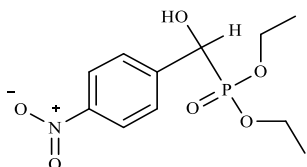
5.3.4 3-Nitrobenzyl- α -hydroxy diethyl phosphonate (15).



3-Nitrobenzaldehyde (1.51 g, 10.0 mmol), diethyl phosphite (1.4 cm³, 10.9 mmol), basic alumina (Al₂O₃) (10.2 g, 100 mmol). Product; colourless solid (2.74 g, 95%). (data for this compound agreed with Goldeman. W, et al 2006, 79%). $R_f = 0.17$; (EtOAc:Hex; 1:1), mp 76-79 °C; $\nu_{\max}/\text{cm}^{-1}$ 3234 (OH), 2981 (C-H), 1540 (NO₂), 1350 (NO₂), 1208 (P=O), 1019 (P-O); δ_{H} (500 MHz, CDCl₃) 1.27 (3 H, t, J 5.0, CH₃), 1.31 (3 H, t, J 7.5, CH₃), 4.09- 4.17 (4 H, m, 2 × CH₂O-), 5.18 (1 H, dd, J 15.0, 10.0, CH-OH), 5.55 (1 H, t, J 10.0, CH-OH), 7.53 (1 H, t, J 7.5, ArH), 7.82 (1 H, d, J 10.0, ArH), 8.17 (1 H, d, J 10.0, ArH), 8.43 (1 H, d, J 5.0, ArH). δ_{C} (126 MHz, CDCl₃) 16.36-16.43 (2 C, m, 2 × CH₃), 63.33 (1 C, d, J 6.3, CH₂O), 63.99 (1 C,

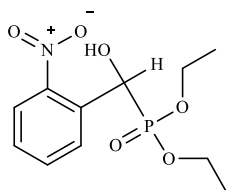
d, J 7.6, CH_2O -) 69.86 (1 C, d, J 160.02, CH-OH), 122.05 (1 C, d, J 5.0, ArC), 122.81 (1 C, d, J 2.5, ArC), 129.01 (1 C, d, J 2.5, ArC), 133.04 (1 C, d, J 5.0, ArC), 139.33 (1 C, d, J 1.3, ArC) 148.22 (1 C, d, J 2.5, ArC). δ_{P} (202 MHz, CDCl_3) 20.36 (1 P, s). m/z (EI^+): 290 ($[\text{M}]^+$, 20%), 272 ($[\text{M}-(\text{OH})]^+$, 3), 244 ($[\text{M}-(\text{OCH}_2\text{CH}_3)]^+$, 3), 152 ($[-\text{CHPO}(\text{OCH}_2\text{CH}_3)_2]^+$, 10), 138 ($[-\text{O}_2\text{NC}_6\text{H}_4\text{CH}]^+$, 100), 77 ($[\text{C}_6\text{H}_4]^+$, 42).

5.3.5 4-Nitrobenzyl- α -hydroxy diethyl phosphonate (16).



4-Nitrobenzaldehyde (1.51 g, 10.0 mmol) diethyl phosphite (1.4 cm^3 , 10.9 mmol) basic alumina (Al_2O_3) (10.2 g, 100 mmol). Product; brown solid (2.83 g, 98%). (data for this compound agreed with Pandi. M, et al 2012, 98%). R_f = 0.17; (EtOAc:Hex; 1:1), mp 75-78 $^\circ\text{C}$; ν_{max} / cm^{-1} 3231 (OH), 2990 (C-H), 1521 (NO_2), 1350 (NO_2), 1238 (P=O), 1019 (P-O); δ_{H} (500 MHz, CDCl_3) 1.26-1.31 (6 H, m, $2 \times \text{CH}_3$), 4.09-4.15 (4 H, m, $2 \times \text{CH}_2\text{O}$), 5.18 (1 H, d, J 10.0, CH-OH), 5.11 (1 H, br, CH-OH), 7.68 (2 H dd, J 2.5, $2 \times \text{ArH}$), 8.23 (2 H, d, J 2.5, $2 \times \text{ArH}$). δ_{C} (126 MHz, CDCl_3) 16.36-16.45 (2 C, m, $2 \times \text{CH}_3$), 63.32 (1 C, d, J 7.6, CH_2O -), 63.99 (1 C, d, J 7.6, CH_2O -) 70.11 (1 C, d, J 157.50, CH-OH), 123.33 (2 C, d, J 2.5, $2 \times \text{ArC}$), 127.66 (2 C, d, J 6.3, $2 \times \text{ArC}$), 142.20 (1 C, d, J 2.5, ArC), 147.53 (1 C, d, J 2.5, ArC). δ_{P} (202 MHz, CDCl_3) 20.20 (1 P, s). m/z (EI^+): 290 ($[\text{M}]^+$, 100%), 272 ($[\text{M}-(\text{OH})]^+$, 10) 262 ($[\text{M}-(\text{CH}_3\text{CH}_2)]^+$, 1), 244 ($[\text{M}-(\text{OCH}_2\text{CH}_3)]^+$, 13), 228 ($[\text{M}-\text{O}(\text{OCH}_2\text{CH}_3)]^+$, 1), 152 ($[-\text{CH-PO}(\text{OCH}_2\text{CH}_3)_2]^+$, 6.3), 138 ($[-\text{O}_2\text{NC}_6\text{H}_4\text{-CH}]^+$, 100), 77 ($[\text{C}_6\text{H}_4]^+$, 45).

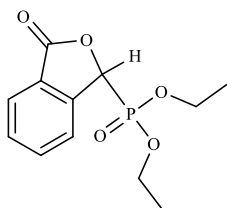
5.3.6 2-Nitrobenzyl- α -hydroxy diethyl phosphonate (17).



2-Nitrobenzaldehyde (1.51 g, 10.0 mmol), diethyl phosphite (1.3 cm^3 , 10.1 mmol), basic alumina (Al_2O_3) (10.2 g, 100 mmol). Product; colourless solid (2.16 g, 74%). (data for this

compound agreed with *Pandi. M, et al 2012, 97%*). $R_f = 0.28$; (EtOAc:Hex; 1:1), mp 109-111 °C; $\nu_{\max}/\text{cm}^{-1}$ 3231 (OH), 2985 (C-H), 1532 (NO₂), 1350 (NO₂), 1205 (P=O), 1015 (P-O); δ_{H} (500 MHz, CDCl₃) 1.21 (3 H, t, J 7.5, 1 × CH₃), 1.27 (3 H, t, J 7.5, 1 × CH₃), 4.07- 4.16 (4 H, m, 2 × CH₂O), 5.40 (1 H, t, J 7.5, CH-OH), 6.29 (1 H, dd, J 15.0, 10.0, CH-OH), 7.46 (1 H, t, J 7.5, ArH), 7.69 (1 H, t, J 7.5, ArH), 7.99-8.01 (2 H, m, 2 × ArH). δ_{C} (126 MHz, CDCl₃) 16.17 (1 C, d, J 6.3, CH₃), 16.27 (1 C, d, J 5.0, CH₃), 63.35 (1 C, d, J 7.6, CH₂O), 64.10 (1 C, d, J 7.6, CH₂O-), 65.62 (1 C, d, J 161.28, CH-OH), 124.72 (1 C, d, J 3.8, ArC), 128.40 (1 C, d, J 3.8, ArC) 128.87 (1 C, d, J 5.0, ArC), 132.90 (1 C, s, ArC), 133.34 (1 C, d, J 3.8, ArC), 147.61 (1 C, d, J 6.3, ArC). δ_{P} (202 MHz, CDCl₃) 20.58 (1 P, s). m/z (ES⁺): 290 ([M]⁺, 35%), 272 ([M-(OH)]⁺, 3), 244 ([M-(OCH₂CH₃)]⁺, 6), 152 ([-CH-PO(OCH₂CH₃)₂]⁺, 21), 138 ([O₂N-C₆H₄-CH]⁺, 73), 77 [C₆H₄]⁺, 84).

5.3.7 Attempted synthesis of 2-cyanobenzyl- α -hydroxy diethyl phosphonate (18) (data for this compound agreed with *Menear. K. A, et al 2012, US008247416B2*).



2-Cyanobenzaldehyde (1.5g, 11.5 mmol), diethylphosphite (1.5cm³, 11.7 mmol), basic Alumina (Al₂O₃) (11.68 g, 114.5 mmol) (silica gel 70 g, hexane: ethyl acetate, 1:1, 200 cm³, 2:8, 400 cm³, 1:9, 400 cm³). Product; yellow solid, (0.7990g, 25.84%). (data for this compound agreed with *Menear. K. A, et al 2012*). $R_f = 0.5$, (EtOAc:Hex; 9:1), mp 58-61 °C; $\nu_{\max}/\text{cm}^{-1}$ 2936 (C-H), 1771 (C=O), 1290 (P=O), 1268 (C-O), 996 (P-O); δ_{H} (500 MHz, CDCl₃) 1.09 (3 H, t, J 7.5, CH₃), 1.41 (3 H, t, J 7.5, CH₃), 3.87- 3.88 (1 H, m, CH₂O-), 3.99-4.02 (1 H, m, CH₂O), 4.28- 4.32 (2 H, m, CH₂O-), 5.69 (1 H, d, J 15.0, -CH-), 7.60 (1 H, t, J 7.5, ArH- γ -lactone), 7.75 (1 H, t, J 7.5, ArH- γ -lactone), 7.78 (1 H, d, J 5.0, ArH- γ -lactone), 7.95 (1 H, d, J 10.0, ArH- γ -lactone). δ_{C} (126 MHz, CDCl₃) 16.19 (1 C, d, J 6.3, CH₃), 16.46 (1 C, d, J 6.3, CH₃), 64.01 (1 C, d, J 6.3, CH₂O-), 64.30 (1 C, d, J 6.3, CH₂O), 75.56 (1 C, d, J 165.06, CH),

123.66 (1 C, d, J 2.5, ArC- γ -lactone), 125.33 (1 C, d, J 3.8, ArC- γ -lactone), 125.97 (1 C, d, J 1.3, ArC- γ -lactone), 129.81 (1 C, d, J 1.3, ArC- γ -lactone), 134.42 (1 C, d, J 2.5, ArC- γ -lactone), 143.83 (1 C, d, J 3.8, ArC- γ -lactone), 169.77 (1 C, d, J 2.5, C=O- γ -lactone). δ_P (202 MHz, CDCl₃) 13.80 (1 P, s). m/z (TOF ES⁺): 271 ([M+H]⁺, 35%), 243 ([M-CH₂CH₃]⁺, 21), 133 ([C₈H₅O₂]⁺, 18), 293 ([M+ Na⁺]⁺, 100).

5.4 Conversion of the substituted benzyl- α -hydroxy to the substituted benzyl- α -methylene-phosphonates and substituted benzyl-dialkyl-phosphates

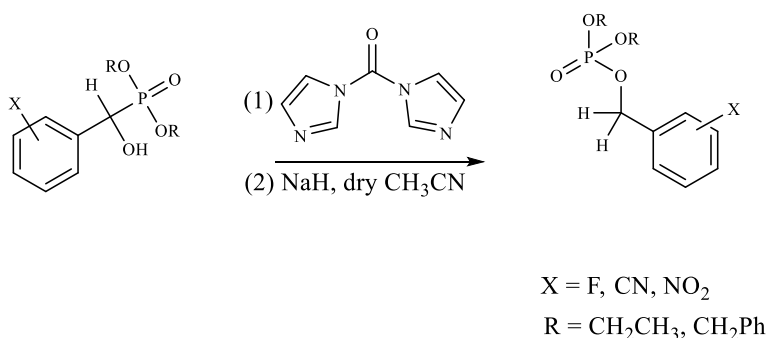
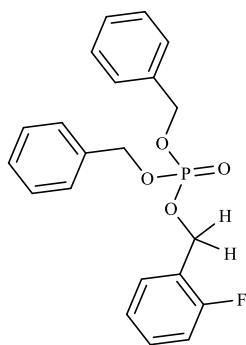


Figure 5.4.1: Synthesis of substituted benzyl-dialkyl phosphonates general reaction scheme

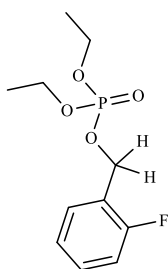
To a round bottomed flask containing, substituted benzyl- α -hydroxy- phosphonate and 1, 1 carbonyl diimidazole were dissolved in dry acetonitrile/ dry tetrahydrofuran (THF) (10 cm³). Sodium hydride was added and the reaction mixture stirred for 2 hours at room temperature. After which, dichloromethane (70 cm³) and water (30 cm³) were added to the reaction mixture and the organic layer was extracted. The organic layer was then washed with dilute hydrochloric acid (10 cm³), saturated sodium hydrogen carbonate (NaHCO₃) (6.0 cm³), water (6.0 cm³), extracted and dried over MgSO₄. The crude reaction mixture was concentrated under reduced pressure and purified with column chromatography.

5.4.1 2-Fluorobenzyl-dibenzyl phosphate (19)



2-Fluorobenzyl- α -hydroxyl-dibenzyl phosphonate (0.70 g, 2.0 mmol), 1,1 carbonyl diimidazole (0.29 g, 1.8 mmol), sodium hydride (NaH) (0.25 g, 10.4 mmol) (silica gel; 40 g, hexane: ethyl acetate, 1:1, 400 cm³). Product; oil, (0.18 g, 24%). R_f = 0.67; (EtOAc: Hex; 1:1); $\nu_{\max}/\text{cm}^{-1}$ 2925 (C-H), 1272 (P=O), 1000 (P-O); δ_{H} (500 MHz, CDCl₃) 5.03 (4 H, d, J 10.0, 2 \times PhCH₂O-), 5.09 (2 H, d, J 5.0, CH₂), 7.04 (1 H, t, J 10.0, ArH), 7.11 (1 H, t, J 7.5, ArH), 7.26-7.35 (12 H, m, 12 \times ArH). δ_{C} (126 MHz, CDCl₃) 63.14 (1 C, t, J 5.0, CH₂-), 69.34 (2 C, d, J 6.3, 2 \times PhCH₂O-), 115.40 (1 C, d, J 20.16, ArC), 124.21 (1 C, d, J 3.8, ArC), 126.98-127.95 (3 C, m, 3 \times ArC), 128.53-128.56 (6 C, m, 6 \times ArC), 130.31 (1 C, d, J 3.8, ArC), 130.47 (1 C, d, J 7.6, ArC), 135.67 (1 C, d, J 7.6, ArC), 160.59 (1 C, d, J 249.48, ArCF). δ_{P} (202 MHz, CDCl₃) -0.51 (1 P, s). m/z (EI⁺): 387 ([C₂₁H₂₀O₄PF]⁺, 47%), 277 ([M-C₆H₄FCH₂]⁺, 80%) 199 ([C₆H₅CH₂O)(OCH₂)PO-CH₂-]⁺, 71), 91 ([C₆H₄CH₂]⁺, 100).

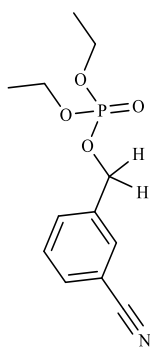
5.4.2 2-Fluorobenzyl-diethyl phosphate (20)



2-Fluorobenzyl- α -hydroxyl-diethyl phosphonate (0.6 g, 2.4 mmol), 1, 1 carbonyl diimidazole (0.37 g, 2.3 mmol), Sodium hydride (NaH) (0.28 g, 11.5 mmol) (silica gel; 40 g, hexane: ethyl acetate, 1:1, 400 cm³). Product; oil (0.52 g, 93%). (data for this compound agreed with Pallikonda. G, et al 2015, 92%). R_f = 0.43; (EtOAc:Hex; 1:1); $\nu_{\max}/\text{cm}^{-1}$ 2985 (C-H), 1268 (P=O), 1011 (C-F), 974 (P-O); δ_{H} (500 MHz, CDCl₃) 1.32 (6 H, t, J 7.5, 2 \times CH₃), 4.07-4.15

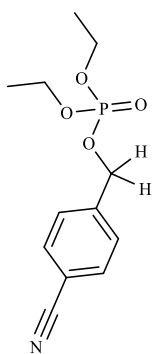
(4 H, m, $2 \times \text{CH}_2\text{O}^-$), 5.14 (2 H, d, 10.0, CH_2), 7.08 (1 H, t, J 7.5, ArH), 7.16 (1 H, t, J 7.5, ArH), 7.32-7.36 (1 H, m, ArH), 7.47 (1 H, t, J 5.0, ArH). δ_{C} (126 MHz, CDCl_3) 16.01 (1 C, s, CH_3), 16.07 (1 C, s, CH_3), 62.88 (1 C, t, J 5.0, CH_2), 63.88 (1 C, s, CH_2O^-), 63.93 (1 C, s, CH_2O), 115.40 (1 C, d, J 21.42, ArC), 123.35 (1 C, dd, J 22.68, 7.6, ArC), 124.23 (1 C, d, J 3.8, ArC), 130.30 (1 C, d, J 3.8, ArC), 130.44 (1 C, d, J 8.8, ArC), 160.65 (1C, d, J 249.48, ArCF). δ_{P} (202 MHz, CDCl_3) -0.60 (1 P, s). m/z (EI^+): 262 ($[\text{C}_{11}\text{H}_{16}\text{PO}_4\text{F}]^+$, 34%), 233 ($[\text{M}-\text{CH}_3\text{CH}_2]^+$, 11%), 214 ($[(\text{CH}_2\text{O})(\text{CH}_3\text{CH}_2\text{O})-\text{POCH}_2\text{C}_6\text{H}_4]^+$, 6), 186 ($[\text{FC}_6\text{H}_4\text{CPO}_3]^+$, 30), 109 ($[\text{FC}_6\text{H}_4\text{CH}_2]^+$, 60).

5.4.3 3-Cyanobenzyl-diethyl phosphate (21)



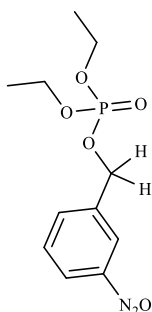
3-Cyanobenzyl- α -hydroxy diethyl phosphonate (0.55 g, 2.03 mmol), 1:1 carbonyl diimidazole (0.36 g, 2.0 mmol), Sodium hydride (NaH) (0.34 g, 14.2 mmol) (silica gel; 50 g, hexane: ethyl acetate, 1:1, 400 cm^3 and hexane: ethyl acetate, 2:8, 200 cm^3). Product; oil (0.07 g, 14%). R_{f} = 0.14; (EtOAc:Hex; 1:1); $\nu_{\text{max}}/\text{cm}^{-1}$ 2985 (C-H), 2233 (CN), 1458 (CH_2), 1268 (P=O), 1022 (P-O); δ_{H} (500 MHz, CDCl_3) 1.34 (6 H, t, J 7.5, $2 \times \text{CH}_3$), 4.11-4.16 (4 H, m, $2 \times \text{CH}_2\text{O}^-$), 5.09 (2 H, d, 10.0, CH_2), 7.50 (1 H, t, J 7.5, ArH), 7.62-7.64 (2 H, m, $2 \times \text{ArH}$), 7.69 (1 H, d, J 5.0, ArH), δ_{C} (126 MHz, CDCl_3) 16.09 (1 C, s, CH_3), 16.14 (1 C, s, CH_3), 64.16 (1 C, s, CH_2O), 64.21 (1 C, s, CH_2O^-), 67.51 (1 C, s, CH_2), 112.85 (1 C, s, ArC), 118.42 (1 C, s, ArCN), 129.47 (1 C, s, ArC), 130.94 (1 C, s, ArC), 131.79 (1 C, s, ArC), 132.02 (1C, s, ArC) 137.75 (1C, d, J 7.6, ArC). δ_{P} (202 MHz, CDCl_3) -0.49 (1 P, s). m/z (EI^+) 270 ($[\text{C}_{11}\text{H}_{16}\text{PO}_4\text{CN}]^+$, 48%), 256 ($[\text{M}-\text{CH}_3]^+$, 1), 241 ($[\text{M}-(\text{CH}_3\text{CH}_2)]^+$, 5), 226 ($[\text{M}-(\text{CH}_3)_2\text{CH}_2]^+$, 1), 213 ($[\text{C}_6\text{H}_4\text{CH}_2\text{PO}(\text{OCH}_2)(\text{OCH}_2\text{CH}_3)]^+$, 33), 197 ($[\text{C}_6\text{H}_4\text{CH}_2\text{PO}(\text{OCH}_2)_2]^+$, 1), 116 ($[\text{CNC}_6\text{H}_4\text{CH}_2]^+$, 100), 89 ($[\text{C}_7\text{H}_7]^+$, 43).

5.4.4 4-Cyanobenzyl-diethyl phosphate (22)



4-Cyanobenzyl diethyl phosphonate (0.76 g; 3.0 mmol), 1, 1 carbonyl diimidazole (0.46 g, 3.0 mmol), sodium hydride (NaH) (0.34 g, 15 mmol) (silica gel; 40 g, hexane: ethyl acetate, 1:1, 400 cm³). Product; oil (0.43 g, 59%). $R_f = 0.5$; (EtOAc:Hex; 1:1); $\nu_{\max}/\text{cm}^{-1}$ 2985 (C-H), 2233 (CN), 1264 (P=O), 1019 (P-O); δ_{H} (500 MHz, CDCl₃) δ /ppm 1.33 (3 H, t, J 7.5, CH₃), 1.34 (3 H, t, J 7.5, CH₃), 4.12-4.16 (4 H, m, 2 × CH₂O-), 5.13 (2 H, d, 5.0, CH₂), 7.51 (2 H, d, J 10.0, 2 × ArH), 7.69 (2 H, d, J 5.0, 2 × ArH). δ_{C} (126 MHz, CDCl₃) 16.10 (1 C, s, CH₃), 16.15 (1 C, s, CH₃), 64.16 (1 C, s, CH₂O-), 64.21 (1 C, s, CH₂O), 67.64 (1 C, d, J 6.3, CH₂), 112.16 (1 C, s, ArC), 118.53 (1 C, s, ArCN), 127.55 (2 C, s, 2 × ArC), 132.41 (2 C, s, 2 × ArC), 141.34 (1 C, d, J 7.6, ArC). δ_{P} (202 MHz, CDCl₃) -0.49 (1 P, s). m/z (EI⁺): 270 ([C₁₁H₁₆PO₄CN]⁺, 39%), 241 ([M-CH₃CH₂]⁺, 4), 228 ([C₆H₄CH₂PO(OCH₂CH₃)₂]⁺, 24), 213 ([C₆H₄CH₂PO(OCH₂)(OCH₂CH₃)]⁺, 24), 137 ([PO(OCH₂CH₃)₂]⁺, 67) 116 ([CNC₆H₄CH₂]⁺, 100), 102 ([CNC₆H₄]⁺, 29).

5.4.5 3-Nitrobenzyl-diethyl phosphate (23)



3-Nitrobenzyl- α -hydroxy diethyl phosphonate (1.00 g, 3.7 mmol), 1:1 carbonyldiimidazole (0.56 g, 3.5 mmol), sodium hydride (NaH) (0.42 g, 17.4 mmol) (silica gel; 60g, hexane: ethyl acetate, 1:1, 400 cm³ and hexane: ethyl acetate, 2:8, 200 cm³). Product; oil (0.44 g, 47%). R_f

= 0.19; (EtOAc:Hex; 1:1); $\nu_{\max}/\text{cm}^{-1}$ 2985 (C-H), 1532 (NO₂), 1354 (NO₂), 1264 (P=O), 1022 (P-O); δ_{H} (500 MHz, CDCl₃) 1.34 (3 H, t, *J* 7.5, CH₃), 1.35 (3 H, t, *J* 7.5, CH₃), 4.12-4.18 (4 H, m, 2 × CH₂O), 5.17 (2 H, d, 5.0, CH₂), 7.57 (1 H, t, *J* 7.5, ArH), 7.73 (1 H, d, *J* 10.0, ArH), 8.21 (1 H, d, *J* 5.0, ArH), 8.27 (1 H, s, ArH). δ_{C} (126 MHz, CDCl₃) 16.10 (1 C, s, CH₃), 16.15 (1 C, s, CH₃), 64.17 (1 C, s, CH₂O-), 64.21 (1 C, s, CH₂O), 67.42 (1 C, d, *J* 5.0, CH₂), 122.36 (1 C, s, ArC), 123.33 (1 C, s, ArC), 129.66 (1 C, s, ArC), 133.36 (1 C, s, ArC), 138.31 (1 C, d, *J* 7.6, ArC), 148.42 (1 C, s, ArC). δ_{P} (202MHz, CDCl₃) -0.46 (1P, s). *m/z* (EI⁺): 290 ([C₁₁H₁₆PO₆N]⁺, 39%), 272 ([O₂NC₆H₄CH₂OPO(OCH₂CH)(OCH)]⁺, 57), 244 ([M-(CH₃CH₂O)]⁺, 22), 216 ([O₂NC₆H₄CH₂PO(OCH₂)]⁺, 16), 186 ([O₂NC₆H₄CH₂PO]⁺, 12), 153 ([CH₂PO(OCH₂CH₃)₂]⁺, 26) 136 ([O₂NC₆H₄CH₂]⁺, 100), 90 ([C₆H₄CH₂]⁺, 34).

5.5 Substituted benzyl- benzyl- α -methylene phosphonates

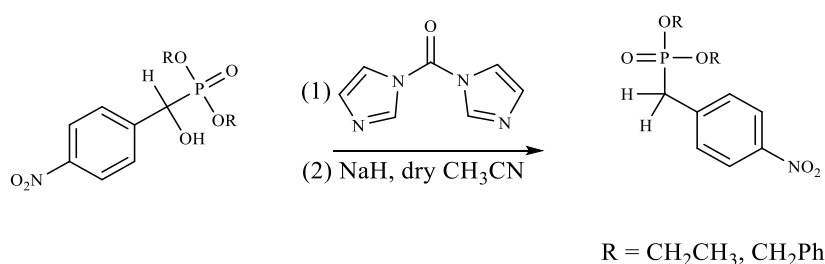
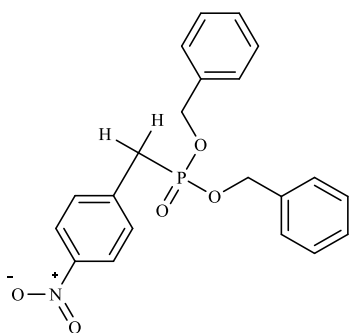


Figure 5.5.1: Synthesis of substituted benzyl- phosphates general reaction scheme

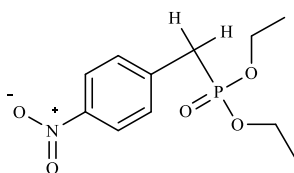
5.5.1 4-Nitrobenzyl- α -methylene-dibenzyl phosphonate (24)



4-Nitrobenzyl- α -hydroxy dibenzyl phosphonate (1.00 g, 2.4 mmol), 1:1 carbonyldiimidazole (0.39g; 2.42 mmol), NaH (0.30 g, 12.6 mmol). (silica gel; 51 g, hexane: ethyl acetate, 6:4, 400 cm³). Product; oil (0.24 g, 25%). *R_f* = 0.70; (EtOAc:Hex; 1:1); Elemental data Anal. Expected. C₂₂H₂₀PO₃N; C; 63.48%, H; 5.04%, N; 3.53%. Found. C; 63.62%, H; 4.95%, N; 3.61%; $\nu_{\max}/\text{cm}^{-1}$ 2925 (C-H), 1514 (NO₂), 1346 (NO₂), 1246 (P=O), 974 (P-O); δ_{H} (500 MHz, CDCl₃)

3.21 (2 H, d, J 25.0, CH_2), 4.89-5.02 (4 H, m, $2 \times \text{PhCH}_2\text{O}$), 7.25-7.26 (4 H, m, $4 \times \text{ArH}$), 7.28 (1 H, d, J , 5.0, ArH), 7.30 (1 H, d, J , 5.0, ArH), 7.33-7.34 (6 H, m, $6 \times \text{ArH}$), 8.06 (1 H, d, J 10.0, ArH). δ_{C} (126 MHz, CDCl_3) 34.33 (1 C, d, J 137.34, CH_2), 67.97 (1 C, s, $1 \times \text{PhCH}_2\text{O}$), 68.02 (1 C, s, PhCH_2O -), 123.62 (2 C, d, J 2.5, $2 \times \text{ArC}$), 128.15 (4 C, s, $4 \times \text{ArC}$), 128.65-128.67 (6 C, m, $6 \times \text{ArC}$), 130.61 (1 C, s, ArC), 130.66 (4 C, s, $4 \times \text{ArC}$), 135.87 (1 C, d, J 5.0, ArC), 139.09 (1 C, d, J 10.08, ArC), 146.97 (1 C, d, J 3.8, ArC). δ_{P} (202 MHz, CDCl_3) 25.85 (1 P, s). m/z (EI^+): 398 ($[\text{M}]^+$, 1%), 306 ($[\text{M}-\text{C}_6\text{H}_5\text{CH}_2]^+$, 80), 260 ($[(\text{C}_6\text{H}_5\text{CH}_2\text{O})_2\text{PO}]^+$, 1), 180 ($[(\text{C}_6\text{H}_5\text{CH}_2\text{O})(\text{OCH}_2)\text{PC}]^+$, 90), 136 ($[\text{O}_2\text{NC}_6\text{H}_4\text{CH}_2]^+$, 12), 91 ($[\text{C}_6\text{H}_4\text{CH}_2]^+$, 100).

5.5.2 4-Nitrobenzyl- α -methylene-diethyl phosphonate (25).



4-Nitrobenzyl- α -hydroxy diethyl phosphonate (1.00 g, 3.5 mmol), 1:1 carbonyldiimidazole (0.56 g, 3.47 mmol), sodium hydride NaH (0.42 g, 17.4 mmol) (silica gel; 60g, hexane: ethyl acetate, 1:1, 400 cm^3 and hexane: ethyl acetate, 4:6, 200 cm^3). Product; oil (0.19 g, 20%). (data for this compound agreed with Döpp, D., (2000), (57%). R_f = 0.33; (EtOAc:Hex; 1:1), Elemental data Anal. Expected. $\text{C}_{12}\text{H}_{16}\text{PO}_3\text{N}$; C; 48.35%, H; 5.86%, N; 5.13%. Found: C; 48.45%, H; 6.00%, N; 5.27%; $\nu_{\text{max}}/\text{cm}^{-1}$ 2985 (C-H), 1521 (NO_2), 1346 (NO_2), 1246 (P=O), 1022 (P-O); δ_{H} (500 MHz, CDCl_3) 1.27 (6 H, t, J 7.5, $2 \times \text{CH}_3$), 3.25 (1 H, d, 20.0, CH_2 -), 4.03-4.09 (4 H, m, $2 \times \text{CH}_2\text{O}$ -), 7.47 (1 H, d, J 5.0, ArH), 7.49 (1 H, d, J 5.0, ArH), 8.18 (2 H, d, J 5.0, $2 \times \text{ArH}$). δ_{C} (126 MHz, CDCl_3) 16.36 (1 C, s, CH_3), 16.40 (1 C, s, CH_3), 34.01 (1 C, d, J 137.34, CH_2), 62.44 (1 C, s, CH_2O), 62.49 (1 C, s, CH_2O -), 123.72 (1 C, d, J 3.8, ArC), 130.61 (1 C, s, ArC), 130.66 (1 C, s, ArC), 139.73 (2 C, d, J 8.8, $2 \times \text{ArC}$), 147.05 (1 C, s, ArC). δ_{P} (202 MHz, CDCl_3) 24.61 (1 P, s). m/z (EI^+): 274 ($[\text{M}]^+$, 41%), 246 ($[\text{M}-\text{CH}_3\text{CH}_2]^+$, 3), 215 ($[\text{O}_2\text{NC}_6\text{H}_4\text{CH}_2\text{PO}_2\text{CH}_2]^+$, 14), 187 ($[\text{O}_2\text{NC}_6\text{H}_4\text{CH}_2\text{PO}]^+$, 16), 153 ($[\text{CH}_2\text{PO}(\text{OCH}_2\text{CH}_3)_2]^+$, 6), 136 ($[\text{O}_2\text{NC}_6\text{H}_4\text{CH}_2]^+$, 35), 124 ($[\text{O}_2\text{NC}_6\text{H}_4]^+$, 71), 89 ($[\text{C}_6\text{H}_4\text{CH}_2]^+$, 76), 78 ($[\text{C}_6\text{H}_4]^+$, 31).

5.6 Synthesis of substituted benzyl- α -hydroxyl phosphonic acids from their diethyl phosphonates precursors.

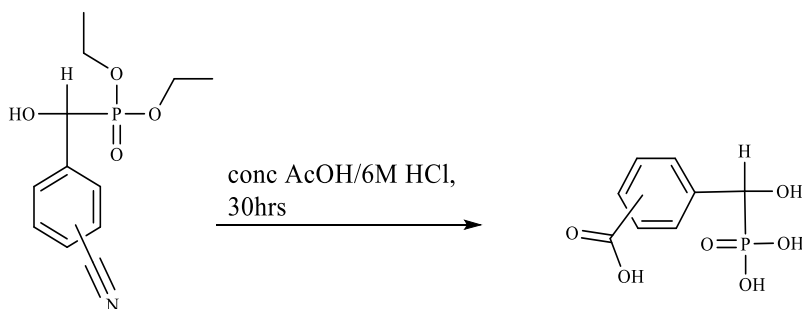
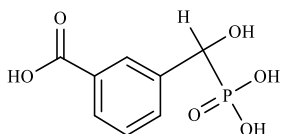


Figure 5.6.1: Acid hydrolysis of the substituted benzyl- α -hydroxy diethyl phosphonates general reaction scheme

Substituted benzyl- α -hydroxy diethyl phosphonate was dissolved in 6M hydrochloric acid/concentrated acetic acid (100 cm³) in a round bottomed flask. The resultant mixture was heated under reflux for 30 hours. After which, the resultant mixture was concentrated under reduced pressure. The resultant product was then washed three times with diethyl ether (20 cm³) and dried under reduced pressure for an hour.

5.7 Synthesis of substituted benzyl- α -hydroxy phosphonic acids from their diethyl phosphonates by acid hydrolysis

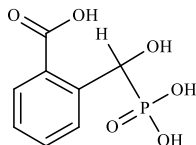
5.7.1 3-Carboxy benzyl- α -hydroxy phosphonic acid (26)



3-Cyanobenzyl- α -hydroxy-diethyl phosphonate (0.4g, 1.5mmol), 6 M hydrochloric acid. Product; colourless solid (0.3456g, 96.55%). $R_f = 0.26$; (butanol: H₂O:Acetic acid; 4:1:0.5), mp 164-167 °C; $\nu_{\max}/\text{cm}^{-1}$ 2963 (C-H), 1699 (C=O), 1246 (P=O); δ_{H} (500 MHz, MeOD) 3.62 (1 H, d, J 280.0, CH-OH), 7.45 (1 H, t, J 10.0, ArH), 7.74 (1 H, d, J 10.0, ArH), 7.94 (1 H, d, J 5.0, ArH), 8.20 (1 H, s, ArH). δ_{C} (126 MHz, MeOD) 71.87 (1 C, d, J 163.8, CH-OH), 129.16 (1 C, s, ArC), 129.85 (1 C, d, J 6.3, ArC), 129.98 (1 C, d, J 2.5, ArC), 131.79 (1 C, s, ArC), 133.17 (1 C, d, J 5.0, ArC) 140.81 (1 C, s, ArC), 169.98 (1 C, s, ArCOOH). δ_{P} (202 MHz,

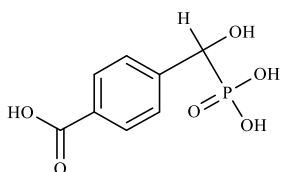
MeOD) 20.68 (1 P, s). m/z (TOF ES⁻): 232 ([M]⁻, 100%), 464 ([2M]⁻, 212 ([M-H₂O]⁻, 25), 81 ([PO₃H]⁻, 8).

5.7.2 2-Carboxyl benzyl- α -hydroxy phosphonic acid (27)



1,2-Benzyl lactone-2- diethyl phosphonate (0.3g, 1.1 mmol), 6 M hydrochloric acid (100cm³)
Product; colourless solid (0.037g, 14.35%). R_f = 0.27; (butanol: H₂O: Acetic acid; 4:1:0.5),
mp 198-201 °C; $\nu_{\max}/\text{cm}^{-1}$ 1701 (C=O), 1285 (P=O); δ_{H} (500 MHz, MeOD) 5.80 (1 H, d, J 10.0,
CH-OH), 7.62 (1 H, t, J 7.5, ArH), 7.78-7.80 (2 H, m, 2 \times ArH), 7.90 (1 H, d, J 5.0, ArH).
 δ_{C} (126 MHz, MeOD) 78.55 (1 C, d, J 158.8, CH-OH), 124.76 (1 C, s, ArC), 126.43 (1 C, s,
ArC) 126.54 (1 C, d, J 5.0, ArC), 130.62 (1 C, s, ArC), 135.57 (1 C, s, ArC), 146.88 (1 C, d,
 J 3.8, ArC), 172.48 (1 C, s, ArCOOH). δ_{P} (202 MHz, MeOD) 12.86 (1 P, s). m/z (TOF ES⁻):
232 ([M-H]⁻, 2%).

5.7.3 4-Carboxylbenzyl- α -hydroxy phosphonic acid (28)



4-Cyanobenzyl- α -hydroxy-diethyl phosphonate (0.8g, 3.0 mmol), concentrated Acetic acid
(100cm³). Product; yellow solid (0.5879g, 85%); R_f = 0.17; (butanol: H₂O: Acetic acid;
4:1:0.5), mp 184-186 °C; $\nu_{\max}/\text{cm}^{-1}$ 3460 (O-H), 1647 (C=O), 1261 (P=O); δ_{H} (500 MHz, D₂O
SUPPRESSED), 4.77 (1 H, d, J 15.0, CH-OH), 7.51 (2 H, d, J 10.0, 2 \times ArH), 7.82 (2 H, d, J
10.0, 2 \times ArH). δ_{C} (126 MHz, D₂O) 76.70 (1 C, d, J 139.86, CH-OH), 129.56 (1 C, s, ArC),
129.60 (1 C, s, ArC), 131.22 (1 C, s, ArC), 137.31 (1 C, s, ArC), 147.71 (1 C, s, ArC), 163.70
(1 C, s, ArC), 178.70 (1 C, s, ArCOOH). δ_{P} (202 MHz, D₂O) 15.11 (1 P, s). m/z (TOF ES⁻):
231 ([M]⁻, 100%), 463 ([2M]⁻, 1), 253 ([M+Na]⁺, 1), 213 ([M-H₂O]⁻, 1), 81 ([PO₃H]⁺, 3).

5.8 Synthesis of substituted benzyl- α -hydroxy phosphonic acids by dealkylation of the substituted benzyl- α -hydroxy diethyl phosphonate precursors with bromotrimethylsilane

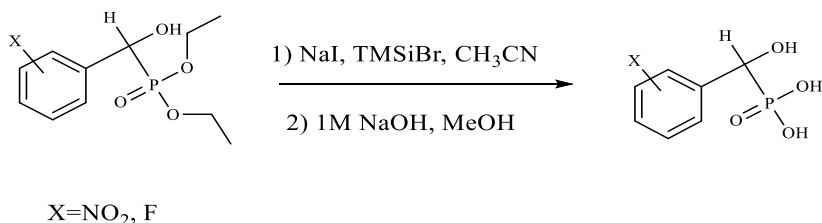
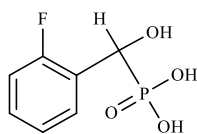


Figure 5.8.1: Reaction scheme for the dealkylation of the substituted benzyl- α -hydroxy diethyl phosphonates by TMSiBr

Substituted benzyl- α -hydroxy diethyl phosphonate and 2 molar equivalents of sodium iodide (NaI) were dissolved in dry acetonitrile (20 cm³) in a round bottomed flask. Chlorotrimethylsilane (TMSiCl)/bromotrimethylsilane (TMSiBr) 1.5 molar equivalent was added and the resultant mixture was left to stir for 48 hours at 50 °C. After which, the filtrate was concentrated under reduced pressure at 40 °C to give an oily residue. 1 M sodium hydroxide (1.0 cm³) was dissolved in methanol (5 cm³) and added to the oily residue and the resultant mixture was stirred for 24 hours at room temperature. After which, the resultant product was filtered under reduced pressure, washed three times with diethyl ether (20 cm³) and dried under reduced pressure overnight.

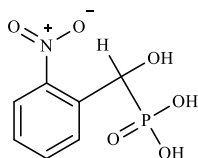
5.8.1 2-Fluorobenzyl- α -hydroxy phosphonic acid (29).



2-Fluorobenzyl- α -hydroxyl diethyl phosphonate (0.5 g, 1.9 mmol), sodium iodide (NaI) (0.58 g, 3.8 mmol), chlorotrimethylsilane (TMSiCl) (0.4 cm³, 2.9 mmol) 1 M sodium hydroxide (1.0 cm³). Product colourless solid (0.083 g, 19.80%). (data for this compound agreed with Murai, K, et al 2016). R_f = 0.27; (butanol: H₂O: Acetic acid; 4:1:0.5), mp >300 °C; $\nu_{\max}/\text{cm}^{-1}$ 3238 (O-H), 1228 (P=O); δ_{H} (500 MHz, MeOD) 5.13 (1 H, d, *J* 10, CH-OH), 6.98 (1 H, t, *J* 5.0, ArH), 7.12 (1 H, t, *J* 7.5, ArH), 7.14-7.23 (1 H, m, ArH), 7.74 (1 H, tt, *J*, 10.0, 5.0, ArH). δ_{C} (126 MHz, MeOD) 66.52 (1 C, d, *J* 152.5, CH-OH), 115.48 (1 C, s, ArC), 115.66 (1 C, s,

ArC), 124.79 (1 C, m, ArC), 129.36 (1 C, dd, J 10.80, 2.5, ArC), 129.86 (1 C, d, J 12.6, ArC), 130.75 (1 C, t, J 3.8, ArC). δ_{H} (202 MHz, MeOD) 16.55 (1 P, d, J 6.06). m/z (TOF ES⁺): 413 ([2M⁺], 84%), 191 ([M-OH]⁺, 3), 229 ([M+Na⁺]⁺, 14), 127 ([FC₆H₄CH(OH)]⁺, 4), 85 ([-PO(OH)₂]⁺, 5).

5.8.2 2-Nitrobenzyl- α -hydroxy phosphonic acid (30).



2-Nitrobenzyl- α -hydroxyl diethyl phosphonate (0.4 g, 1.3 mmol), sodium iodide (NaI) (0.58 g, 3.5 mmol), chlorotrimethylsilane (TMSiCl) (0.5 cm³, 3.5 mmol). Product; yellow solid (0.2208 g, 68.35%). (data for this compound agreed with *Uhlmann, E, et al 2000*). R_f = 0.18; (butanol:H₂O:Acetic acid; 4:1:0.5), mp 155-158 °C; $\nu_{\text{max}}/\text{cm}^{-1}$ 3238 (O-H), 2842 (P-OH), 1513 (NO₂), 1347 (NO₂), 1174 (P=O); δ_{H} (500 MHz, MeOD) 5.76 (1 H, d, J 15, CH-OH), 7.34 (1 H, t, J 10.0, ArH), 7.57 (1 H, t, J 10, ArH), 7.83 (1 H, d, J 10.0, ArH), 8.03 (1 H, d, J 10, ArH). δ_{C} (126 MHz, MeOD) 69.05 (1 C, d, J 142.38, CH-OH), 125.00 (1 C, s, ArC), 127.82 (1 C, s, ArC), 130.48 (1 C, d, J 3.8, ArC), 133.39 (1 C, s, ArC), 139.14 (1 C, s, ArC), 150.06 (1 C, s, ArC). δ_{P} (202 MHz, MeOD) 15.57 (1 P, s). m/z (TOF ES⁻): 232 ([M-H]⁻, 100%), 79 ([CH(OH)PO]⁻, 40).

5.9 Synthesis of substituted benzyl- α -amino phosphonic acids

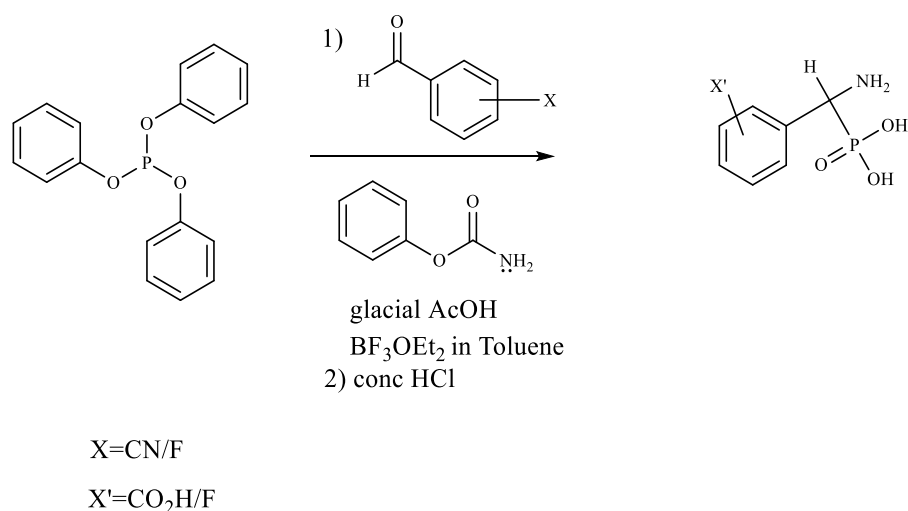
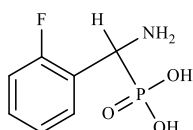


Figure 5.9.1: Synthesis of substituted benzyl- α -amino phosphonic acid reaction scheme

Equimolar amounts of triphenylphosphite, substituted benzylaldehyde and benzyl carbamate were dissolved in glacial acetic acid (80 cm³) in a round bottomed flask at room temperature. Boron trifluoride in diethyl ether (BF₃.OEt₂) (2.5% v/v) in toluene (50 cm³) was added to the reaction mixture and the resultant mixture was left to stir for 30 minutes at room temperature and then heated under reflux for 4 hours. The resultant solution was concentrated under reduced pressure and then refluxed for a further 4 hours in concentrated hydrochloric acid (HCl) (100 cm³). The aqueous layer was extracted and washed with toluene (50 cm³). The resultant mixture was concentrated under reduced pressure and triturated 3 times with diethyl ether (30 cm³). The resultant reaction mixture was dissolved in methanol (4 cm³) and added to a round bottomed flask containing chloroform (400 cm³) dropwise, stirred and left to settle overnight. The solid product was filtered out under reduced pressure, washed three times with dichloromethane (20 cm³) and dried under reduced pressure for 24 hours.

5.9.1 2-Fluorobenzyl- α - amino phosphonic acids (34)



Triphenylphosphite (2.6 cm³; 10mmols), 2-fluorobenzylaldehyde (1.2 cm³; 10 mmols) and benzyl carbamate (1.52 g; 10 mmols). Product; colourless solid (0.73 g 35.60%,). R_f = 0.5;

(EtOAc: methanol; 6:4), mp 232-235 °C; $\nu_{\max}/\text{cm}^{-1}$ 3126 (OH), 2828 (NH₂), 2616 (P-OH), 1235 (P=O); δ_{H} (500 MHz, NaOD, D₂O) 4.13 (1 H, d, *J* 20.0, CH-NH₂), 7.12-7.14 (1 H, m, ArH), 7.22-7.24 (1 H, m, ArH), 7.30-7.31 (1 H, m, ArH), 7.46 (1 H, tt, *J* 10.0, 5.0, ArH). δ_{C} (126 MHz, D₂O, NaOD) 51.00 (1 C, d, *J* 132.30, CH-NH₂), 117.60 (1 C, d, *J* 22.68, ArC), 126.67 (1 C, s, ArC), 130.39 (1 C, dd, *J* 6.30, 1.30, ArC), 131.55 (1 C, s, ArC), 132.36 (1C, s, ArC), 162.54 (1 C, d, *J* 243.18, ArC). δ_{P} (202 MHz, D₂O, NaOD) 18.20 (1 P, s). *m/z* (EI⁺): 109 ([FC₆H₄CH]⁺, 56%), 83 ([PO₃H₃]⁺, 11).

5.10 Protocols and procedures for the antimalarial evaluations

5.10.1 *P. falciparum* drug assay method

Parasites (*Pf* 3D7 and *Pf* Dd2 strains) were propagated as previously described (*Trager W, Jensen JB, Science 1976, PMID: 781840*) in RPMI-1640 that was supplemented with 50 mg/l hypoxanthine, 0.25 % sodium bicarbonate, 0.5 % Albumax II, 25 mM HEPES and GlutaMAX at 1x concentration. To assay their antimalarial activity, a two-fold serial dilution of compounds was performed in duplicate, in 96-well flat bottom plates. Parasites at predominantly ring-stage were added at 1% parasitemia, with a final haematocrit of 1% red blood cells (RBCs). No-drug wells (i.e. maximum growth) and RBC only wells were also included. Plates were incubated at 37 °C for 72 hours before measurement of parasite growth using SYBR green stain. Cells were re-suspended in SYBR lysis buffer (final concentration 1xSYBR green stain in 5 mM Tris-HCl, 1.5 mM EDTA, 0.05% w/v saponin, 0.5% v/v Triton X-100), incubated at 37 °C for 30 minutes, and fluorescence signal measured on a FLUOstar Omega (BMG Biotech, ex. 485 nm, em. 535 nm).

5.11 Protocols and procedures for the testing against other parasites, (*T. brucei*, *T. cruzi*, *L. major* and HeLa).

5.11.1 Cell lines and cell culture

Bloodstream form (BSF) *Trypanosoma. brucei* strain 427, hereafter referred to as ‘wild-type’. BSF *T. brucei* were grown in either HMI-11 media supplemented with 10% foetal bovine serum (Gibco) and 2.5 µg/mL G418 (Calbiochem) at 37°C with 5% v/v CO₂ as described

elsewhere (*Hirumi et al, 1989*). Cells were routinely grown in 10 mL media in 75 cm² vented flasks and passaged three times per week to maintain cells in mid-log phase (i.e. below 2 x10⁶/mL).

Epimastigote *Trypanosoma cruzi* CL Brener strain expressing pLEW13, hereafter referred to as ‘wild-type’ were grown at 28°C in RTH media (RPMI 1640 medium (Sigma) supplemented with 20 mM HEPES pH 7.2 (Sigma), 4.9 mg/mL tryptone (Sigma), PGAB (2 mM sodium glutamate, 2 mM sodium pyruvate, 100 µg/mL streptomycin and 100 U/mL penicillin, all Sigma), 20 µg/mL haemin and 10% HI-FBS). Cells were routinely grown in 10 mL media in 75 cm² flasks and passaged three times per week by splitting cultures 1 in 10 to maintain cultures in log phase between 1 x10⁶/mL and 1 x10⁷/mL.

Promastigote *L. major* MHOM/IL/80/Friedlin were grown at 28°C in M199 media (Sigma) pH 7.4, supplemented with 40 mM HEPES pH 7.4, 100 µM adenosine, 5 µg/mL haemin and 10% HI-FBS. Cells were routinely grown in 10 mL media in 75 cm² non-vented flasks (MANU) and passaged three times per week to maintain cells in mid-log phase, below 1 x10⁷/mL.

HeLa cells were cultured in Dulbecco’s Modified Eagle Medium (DMEM) (Sigma) supplemented with 10% HI-FBS and grown at 37°C in 5% CO₂ atmosphere. Cells were grown in 75 cm² vented flasks and passaged twice per week by trypsinization when monolayers reached ~90% confluency. All media was removed, the monolayer washed in PBS, and trypsinized with 2 mL Trypsin-EDTA, incubated at 37°C until the monolayer detached, following which 8 mL fresh media was added to neutralize the trypsin. Cell culture was then split at a 1 in 5 ratio in fresh media.

5.11.2 Cytotoxicity EC₅₀ assay

The EC₅₀ of the compounds (in DMSO) was determined using two-fold serial dilutions of compound in media, these were carried out in a 96-well plate in quadruplicate. Cells were counted using CASY TT Cell Counter and seeded as specified below. For Alamar Blue assays, cell viability was quantified using an FLx 800 plate reader (BioTek) with excitation

wavelength 540/35nm and emission wavelength at 590/10nm using Gen5 Reader Control 2.0 Software (BioTek). EC₅₀ values were determined using a 4-parameter logistic regression equation using GraFit 5.0 (Erithacus Software).

Bloodstream form *T. brucei* were seeded in 96-well plates at 1 x10³ cells/well in HMI-11 with serial dilutions of test compound and incubated at 37 °C 5% CO₂ for 72 hours, after which 20 µL Alamar Blue (0.125 mg/mL resazurin salt in PBS) was added to all wells and incubated for a further 6 hours.

For HeLa cell assays, monolayer cells were detached, diluted in DMEM with 10% HI-FBS and seeded at 4 x10³ cells per well. Plates were incubated at 37°C with 5% CO₂ for 24 hours to allow attachment, after which media was removed and replaced with fresh media containing serial dilutions of the compound. Drug diluted in media was added and plates were incubated for 72 hours, after which 10 µL Alamar Blue was added to all wells and incubated for a further 2 hours.

Mid-log *L. major* promastigotes were diluted in media and seeded at 2 x10⁵ per well. Negative controls of DMSO and positive controls of pentamidine were included. Plates were incubated at 28 °C for 72 hours, after which 20 µL Alamar Blue was added to all wells and incubated for a further 6 hours. After 72 hours' incubation at 37°C with 5% CO₂ cell viability was determined using 20 µL Alamar Blue for 6 hours.

Mid-log *T. cruzi* epimastigotes were diluted in RTH media and seeded at 5 x10⁵ per well. Negative controls of DMSO only and positive control of nifurtimox were included. Plates were incubated at 28 °C for 72 hours, after which 10 µL Alamar Blue was added to all wells and incubated for a further 6 hours.

All plates were read at 570 nm and EC₅₀ values were determined using a 4-parameter logistic regression equation using GraFit 5.0.

6 REFERENCES

- AbbVie Inc (2020). *Anti-infective agents and uses thereof*. US009095590B2.
- Advinus Therapeutics Limited (2017). *Amide compounds, compositions and applications thereof*. US009682953B2.
- African Animal Trypanosomiasis. (2018). *The Institute for International cooperation in animal Biologics*, pp.1-8.
- Águas, R., White, L., Snow, R., Gomes, M. (2008). Prospects for Malaria Eradication in Sub-Saharan Africa. *PLoS ONE*, 3(3), pp.1767.
- Akerfeldt, K. and Bartlett, P. (1991). Synthesis and evaluation of glucose-ADP hybrids as inhibitors of hexokinase. *The Journal of Organic Chemistry*, 56(25), pp.7133-7144.
- Ambre, P., Wavhale, R. and Coutinho, E. (2015). New Horizons in Antimalarial Drug Discovery in the Last Decade by Chemoinformatic Approaches. *Combinatorial Chemistry & High Throughput Screening*, 18(2), pp.129-150.
- Andrade-Neto, V., Brandão, M., Nogueira, F., Rosário, V. and Krettli, A. (2008). *Ampeloziziphus amazonicus* Ducke (Rhamnaceae), a medicinal plant used to prevent malaria in the Amazon Region, hampers the development of *P. berghei* sporozoites. *International Journal for Parasitology*, 38(13), pp.1505-1511.
- Andrianov, K., (1971). Rearrangements and polymerization of cyclic organosilicon compounds. *Polymer Science U.S.S.R.*, 13(2), pp.284-298.
- Andricopulo, A. and Montanari, C. (2005). Structure-Activity Relationships for the Design of Small-Molecule Inhibitors. *Mini-Reviews in Medicinal Chemistry*, 5(6), pp.585-593.
- Anon, (2018). [online] Available at: <http://WHO> Global malaria programme, world malaria report 2011 [Accessed 9 Jan. 2018].

- Anon, (2018). [online] Available at: <http://WHO Malaria report 2008> [Accessed 9 Jan. 2018].
- Anon, (2018). [online] Available at: <http://WHO Malaria report 2009> [Accessed 9 Jan. 2018].
- Anon, (2018). [online] Available at: <http://WHO Malaria report 2010> [Accessed 9 Jan. 2018].
- Anon, (2020). [online] Available at: <http://WHO Malaria report 2019> [Accessed 23 Mar. 2020].
- Aparicio, I., Marín-Menéndez, A., Bell, A. and Engel, P. (2010). Susceptibility of *P. falciparum* to glutamate dehydrogenase inhibitors—A possible new antimalarial target. *Molecular and Biochemical Parasitology*, 172(2), pp.152-155.
- Arévalo-Herrera, M. and Herrera, S. (2001). *P. vivax* malaria vaccine development. *Molecular Immunology*, 38(6), pp.443-455.
- Arya, S. (2002). Malaria transmission, antimalarial-drug use, and resistance. *Transactions of the Royal Society of Tropical Medicine and Hygiene*, 96(6), pp.704.
- Aschenbrenner, D., 2020. Remdesivir Receives Emergency Use Authorization for Severely Ill Patients with COVID-19. *AJN, American Journal of Nursing*, 120(7), pp.26.
- Aslan, M., Thornley-Brown, D., Freeman, B. (2006). Reactive Species in Sickle Cell Disease. *Annals of the New York Academy of Sciences*, 899(1), pp.375-391.
- Atamna, H. and Ginsburg, H. (1997). The Malaria Parasite Supplies Glutathione to its Host Cell - Investigation of Glutathione Transport and Metabolism in Human Erythrocytes Infected with *P. falciparum*. *European Journal of Biochemistry*, 250(3), pp.670-679.
- Atan, N., Koushki, M., Ahmadi, N. and Rezaei-Tavirani, M. (2018). Metabolomics-based studies in the field of Leishmania/leishmaniasis. *Alexandria Journal of Medicine*, 54(4), pp.383-390.
- Atwood, J. (2005). The Trypanosoma cruzi Proteome. *Science*, 309(5733), pp.473-476.

- Avery, M., Choi, S. and Mukherjee, P. (2008). The Fight Against Drug-Resistant Malaria: Novel Plasmodial Targets and Antimalarial Drugs. *Current Medicinal Chemistry*, 15(2), pp.161-171.
- Ayi, K., Cappadoro, M., Branca, M., Turrini, F. and Arese, P. (1998). *P. falciparum* glutathione metabolism and growth are independent of glutathione system of host erythrocyte. *FEBS Letters*, 424(3), pp.257-261.
- Babokhov, P., Sanyaolu, A., Oyibo, W., Fagbenro-Beyioku, A. and Iriemenam, N. (2013). A current analysis of chemotherapy strategies for the treatment of human African trypanosomiasis. *Pathogens and Global Health*, 107(5), pp.242-252.
- Bakht, M., Alajmi, M., Alam, P., Alam, A., Alam, P. and Aljarba, T., 2014. Theoretical and experimental study on lipophilicity and wound healing activity of ginger compounds. *Asian Pacific Journal of Tropical Biomedicine*, 4(4), pp.329-333.
- Banerjee, M., Parai, D., Dhar, P., Roy, M., Barik, R., Chattopadhyay, S., Mukherjee, S. (2017). Andrographolide induces oxidative stress-dependent cell death in unicellular protozoan parasite *Trypanosoma brucei*. *Acta Tropica*, 176, pp.58-67.
- Banerjee, M., Parai, D., Dhar, P., Roy, M., Barik, R., Chattopadhyay, S. and Mukherjee, S. (2017). Andrographolide induces oxidative stress-dependent cell death in unicellular protozoan parasite *Trypanosoma brucei*. *Acta Tropica*, 176, pp.58-67.
- Barnes, K., Watkins, W. and White, N. (2008). Antimalarial dosing regimens and drug resistance. *Trends in Parasitology*, 24(3), pp.127-134.
- Bathurst, I. and Hentschel, C. (2006). Medicines for Malaria Venture: sustaining antimalarial drug development. *Trends in Parasitology*, 22(7), pp.301-307.
- Becker, K., Rahlfs, S., Nickel, C. and Schirmer, R. (2003). Glutathione – Functions and Metabolism in the Malarial Parasite *P. falciparum*. *Biological Chemistry*, 384(4), pp.551-556.

- Becker, K., Tilley, L., Vennerstrom, J., Roberts, D., Rogerson, S. and Ginsburg, H. (2004). Oxidative stress in malaria parasite-infected erythrocytes: host–parasite interactions. *International Journal for Parasitology*, 34(2), pp.163-189.
- Bermudez, L. Meek, L., 2014. Mefloquine and Its Enantiomers Are Active against *Mycobacterium tuberculosis* In Vitro and in Macrophages. *Tuberculosis Research and Treatment*, 2014, pp.1-5.
- Bermudez, L., Inderlied, C., Kolonoski, P., Chee, C., Aralar, P., Petrofsky, M., Parman, T., Green, C., Lewin, A., Ellis, W. Young, L., 2012. Identification of (+)-Erythro-Mefloquine as an Active Enantiomer with Greater Efficacy than Mefloquine against *Mycobacterium avium* Infection in Mice. *Antimicrobial Agents and Chemotherapy*, 56(8), pp.4202-4206.
- Berriman, M. (2005). The Genome of the African Trypanosome *Trypanosoma brucei*. *Science*, 309(5733), pp.416-422.
- Biamonte, M., Wanner, J. and Le Roch, K. (2013). Recent advances in malaria drug discovery. *Bioorganic & Medicinal Chemistry Letters*, 23(10), pp.2829-2843.
- Biot, C. and Chibale, K. (2006). Novel Approaches to Antimalarial Drug Discovery. *Infectious Disorders - Drug Targets*, 6(2), pp.173-204.
- Biot, C., Bauer, H., Schirmer, R. and Davioud-Charvet, E. (2004). 5-Substituted Tetrazoles as Bioisosteres of Carboxylic Acids. Bioisosterism and Mechanistic Studies on Glutathione Reductase Inhibitors as Antimalarials. *Journal of Medicinal Chemistry*, 47(24), pp.5972-5983.
- Biot, C., Nosten, F., Fraisse, L., Ter-Minassian, D., Khalife, J. and Dive, D. (2011). The antimalarial ferroquine: from bench to clinic. *Parasite*, 18(3), pp.207-214.
- Björkman, A. (2002). Malaria associated anaemia, drug resistance and antimalarial combination therapy. *International Journal for Parasitology*, 32(13), pp.1637-1643.

- Björkman, A. and Phillips-Howard, P. (1990). The epidemiology of drug-resistant malaria. *Transactions of the Royal Society of Tropical Medicine and Hygiene*, 84(2), pp.177-180.
- Bononi, A., Agnoletto, C., De Marchi, E., Marchi, S., Patergnani, S., Bonora, M., Giorgi, C., Missiroli, S., Poletti, F., Rimessi, A. and Pinton, P. (2011). Protein Kinases and Phosphatases in the Control of Cell Fate. *Enzyme Research*, 2011, pp.1-26.
- Bose, A. and Lal, B. (1973). ChemInform Abstract: A Facile Replacement of Hydroxyl by Halogen with Inversion. *Chemischer Informationsdienst*, 5(1), pp.3937-3940.
- Breman, J., Egan, A. and Keusch, G. (2001). The intolerable burden of malaria: a new look at the numbers. *The American Journal of Tropical Medicine and Hygiene*, 64(1_suppl), (pp.4-7).
- Britton, K., Baker, P., Borges, K., Engel, P., Pasquo, A., Rice, D., Robb, F., Scandurra, R., Stillman, T. and Yip, K. (1995). Insights into Thermal Stability from a Comparison of the Glutamate Dehydrogenases from *Pyrococcus furiosus* and *Thermococcus litoralis*. *European Journal of Biochemistry*, 229(3), pp.688-695.
- Brook, A., (1974). Molecular rearrangements of organosilicon compounds. *Accounts of Chemical Research*, 7(3), pp.77-84.
- Brun, R., Burri, C. and Blum, J. (2018). Human African trypanosomiasis. pp. 966.
- Buffington, G., Hunt, N., Cowden, W. and Clark, I. (1986). Malaria: a role for reactive oxygen species in parasite killing and host pathology. *Free Rad Cell Dam Dis*, pp.201-220.
- Burrows, J., Leroy, D., Lotharius, J. and Waterson, D. (2011). Challenges in antimalarial drug discovery. *Future Medicinal Chemistry*, 3(11), pp.1401-1412.

- Burrows, N. J., Chibale, K. and N.C. Wells, T. (2011). The State of the Art in Antimalarial Drug Discovery and Development. *Current Topics in Medicinal Chemistry*, 11(10), pp.1226-1254.
- Büscher, P., Cecchi, G., Jamonneau, V. and Priotto, G. (2017). Human African trypanosomiasis. *The Lancet*, 390, pp.2397-2409.
- Capes-Davis, A., Theodosopoulos, G., Atkin, I., Drexler, H., Kohara, A., MacLeod, R., Masters, J., Nakamura, Y., Reid, Y., Reddel, R. and Freshney, R. (2010). Check your cultures! A list of cross-contaminated or misidentified cell lines. *International Journal of Cancer*, 127(1), pp.1-8.
- Cappadoro, M., Giribaldi, G., O'Brien, E., Turrini, F., Mannu, F. and Ulliers, F. (1998). Early phagocytosis of glucose6-phosphate dehydrogenase (G6PD)-deficient erythrocytes parasitized by *P. falciparum* may explain malaria protection in G6PD deficiency. *Blood*, 92, pp.2527– 2534.
- Carraz, M., Jossang, A., Franetich, J., Siau, A., Ciceron, L., Hannoun, L., Sauerwein, R., Frappier, F., Rasoanaivo, P., Snounou, G. and Mazier, D. (2006). A Plant-Derived Morphinan as a Novel Lead Compound Active against Malaria Liver Stages. *PLoS Medicine*, 3(12), pp. 513.
- Carvalho, L. and Krettli, A. (1991). Antimalarial chemotherapy with natural products and chemically defined molecules. *Memórias do Instituto Oswaldo Cruz*, 86(suppl 2), pp.181-184.
- Caughey, W., Smiley, J. and Hellerman, L. (1957). L-Glutamic acid dehydrogenase: structural requirements for substrate competition: effect of thyroxine. *J.Biol. Chem*, 224, pp.591-607.
- Choudhury, R. and Punekar, N. (2007). Competitive inhibition of glutamate dehydrogenase reaction. *FEBS Letters*, 581(14), pp.2733-2736.

- Clark, I., Alleva, L., Cowden, W. and Budd, A. (2006). Human malarial disease: a consequence of inflammatory cytokine release. *malaria journal*, (5), pp.85.
- Conners, E., Vinetz, J., Weeks, J. and Brouwer, K. (2016). A global systematic review of Chagas disease prevalence among migrants. *Acta Tropica*, 156, pp.68-78.
- Coronado, L., Nadovich, C. and Spadafora, C. (2014). Malarial hemozoin: From target to tool. *Biochimica et Biophysica Acta (BBA) - General Subjects*, 1840(6), pp.2032-2041.
- Crabb, B. (2002). Transfection technology and the study of drug resistance in the malaria parasite *P. falciparum*. *Drug Resistance Updates*, 5(3-4), pp.126-130.
- Croft, S. (2001). Antimalarial Chemotherapy: Mechanisms of Action, Resistance and New Directions in Drug Discovery. *Drug Discovery Today*, 6(22), pp.1151.
- Das, N., Dhanawat, M., Dash, B., Nagarwal, R. and Shrivastava, S. (2010). Codrug: An efficient approach for drug optimization. *European Journal of Pharmaceutical Sciences*, 41(5), pp.571-588.
- de Pilla Varotti, F., Botelho, A., Andrade, A., de Paula, R., Fagundes, E., Valverde, A., Mayer, L., Mendonca, J., de Souza, M., Boechat, N. and Krettli, A. (2008). Synthesis, antimalarial activity, and intracellular targets of mefas, a new hybrid compound derived from mefloquine and artesunate. *Antimicrobial Agents and Chemotherapy*, 52(11), pp.3868-3874.
- Delespaux, V. and Dekoning, H. (2007). Drugs and drug resistance in African trypanosomiasis. *Drug Resistance Updates*, 10(1-2), pp.30-50.
- Demidov, V. (2003). Infection stage clues to new antimalarial medicines. *Drug Discovery Today*, 8(20), pp.913-915.
- Derbyshire, E., Mazitschek, R. and Clardy, J., 2012. Characterization of Plasmodium Liver Stage Inhibition by Halofuginone. *ChemMedChem*, 7(5), pp.844-849.

- Devine, K., McGuigan, C., O'Connor, T., Nicholls, S. and Kinchington, D. (1990). Novel phosphate derivatives of zidovudine as anti-HIV compounds. *AIDS*, 4(4), pp.371-374.
- Dhanawat, M., Das, N., Nagarwal, R. and Shrivastava, S. (2009). Antimalarial Drug Development: Past to Present Scenario. *Mini-Reviews in Medicinal Chemistry*, 9(12), pp.1447-1469.
- Diagana, T. (2015). Supporting malaria elimination with 21st century antimalarial agent drug discovery. *Drug Discovery Today*, 20(10), pp.1265-1270.
- Dondorp, A., Nosten, F., Yi, P., Das, D., Phyto, A., Tarning, J., Lwin, K., Ariey, F., Hanpithakpong, W., Lee, S., Ringwald, P., Silamut, K., Im-wong, M., Chotivanich, K., Lim, P., Herdman, T., An, S., Yeung, S., Singhasivanon, P., Day, N., Lindegardh, N., Socheat, D. and White, N. (2009). Artemisinin resistance in *P. falciparum* malaria. *N Engl J Med*, 361, pp.455-467.
- Döpp, D., (2000). Preparation of 4-(N,N-dihexylamino)-4'-nitrostilbene (DHANS). *Arkivoc*, 2000(6), pp.939-944.
- Downey, A., Cairo, C. (2014). Synthesis of α -brominated phosphonates and their application as phosphate bioisosteres. *Med. Chem. Commun.*, 5(11), pp.1619-1633.
- Drug-Resistant Malaria. (1981). *The Lancet*, 318(8255), pp.1087-1088.
- Eacquerra, J., Pedregal, C., Micó, I. and Nájera, C. (1994). Efficient synthesis of 4-Methylene-L-glutamic acid and its cyclopropyl analogue. *Tetrahedron: Asymmetry*, 5(5), pp.921-926.
- Eastman, R., Roth, J., Brimacombe, K., Simeonov, A., Shen, M., Patnaik, S. and Hall, M., 2020. Remdesivir: A Review of Its Discovery and Development Leading to Emergency Use Authorization for Treatment of COVID-19. *ACS Central Science*, 6(5), pp.672-683.

- Eaton, J., Eckman, J., Beger, E., Jacob, H. (1976). Suppression of malaria infection by oxidant-sensitive host erythrocytes. *Nature*, 264(5588), pp.758-760.
- Eckstein-Ludwig, U., Webb, R., van Goethem, I., East, J., Lee, A., Kimura, M., O'Neill, P., Bray, P., Ward, S. and Krishna, S. (2003). Artemisinin target the SERCA of *P. falciparum*. *Nature*, 424(6951), pp.957-961.
- Egan, T. (2003). Haemozoin (malaria pigment): a unique crystalline drug target. *TARGETS*, 2(3), pp.115-124.
- Egan, T., Combrinck, J., Egan, J., Hearne, G., Marques, H., Ntenti, S., Sewell, B., Smith, P., Taylor, D., van Schalkwyk, D., Walden, J. (2002). Fate of haem iron in the malaria parasite *P. falciparum*. *Biochemical Journal*, 365(2), pp.343-347.
- Elliott, T., Slowey, A., Ye, Y. and Conway, S. (2012). The use of phosphate bioisosteres in medicinal chemistry and chemical biology. *Med Chem Comm*, 3(7), pp.735.
- El-Sayed, N. (2005). The Genome Sequence of *Trypanosoma cruzi*, Etiologic Agent of Chagas Disease. *Science*, 309(5733), pp.409-415.
- Emanuelsson, O., Nielsen, H., Brunak, S. and von Heijne, G. (2000). Predicting Subcellular Localization of Proteins Based on their N-terminal Amino Acid Sequence. *Journal of Molecular Biology*, 300(4), pp.1005-1016.
- Fairfield, A., Meshnick and Eaton, J. (1983). Malaria parasites adopt host cell superoxide dismutase. *Science*, 221(4612), pp.764-766.
- Famin, O., Krugliak, M. and Ginsburg, H. (1999). Kinetics of inhibition of glutathione-mediated degradation of ferriprotoporphyrin IX by antimalarial drugs. *Biochemical Pharmacology*, 58(1), pp.59-68.

- Färber, P., Arscott, L., Williams, C., Becker, K. and Schirmer, R. (1998). Recombinant *P. falciparum* glutathione reductase is inhibited by the antimalarial dye methylene blue. *FEBS Letters*, 422(3), pp.311-314.
- Farber, P., Becker, K., Muller, S., Schirmer, R. and Franklin, R. (1996). Molecular Cloning and Characterization of a Putative Glutathione Reductase Gene, the PfGR2 Gene, from *P. falciparum*. *European Journal of Biochemistry*, 239(3), pp.655-661.
- Felger, I. and Beck, H. (2008). Fitness costs of resistance to antimalarial drugs. *Trends in Parasitology*, 24(8), pp.331-333.
- Fernandes, A. and Holmgren, A. (2004). Glutaredoxins: Glutathione-Dependent Redox Enzymes with Functions Far Beyond a Simple Thioredoxin Backup System. *Antioxidants & Redox Signalling*, 6(1), pp.63-74.
- Fidock, D. (2000). Mutations in the *P. Falciparum* Digestive Vacuole Transmembrane Protein PfCRT and Evidence for Their Role in Chloroquine Resistance. *Molecular Cell*, 6(4), pp.861-871.
- Fidock, D., Rosenthal, P., Croft, S., Brun, R. and Nwaka, S. (2004). Antimalarial drug discovery: efficacy models for compound screening. *Nature Reviews Drug Discovery*, 3(6), pp.509-520.
- Filomeni, G., Rotilio, G. and Ciriolo, M. (2002). Cell signalling and the glutathione redox system. *Biochemical Pharmacology*, 64(5-6), pp.1057-1064.
- Flengte, C., Hutchinson, D., Betebenner, D., DeGoey, D., Donner, P., Kati, W., Krueger, A., Liu, D., Liu, Y., Longenecker, K., Maring, C., Motter, C., Pratt, J., Randolph, J., Rockway, T., Stewart, K., Wagner, R., Chen, S., Yi, G., Lou, X. and Zhang, G. (2012). *Anti-Infective Agents and uses thereof*. US008188104B2.
- Fletcher, A. and Shepherd, R., 2003. *Use of (+)-mefloquine for the treatment of malaria*. US006664397B1.

- Fonken, G., Herr, M., Murray, H. and Reineke, L., (1967). Microbiological Hydroxylation of Monocyclic Alcohols. *Journal of the American Chemical Society*, 89(3), pp.672-675.
- Foth, B. (2003). Dissecting Apicoplast Targeting in the Malaria Parasite *P. falciparum*. *Science*, 299(5607), pp.705-708.
- Foth, B., Stimmler, L., Handman, E., Crabb, B., Hodder, A. and McFadden, G. (2004). The malaria parasite *P. falciparum* has only one pyruvate dehydrogenase complex, which is located in the apicoplast. *Molecular Microbiology*, 55(1), pp.39-53.
- França, T., Wilter, A., Ramalho, T., Pascutti, P. and Figueroa-Villar, J. (2006). Molecular dynamics of the interaction of *P. falciparum* and human serine hydroxymethyltransferase with 5-formyl-6-hydrofolic acid analogues: design of new potential antimalarials. *Journal of the Brazilian Chemical Society*, 17(7), pp.1383-1392.
- Gallup, J. and Sachs, J. (2001). The economic burden of malaria. *The American Journal of Tropical Medicine and Hygiene*, 64(1_suppl), pp.85-96.
- Gamo, F. (2014). Antimalarial drug resistance: new treatments options for Plasmodium. *Drug Discovery Today: Technologies*, 11, pp.81-88.
- Gelb, M. (2007). Drug discovery for malaria: a very challenging and timely endeavour. *Current Opinion in Chemical Biology*, 11(4), pp.440-445.
- Ghosh, S., Kumar Das, A., Sarkar, P. and Sil, P. (2019). 6 - Oxidative stress in schistosomiasis, echinococcosis, and trypanosomiasis: a therapeutic approach. *Discovery and Development of Therapeutics from Natural Products Against Neglected Tropical Diseases*, [online] pp.219-239. Available at: <https://doi.org/10.1016/B978-0-12-815723-7.00006-7>.
- Giha, H. (2009). Artemisinin derivatives for treatment of uncomplicated *P. falciparum* malaria in Sudan: too early for too much hope. *Parasitology Research*, 106(3), pp.549-552.

- Gillard, J. and Israel, M. (1981). Trimethylsilyl bromide as a mild, stereoselective anomeric brominating agent. *Tetrahedron Letters*, 22(6), pp.513-516.
- Gillespie, R., Adams, D., Bebbington, D., Benwell, K., Cliffe, I., Dawson, C., Dourish, C., Fletcher, A., Gaur, S., Giles, P., Jordan, A., Knight, A., Knutsen, L., Lawrence, A., Lerpiniere, J., Misra, A., Porter, R., Pratt, R., Shepherd, R., Upton, R., Ward, S., Weiss, S. and Williamson, D., 2008. Antagonists of the human adenosine A2A receptor. Part 1: Discovery and synthesis of thieno [3,2-d] pyrimidine-4-methanone derivatives. *Bioorganic & Medicinal Chemistry Letters*, 18(9), pp.2916-2919.
- Ginsburg, H. and Atamina, H. (1994). The redox status of malaria-infected erythrocytes: an overview with an emphasis on unresolved problems. *Parasite*, 1(1), pp.5-13.
- Ginsburg, H., Famin, O., Zhang, J. and Krugliak, M. (1998). Inhibition of glutathione-dependent degradation of heme by chloroquine and amodiaquine as a possible basis for their antimalarial mode of action. *Biochemical Pharmacology*, 56(10), pp.1305-1313.
- Gleeson, M., Hersey, A., Montanari, D. and Overington, J. (2011). Probing the links between in vitro potency, ADMET and physicochemical parameters. *Nature Reviews Drug Discovery*, 10(3), pp.197-208.
- Green, D., Elgendy, S., Patel, G., Baban, J., Skordalakes, E., Husman, W., Kakkar, V. and Deadman, J. (1996). The facile synthesis of O,O-Dialkyl α -halobenzylphosphonates from O,O-Dialkyl α -hydroxy benzyl phosphonates. *Tetrahedron*, 52(30), pp.10215-10224.
- Greenwood, B., Fidock, D., Kyle, D., Kappe, S., Alonso, P., Collins, F. and Duffy, P. (2008). Malaria: progress, perils, and prospects for eradication. *Journal of Clinical Investigation*, 118(4), pp.1266-1276.
- Gué, A., Lattes, A., Laurent, E., Mauzac, M. and Mingotaud, A. (2008). Characterization of recognition sites for diethyl 4-nitrobenzylphosphonate, an organophosphate pesticide analogue. *Analytica Chimica Acta*, 614(1), pp.63-70.

- Hansch, C., Björkroth, J. and Leo, A., 1987. Hydrophobicity and Central Nervous System Agents: On the Principle of Minimal Hydrophobicity in Drug Design. *Journal of Pharmaceutical Sciences*, 76(9), pp.663-687.
- Hastings, I. and Donnelly, M. (2005). The impact of antimalarial drug resistance mutations on parasite fitness, and its implications for the evolution of resistance. *Drug Resistance Updates*, 8(1-2), pp.43-50.
- Hastings, I. and Watkins, W. (2006). Tolerance is the key to understanding antimalarial drug resistance. *Trends in Parasitology*, 22(2), pp.71-77.
- Hayashi, M. and Nakamura, S., (2011). Catalytic Enantioselective Protonation of α -Oxygenated Ester Enolates Prepared through Phospha-Brook Rearrangement. *Angewandte Chemie International Edition*, 50(10), pp.2249-2252.
- He, L., Cai, Z., Pian, J. and Du, G. (2013). NHCs Catalysed Hydrophosphonylation of α -Ketoesters and α -Trifluoromethyl Ketones. *The Scientific World Journal*, 2013, pp.1-6.
- Hecker, S., Erion, M. (2008). ChemInform Abstract: Prodrugs of Phosphates and Phosphonates. *Journal of Medicinal Chemistry*, (51), pp. 2328-2345.
- Held, J., Kreidenweiss, A. and Mordmüller, B. (2013). Novel approaches in antimalarial drug discovery. *Expert Opinion on Drug Discovery*, 8(11), pp.1325-1337.
- Held, J., Supan, C., Salazar, C., Tinto, H., Bonkian, L., Nahum, A., Sié, A., Abdulla, S., Cantalloube, C., Djeriou, E., Bouyou-Akotet, M., Ogutu, B., Mordmüller, B., Kreidenweiss, A., Siribie, M., Sirima, S. and Kremsner, P. (2017). Safety and efficacy of the choline analogue SAR97276 for malaria treatment: results of two phase 2, open-label, multicenter trials in African patients. *Malaria Journal*, 16(1), pp.1-12.
- Herrera, S., Corradin, G. and Arévalo-Herrera, M. (2007). An update on the search for a *P. vivax* vaccine. *Trends in Parasitology*, 23(3), pp.122-128.

- Hirumi, H. and Hirumi, K. (1989). Continuous Cultivation of *Trypanosoma brucei* Blood Stream Forms in a Medium Containing a Low Concentration of Serum Protein without Feeder Cell Layers. *The Journal of Parasitology*, 75(6), pp.985.
- Hocart, S., Liu, H., De, D., Krogstad, F. and Krogstad, D. (2008). Quantitative Structure-Activity Relationships of Potential Antimalarial Drugs Active Against Chloroquine-Resistant *P. falciparum*. *Planta Medica*, 74(03), pp.203-304
- Hocart, S., Liu, H., Deng, H., De, D., Krogstad, F. and Krogstad, D. (2011). 4-Aminoquinolines Active against Chloroquine-Resistant *P. falciparum*: Basis of Antiparasite Activity and Quantitative Structure-Activity Relationship Analyses. *Antimicrobial Agents and Chemotherapy*, 55(5), pp.2233-2244.
- Hunter, T. (1995). Protein kinases and phosphatases: The Yin and Yang of protein phosphorylation and signalling. *Cell*, 80(2), pp.225-236.
- Hyde, J. (2002). Mechanisms of resistance of *P. falciparum* to antimalarial drugs. *Microbes and Infection*, 4(2), pp.165-174.
- Hyde, J. (2005). Drug-resistant malaria. *Trends in Parasitology*, 21(11), pp.494-498.
- Imlay, J. (2003). Pathways of Oxidative Damage. *Annual Review of Microbiology*, 57(1), pp.395-418.
- Ismail, F. (2002). Important fluorinated drugs in experimental and clinical use. *Journal of Fluorine Chemistry*, 118(1-2), pp.27-33.
- Ismail, F., Dascombe, M., Carr, P., Mérette, S. and Rouault, P. (1998). Novel Aryl-bis-quinolines with Antimalarial Activity In-vivo. *Journal of Pharmacy and Pharmacology*, 50(5), pp.483-492.

- Izumi, M., Fukase, K. and Kusumoto, S. (2002). TMSiCl as a Mild and Effective Source of Acidic Catalysis in Fischer Glycosidation and Use of Propargyl Glycoside for Anomeric Protection. *Bioscience, Biotechnology, and Biochemistry*, 66(1), pp.211-214.
- Jackson, R. and Malek, F. (1980). ChemInform Abstract: Radical-Initiated Reduction of Chloroformates to Alkanes by Tri-N-Propylsilane. A Method for removal of unwanted Hydroxy-groups from Organic molecules. *Chemischer Informationsdienst*, 11(35), pp.344-345.
- Jamieson, A. (2006). Malaria prevention and treatment. *South African Family Practice*, 48(9), pp.38-41.
- Joshi, A. and Viswanathan, C. (2006). Recent Developments in Antimalarial Drug Discovery. *Anti-Infective Agents in Medicinal Chemistry*, 5(1), pp.105-122.
- Ju, K., Gao, J., Doroghazi, J., Wang, K., Thibodeaux, C., Li, S., Metzger, E., Fudala, J., Su, J., Zhang, J., Lee, J., Cioni, J., Evans, B., Hirota, R., Labeda, D., van der Donk, W. and Metcalf, W. (2015). Discovery of phosphonic acid natural products by mining the genomes of 10,000 actinomycetes. *Proceedings of the National Academy of Sciences*, 112(39), pp.12175-12180.
- Kafarski, P. (2020). *Phosphonates: Their Natural Occurrence and Physiological Role*.
- Kamel, A. (2015). phosphorus compounds in pharmaceutical drugs and their rising role as antioxidants and anti-diabetics: a review. *International Journal of Chemical and Biomedical Science*, 1(3), pp.56-69.
- Kamijo, T., Harada, H. and Iizuka, K. (1983). A novel one step conversion of alcohols into alkyl bromides or iodides. *Chemical & pharmaceutical bulletin*, 31(11), pp.4189-4192.
- Karunamoorthi, K. (2011). Vector control: a cornerstone in the malaria elimination campaign. *Clinical Microbiology and Infection*, 17(11), pp.1608-1616.

- Khan, S., Battula, S. and Ahmed, Q., (2016). Aroyl group driven [1,2] phosphonate-phosphate/phosphine oxide-phosphinate rearrangement. *Tetrahedron*, 72(29), pp.4273-4279.
- Kiso, Y., Nakamura, S., Ito, K., Ukawa, K., Kitagawa, K., Akita, T. and Moritoki, H., 1979. Deprotection of O-methyltyrosine by a 'push-pull' mechanism using the thioanisole-trifluoromethanesulphonic acid system. Application to the convenient synthesis of a potent N-methylenkephalin derivative. *J. Chem. Soc., Chem. Commun.*, (21), pp.971-972.
- Kiso, Y., Nakamura, S., Ito, K., Ukawa, K., Kitagawa, K., Akita, T. and Moritoki, H., (1979). Deprotection of O-methyltyrosine by a 'push-pull' mechanism using the thioanisole-trifluoromethanesulphonic acid system. Application to the convenient synthesis of a potent N-methylenkephalin derivative. *J. Chem. Soc., Chem. Commun.*, (21), pp.971-972.
- Kiso, Y., Ukawa, K. and Akita, T., (1980). Efficient removal of N-benzyloxycarbonyl group by a 'push-pull' mechanism using thioanisole-trifluoroacetic acid, exemplified by a synthesis of Met-enkephalin. *J. Chem. Soc., Chem. Commun.*, (3), pp.101-102.
- Kiso, Y., Ukawa, K., Nakamura, S., Ito, K. and Akita, T., (1980). Efficient removal of protecting groups by a 'push-pull' mechanism. II. Deprotection of O-benzylytyrosine with a thioanisole-trifluoroacetic acid system without O-to-C rearrangements. *Chemical & Pharmaceutical Bulletin*, 28(2), pp.673-676.
- Kondoh, A., Aita, K., Ishikawa, S. and Terada, M., (2020). Synthesis of Tetrasubstituted Furans through One-Pot Formal [3 + 2] Cycloaddition Utilizing [1,2]-Phospha-Brook Rearrangement. *Organic Letters*, 22(5), pp.2105-2110.
- Kondoh, A., Koda, K., Kamata, Y. and Terada, M., (2017). Synthesis of Indolizine Derivatives Utilizing [1,2]-Phospha-Brook Rearrangement/Cycloisomerization Sequence. *Chemistry Letters*, 46(7), pp.1020-1023.

- Kondoh, A., Tasato, N., Aoki, T. and Terada, M., (2020). Brønsted Base-Catalyzed Transformation of α,β -Epoxyketones Utilizing [1,2]-Phospha-Brook Rearrangement for the Synthesis of Allylic Alcohols Having a Tetrasubstituted Alkene Moiety. *Organic Letters*, 22(13), pp.5170-5175.
- Kortagere, S., Welsh, W., Morrisey, J., Daly, T., Ejigiri, I., Sinnis, P., Vaidya, A. and Bergman, L. (2010). Structure-based Design of Novel Small-Molecule Inhibitors of *P. falciparum*. *Journal of Chemical Information and Modelling*, 50(5), pp.840-849.
- Kosolapoff, G. (1945). Isomerization of Alkyl Phosphites. IV. The Synthesis of Some Alkaryl Phosphonic Acids and Esters. *Journal of the American Chemical Society*, 67(12), pp.2259-2260.
- Krauth-Siegel, L. and Schmdt, H. (2020). Trypanothione and Tryparedoxin in Ribonucleotide Reduction. *Methods in enzymology*, 347, pp.259-270.
- Krauth-Siegel, R., Muller, J., Lottspeich, F. and Schirmer, R. (1996). Glutathione Reductase and Glutamate Dehydrogenase of *P. falciparum*, The Causative Agent of Tropical Malaria. *European Journal of Biochemistry*, 235(1-2), pp.345-350.
- Krettli, A. (2009). Antimalarial drug discovery: screening of Brazilian medicinal plants and purified compounds. *Expert Opinion on Drug Discovery*, 4(2), pp.95-108.
- Krettli, A., Adebayo, J. and Krettli, L. (2009). Testing of Natural Products and Synthetic Molecules Aiming at New Antimalarials. *Current Drug Targets*, 10(3), pp.261-270.
- Krishna, S., Kleine, C. and Stich, A. (2020). Hunter's Tropical Medicine and Emerging Infectious Diseases (Tenth Edition). pp.755-761.
- Kulkarni, M., Lad, U., Desai, U., Mitragotri, S. and Wadgaonkar, P. (2013). Mechanistic approach for expeditious and solvent-free synthesis of α -hydroxy phosphonates using potassium phosphate as catalyst. *Comptes Rendus Chimie*, 16(2), pp.148-152.

- Kumar, S., Bhardwaj, T., Prasad, D. and Singh, R. (2018). Drug targets for resistant malaria: Historic to future perspectives. *Biomedicine & Pharmacotherapy*, 104, pp.8-27.
- Kuroboshi, M., Ishihara, T. and Ando, T., (1988). Reaction of fluorinated ketones with dialkyl phosphites: An efficient and selective transformation of aryl F-alkyl ketones into dialkyl aryl (F-alkyl) methyl phosphates. *Journal of Fluorine Chemistry*, 39(2), pp.293-298.
- Laufer, M. and Plowe, C. (2004). Withdrawing antimalarial drugs: impact on parasite resistance and implications for malaria treatment policies. *Drug Resistance Updates*, 7(4-5), pp.279-288.
- Lawrence, N., Drew, M. and Bushell, S. (1999). Polymethylhydrosiloxane: a versatile reducing agent for organic synthesis. *Journal of the Chemical Society, Perkin Transactions 1*, (23), pp.3381-3391.
- Leroux, A., Krauth-Siegel, R. (2016). Thiol redox biology of trypanosomatids and potential targets for chemotherapy. *Molecular and Biochemical Parasitology*, 206(1-2), pp.67-74.
- Leysens, T. and Peeters, D. (2004). Theoretical study of the influence of phosphorus containing substituents on organic molecules. *Journal of Molecular Structure: Theochem*, 686(1-3), pp.71-82.
- Li, M., Smith, C., Walker, M. and Smith, T. (2009). Novel Inhibitors Complexed with Glutamate Dehydrogenase. *Journal of Biological Chemistry*, 284(34), pp.22988-23000.
- Lipinski, C., Lombardo, F., Dominy, B. and Feeney, P. (1997). Experimental and computational approaches to estimate solubility and permeability in drug discovery and development settings. *Advanced Drug Delivery Reviews*, 23(1-3), pp.3-25.
- Llanos-Cuentas, A., Lacerda, M., Rueangweerayut, R., Krudsood, S., Gupta, S., Kochar, S., Arthur, P., Chuenchom, N., Möhrle, J., Duparc, S., Ugwuegbulam, C., Kleim, J., Carter, N., Green, J. and Kellam, L. (2014). Tafenoquine plus chloroquine for the treatment and

- relapse prevention of *P. vivax* malaria (DETECTIVE): a multicentre, double-blind, randomised, phase 2b dose-selection study. *The Lancet*, 383(9922), pp.1049-1058.
- Ludin, P., Woodcroft, B., Ralph, S. and Mäser, P. (2012). In silico prediction of antimalarial drug target candidates. *International Journal for Parasitology: Drugs and Drug Resistance*, 2, pp.191-199.
- Lugovkin, B. (1970). Synthesis of dialkyl esters of aryl amino(2-pyridyl) methyl-phosphonic acids. *Chemistry of Heterocyclic Compounds*, 4(1), pp.91-93.
- Maaswinkel, H., Zhu, L. and Weng, W., (2015). A small-fish model for behavioural-toxicological screening of new antimalarial drugs: a comparison between erythro- and threo-mefloquine. *BMC Research Notes*, 8(1), pp.1-7.
- Macreadie, I., Ginsburg, H., Sirawaraporn, W. and Tilley, L. (2000). Antimalarial Drug Development and New Targets. *Parasitology Today*, 16(10), pp.438-444.
- Mahidol, C. (2004). Malaria: integrated approaches for prevention and treatment. *Acta Tropica*, 89(3), pp.265-269.
- Maienfisch, P. and Hall, R. (2004). The Importance of Fluorine in the Life Science Industry. *CHIMIA International Journal for Chemistry*, 58(3), pp.93-99.
- Makhaeva, G., Aksinenko, A., Sokolov, V., Serebryakova, O. and Richardson, R., (2009). Synthesis of organophosphates with fluorine-containing leaving groups as serine esterase inhibitors with potential for Alzheimer disease therapeutics. *Bioorganic & Medicinal Chemistry Letters*, 19(19), pp.5528-5530.
- Martin, D. and Griffin, C. (1964). Phosphonic acids and esters. *Journal of Organometallic Chemistry*, 1(3), pp.292-296.
- Maxwell, R. (1984). The state of the art of the science of drug discovery? An opinion. *Drug Development Research*, 4(4), pp.375-389.

- McCarthy, J., Lotharius, J., Rückle, T., Chalon, S., Phillips, M., Elliott, S., Sekuloski, S., Griffin, P., Ng, C., Fidock, D., Marquart, L., Williams, N., Gobeau, N., Bebrevska, L., Rosario, M., Marsh, K. and Möhrle, J. (2017). Safety, tolerability, pharmacokinetics, and activity of the novel long-acting antimalarial DSM265: a two-part first-in-human phase 1a/1b randomised study. *The Lancet Infectious Diseases*, 17(6), pp.626-635.
- McCarthy, J., Rückle, T., Elliott, S., Ballard, E., Collins, K., Marquart, L., Griffin, P., Chalon, S. and Möhrle, J. (2019). A Single-Dose Combination Study with the Experimental Antimalarials Artefenomel and DSM265 to Determine Safety and Antimalarial Activity against Blood-Stage *P. falciparum* in Healthy Volunteers. *Antimicrobial Agents and Chemotherapy*, 64(1), pp.1-10.
- McKenna, C. and Schmidhuser, J. (1979). Functional selectivity in phosphonate ester dealkylation with bromotrimethylsilane. *Journal of the Chemical Society, Chemical Communications*, (17), pp.739.
- Mehellou, Y., Balzarini, J. and McGuigan, C., (2009). Aryloxy Phosphoramidate Triesters: A Technology for Delivering Monophosphorylated Nucleosides and Sugars into Cells. *Chem Med Chem*, 4(11), pp.1779-1791.
- Mehellou, Y., Rattan, H. and Balzarini, J. (2017). The ProTide Prodrug Technology: From the Concept to the Clinic. *Journal of Medicinal Chemistry*, 61(6), pp.2211-2226.
- Mehlin, C. (2005). Structure-Based Drug Discovery for *P. falciparum*. *Combinatorial Chemistry & High Throughput Screening*, 8(1), pp.5-14.
- Meierjohann, S., Walter, R., Müller, S. (2002). Regulation of intracellular glutathione levels in erythrocytes infected with chloroquine-sensitive and chloroquine-resistant *P. falciparum*. *Biochemical Journal*, 368(3), pp.761-768.
- Meister, S., Plouff, D., Kuhen, K., Bonamy, G., Wu, T., Barnes, W., Bopp, S., Borboa, R., Bright, T., Che, J., Cohen, S., Dharia, N., Gagaring, K., Gettayacamin, M., Gordon, P.,

- Groessl, T., Kato, N., Lee, M., McNamara, C., Fidock, D., Nagle, A., Nam, T., Richmond, W., Roland, J., Rottmann, M., Zhou, B., Froissard, P., Glynn, R., Mazier, D., Sattabongkot, J., Schultz, P., Tuntland, T., Walker, J., Zhou, Y., Chatterjee, A., Diagana, T. and Winzeler, E., 2011. Imaging of Plasmodium liver stages to drive next-generation antimalarial drug discovery. *Science*, 334(6061), pp.1372-1377.
- Meneer, K., Ottridge, A., Londesbrough, D., Hallet, M., Mulholland, R., Pittam, J., Laffan, D., Ashworth, I., Jones, M. and Cherryman, J. (2012). *Phthalazinone Derivative*. US008247416B2.
- Meshnick, S. (2002). Artemisinin: mechanisms of action, resistance and toxicity. *International Journal for Parasitology*, 32(13), pp.1655-1660.
- Methyl groups by reduction of Aromatic Carboxylic acids with Trimethylchlorosilane - Tri-n-Propylamine: 2-Methylbiphenyl. (1977). *Organic Syntheses*, 56, pp.83.
- Mignani, S., Rodrigues, J., Tomas, H., Jalal, R., Singh, P., Majoral, J. and Vishwakarma, R. (2018). Present drug-likeness filters in medicinal chemistry during the hit and lead optimization process: how far can they be simplified? *Drug Discovery Today*, 23(3), pp.605-615.
- Milek, A. (2008). Design and synthesis of novel GDH-inhibitors as potential new antimalarials. *MSc thesis*, London Metropolitan University.
- Miller, L. and Good, M. (1988). The main obstacle to a malaria vaccine: the malaria parasite. *Vaccine*, 6(2), pp.104-106.
- Miller, L., Good, M. and Milon, G. (1994). Malaria pathogenesis. *Science*, 264(5167), pp.1878-1883.
- Moedritzer, K. and Irani, R. (1966). The Direct Synthesis of α -Amino methyl phosphonic Acids. Mannich-Type Reactions with Orthophosphorous Acid. *The Journal of Organic Chemistry*, 31(5), pp.1603-1607.

- Monitoring antimalarial drug resistance within National Malaria Control Programmes: the EANMAT experience. (2001). *Tropical Medicine and International Health*, 6(11), pp.891-898.
- Moore, B., Jago, J. and Batty, K. (2008). *P. berghei*: Parasite clearance after treatment with dihydroartemisinin in an asplenic murine malaria model. *Experimental Parasitology*, 118(4), pp.458-467.
- Müller, I. and Hyde, J. (2010). Antimalarial drugs: modes of action and mechanisms of parasite resistance. *Future Microbiology*, 5(12), pp.1857-1873.
- Müller, S. (2004). Redox and antioxidant systems of the malaria parasite *P. falciparum*. *Molecular Microbiology*, 53(5), pp.1291-1305.
- Müller, S. (2015). Role and Regulation of Glutathione Metabolism in *P. falciparum*. *Molecules*, 20(6), pp.10511-10534.
- Murai, K. and Fujioka, H., (2016). Enantioselective, Metal-Catalyzed Addition of Phosphites to Aldehydes (Pudovik Reaction). *Science of Synthesis Knowledge Updates*, 2, pp.303.
- Muregi, F. and Ishih, A. (2009). Next-generation antimalarial drugs: hybrid molecules as a new strategy in drug design. *Drug Development Research*, pp.20-32.
- Noedl, H., Wongsrichanalai, C. and Wernsdorfer, W. (2003). Malaria drug-sensitivity testing: new assays, new perspectives. *Trends in Parasitology*, 19(4), pp.175-181.
- Nowicki, C., Cazzulo, J. (2008). Aromatic amino acid catabolism in trypanosomatids. *Comparative Biochemistry and Physiology Part A: Molecular & Integrative Physiology*, 151(3), pp.381-390.
- Olah, G. and Narang, S. (1982). ChemInform Abstract: Iodotrimethylsilane, a versatile synthetic reagent. *Chemischer Informationsdienst*, 13(50), pp.2225-2277.

- Olah, G., Gupta, B., Malhotra, R., Narang, S. (1980). ChemInform Abstract: Chlorotrimethylsilane/Lithium Bromide and hexamethyldisilane/Pyridinium Bromide Perbromide: Effective and selective reagents for the effective and selective reagents for the conversion of alkyl (Cycloalkyl and Aalkyl) alcohols into Bromides. *The Journal of Organic chemistry*, 45, pp.1638-1639.
- Olah, G., Narang, S., Gupta, B. and Malhotra, R. (1979). Hexamethyldisilane/Iod: Bequeme Erzeugung von Iodtrimethylsilane in situ. *Angewandte Chemie*, 91(8), pp.648-649.
- Olah, G., Narang, S., Olah, J., Pearson, R. and Cupas, C. (1980). ChemInform Abstract: Aromatic substitution. 45. Transfer nitration of aromatics with N-Nitropyridinium and Quinollinum ions. *Chemischer Informationsdienst*, 11(32), pp.3507-3510.
- Olliaro, P. (2001). Mode of action and mechanisms of resistance for antimalarial drugs. *Pharmacology & Therapeutics*, 89(2), pp.207-219.
- Olliaro, P. and Wirth, D. (1997). New Targets for Antimalarial Drug Discovery. *Journal of Pharmacy and Pharmacology*, 49(S2), pp.29-33.
- Olliaro, P. and Yuthavong, Y. (1999). An Overview of Chemotherapeutic Targets for Antimalarial Drug Discovery. *Pharmacology & Therapeutics*, 81(2), pp.91-110.
- O'Neill, M., Bray, D., Boardman, P., Chan, K., Phillipson, J., Warhurst, D. and Peters, W. (1987). Plants as Sources of Antimalarial Drugs, Part 4: Activity of *Brucea javanica* Fruits Against Chloroquine-Resistant *P. falciparum* in vitro and Against *P. berghei* in vivo. *Journal of Natural Products*, 50(1), pp.41-48.
- Oyeyinka, G. (2005). Review Article: Vaccine for Malaria – How Far? *African Journal of Clinical and Experimental Microbiology*, 6(2), pp.139-143.
- Pallikonda, G., Santosh, R., Ghosal, S. and Chakravarty, M., (2015). BuLi-triggered phospho-Brook rearrangement: efficient synthesis of organophosphates from ketones and aldehydes. *Tetrahedron Letters*, 56(24), pp.3796-3798.

- Pallikonda, G., Santosh, R., Ghosal, S. and Chakravarty, M., (2015). BuLi-triggered phospho-Brook rearrangement: efficient synthesis of organophosphates from ketones and aldehydes. *Tetrahedron Letters*, 56(24), pp.3796-3798.
- Pandi, M., Chanani, P. and Govindasamy, S. (2012). An efficient synthesis of α -hydroxy phosphonates and 2-nitroalkanols using Ba(OH)₂ as catalyst. *Applied Catalysis A: General*, 441-442, pp.119-123.
- Pawar, V., Bettigeri, S., Weng, S., Kao, J. and Chen, C., (2006). Highly Enantioselective Aerobic Oxidation of α -Hydroxyphosphonates Catalyzed by Chiral Vanadyl(V) Methoxides Bearing N-Salicylidene- α -aminocarboxylates. *Journal of the American Chemical Society*, 128(19), pp.6308-6309.
- Pechan, T. and Gwaltney, S. (2012). Calculations of relative intensities of fragment ions in the MSMS spectra of a doubly charged penta-peptide. *BMC Bioinformatics*, 13(S15).
- Pereira, E., Ishikawa, E. and Fontes, C. (2011). Adherence to *P. vivax* malaria treatment in the Brazilian Amazon Region. *Malaria Journal*, 10(1), pp.355.
- Peterson, P. and Smith, T. (1999). The structure of bovine glutamate dehydrogenase provides insights into the mechanism of allostery. *Structure*, 7(7), pp.769-782.
- Peyman, A., Uhlmann, E., Budt, K., Knolle, J., Winkler, I. and Helsenberg, M. (1993). *Use of Benzylphosphonic acid derivatives for their treatment of diseases caused by viruses.* US005242908A.
- Phosphonates: Their Natural Occurrence and Physiological Role. (2019). 1st ed.
- Phyo, A., Jittamala, P., Nosten, F., Pukrittayakamee, S., Imwong, M., White, N., Duparc, S., Macintyre, F., Baker, M. and Möhrle, J. (2016). Antimalarial activity of artefenomel (OZ439), a novel synthetic antimalarial endoperoxide, in patients with *P. falciparum* and *P. vivax* malaria: an open-label phase 2 trial. *The Lancet Infectious Diseases*, 16(1), pp.61-69.

- Plowe, C. (2003). Monitoring antimalarial drug resistance: making the most of the tools at hand. *Journal of Experimental Biology*, 206(21), pp.3745-3752.
- Plowe, C. (2005). Antimalarial drug resistance in Africa: strategies for monitoring and deterrence. *Curr. Top. Microbiol. Immunol.*, (295), pp.55-79.
- Pogatchnik, D. and Wiemer, D., (1997). Enantioselective synthesis of α -hydroxy phosphonates via oxidation with (camphorsulfonyl)oxaziridines. *Tetrahedron Letters*, 38(20), pp.3495-3498.
- Prechelmacher, S., Mereiter, K. and Hammerschmidt, F., (2018). The α -hydroxyphosphonate-phosphate rearrangement of a noncyclic substrate – some new observations. *Organic & Biomolecular Chemistry*, 16(19), pp.3672-3680.
- Price, R. and Nosten, F. (2001). Drug resistant *P. falciparum* malaria: clinical consequences and strategies for prevention. *Drug Resistance Updates*, 4(3), pp.187-196.
- Pudovik, A. and Yarmukhametova, D. (1954). New method of synthesis of esters of phosphonic and thiophosphonic acids. *Bulletin of the Academy of Sciences of the USSR Division of Chemical Science*, 3(4), pp.543-550.
- Pudovik, A. and Zimin, M., (1980). ChemInform Abstract: Addition reactions of partially-esterified phosphorus acids. rearrangements of α -hydroxyalkyl phosphorus esters and their α -mercapto an α -amino-analogs. *Chemischer Informationsdienst*, 11(31).
- Pudovik, A. and Zimin, M., (1980). Reactions of the addition of phosphorus acids partial esters multiple bonds and the rearrangements of addition products. *Pure and Applied Chemistry*, 52(4), pp.989-1011.
- Rádai, Z. and Keglevich, G. (2018). Synthesis and Reactions of α -Hydroxyphosphonates. *Molecules*, 23(6), pp.1493.

- Rahbari, R., Sheahan, T., Modes, V., Collier, P., Macfarlane, C. and Badge, R. (2009). A novel L1 retrotransposon marker for HeLa cell line identification. *BioTechniques*, 46(4), pp.277-284.
- Ranga, S., Chakravarty, M., Chatterjee, T. and Ghosal, S., (2019). Mechanistic insights into n-BuLi mediated phospho-Brook rearrangement. *New Journal of Chemistry*, 43(25), pp.9886-9890.
- Ranga, S., Chakravarty, M., Chatterjee, T. and Ghosal, S., (2019). Mechanistic insights into n-BuLi mediated phospho-Brook rearrangement. *New Journal of Chemistry*, 43(25), pp.9886-9890.
- Rassi Jr, A., Rassi, A. and Marin-Neto, J. (2010). Chagas disease. *The Lancet*, 375(9723), pp.1388-1402.
- Redmore, D. (1978). Chemistry of phosphorous acid: new routes to phosphonic acids and phosphate esters. *The Journal of Organic Chemistry*, 43(5), pp.992-996.
- Ritchie, T. and Macdonald, S. (2014). How drug-like are 'ugly' drugs: do drug-likeness metrics predict ADME behaviour in humans? *Drug Discovery Today*, 19(4), pp.489-495.
- Rodrigues, T., Lopes, F. and Moreira, R. (2010). Inhibitors of the Mitochondrial Electron Transport Chain and de novo Pyrimidine Biosynthesis as Antimalarials: The Present Status. *Current Medicinal Chemistry*, 17(10), pp.929-956.
- Rosenthal, P. (2003). Antimalarial drug discovery: old and new approaches. *Journal of Experimental Biology*, 206(21), pp.3735-3744.
- Sachs, J. and Malaney, P. (2002). The economic and social burden of malaria. *Nature*, 415(6872), pp.680-685.
- Sahu, N., Sahu, S. and Kohli, D. (2008). Novel Molecular Targets for Antimalarial Drug Development. *Chemical Biology & Drug Design*, 71(4), pp.287-297.

- Salom-Roig, X., Hamze, A., Calas, M. and Vial, H. (2005). Dual Molecules as New Antimalarials. *Combinatorial Chemistry & High Throughput Screening*, 8(1), pp.49-62.
- Samanta, S. and Zhao, C. (2006). Organocatalytic Enantioselective Synthesis of α -Hydroxy Phosphonates. *ChemInform*, 37(43).
- Sandro, P., Moreira, D., Gomes, B., Ferreira, M., Goncalves, A., Laurindo, P., Vilhena, T., Dolabela, M. and , Green, M. (2012). Review: Oxidative Stress in Malaria, International Journal of Molecular Science. *International Journal of Molecular Science*, 13, pp.16346-16372.
- Scherer, W. (1953). Studies on the propagation of in vitro of Poliomyelitis virus: IV. Viral multiplication in stable strain of human malignant epithelial cells (strain HeLa) derived from an epidermoid carcinoma of the cervix. *Journal of Experimental Medicine*, 97(5), pp.695-710.
- Schlagenhauf, P. (1999). Mefloquine for Malaria Chemoprophylaxis 1992–1998: A Review. *Journal of Travel Medicine*, 6(2), pp.122-133.
- Schofield, C., Jannin, J. and Salvatella, R. (2006). The future of Chagas disease control. *Trends in Parasitology*, 22(12), pp.583-588.
- Schwartz, L., Brown, G., Genton, B. and Moorthy, V. (2012). A review of malaria vaccine clinical projects based on the WHO rainbow table. *Malaria Journal*, 11(1), pp.11.
- Sevrain, C., Berchel, M., Couthon, H. and Jaffrès, P. (2017). Phosphonic acid: preparation and applications. *Beilstein Journal of Organic Chemistry*, 13, pp.2186-2213.
- Shafiq, N., Rajagopalan, S., Kushwaha, H., Mittal, N., Chandurkar, N., Bhalla, A., Kaur, S., Pandhi, P., Puri, G., Achuthan, S., Pareek, A., Singh, S., Srivastava, J., Gaur, S. and Malhotra, S. (2014). Single Ascending Dose Safety and Pharmacokinetics of CDRI-97/78: First-in-Human Study of a Novel Antimalarial Drug. *Malaria Research and Treatment*, 2014, pp.1-10.

- Shahinas, D., Folefoc, A. and Pillai, D. (2013). Targeting *P. falciparum* Hsp90: Towards Reversing Antimalarial Resistance. *Pathogens*, 2(1), pp.33-54.
- Shandilya, A., Chacko, S., Jayaram, B. and Ghosh, I. (2013). A plausible mechanism for the antimalarial activity of artemisinin: A computational approach. *Scientific Reports*, 3(1).
- Shavlev, O., Repka, T., Goldfarb, A., Grinberg, L., Abrahamov, A. and Olivier, N. (1995). Deferipron (L1) chelates pathologic iron deposits from membranes of intact thalassaemic and sickle red blood cells both in vitro, *Blood*, 86, pp.2008-2013.
- Sherman, I. (1965). Glucose-6-phosphate Dehydrogenase and Reduced Glutathione in Malaria-Infected Erythrocytes (*Plasmodium lophurae* and *P. berghei**). *The Journal of Protozoology*, 12(3), pp.394-396.
- Sherman, I. (1998). Carbohydrate metabolism in asexual stages. In *Malaria. Parasite Biology, Pathogenesis, and Protection*, ASM Press, pp.135–144.
- Sibley, C. and Price, R. (2012). Monitoring antimalarial drug resistance: Applying lessons learned from the past in a fast-moving present. *International Journal for Parasitology: Drugs and Drug Resistance*, 2, pp.126-133.
- Sibley, C., Barnes, K., Watkins, W. and Plowe, C. (2008). A network to monitor antimalarial drug resistance: a plan for moving forward. *Trends in Parasitology*, 24(1), pp.43-48.
- Sibley, C., Guerin, P. and Ringwald, P. (2010). Monitoring antimalarial resistance: launching a cooperative effort. *Trends in Parasitology*, 26(5), pp.221-224.
- Siegel, D., Hui, H., Doerffler, E., Clarke, M., Chun, K., Zhang, L., Neville, S., Carra, E., Lew, W., Ross, B., Wang, Q., Wolfe, L., Jordan, R., Soloveva, V., Knox, J., Perry, J., Perron, M., Stray, K., Barauskas, O., Feng, J., Xu, Y., Lee, G., Rheingold, A., Ray, A., Bannister, R., Strickley, R., Swaminathan, S., Lee, W., Bavari, S., Cihlar, T., Lo, M., Warren, T. and Mackman, R., (2017). Discovery and Synthesis of a Phosphoramidate Prodrug of a

- Pyrrolo[2,1-f][triazin-4-amino] Adenine C-Nucleoside (GS-5734) for the Treatment of Ebola and Emerging Viruses. *Journal of Medicinal Chemistry*, 60(5), pp.1648-1661.
- Silva, N., Gonçalves, L., Duarte, J., Silva, J., Santos, C., Braga, F., Silva, R., Costa, J., Hagemelin, L. and dos Santos, C. (2014). Computational Analysis of Physicochemical, Pharmacokinetic and Toxicological Properties of Deoxyhypusine Synthase Inhibitors with Antimalarial Activity. *Computational Molecular Bioscience*, 04(04), pp.47-57.
- Singh, C., Gupta, N. and Puri, S. (2004). Geraniol-Derived 1,2,4-Trioxanes with Potent in vivo Antimalarial Activity. *Bioorganic and Medicinal Chemistry Letters*, 13(20). *ChemInform*, 13(20), pp.3447-3450.
- Smith, A., Xian, M., Kim, W. and Kim, D., (2006). The [1,5]-Brook Rearrangement: An Initial Application in Anion Relay Chemistry. *Journal of the American Chemical Society*, 128(38), pp.12368-12369.
- Sobhani, S. and Tashrifi, Z. (2010). Synthesis of α -functionalized phosphonates from α -hydroxyphosphonates. *Tetrahedron*, 66(7), pp.1429-1439.
- Sohrabi, Y. and Lipoldová, M. (2018). Mannose Receptor and the Mystery of Non healing *Leishmania major* Infection. *Trends in Parasitology*, 34(5), pp.354-356.
- Solomon, V., Haq, W., Smilkstein, M., Srivastava, K., Rajakumar, S., Puri, S. and Katti, S. (2008). Synthesis and Antimalarial Activity of Novel Side Chain Modified Antimalarial Agents Derived from 4-Aminoquinoline. *Medicinal Chemistry*, 4(5), pp.446-456.
- Song, Y. (2005). To what extent is it possible to design selective L-glutamate dehydrogenase inhibitors? *MSc thesis*, University College Dublin.
- Stanaway, J. and Roth, G. (2015). The Burden of Chagas Disease. *Global Heart*, 10(3), pp.139-144.

- Storm, J., Perner, J., Aparicio, I., Patzewitz, E., Olszewski, K., Llinas, M., Engel, P. and Müller, S. (2011). *P. falciparum* glutamate dehydrogenase is dispensable and not a drug target during erythrocytic development. *Malaria Journal*, 10(1), pp.193.
- Tam, J., Heath, W. and Merrifield, R., (1986). Mechanisms for the removal of benzyl protecting groups in synthetic peptides by trifluoromethanesulfonic acid-trifluoroacetic acid-dimethyl sulfide. *Journal of the American Chemical Society*, 108(17), pp.5242-5251.
- Taylor-Robinson, A. (1999). Immunity to Asexual Blood Stages of Plasmodium: Is Resistance to Acute Malaria Adaptive or Innate? – A Response. *Parasitology Today*, 15(5), pp.208.
- Thornton, P., Kadri, H., Miccoli, A. and Mehellou, Y. (2016). Nucleoside Phosphate and Phosphonate Prodrug Clinical Candidates. *Journal of Medicinal Chemistry*, 59(23), pp.10400-10410.
- Trafford, H. (2005). Antimalarial therapies. *Drug Discovery Today*, 10(23-24), pp.1588-1590.
- Trager, W. and Jensen, J. (1976). Human malaria parasites in continuous culture. *Science*, 193(4254), pp.673-675.
- Trape, J., Pison, G., Spiegel, A., Enel, C. and Rogier, C. (2002). Combating malaria in Africa. *Trends in Parasitology*, 18(5), pp.224-230.
- Triglia, T. and Cowman, A. (1999). The mechanism of resistance to sulfur drugs in *P. falciparum*. *Drug Resistance Updates*, 2(1), pp.15-19.
- Tripathy, S. and Roy, S. (2015). Redox sensing and signalling by malaria parasite in vertebrate host. *Journal of Basic Microbiology*, 55(9), pp.1053-1063.
- Trypanosomiasis and Tsetse flies. (1946). *The Lancet*, 247(6397), pp.509.
- Ugwuozor, D. (2008). Synthesis of l-glutamate analogues as potential new antimalarials. *MSc thesis, London Metropolitan University*.

- Uhlmann, E. and Meier, C. (2000). *Methyl phosphonic acid esters, processes for their preparation, and their use*. US006028182A.
- Van Aalten, D., Milne, K., Zou, J., Kleywegt, G., Bergfors, T., Ferguson, M., Knudsen, J. and Jones, T. (2001). Binding site differences revealed by crystal structures of *P. falciparum* and bovine Acyl-CoA binding protein. *Journal of Molecular Biology*, 309(1), pp.181-192.
- Vepsäläinen, J., Nupponen, H. and Pohjala, E. (1993). Bisphosphonic compounds v. selective preparation of (dichloromethylene)bisphosphonate partial esters. *Tetrahedron Letters*, 34(28), pp.4551-4554.
- Wagner, J., Ludemann, H., Farber, P., Lottspeich, F. and Krauth-Siegel, R. (1998). Glutamate dehydrogenase, the marker protein of *P. falciparum*. Cloning, expression and characterization of the malarial enzyme. *European Journal of Biochemistry*, 258(2), pp.813-819.
- Wani, W., Jameel, E., Baig, U., Mumtazuddin, S. and Hun, L. (2015). ChemInform Abstract: Ferroquine and Its Derivatives: New Generation of Antimalarial Agents. *ChemInform*, 46(41), pp.534-551.
- Warhurst, D. (1985). Antimalarial drugs II: Current antimalarials and new drug development. *Trends in Pharmacological Sciences*, 6, pp.302-304.
- Wein, S., Maynadier, M., Bordat, Y., Perez, J., Maheshwari, S., Bette-Bobillo, P., Tran Van Ba, C., Penarete-Vargas, D., Fraisse, L., Cerdan, R. and Vial, H. (2012). Transport and pharmacodynamics of albitiazolium, an antimalarial drug candidate. *British Journal of Pharmacology*, 166(8), pp.2263-2276.
- Wells, T., van Huijsduijnen, R. and Van Voorhis, W. (2015). Malaria medicines: a glass half full? *Nature Reviews Drug Discovery*, 14(6), pp.424-442.

- Wendo, C. (2002). African scientists discuss drug-resistant malaria. *The Lancet*, 359(9308), pp.770.
- Weng, S., Lin, G., Li, H., Yang, K., Yang, T., Liu, H. and Sie, S. (2012). Nafion®-supported oxovanadium-catalyzed hydrophosphonylation of aldehydes under solventless conditions. *Applied Organometallic Chemistry*, 26(9), pp.455-460.
- Werner, C., Stubbs, M., Krauth-Siegel, R. and Klebe, G. (2005). The Crystal Structure of *P. falciparum* Glutamate Dehydrogenase, a Putative Target for Novel Antimalarial Drugs. *Journal of Molecular Biology*, 349(3), pp.597-607.
- Wernsdorfer, W. H, and Payne, D. (1991). The dynamics of drug resistance in *P. falciparum*. *Pharmacology & Therapeutics*, 50(1), pp.95-121.
- White, N. (2002). The assessment of antimalarial drug efficacy. *Trends in Parasitology*, 18(10), pp.458-464.
- White, N. (2010). Artemisinin resistance—the clock is ticking. *The Lancet*, 376(9758), pp.2051-2052.
- White, N. (2011). The parasite clearance curve. *Malaria Journal*, 10(1), pp.278.
- White, N., Duong, T., Uthaisin, C., Nosten, F., Phyo, A., Hanboonkunupakarn, B., Pukrittayakamee, S., Jittamala, P., Chuthasmit, K., Cheung, M., Feng, Y., Li, R., Magnusson, B., Sultan, M., Wieser, D., Xun, X., Zhao, R., Diagana, T., Pertel, P. and Leong, F. (2016). Antimalarial Activity of KAF156 in *Falciparum* and *Vivax* Malaria. *New England Journal of Medicine*, 375(12), pp.1152-1160.
- White, N., Stepniewska, K., Barnes, K., Price, R. and Simpson, J. (2008). Simplified antimalarial therapeutic monitoring: using the day-7 drug level? *Trends in Parasitology*, 24(4), pp.159-163.

- Whitelaw, B. and Robinson, M. (2013). Inhibitors of Glutamate Dehydrogenase Block Sodium-Dependent Glutamate Uptake in Rat Brain Membranes. *Frontiers in Endocrinology*, 4(article 123), pp.1-9.
- Wiemer, A., Wiemer, D. (2016). ChemInform Abstract: Prodrugs of Phosphonates and Phosphates: Crossing the Membrane Barrier. *ChemInform*, 47(50).
- Wongsrichanalai, C., Pickard, A., Wernsdorfer, W. and Meshnick, S. (2002). Epidemiology of drug-resistant malaria. *The Lancet Infectious Diseases*, 2(4), pp.209-218.
- Wright, C. (2005). Traditional antimalarials and the development of novel antimalarial drugs. *Journal of Ethnopharmacology*, 100(1-2), pp.67-71.
- Yeh, I. (2004). Computational Analysis of *P. falciparum* Metabolism: Organizing Genomic Information to Facilitate Drug Discovery. *Genome Research*, 14(5), pp.917-924.
- Yektaeian, N., Mehrabani, D., Sepaskhah, M., Zare, S., Jamhiri, I. and Hatam, G. (2019). Lipophilic tracer Dil and fluorescence labelling of acridine orange used for *Leishmania major* tracing in the fibroblast cells. *Heliyon*, 5(12), pp.03-73.
- Yokomatsu, T., Yamagishi, T. and Shibuya, S. (2010). ChemInform Abstract: Enantioselective Synthesis of α -Hydroxyphosphonates Through Asymmetric Pudovik Reactions with Chiral Lanthanoid and Titanium Alkoxides. *ChemInform*, 28(43).
- Yokomatsu, T., Yamagishi, T., Shibuya, S. (1997). Enantioselective synthesis of α -hydroxyphosphonates through asymmetric Pudovik reactions with chiral lanthanoid and titanium alkoxides. *Journal of the Chemical Society, Perkin Transactions 1*, (10), pp.1527-1534.
- Zahirnia, A., Bordbar, A., Ebrahimi, S., Spotin, A., Mohammadi, S., Ghafari, S., Ahmadvand, S., Jabbari, N., Esmaili Rastaghi, A. and Parvizi, P. (2018). Predominance of *Leishmania major* and rare occurrence of *Leishmania tropica* with haplotype variability at the center of Iran. *The Brazilian Journal of Infectious Diseases*, 22(4), pp.278-28

